

Mechanismen der CO₂ Toleranz bei Seeigeln des Genus
Strongylocentrotus

Mechanisms of CO₂ tolerance in sea urchins of the genus
Strongylocentrotus

Dissertation
zur Erlangung des akademischen Grades
Dr. rer. nat.
der Mathematisch-Naturwissenschaftlichen Fakultät
der Christian-Albrechts-Universität zu Kiel
vorgelegt von

Meike Stumpp
Kiel, 2011

Referent: Prof. Dr. Frank Melzner
Koreferent: Prof. Dr. Markus Bleich

Tag der mündlichen Prüfung: 16.09.2011

Zum Druck genehmigt am: 16.09.2011

Summary

Increasing atmospheric $p\text{CO}_2$ due to anthropogenic CO_2 emissions are altering the carbonate chemistry of the oceans, inducing a drop in surface seawater pH (pH_{sw}) and $[\text{CO}_3^{2-}]$ and an increase in seawater $p\text{CO}_2$ and $[\text{HCO}_3^-]$. This phenomenon has been termed “ocean acidification” and has lately received considerable public and scientific attention. Atmospheric $p\text{CO}_2$ of 1000 ppm and a concomitant decrease in surface ocean pH of 0.4 units can be expected by the year 2100-2300. The organisms examined in this study – echinoids – are keystone species in several ecosystems as well as economically important. Echinoids are characterized by a calcified skeleton in adult as well as larval stages. Calcifying invertebrates have been shown to be relatively vulnerable to CO_2 induced changes in seawater carbonate chemistry. In most studies, echinoid adults and larvae responded with reduced growth and developmental rates to elevated seawater $p\text{CO}_2$, but the underlying mechanisms are unknown. In order to fill some of the gaps in knowledge, the present work was aimed at characterizing $p\text{CO}_2$ induced changes in acid-base regulatory capacity and energy budgets in two sea urchin species, *Strongylocentrotus droebachiensis* and *S. purpuratus*. Furthermore, this study investigated the adults’ physiological acclimation potential and studied ‘carry-over’ effects between different life cycle stages in response to environmental hypercapnia.

Using feeding rates, aerobic metabolic rates and egestion/excretion rates measured in larval and adult sea urchins exposed to current (approx. 40 Pa, 390 μatm) and elevated $p\text{CO}_2$ conditions (100 - 385 Pa, 990 - 3800 μatm), the present study demonstrated that the

energy available for growth and development – so called ‘scope for growth (SfG)’ – was reduced in response to hypercapnic conditions and that SfG correlated with observed decreases in growth and development. In *S. purpuratus* larvae, the reduction in SfG was due to elevated energy demands for maintenance processes as indicated by highly increased metabolic rates which rose by up to 100%, while food ingestion was slightly but not significantly reduced. In adult *S. droebachiensis*, SfG was reduced due to a significant decrease in feeding rates and an increase in N excretion, while aerobic metabolic rates were not altered in response to elevated seawater $p\text{CO}_2$. This drop in SfG significantly reduced gonad growth and fertilization success in sea urchins exposed to hypercapnic conditions for up to 4 months.

In order to identify the processes that were supplied with increased energy in response to elevated $p\text{CO}_2$, extracellular pH (pH_e) was determined in larval and adult *S. droebachiensis*. Planktotrophic sea urchin larvae basically have two fluid compartments that could be impacted by changes in seawater carbonate chemistry: 1. the digestive system consisting of mouth, stomach and intestine and 2. the primary body cavity (PBC), filled with an extracellular matrix similar in structural appearance to the scyphozoan mesoglea, in which the calcifying primary mesenchyme cells (PMCs) construct the larval spicules. Acute and chronic declines in pH_{SW} both led to linear decreases in PBC pH_e indicating that PBC pH_e is pH conform to the surrounding seawater and that no pH_e compensation occurs in this cell free gelatinous space. Furthermore, environmental hypercapnia (250 Pa, 2470 μatm) led to a 0.4 units decrease in the highly alkaline stomach pH (pH 9.5) and may thus negatively impact energy acquisition by potentially reducing larval digestion potential. While several genes important for ion regulation and calcification were down regulated in *S. purpuratus* pluteus larvae, gene transcript abundance of several metabolic genes and Na^+/K^+ -ATPase were increased in response to elevated $p\text{CO}_2$ conditions. This is in line with the observed increased metabolic rates which may be due to increased energetic demands for ion regulation, particularly for additional alkalization of the stomach lumen. Furthermore, albeit larval survival was not impacted by larval exposure to elevated $p\text{CO}_2$ (1175 μatm), a 5 times higher mortality of *S. droebachiensis* juveniles after metamorphosis of exposed larvae indicated a clear bottleneck at the transition from the larva to the juvenile.

Adult *S. droebachiensis* fully compensated hypercapnia induced acid-base disturbances by significantly accumulating $[\text{HCO}_3^-]_e$ after 10 days of exposure to 145 Pa CO_2 (1430 μatm). Furthermore, they could sustain full pH_e compensation and high $[\text{HCO}_3^-]_e$ for 45 days. Adult *S. droebachiensis* exposed to 123 Pa $p\text{CO}_2$ for 16 months exhibited a fertility rate not different from control animals. Both experiments suggest that there is acclimation/adaptation potential in *S. droebachiensis* which is possibly due to its current distribution in a habitat with seasonal hypercapnic conditions. In contrast, sea urchins exposed to >284 Pa CO_2 (2800 μatm) only partially compensated pH_e changes with $[\text{HCO}_3^-]_e$ accumulation of maximal 2.5 mM above control values similar to the $[\text{HCO}_3^-]_e$ values of animals exposed to the intermediate $p\text{CO}_2$. 71% of all animals could not sustain this compensation for 45 days exhibiting a strong metabolic acidosis. Possibly, $p\text{CO}_2$ conditions above 280 Pa (2760 μatm) exceed the acclimation potential of *S. droebachiensis*.

Accordingly, the present thesis demonstrated that environmental hypercapnia primarily impacts the energy balance and energy partitioning of different ontogenetic stages of Strongylocentrotid sea urchins leading to the observed reductions in growth and development. Shifts in energy partitioning likely disturb transitions between life cycle stages and may thus decrease recruitment success of sea urchins.

Zusammenfassung

Die Zunahme des Kohlendioxids in der Atmosphäre aufgrund anthropogener CO₂-Emissionen führt im Oberflächenwassers der Meere einerseits zu einem Abfall des pH Wertes und der Karbonationen-Konzentration und andererseits zu einem Anstieg des pCO₂ Wertes und der Bikarbonat-Konzentration. Aktuelle Voraussagen zu Folge wird der pCO₂ der Atmosphäre in den nächsten 100 Jahren auf ca. 1000 ppm ansteigen und somit einen pH Abfall von 0,4 Einheiten im Oberflächenwasser der Ozeane hervorrufen. Es kommt zu einer Versauerung des Meerwassers, weshalb dieses Phänomen auch „Ozeanversauerung“ genannt wird.

Die vorliegende Studie befasst sich mit Echinoiden – den Seeigeln -, die Schlüsselarten in ökologischen Systemen sind, und ökonomisch als begehrtes Nahrungsmittel eine wichtige Rolle spielen. Seeigel sind durch skelettbildende Kalkstrukturen sowohl im Adulten- als auch im Larvalstadium charakterisiert und wurden deshalb als empfindlichere Organismengruppe gegenüber der Ozeanversauerung eingestuft. Bisherige Studien zeigten, dass die Gruppe der Echinoiden im Adulten- so wie auch im Larvalstadium mit verzögerten und verringerten Wachstumsraten auf erhöhten Meerwasser pCO₂ reagierten. Die Mechanismen, die dieser Entwicklungs- und Wachstumsverzögerung zu Grunde liegen, sind jedoch bisher noch nicht geklärt und sind Thema der vorliegenden Arbeit.

Zunächst wurden Energiebilanzen für verschiedene Lebensstadien der beiden Seeigelarten *Strongylocentrotus droebachiensis* und *S. purpuratus* erstellt, um herauszufinden, ob eine energetische Verschiebung stattfindet, d. h. ob möglicherweise Energie von Wachstumsprozessen auf lebenserhaltenden Prozessen (z.B. der Ionenregulation) umgelagert wird. Als ein lebenswichtiger Prozess, der mit

hyperkapnischen Bedingungen verknüpft ist, wurden die extrazellulären Säure-base-regulatorischen Fähigkeiten verschiedener ontogenetischer Stadien genauer betrachtet. Weiterhin sollte geklärt werden, in wieweit die adulten Tiere in der Lage sind, sich an die erwarteten klimatischen Veränderungen anzupassen und wie sich eine Akklimierung unterschiedlicher Lebensstadien des Seeigels (Adulte und Larven) an erhöhten $p\text{CO}_2$ auf die Fitness der darauffolgenden Lebensstadien (Larven und Juvenile) auswirkt.

Mit Hilfe der Ermittlung von Futteraufnahme, aeroben metabolischen Raten und Exkretionsraten in Adulten und Larven, die jetzigen (40 Pa, 390 μatm) und erhöhten $p\text{CO}_2$ (100 – 385 Pa, 990 – 3800 μatm) ausgesetzt wurden, konnte diese Studie zeigen, dass sich die Menge an Energie, die für das Wachstum und die Entwicklung der Tiere bereitgestellt werden konnte, unter erhöhten $p\text{CO}_2$ verringerte. In Larven des Seeigels *S. purpuratus* lag dieser Verringerung eine Erhöhung (bis zur Verdopplung) der metabolischen Raten zu Grunde. Dies deutet darauf hin, dass die Tiere einen erhöhten Energiebedarf für lebenserhaltende Prozesse hatten und ihre Entwicklung mit dementsprechend weniger Energie versorgen konnten. Bei adulten Tieren konnte die Abnahme von Wachstumsraten auf reduzierte Fraßraten (um bis zu 30%) und erhöhte Stickstoff-Exkretion zurückgeführt werden. Diese führte bei einer Inkubationsdauer von 6 Wochen bis zu 4 Monaten zu einer signifikant erniedrigten Gewichtszunahme der Gonaden bzw. einer Einschränkung der Fertilität der Weibchen.

Untersuchungen des extrazellulären pH (pH_e) in Larven und Adulten des Seeigels *S. droebachiensis* dienten einerseits dem Aufschluss, ob die Tiere in der Lage sind ihren extrazellulären pH zu regulieren und ob möglicherweise ein erhöhter Energiebedarf für die pH- und Ionen-Regulation besteht. Bei Seeigellarven gibt es zwei flüssigkeitsgefüllte Kompartimente: zum einen den larvalen Verdauungsapparat bestehend aus Mund, Magen und Darm und zum anderen die primäre Körperhöhle, den gelatinösen zell-freien Raum zwischen äußerem Epithel und dem Verdauungssystem, in dem die kalzifizierenden primären mesenchymalen Zellen (PMC) das larvale Skelett aufbauen. Untersuchungen unter akuter und chronischer $p\text{CO}_2$ -Exposition von Larven konnten zeigen, dass der pH_e der Körperhöhle mit dem pH des Seewassers (pH_{SW}) konform ist. Weiterhin führte eine chronische Inkubation der Larven in erhöhtem Seewasser $p\text{CO}_2$ (250 Pa, 2470 μatm) zu einer Erniedrigung des alkalischen (pH 9.5) Magen pH um bis zu 0.4 Einheiten. Ein solcher Einbruch des Magen pH könnte zu einer Einschränkung der larvalen

Verdauungseffizienz führen und somit ebenfalls zu einer Verringerung der Energieaufnahme. Genetische Analysen unterstützen die beobachteten erhöhten metabolischen Raten durch erhöhte Transkription metabolischer Gene. Weiterhin deutet die Erhöhung der Na^+/K^+ -ATPase-Transkriptkonzentration darauf hin, dass in Larven möglicherweise ein erhöhter Energiebedarf für Ionenregulation (z.B. für die Alkalinisierung des Magens) besteht. Andere wichtige Gene für Kalzifizierung und Ionenregulation waren jedoch nicht unterschiedlich exprimiert. Weiterhin war die Mortalitätsrate der Juvenilen, nachdem die Larven erhöhtem $p\text{CO}_2$ ausgesetzt waren, extrem erhöht (5-fach geringeres Überleben). Man kann daher vermuten, dass durch den erhöhten Energiebedarf der Larven weniger Energie für das Überleben der Juvenilen nach der Metamorphose bereitgestellt werden konnte.

In adulten Seeigeln (*S. droebachiensis*) konnte gezeigt werden, dass die Tiere nach 10 Tagen bei einem $p\text{CO}_2$ von 145 Pa (1430 μatm) durch $[\text{HCO}_3^-]_e$ Akkumulation einen CO_2 induzierten Abfall des pH_e vollständig und langfristig (6 Wochen) kompensieren konnten. Dies kann möglicherweise als Anpassung der Tiere an ihr natürliches Habitat gewertet werden, das schon heute durch saisonale hyperkapnische Bedingungen (bis zu 243 Pa, 2400 μatm) geprägt ist. Bei einer Inkubation zwischen 300 und 400 Pa CO_2 (2960 bis 3950 μatm) konnten die Tiere mit der gleichen $[\text{HCO}_3^-]_e$ von +2.5 mM jedoch nur eine partielle pH_e Kompensation erzielen. Außerdem konnten ein Großteil der Tiere (71%) die partielle Kompensation nicht über sechs Wochen aufrechterhalten und zeigte nach dieser Inkubationszeit eine starke metabolische Azidose. Offensichtlich wurde mit diesen hohen $p\text{CO}_2$ Werten das Anpassungspotential der erwachsenen Tiere überschritten.

Zusammenfassend konnte die vorliegende Arbeit zeigen, dass den verringerten Wachstums- und Entwicklungsraten der Seeigel eine Umstrukturierung der Energiebilanzen zu Grunde liegt. Die beiden Seeigelarten *S. droebachiensis* und *S. purpuratus* weisen weiterhin eine gewisse Robustheit gegenüber moderaten Anstiegen in Seewasser $p\text{CO}_2$ aufweisen (bis zu 150 Pa, 1480 μatm). Dennoch stellen anthropogene CO_2 -Emissionen insbesondere für den Übergang von einem Lebensstadium zum anderen und in Bezug auf lokal und saisonal extrem erhöhte $p\text{CO}_2$ -Bedingungen (>300 Pa, 2960 μatm) eine ernstzunehmende Bedrohung für die Seeigel dar.

Contents

1 Introduction	1
1.1 <i>Ocean acidification</i>	1
1.2 <i>Biological Impacts</i>	5
1.3 <i>Physiology of hypercapnia tolerance</i>	6
1.4 <i>Echinoids</i>	8
1.4.1 Evolution	8
1.4.2 Biological relevance	9
1.4.3 Reproduction and development	10
1.5 <i>Research hypotheses</i>	12
2 Material and Methods	17
2.1 <i>Origin and maintenance of adult sea urchins</i>	17
2.2 <i>Experimental design</i>	18
2.2.1 Larval experiments	18
2.2.2 Adult experiments	19
2.3 <i>Determination of seawater carbonate chemistry speciation</i>	20
2.3.1 Experiments at the IFM-GEOMAR and AWI Sylt, Germany	20
2.3.2 Experiments at the SLC, Sweden	21
2.4 <i>Whole animal performance: development, growth and reproduction</i>	21
2.4.1 Larval development	21
2.4.2 Larval settlement success in response to adult acclimation to elevated $p\text{CO}_2$	22
2.4.3 Juvenile growth and survival in response to larval exposure to elevated $p\text{CO}_2$	22
2.4.4 Adult growth	23
2.4.5 Fertility	23
2.5 <i>Energy metabolism</i>	24
2.5.1 Feeding and fecal pellet production	24
2.5.2 Routine metabolic rates	26
2.5.3 NH_4^+ excretion rate and O:N ratio	28
2.5.4 Energy budget calculations	28

2.6 <i>Molecular techniques</i>	30
2.6.1 Reverse transcription quantitative polymerase chain reaction (RT qPCR)	30
2.6.2 Immunocytochemistry	32
2.7 <i>Determination of acid-base status</i>	33
2.7.1 Measurements of extracellular pH (pH _e) in sea urchin larvae	33
2.7.2 Extracellular carbonate system speciation of perivisceral coelomic fluid	37
3 Publications and unpublished results	41
I CO ₂ induced seawater acidification impacts sea urchin larval development I: elevated metabolic rates decrease scope for growth and induce developmental delay	43
II CO ₂ induced seawater acidification impacts sea urchin larval development II: gene expression patterns in pluteus larvae	101
III Resource allocation and extracellular acid-base status in <i>Strongylocentrotus droebachiensis</i> in response to CO ₂ induced seawater acidification.	157
IV Impact of long term and trans-life-cycle acclimation to near-future ocean acidification on the green sea urchin <i>Strongylocentrotus droebachiensis</i> .	217
4 Discussion	255
4.1 <i>CO₂ induced changes in growth and energy budgets</i>	258
4.1.1 Growth and energy budgets of larval sea urchins	258
4.1.2 Growth and energy budgets of adult sea urchins	261
4.2 <i>Energy partitioning</i>	264
4.2.1 Calcification, ion regulation and metabolism: changes in larval gene transcript levels	264
4.2.2 Extracellular pH homeostasis in <i>S. droebachiensis</i> larvae	268
4.2.3 Extracellular pH homeostasis in <i>S. droebachiensis</i> adults	274
5 Conclusion	277
6 References	281

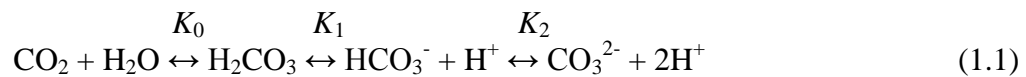
Abbreviations:

A	absorbed energy
A_T	total alkalinity
ADM	ash dry mass
AFDM	ash free dry mass
ASW	artificial seawater
C	consumed energy (=I in publication 1)
C_T	total dissolved inorganic carbon
DM	dry mass
DOM	dissolved organic matter
dpf	days post-fertilization
ECM	extracellular matrix
E_{OM}	organic matter absorption efficiency
FSW	filtered seawater
G_X	energy deposited in body organ growth (X= gonad, gut or test)
MO_2	aerobic metabolic rate
NKA	Na^+/K^+ -ATPase
OM	organic matter
O:N	atomic oxygen to nitrogen ratio
PBC	primary body cavity
PCF	perivisceral coelomic fluid
PFA	paraformaldehyde
pH_c	extracellular pH
pH_{NBS}	pH NBS scale
pH_{SW}	seawater pH
pH_T	pH total scale
R	respired energy
RMR	routine metabolic rate
RT qPCR	reverse transcription quantitative polymerase chain reaction
SfG	scope for growth
SW	seawater
U	excreted energy (as NH_4^+)
WM	wet mass

1 Introduction

1.1 Ocean acidification

Anthropogenic release of carbon dioxide (CO_2) and the simultaneous increase in CO_2 partial pressure ($p\text{CO}_2$) of the atmosphere has lately received considerable attention: CO_2 acts as a greenhouse gas and thus increases global temperatures. In addition, dissolution of CO_2 in the world oceans causes a change in carbonate chemistry speciation of seawater leading to an acidification of the oceans. Dissolution of CO_2 in seawater leads to the formation of carbonic acid (H_2CO_3) which dissociates into a proton and HCO_3^- , decreasing seawater pH (equation 1.1, Zeebe and Wolf-Gladrow, 2001). This phenomenon was termed ocean acidification. Excess protons react with CO_3^{2-} resulting in the formation of HCO_3^- . The net effect of adding CO_2 to seawater is thus increasing the concentration of dissolved CO_2 and HCO_3^- and decreasing $[\text{CO}_3^{2-}]$ and seawater pH.



The different carbon species in seawater are in chemical equilibrium, which is described by the three equilibrium constants K_0 , K_1 and K_2 . K_0 defines the equilibrium between CO_2 and H_2CO_3 , K_1 defines the equilibrium between H_2CO_3 and HCO_3^- and K_2 defines the equilibrium between HCO_3^- and CO_3^{2-} . The equilibrium constants are dependent on temperature, salinity and pressure. Total dissolved inorganic carbon (C_T) is the sum of all carbon species in seawater (equation 1.2):

$$C_T = [\text{H}_2\text{CO}_3^*] + [\text{HCO}_3^-] + [\text{CO}_3^{2-}] \quad (1.2)$$

with $[\text{H}_2\text{CO}_3^*]$ being the sum of dissolved CO_2 ($\text{CO}_2(\text{aq})$) and H_2CO_3 . At a pH of 8.1, a temperature of 25°C and a salinity of 35, only $\sim 0.5\%$ of the inorganic carbon is in the form of H_2CO_3^* , 13% in the form of CO_3^{2-} and the majority of $\sim 86\%$ is in the form of HCO_3^- .

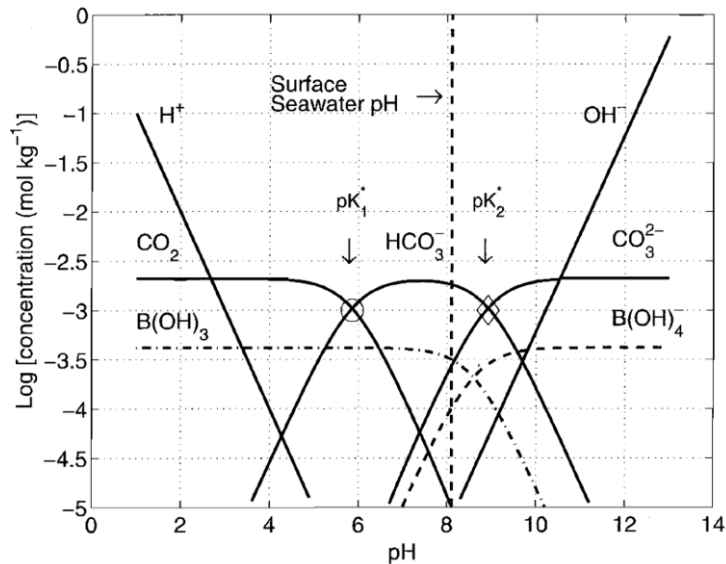


Figure 1.1: Bjerrum plot (from Zeebe and Wolf-Gladrow, 2001). Graphical representation of dissolved inorganic carbon species ($[\text{CO}_2]$, $[\text{HCO}_3^-]$ and $[\text{CO}_3^{2-}]$) with respect to pH (at $T = 25^\circ\text{C}$, $S = 35$ and atmospheric pressure of 1 atm). pK_1 (pK_2) is the negative logarithm to the base of 10 for the first (second) dissociation constant.

The oceans cover two thirds of the world surface and play an essential role in determining world climate. Since the beginning of the industrial revolution about 250 years ago and the concomitant increase in anthropogenic CO_2 emissions, the oceans have served as a carbon sink, absorbing about half of the CO_2 produced by human activity (Sabine et al., 2004). Atmospheric $p\text{CO}_2$ has increased by >100 ppm above pre-industrial to a current $p\text{CO}_2$ of 394 ppm (NOAA/ESRL, www.esrl.noaa.gov/gmd/ccgg/trends) already, having induced a drop in surface ocean pH by >0.1 units (Caldeira and Wickett, 2003; Orr et al., 2006). Based on different scenarios of future human and technological development, the Intergovernmental Panel on Climate Change presented several predictions on atmospheric $p\text{CO}_2$ increases (SRES, Special Report on Emission Scenarios) and $p\text{CO}_2$ stabilization scenarios (WRE or SP scenarios) for the next centuries (IPCC, 2001; IPCC, 2007). The highest emission scenario of SRE scenarios (A2) is assuming an increase in CO_2 emissions based on a continuously increasing population with slow technological change and predicts an increase of atmospheric $p\text{CO}_2$ to 970 ppm by the end of this century (figure 1.2). Stabilization scenarios (WRE450 to WRE1000) assume human awareness of climate change and an arrest of CO_2 emissions at different

time scales in order to stabilize atmospheric CO₂ levels at certain thresholds (e.g. 450 to 1000 ppm) by the end of year 2300 (figure 1.2, Caldeira and Wickett, 2005; IPCC, 2007; Cao and Caldeira, 2008). An atmospheric pCO₂ of 1000 ppm would lead to a 0.5 pH unit decrease in ocean surface waters. Further scenarios are based on complete combustion of fossil fuel reserves. The burning of 5000 Pg C, current estimates of global carbon fossil fuel resources (IPCC, 2001), would result in atmospheric pCO₂ of 2000 ppm by the year 2300 and a pH decrease in ocean surface waters by 0.8 units (Caldeira and Wickett, 2005).

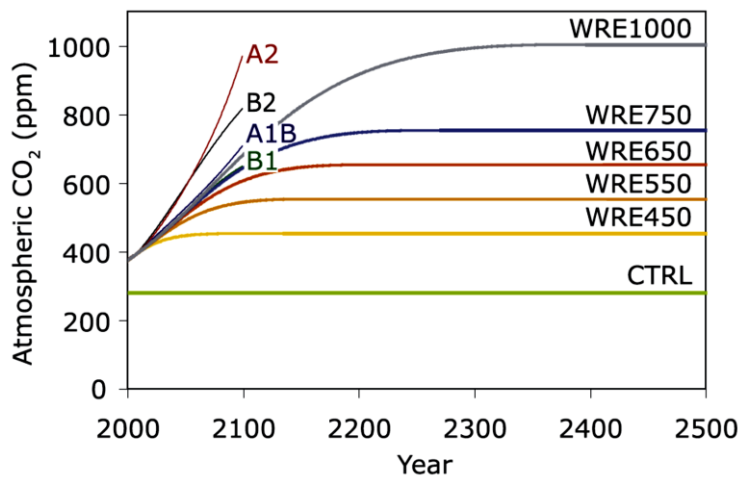


Figure 1.2: CO₂ emission scenarios based on different predictive models: A1-2 and B1 are SRE scenarios. WRE are stabilization scenarios with final atmospheric pCO₂ levels of 450, 550, 650, 750 and 1000 ppm (from Caldeira and Wickett, 2005).

As a consequence, a reduction in pH decreases the saturation states of calcite (Ω_{Ca}) and aragonite (Ω_{Ar}) in the oceans. Aragonite and calcite are the two most common CaCO₃ polymorphs formed by marine organisms. The calcite and aragonite saturation states are the products of [Ca²⁺] and [CO₃²⁻] divided by the stoichiometric solubility constants for calcite and aragonite, respectively (equation 1.3).

$$\Omega_{sp} = [Ca^{2+}] [CO_3^{2-}] K_{sp}^*^{-1} \tag{1.3}$$

The solubility of CaCO₃ decreases with increasing pressure and decreasing temperature and pH. If Ω drops below unity, CaCO₃ is prone to dissolution (Feely et al., 2004). Models for future ocean surface saturation states predict that CaCO₃ saturation will reach unity in polar regions at atmospheric pCO₂ of ca. 500 ppm (aragonite) and ca. 1000 ppm (calcite), clearly identifying these regions as especially vulnerable to increases in atmospheric pCO₂ (figure 1.3, Cao and Caldeira, 2008). Although CaCO₃ structures constructed by most marine organism are organic – inorganic compound materials, it has

been proposed that the increase in $p\text{CO}_2$ might threaten marine calcifiers - eventually by dissolution of external shells (e.g. Orr et al., 2006; Lischka et al., 2011). Since comparably high atmospheric $p\text{CO}_2$ have not existed on earth during the last 450,000 years (Petit et al., 1999), it is unknown, how marine calcifiers will cope with such rapidly changing and exceptional high seawater $p\text{CO}_2$ in the future.

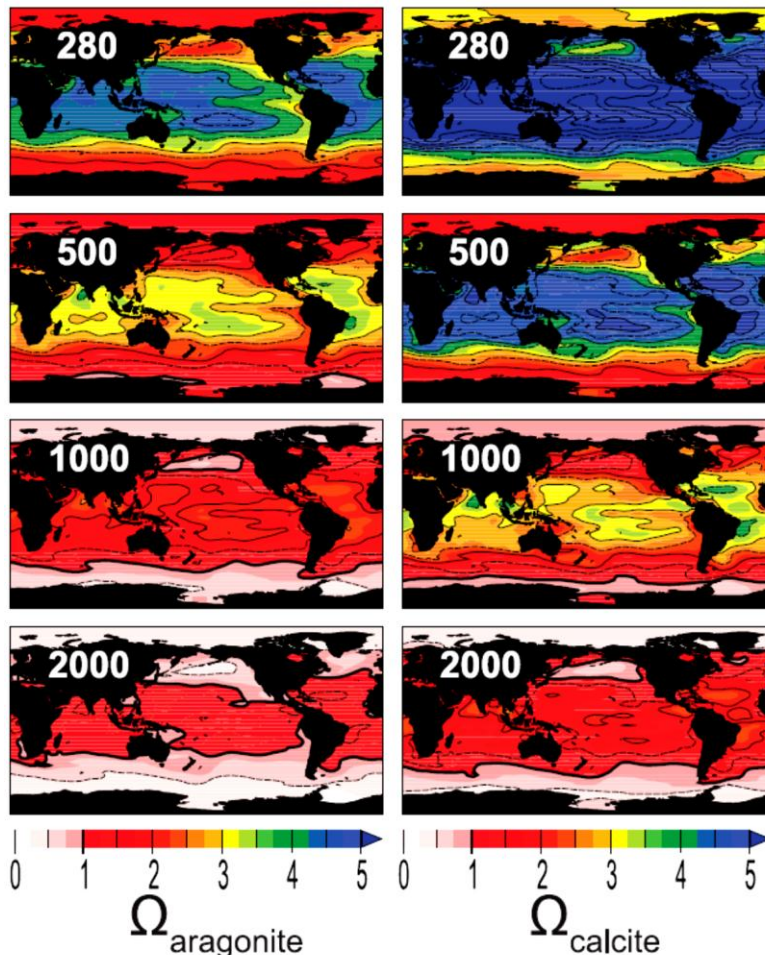


Figure 1.3: Aragonite and calcite saturation states ($\Omega_{\text{aragonite}}$ and Ω_{calcite} , respectively) for different CO₂ stabilization scenarios suggested by the IPCC (from Cao and Caldeira, 2008)

Of special interest in this matter are habitats that are naturally enriched with CO₂ already today either by naturally occurring CO₂ seeps (Hall-Spencer et al., 2008; Fabricius et al., 2011) or due to increased biological activity (Thomsen et al., 2010), as these could serve as analogues of a future, more acidified ocean. Upwelling of CO₂ enriched water masses along coasts which is happening at the continental shelf of western North America (Feely et al., 2008) or in the Baltic Sea (Thomsen et al., 2010) can lead to elevated $p\text{CO}_2$ in shallow water ecosystems confronting the inhabitants of these with elevated $p\text{CO}_2$. In the Baltic Sea (Kiel Fjord), average summer (July-August) surface $p\text{CO}_2$ values of 100 Pa (1000 μatm) were observed, while peak values could even reach

230 Pa (2300 μatm) (Thomsen et al., 2010). On the one hand, organisms living in naturally seasonal CO_2 enriched habitats may be pre-adapted to hypercapnic conditions resulting in a higher resilience towards moderately elevated $p\text{CO}_2$ (Thomsen et al., 2010; Thomsen and Melzner, 2010). On the other hand, further increases in atmospheric $p\text{CO}_2$ will lead to a higher rate of increase in $p\text{CO}_2$ in already CO_2 enriched habitats: peak $p\text{CO}_2$ values of >300-400 Pa by the end of the century seem likely in some CO_2 enriched habitats (Thomsen et al., 2010). Such high seawater $p\text{CO}_2$ may exceed the organisms' acclimation and/or adaptation potential.

1.2 Biological Impacts

Apart from direct effects, i.e. external dissolution of shells and tests, elevated seawater $p\text{CO}_2$ challenges all marine organisms by affecting physiological processes ranging from the organismic to the cellular level. Calcifying organisms are regarded particularly sensitive to increases in seawater $p\text{CO}_2$ and decreases in the CaCO_3 saturation state (Fabry, 2008). In fact, decreased calcification and/or growth rates in response to hypercapnia were found in many organisms (Ries et al., 2009) such as coccolithophores (Riebesell et al., 2000), corals (Langdon and Atkinson, 2005; Silverman et al., 2009), bivalve molluscs (Thomsen et al., 2010), pteropod mollusks (Lischka et al., 2011) and echinoderms (Dupont et al., 2010c). Special attention was dedicated to planktonic (i.e. coccolithophores, foraminifera, pteropods), but also to benthic calcifying organisms (echinoderms, molluscs) and fish due to their importance in contribution to the global carbon cycle (Bathmann et al., 1991; Westbroeck et al., 1993; Schiebel, 2002; Feely et al., 2004; Hunt et al., 2008; Wilson et al., 2008; Lebrato et al., 2010). Calcium carbonate precipitated by organisms at the oceans' surface sinks to deeper water layers where it can either dissolve or be buried in sediments and is thus removed from the inorganic carbon cycle. This phenomenon is known as the "biological carbon pump". It has been hypothesized, that impaired calcification processes in marine organisms (i.g. coccolithophores, foraminifera, pteropods, echinoderms) due to seawater acidification may impact the inorganic carbon cycle of the ocean (Riebesell et al., 2000; Feely et al., 2004; Riebesell et al., 2007; Lebrato et al., 2010; Beaufort et al., 2011; Lischka et al., 2011).

Teleost fish (Checkley et al., 2009; Munday et al., 2009), decapod crustaceans (Ries et al., 2009) and cephalopod molluscs (Gutowska et al., 2008; Gutowska et al., 2010b; Hu et al., 2011) appear to be more tolerant towards elevated seawater $p\text{CO}_2$. Some species from these taxa are characterized by even higher calcification and growth rates under hypercapnic conditions. However, a high species and ontogeny dependent degree of sensitivity has been described for many taxonomic groups (Langer et al., 2006; Kurihara, 2008; Dupont et al., 2010c; Hu et al., 2011) making predictions on the ecosystem level very difficult. In particular, early developmental stages are expected to be characterized by a higher sensitivity towards environmental stressors when compared to juveniles or adults, because larval or embryonic stages are most often lacking specialized regulatory tissues (e.g. gills for ion and pH homeostasis in fish or cephalopods, Hu et al., 2011) or adult defense systems such as immune response systems (e.g. coelomocytes in sea urchin adults). Furthermore, most often embryonic stages have to undergo severe transitions to reach the following developmental stage and are especially sensitive during these transitions (Kobayashi, 1980; Walther et al., 2010). For example, during sea urchin larval development, gastrulation and metamorphosis, which are characterized by extremely complex and tightly regulated morphological changes, were found to be extremely sensitive to toxins (Kobayashi, 1980) and can thus be expected to be especially sensitive to changes in environmental $p\text{CO}_2$ or other abiotic factors.

1.3 Physiology of hypercapnia tolerance

It has been suggested that higher tolerance towards sea water hypercapnia is directly related to an organism's ability to regulate acid-base disturbances. Active ectothermic organisms with high metabolic rates and rate fluctuations such as fish, crustaceans and cephalopods experience strong $p\text{CO}_2$ variations in their body fluids and are therefore believed to be pre-adapted, at least to a certain degree, towards environmental hypercapnia (Melzner et al., 2009). The major mechanism to counter hypercapnia induced extracellular acidosis is the active accumulation of HCO_3^- in order to buffer the excess of protons in body fluids (Heisler, 1989; Gutowska et al., 2010a). Active accumulation of bicarbonate is achieved by secondary active transporters depending on the

electrochemical gradient created by the Na^+/K^+ -ATPase (NKA), which are localized in specialized ion-regulatory epithelia in gills or digestive organs. The establishment of an electrochemical gradient over the cell membrane is highly energy consuming. For instance, in sea urchin larvae, NKA alone is utilizing up to 77% of the energy provided by aerobic metabolism (Leong and Manahan, 1999). Thus, increases in extra- and intracellular acid loads are accompanied with an increased need for transport processes and may thus either lead to increases in metabolic rates (Wood et al., 2008; Thomsen and Melzner, 2010; Lischka et al., 2011) to fuel NKA or to a reorganization of energy budgets to channel energy towards more essential processes to assure survival (e.g. ion regulation, Deigweiher et al., 2010). On the other hand, metabolic depression has been observed in a range of invertebrates, including molluscs (Michaelidis et al., 2005), and a sipunculid worm (Langenbuch and Pörtner, 2002), in response to environmental hypercapnia.

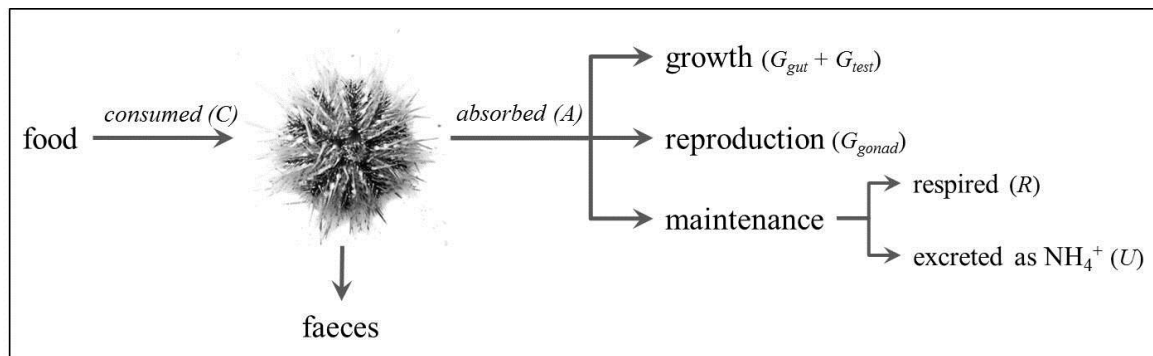


Figure 1.4: Basic composition of a sea urchin's energy budget.

Many of these species specific responses to environmental stress can be explained by linking the organisms' sensitivity to their energy budgets and energy allocation decisions. The analysis of resource allocation within an individual (figure 1.4) in response to changing environmental conditions is considered a useful tool to estimate the severity of a stressful condition for an organism and has been applied in a range of research fields (i.g. toxicology, physiology). The scope for growth (SfG) model is integrating physiological, cellular and biochemical changes to one response variable on the whole organism level, thus providing a robust tool for measuring whole animal performance under stress (Navarro et al., 2006). SfG is estimated from feeding rate, feeding efficiency, respiration rate and excretion rate as stated in the following equation (Widdows and Johnson, 1988):

$$\text{SfG} = A - (R + U) \quad (1.4)$$

where A is the amount of absorbed energy (calculated from absorption efficiency and consumed energy, figure 1.4), R is the respired energy and U is the energy contained in excretion products of nitrogen metabolism (e.g. NH_4^+). A stress induced decrease in feeding rate or increase in respiration or excretion rates consequently results in a decline in SfG and hence reduces the energy available for growth, reproduction or development. SfG measurements are commonly used in measuring animals' responses towards a range of stressors, such as food quality, temperature, salinity or pollution (Shirley and Stickle, 1982; Widdows and Johnson, 1988; Maltby et al., 1990; Otero-Villanueva et al., 2004; Verslycke et al., 2004; Mubiana and Blust, 2007) and have been shown to correlate with growth rate (Navarro et al., 2006). Thus, SfG provides a measure of fitness for the studied organism at a given environmental condition.

1.4 Echinoids

1.4.1 Evolution

Echinoderms represent one of the three major phyla of Deuterostomia (figure 1.5) and evolved around 525 million years ago during of the “Cambrian explosion” (reviewed by Bottjer, 2006) – the start of the rapid diversification of metazoans.

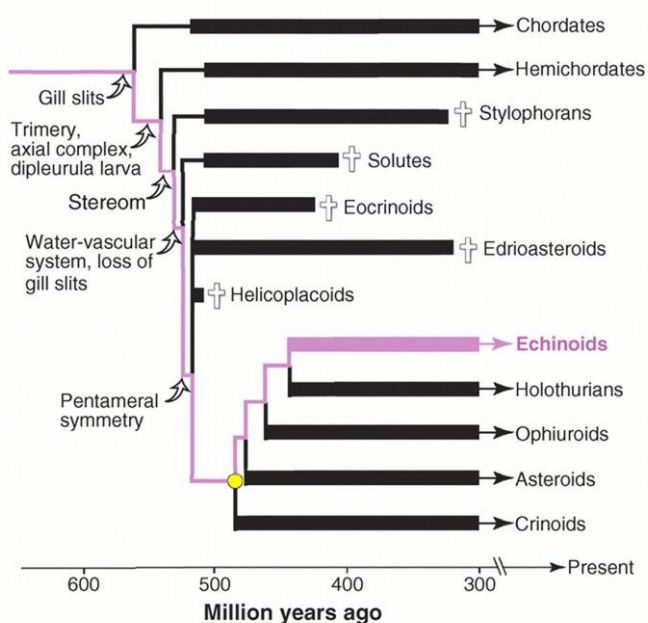


Figure 1.5: Phylogenetic tree of deuterostomia with the major echinoderm groups. Living echinoderms are characterized by the stereom, the water vascular system and the pentamer symmetry. Extinct deuterostomia groups are indicated with crosses. The purple lineage is highlighting the lineage leading to echinoids, to which both species used for this study belong (from Bottjer, 2006).

Echinoderms are characterized by (i) a stereom, the unique endoskeletal structures composed of calcium carbonate and organic matrices (ii) a water vascular system, a closed circulatory system providing the hydraulic force to extend the tube feet, and (iii) the pentameral symmetry characteristic for the adult stages of echinoderms (Bottjer, 2006). Modern echinoderms are divided into five suborders, the sea lilies (crinoids), sea stars (asteroidea), brittlestars (ophiuroida), sea cucumbers (holothurida), and sea urchins (echinoidea). Echinoderms are exclusively found in marine and brackish environments.

1.4.2 Biological relevance

The two sea urchin species studied in this thesis are *Strongylocentrotus droebachiensis* (green sea urchin) and *Strongylocentrotus purpuratus* (purple sea urchin). Both species are regular sea urchins and belong to the family Strongylocentrotidae (Class: Echinoidea, Order: Echinoidea).

The green sea urchin has a wide distribution mainly on the northern hemisphere and inhabits polar to temperate coastal ecosystems (reviewed by Scheibling and Hatcher, 2007). It commonly inhabits the shallow subtidal zone from 0 to 50 m and also occurs in the North-Western part of the Baltic Sea (Skagerrak and Kattegat). The purple sea urchin is a popular model species for evolutionary developmental biology and is commonly found in near shore rocky reef habitats along the North American west coast (reviewed by Rogers-Bennett, 2007). Both species are long-lived and slow-growing (Ebert, 1967; Scheibling and Hatcher, 2007) and are abundant and key components of intertidal and sub-tidal ecosystems. They are important grazers of macroalgae, particularly kelp, and compete with other grazers (for *S. purpuratus*: abalone, *Haliotis* spp., red sea urchin *Strongylocentrotus franciscanus*). Both species are also a food source for many predators, including sea otters, fish and crustaceans (Steneck et al., 2002; Rogers-Bennett, 2007; Scheibling and Hatcher, 2007). Sea urchins are key species significantly shaping kelp forest habitats that alternate between diversity rich kelp forests and sea urchin “barrens” depending on sea urchin recruitment intensity, competition and predatory pressure (Pearse, 2006; Rogers-Bennett, 2007; Scheibling and Hatcher, 2007).

1.4.3 Reproduction and development

In sea urchins, gonads function as both reproductive and nutritive organs (Hughes et al., 2006). Gonad growth increases through summer reaching maximum rates in autumn, when initiation of vitellogenesis in females or spermatogenesis in males occurs (Rogers-Bennett, 2007; Scheibling and Hatcher, 2007). Gonad growth and maturation continues until spring (*S. droebachiensis*) or early summer (*S. purpuratus*) until spawning begins. In mature sea urchins, spawning can be triggered by a range of factors such as temperature, phytoplankton blooms or stressful conditions. During their life cycle, sea urchins experience benthic as well as planktonic conditions (figure 1.6 A). The benthic parents release sperm and eggs into the surrounding water and the planktonic phase begins. At fertilization, sperm penetrates the egg membrane which results in an elevation of the fertilization envelope. The zygote follows through several cleavages developing into a ciliated blastula (Wilt, 1999; Smith et al., 2008) that hatches from the fertilization membrane. At the swimming blastula stage, small micromere descendants start to ingress into the blastocoel (mesenchyme blastula) and form the primary mesenchyme. Subsequently, the vegetal plate invaginates into the blastocoel initiating gastrulation and leading to the formation of the archenteron (figure 1.6 B). Simultaneously, primary mesenchyme cells (PMCs) start the formation of a syncytium and eventually begin the formation of high Mg^{2+} calcite spicules (Okazaki and Inoué, 1976), the larval skeleton (Wilt, 1999). The process of calcification is relatively well studied in sea urchin larvae (Wilt et al., 2003; Killian and Wilt, 2008). Briefly, transient amorphous calcium carbonate (ACC, Beniash et al., 1997; Beniash et al., 1999; Raz et al., 2003; Politi et al., 2004; Politi et al., 2008) is precipitated in vesicles within the PMCs which are then transported through the PMC syncytium to the site of calcification. The ACC and stabilizing matrix proteins are exocytosed into the PMC sheath and incorporated into the larval spicule (Wilt et al., 2008). The space between the cytoplasmic sheath and the spicules is probably connected to the extracellular fluid of the matrix within the primary body cavity (Decker et al., 1987; Wilt, 1999). At the next step, the archenteron breaks through the body wall and opens into the larval mouth. At this stage, development has reached the prism stage. Larval appendages elongate to larval arms and the larva develops into the 4-arm pluteus stage. Soon after, the functional digestive tract has developed and larvae are ready to feed. Echinopluteus larvae feed by creating currents with ciliary bands

running along their body and appendages (larval arms) and capture food particles in their mouth (Strathmann, 1971), which are then transported into the stomach by swallowing. Food is digested in stomach and intestine and indigestible waste is egested through the after (figure 1.6 C). Sea urchin larvae exhibit a high plasticity by increasing growth of feeding appendages to secure sufficient nutrition in low food environments (Miner, 2005; Podolsky and McAlister, 2005). During development, pluteus larvae grow additional arm pairs to support nutrition of the developing juvenile, the so called rudiment.

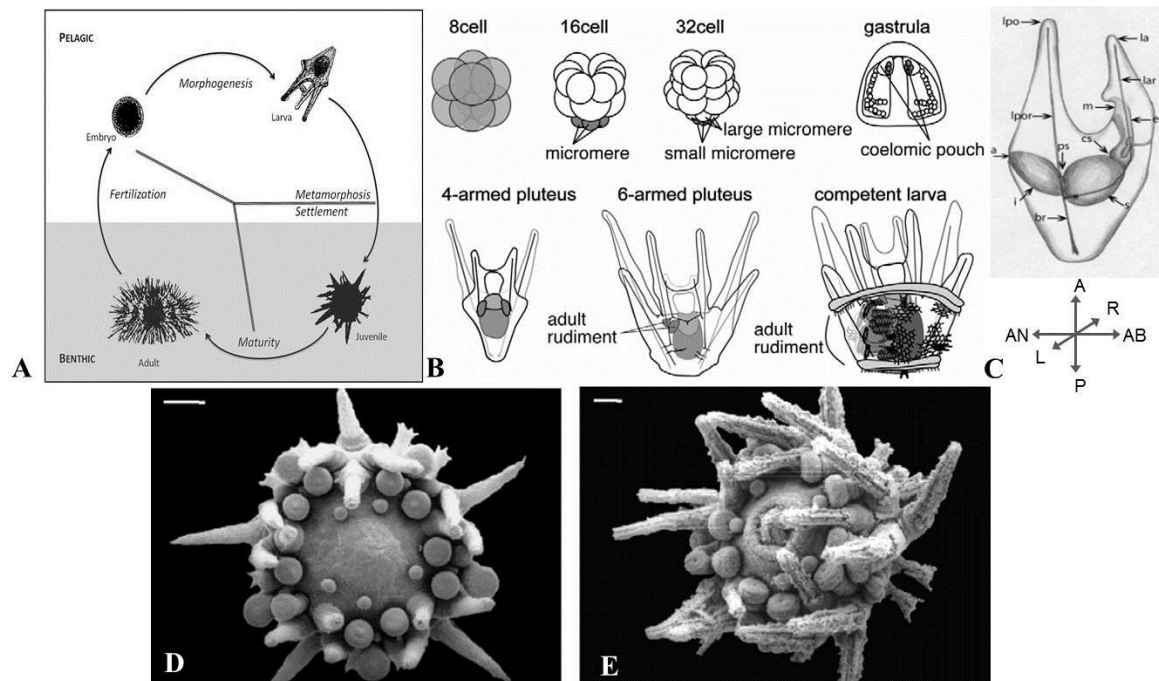


Figure 1.6: Overview about sea urchin development. **A** Schematic drawing of a sea urchin's life cycle (*S. droebachiensis*, publication 4). **B** Summary of embryonic and larval development (for pluteus larvae: view on the abanal side, *S. purpuratus*, modified after Yajima and Wessel, 2011). **C** Left side view of 4-arm pluteus stage larva, *S. purpuratus*. The axial coordinate diagram applies to the orientation of the larvae above it. **Axes:** A anterior, AB abanal, AN anal, L left, P posterior, R right; **Tissues/Structures:** a anus, br body rod, cs cardiac sphincter, e esophagus, i intestine, la left anterolateral arm, lar left anterolateral rod, lpo left postoral arm, lpor left postoral rod, m mouth, ps pyloric sphincter, s stomach (from Smith et al., 2008). The empty appearing space between the larval epidermis and the digestive system was defined as primary body cavity in this study. **D** and **E** scanning electron microscope (SEM) photographs of the oral side of *Paracentrotus lividus* post-metamorphic juveniles: juvenile one day after metamorphosis with no mouth (**D**) and 7 days after metamorphosis with a developed mouth (**E**). Scale bar is 100 μm (from Vaitilingon et al., 2001)

The rudiment is initiated at 25 to 35 days post-fertilization (dpf, 15°C) in *S. purpuratus* (Smith et al., 2008) and around 10 dpf (10°C) in *S. droebachiensis* and develops at the left side of the larva close to the digestive system in coelomic pouches (Hibino et al., 2006). The rudiment subsequently develops into the early juvenile of the sea urchin

having a calcified test and spines, a water vascular system including tube feet and pentamerous symmetry characteristic for the adult stage (Smith et al., 2008). When the rudiment is ready to metamorphose, the larva sinks to the bottom and settles, which occurs in response to a specific environmental cue (Cameron and Hinegardner, 1974; Burke, 1980). After settlement, juveniles need a few days to two weeks to fully develop the mouth, after and digestive tract (figure 1.6 D and E, Vaitilingon et al., 2001). Thus, the benthic juvenile undergoes a further series of metamorphoses until the fully developed adult stage is reached. The whole planktonic larval phase takes about 50 days in *S. purpuratus* (15°C, Smith et al., 2008) and about 30 days in *S. droebachiensis* (10 to 12°C). Under good feeding conditions, both species need around three years to reach maturity after settlement (Lawrence, 2007).

1.5 Research hypotheses

Since echinoids have a calcified skeleton in larval as well as in adult stages, sea urchins were rapidly identified as one of the primary targets in ocean acidification research. Recent studies demonstrated that a range of different echinoid species respond rather uniformly with reduced growth or developmental rates to elevated $p\text{CO}_2$ (Dupont et al., 2010c; Byrne et al., 2011). The mechanisms underlying the observed declines in development and growth rates are still unclear. As mentioned earlier, three general hypotheses have been raised on the question what could cause growth reductions not only observed in echinoids:

- (i) Environmental hypercapnia causes uncompensated extracellular pH, which, in turn, elicits metabolic depression and reductions in growth rates (Langenbuch and Pörtner, 2002; Langenbuch and Pörtner, 2004; Michaelidis et al., 2005)
- (ii) The calcification mechanism itself is impacted by elevated $p\text{CO}_2$ and reduced calcification performance leads to the observed reductions in growth rates (Michaelidis et al., 2005; Fabry, 2008; Ries et al., 2009; Todgham and Hofmann, 2009)

- (iii) Due to a higher acid load in the surrounding seawater, costs for cellular and extracellular ion and pH homeostasis as well as calcification are increased and less energy is available for sustaining high growth rates (Melzner et al., 2009; Comeau et al., 2010b; Deigweiher et al., 2010; Thomsen and Melzner, 2010; Lischka et al., 2011).

During the course of this study, my aim was to examine the energetic mechanisms underlying growth and developmental responses of model echinoid species to hypercapnic stress. I formulated the following specific research hypotheses:

a) Growth reductions in sea urchin larval and adult stages are related to a decrease in scope for growth which is either caused by elevated metabolic rates or decreased feeding rates.

A great body of literature suggests that sea urchin larval development and adult growth is negatively impacted by elevated seawater $p\text{CO}_2$ (reviewed by Dupont et al., 2010c). Growth or developmental retardation is intrinsically linked to an animals' energy budget. When the amount of energy that is available for growth (scope for growth) is reduced due to a reduction in energy input (e.g. a cessation of feeding) or due to elevated energetic costs for maintenance of vital physiological processes (e.g. ion regulation), then an organism's growth rate is reduced. Both, increases in metabolic rates or decreased feeding rates, can be found in animals exposed to a range of pollutants or changing abiotic conditions such as light intensity or temperature (Greenwood, 1980; Wieser and Medgyesy, 1991; Verslycke et al., 2004; Hill and Lawrence, 2006; Siikavuopio et al., 2007a; Siikavuopio et al., 2007b). Feeding rate decreased in *S. droebachiensis* adults (Siikavuopio et al., 2007b) and metabolic as well as N excretion rates increased in Baltic Sea *Mytilus edulis* in response to elevated seawater $p\text{CO}_2$ (Thomsen and Melzner, 2010). So far no energy budget has been constructed for sea urchin larval or adult stages in response to elevated environmental $p\text{CO}_2$.

b) Larval stages are not able to actively control extracellular acid-base disturbances in order to support calcification by PMCs. Calcification and ion regulatory processes are up regulated in order to sustain growth and development.

Studies determining the larval capacity to regulate the pH of extracellular compartments, such as the gel-like structure (extracellular matrix, ECM) filling the primary body cavity or the digestive system, are still lacking. However, such studies are of high importance to understand the impact of CO₂ induced seawater acidification on calcification and digestion in sea urchin larvae. Given that sea urchin larval spicules are grown inside sheaths formed by the PMC syncytium, which probably are connected to the extracellular fluid of the matrix within the primary body cavity (Decker et al., 1987; Wilt, 1999), then an uncompensated extracellular pH could interfere with the calcification process or increase the costs for calcification. It is possible that moderate acid-base disturbances within the primary body cavity is compensated by potential non-bicarbonate buffer substances, the constituents of the gel-like structure such as collagens, fibronectin and glycosaminoglycans (Burke and Tamboline, 1990; Crawford, 1990) in order to facilitate spicule formation by the PMCs. However, it is still unclear, whether hypercapnia effects on growth are due to reductions in calcification performance or whether calcification is affected in a secondary fashion due to changes in somatic growth rate. If calcification performance under acidified conditions is comparable to the performance under ambient conditions, this could then be related to an up regulation of the calcification machinery, as observed in a recent study (Martin et al., 2011), and/or due to compensatory processes in order to maintain a certain pH in extracellular fluids. In order to determine which processes are favored on expense of larval growth, acid-base status of the larval primary body cavity/stomach and the transcript abundance of genes relevant for metabolism, ion regulation and calcification were examined.

c) Sea urchins are regarded as weak acid-base regulators and are using test dissolution in order to buffer excess protons within the perivisceral coelomic fluid during exposure to high seawater pCO₂.

In contrast to more active organism groups such as fish, crustaceans and cephalopods which have specialized epithelia for ion regulation and gas exchange (Heisler, 1989; Hu

et al., 2011), sea urchins are regarded rather weak acid-base regulators (Spicer et al., 1988; Burnett et al., 2002; Miles et al., 2007; Spicer et al., 2011). Recent studies on *Psammechinus miliaris*, *S. purpuratus* and *S. droebachiensis* adults demonstrated that these sea urchins are not able to compensate for hypercapnia (*P. miliaris*) or emersion (*S. purpuratus*) induced acid-base disturbances in the perivisceral coelomic fluid (Burnett et al., 2002; Miles et al., 2007; Spicer et al., 2011). However, when exposing *P. miliaris* and *Echinus esculentus* to air a substantial accumulation of HCO_3^- could be observed (Spicer et al., 1988) and an accompanied increase in Mg^{2+} and Ca^{2+} concentrations in PCF (Spicer et al., 1988; Spicer, 1995; Miles et al., 2007) indicates that elevated $[\text{HCO}_3^-]_e$ in these sea urchin species might be due to shell dissolution as the PCF is most likely undersaturated with respect to calcium carbonate.

d) The green sea urchin has a potential to adapt to environmental hypercapnia, because it occurs in areas with seasonally hypercapnic conditions. Nevertheless, a further increase in seawater $p\text{CO}_2$ may severely threaten echinoids.

Coastal benthic habitats like the Kattegat and the Baltic Sea are experiencing seasonally elevated seawater $p\text{CO}_2$ already today. Peak seawater $p\text{CO}_2$ of ca. 230 Pa (Thomsen et al., 2010) were recently reported due to upwelling of deeper water masses with decreased $p\text{O}_2$ and increased $p\text{CO}_2$. High $p\text{CO}_2$ originates from eutrophication and net heterotrophy in deeper water layers in the summer months (Conley et al., 2007; Zillén et al., 2008; HELCOM, 2009; Beldowski et al., 2010; Thomsen et al., 2010). It can be expected that species living in such habitats must be adapted to seasonal hypoxic hypercapnic events. On the other hand, additional anthropogenic CO_2 will lead to much stronger increases in $p\text{CO}_2$ than expected for the average surface ocean: it has been estimated that in seasonally hypoxic habitats, $p\text{CO}_2$ values of >300-400 Pa (>3000-4000 μatm) could be encountered in the summer months in benthic habitats in the Western Baltic Sea within this century (Thomsen et al., 2010). Based on the fact that the green sea urchin already encounters seasonal hypercapnia and hypoxia, this species may have the potential to overcome short periods of elevated $p\text{CO}_2$, but might be impaired by a continuous increase in seawater $p\text{CO}_2$.

2 Material and Methods

In the course of my doctoral studies, several experiments with sea urchin larvae and adults were conducted. For overview purposes, relevant parameters of larval (L1 to L4) and adult (A1 to A4) experiments are summarized in table 2.1.

Table 2.1: Overview of animals, experiments and experimental parameters used for the present dissertation

ID	experimental time	experimental location	duration of experiments	Species	adult origin	CO ₂ perturbation levels (Pa)	T (°C) / salinity	parameters measured	publication
<u>larval experiments</u>									
L1	July 08	Sweden, SLC Kristineberg	7 days	SP	California	40 (control) & 134	16 / 31	gene expression patterns	discussion, 2
L2	July 09	Sweden, SLC Kristineberg	21 days	SP	California	38 (control) & 128	14 / 31	development, feeding, metabolic rates, energy budget	discussion, 1
L3	March-May 10	Sweden, SLC Kristineberg	28 days	SD	Kattegat/ Skagerrak	36 (control) & 95	12 / 31	extracellular pH (microfluorometry), carry over effects larvae to juvenile	discussion, 4
L4	April 11	Germany, Kiel, IFM-GEOMAR	10 days	SD	Dröbak	46 (control), 103, 249	10 / 31	extracellular pH (microelectrodes), intracellular pH (microfluorometry)	discussion
<u>adult experiments</u>									
A1	August 09	Germany, Kiel, IFM-GEOMAR	10 days	SD	Kattegat	69 (control), 145, 385	10 / 31	extracellular acid-base status	discussion, 3
A2	September-October 10	Germany, Sylt, AWI Wadden Sea Station	45 days	SD	Kattegat	47 (control), 102, 284	10 / 30	growth, feeding, metabolic rates, N excretion, extracellular acid-base status, energy budget	discussion, 3
A3	January 09 - April 09	Sweden, SLC Kristineberg	4 months	SD	Kattegat/ Skagerrak	41 (control) & 123 (A) 44 (control) & 119 (L)	12 / 32	fertility, carry over effects adults to larval settlement	discussion, 4
A4	January 09 - April 10	Sweden, SLC Kristineberg	16 months	SD	Kattegat/ Skagerrak	41 (control) & 123	12 / 32	fertility	discussion, 4

Abbreviations: Sven Lovén Centre for Marine Sciences (SLC), *Strongylocentrotus droebachiensis* (SD), *Strongylocentrotus purpuratus* (SP), Adults (A), Larvae (L)

2.1 Origin and maintenance of adult sea urchins

Adult purple sea urchins (*Strongylocentrotus purpuratus*) were collected off the Californian coast (Kerckhoff Marine Laboratory, California Institute of Technology, USA) and transferred to the Sven Lovén Centre for Marine Science (SLC, Kristineberg, Sweden). They were maintained in natural flowing seawater at 14°C and pH 8.1 on a diet

of *Ulva lactuca*. Adult green sea urchins (*Strongylocentrotus droebachiensis*) were collected in the Kattegat/Skagerrak either by divers (Dröbak, Norway, experiment 4) or by dredging (Anholt, Denmark, A1, A2, table 2.1) and transferred to IFM-GEOMAR (Kiel, Germany, L4, table 2.1) or were collected off the coast of Hammerfest (Norway) or Anholt (Denmark) and transferred to SLC (Kristineberg, Sweden, L3, A3, A4, table 2.1). Green sea urchins for experiments that were conducted in Kiel or on Sylt were fed *ad libitum* with *Fucus vesiculosus* supplemented with mussel flesh (*Mytilus edulis*) and kept for several weeks in a recirculating system at 6 to 8°C, pH 8.0. Three times a week, one third of the water volume (total 800 L) was exchanged with fresh seawater that was prepared from Baltic seawater adjusted to the salinity of 32 by addition of sea salt SequaSal (Münster, Germany). Green sea urchins for experiments that were conducted in Sweden (L3, A3, A4) were fed *ad libitum* with *Ulva lactuca* and were kept in a flow through system with continuous supply of natural seawater at 12°C and a salinity of 31.

2.2 Experimental design

2.2.1 Larval experiments (L1-L4)

Spawning was induced by intra-coelomic injection of 0.5M KCl in 0.2 µm filtered seawater (FSW). After fertilization, cleaving embryos (two cells stage) were placed in 2L (L4), 5L (L2, L3) or 50L (L1, L2) aquaria filled with FSW at a density of 5 to 10 embryos per mL and at a temperature between 9 and 16°C depending on species (for details see publications 1 and 2). The FSW was continuously aerated to maintain oxygen concentrations close to air saturation and mixed by the slow convective current of a stream of single bubbles (approx. 100 bubbles per min). After 3 to 5 days (see publications for details), larvae were fed daily with the cryptophyte algae *Rhodomonas* sp. which were raised in B1 medium (Guillard and Ryther, 1962) at 20°C under a 12:12 h light:dark cycle. Algal strains were provided by the Marine Algal Culture Centre at Gothenburg University (GUMACC). Larvae were fed at a constant concentration of 150 to 200 µg C L⁻¹ (~3000 to 6000 cells ml⁻¹ for diameters ranging between 6 to 8 µm, depending on experiment, see publications for details). The carbon content of the algae was estimated based on biovolume measurements as equivalent spherical diameter (ESD)

with an electronic particle analyzer (Elzone 5380, Micrometrics, Aachen, Germany) and equations provided by Mullin et al. (1966). At the chosen algae concentration, seawater $p\text{CO}_2$ treatment levels and temperatures had no impact on algal growth and survival (Dupont pers. comm.). Cultures were maintained at a salinity of 31 to 32. For experiments in Germany, three different $p\text{CO}_2$ levels (a control $p\text{CO}_2$ level of 46 Pa and two high $p\text{CO}_2$ levels of 103 and 249 Pa, see L4, table 2.1) were used by equilibrating experimental aquaria with an air/ CO_2 gas mixture generated by a central automatic gas mixing-facility (Linde Gas, HTK Hamburg, Germany). In Sweden (L1, L2, L3), pH was maintained in each aquarium using a computerized feedback system (AquaMedic) that regulates pH (NBS scale) by addition of pure gaseous CO_2 directly into the seawater (± 0.02 pH units). In each experiment two $p\text{CO}_2$ levels were applied: one control $p\text{CO}_2$ level between 36 and 40 Pa and one high $p\text{CO}_2$ level between 95 and 134 Pa. For details on experimental parameters measured in each experiment see table 2.1 and the publications.

2.2.2 Adult experiments (A1-A4)

Experiments were conducted either at the facilities of the IFM-GEOMAR in Kiel in summer 2008 (A1, table 2.1), on the island Sylt at the Wadden Sea Station Sylt of the Alfred Wegener Institute for Polar and Marine Research (AWI) in October 2010 (A2, table 2.1) or at the Sven Lovén Centre for Marine Sciences (SLC) Kristineberg in Sweden in 2009 to 2010 (A3, A4).

At the IFM-GEOMAR in Kiel, a salinity of 31.5 was created by mixing distilled water with synthetic sea salt (SeequaSal). Natural flowing seawater with average salinities of 29.5 and 32 was used at the AWI on Sylt and at the SLC in Sweden, respectively. A storage tank was used in experiments at the AWI on Sylt and at the IFM-GEOMAR for thermal equilibration and aeration with pressurized air. Water was distributed to the experimental units via a pump (A1) or via gravity feed (A2). To avoid bacterial infections, seawater was passed over a 15 Watt UV sterilizer (HW-Aquaristik, Germany, A1-A4). In order to avoid alterations of the seawater carbonate system by biological activity of experimental animals and microorganisms, flow rates of seawater were adjusted to a minimum twofold water exchange per tank per day (A1-A4). A light regime with a 12 h/12 h light/dark cycle was chosen. For experiments in Germany, three different $p\text{CO}_2$ levels (47 to 69 Pa (control), and two high $p\text{CO}_2$ levels of 102 to 145 and

284 to 385 Pa, see A1 and A2, table 2.1) were used by equilibrating experimental aquaria with an air/CO₂ gas mixture generated by a central automatic gas mixing-facility (Linde Gas, HTK Hamburg, Germany). The gas mixture (0.8 L min⁻¹) was introduced into the experimental aquaria using diffusor stones (Dohse, Grafschaft-Gelsdorf, Germany). At the SLC in Sweden (A3 and A4), pH was maintained in each aquarium using the same computerized feedback system (AquaMedic) that was used for larval experiments (see details above). Sea urchins were incubated under control conditions for at least one week. Exposure times were 10 days (A1), 48 days (A2), 4 months (A3) and 16 months (A4). For details on parameters measured in each experiment see table 2.1 and publications.

2.3 Determination of seawater carbonate chemistry speciation

2.3.1 Experiments at the IFM-GEOMAR and AWI Sylt, Germany (L4, A1-A2):

Seawater carbonate system speciation was calculated from total alkalinity (A_T) and total dissolved inorganic carbon (C_T) measurements (IFM-GEOMAR, A1) and from C_T and pH_T measurements (AWI Sylt, A2) using CO2SYS software (Lewis and Wallace, 1998), with dissociation constants from Mehrbach et al. (1973) as refitted by Dickson and Millero (1987). A 500 ml water sample was taken for C_T/A_T or C_T/pH_T determinations and immediately poisoned with 100 μ l of saturated HgCl₂ solution. C_T was measured according to Dickson et al. (2007) using either a SOMMA (Marianda, Kiel, Germany) coulometric auto analyzer or an AIRICA (Marianda, Kiel, Germany) analyzer, which is based on infrared-detection of CO₂ purged from an acidified sample. A_T was determined according to Dickson et al. (2007) by means of potentiometric open-cell titration with hydrochloric acid that was performed via a VINDTA (Marianda, Kiel, Germany) auto analyzer. Reference material was used according to Dickson et al. (2007). pH_T measurements were conducted with a Metrohm pH meter (826 pH mobile, Metrohm, Filderstadt, Germany) and a glass electrode calibrated with sea water buffers based on TRIS/HCl and 2-aminopyridine/HCl (for details see Dickson et al., 2007). Seawater salinity and temperature were measured daily (precision \pm 0.1 g/kg respectively °C) with a salinometer (WTW cond 315i, WTW TETRACON 325-measuring chain). Additionally, seawater pH_{NBS} was controlled daily with a pH meter (WTW 340i pH-analyzer, WTW 20

SenTix 81-measuring chain, precision 0.01 units) that was calibrated with Radiometer IUPAC precision pH buffers 7.00 and 10.00 (S11M44, S11 M007).

2.3.2 Experiments at the SLC, Sweden (L1-L3, A3-A4):

The carbonate system speciation ($p\text{CO}_2$, Ω_{Ca} and Ω_{Ar}) was calculated from pH_T and alkalinity using CO2SYS (Lewis and Wallace, 1998, Table 1) with dissociation constants from Mehrbach et al. (1973) refitted by Dickson and Millero (1987). Alkalinity was measured photometrically following Sarazin et al (1999). pH_T measurements were conducted with a Metrohm pH meter (826 pH mobile, Metrohm, Filderstadt, Germany) and a glass electrode calibrated with sea water buffers based on TRIS/HCl and 2-aminopyridine/HCl (for details see Dickson et al., 2007).

2.4 Whole animal performance: development, growth and reproduction

2.4.1 Larval development (L1-L2)

Larval cultures were monitored daily or every other day for the experimental period. Each day, 3 subsamples of more than 50 larvae were removed from each culture and fixed in buffered 4% paraformaldehyde (PFA) in 0.2 μm filtered seawater (FSW) for later analysis. Density at time t (N_t in larvae L^{-1}) was estimated by dividing the number of larvae by the corresponding volume collected. For each replicate, 10 fixed larvae were photographed every (1 to 7 days post-fertilization) or every other day (after 7 days post-fertilization) with a digital camera mounted on a dissecting microscope using polarized light to visualize the skeleton. Five morphometric parameters (L1: body length publication 2; L2: body length, body rod lengths, postoral rod lengths and posterolateral rod length, publication 1 figure 1) were measured for each larva using LAS software (Leica).

2.4.2 Larval settlement success in response to adult acclimation to elevated $p\text{CO}_2$ (A3)

The impact of adult acclimation on larval settlement success was measured after a 4 month acclimation period. Eggs from the different females were pooled and concentrated into 1L FSW at the relevant $p\text{CO}_2$ (control or elevated). Sperm stock solution (mix of 4 males) in FSW was added to each dish to a final concentration of ~ 1000 sperm ml^{-1} . After 15 min, fertilized eggs (mixed females and males, $>95\%$ fertilization success) were rinsed in FSW at the appropriate pH and at the two-cell stage were transferred to 5L aquaria at a density of 10 embryos per ml. The different culture treatments (control $p\text{CO}_2=44$ Pa, or elevated $p\text{CO}_2=119$ Pa) were set up as a 2 x 2 experimental design: 2 acclimation pH treatments (pH of the basin in which the adults were kept 4 months prior to spawning) x 2 larval culture pH treatments (publication 5 figure 2). The experiment was replicated 4 times using the same batch of parental animals. Settlement success was measured after 28 days as the number of larvae reaching the juvenile stage.

2.4.3 Juvenile growth and survival in response to larval exposure to elevated $p\text{CO}_2$ (L3)

Gametes from freshly collected sea urchins from both Denmark and Norway populations were collected, fertilized and cultured using a full-cross design experiment (2 populations x 2 females x 4 males x 2 nominal $p\text{CO}_2$ (control and elevated) for a total of 64 cultures) according to the methods described above. Juveniles were then collected, measured (diameter of the test), pooled to ensure the highest genetic variability representative of the species along the geographical distribution and cultured for 3 months in a 5L system identical to that used for the larvae. pH was maintained in each aquarium using a computerized control system as described above. The different culture treatments (control, $p\text{CO}_2=36$ Pa and elevated $p\text{CO}_2=95$ Pa) were set up as a 2 x 2 experimental design: 2 larval culture pH x 2 juvenile culture pH. Cultures were maintained at 12 °C, a salinity of 32‰ and alkalinity of 2.17 ± 0.06 mM. The entire experiment was replicated 2 times using different parental animals. The juveniles were fed *ad libitum* with small pieces of *Ulva* spp. Juvenile survival (%) and growth ($\text{mm}\cdot\text{mo}^{-1}$, calculated as the difference between average size after 3 months and at the beginning of the exposure) were estimated after 3 months. It is important to notice that because of the high mortality in one of the treatments, juvenile growth may be biased due to size-dependent sensitivity (e.g. see Green et al., 2004).

2.4.4 Adult growth (A2)

Sea urchins had a fresh mass between 7 and 12 g. Growth of sea urchins in the LT experiment was analyzed using wet mass (WM), dry mass (DM), ash-free dry mass (AFDM) and ash content (ash dry mass) of several body parts (Lantern of Aristotle, gonads, gut and test including spines). A random sample of 18 urchins was taken as a reference group at the beginning of the experiment (prior to CO₂ incubation) and randomly grouped into 6 replicates. The diameter (to the nearest 0.1 cm) was recorded using a caliper. Test diameter was recorded before and after experimental incubation. In order to determine the masses of body organs, urchins were dissected (Aristotle Lantern, gonads, gut, test and spines) and organs / body parts blotted dry on paper towels. Wet masses were determined using a precision scale (LC220s, Sartorius, Göttingen, Germany, 1 mg resolution). Organs were dried at 80°C for 20 hours (U30 793 590 Memmert, Schwabach, Germany) and masses were determined again. Ash dry mass of body organs was determined by placing organs in a drying oven at 500°C for 20 hours (M110, Heraeus, Hanau, Germany) prior to mass determination. AFDM was then calculated by subtracting ash dry mass from dry mass of the respective organ.

2.4.5 Fertility (A3-A4)

After 4 (Denmark and Norway populations, April 2009) or 16 months (Denmark population, April 2010) of exposure to control (41 Pa) or elevated *p*CO₂ conditions (123 Pa), spawning of 4 to 11 females and 4 males in each treatment was induced by two intra-coelomic injections with 1 ml of 0.5M KCl in FSW. Females were separately placed in 1L beaker filled with FSW during spawning. Sperm were collected dry using a pipette and kept on ice until use. The collected eggs were used to assess fecundity (number of eggs per female, estimated as the average of 5 sub-samples of 50µL and then fertilized with collected sperm to evaluate further settlement success (number of larvae reaching the juvenile stage).

2.5 Energy metabolism

2.5.1 Feeding and fecal pellet production (L1, A2)

a) Larval experiments (L1):

To assess the impact of elevated seawater $p\text{CO}_2$ on feeding performance, feeding rate was estimated every other day beginning at day 6 (commencement of feeding) up to 21 days post-fertilization in *Strongylocentrotus purpuratus* pluteus larvae. 15 larvae each were transferred to 100 ml glass bottles (7 replicates) with food suspension (*Rhodomonas* sp. at $150 \mu\text{g C L}^{-1}$) in FSW equilibrated with the same $p\text{CO}_2$ the respective experimental animals originated from (pH 8.1 or pH 7.7). Two sets of control bottles (3 replicates for each treatment) without larvae containing the same food suspension were also prepared. The bottles were incubated on a rotating plankton wheel (0.2 rpm) at 14°C . Feeding rate was estimated as clearance rate by measuring the algal concentration ($\Delta \text{cells L}^{-1}$) at the end of the incubation (24h) in control and experimental bottles after collection of the larvae on a $50 \mu\text{m}$ sieve. As nutritional values of algae differ with size, algae cell size was simultaneously measured and feeding rate was expressed in changes in ng C L^{-1} . Feeding rate ($F, \text{ml ind}^{-1} \text{d}^{-1}$) was calculated following Frost (1972), and ingestion ($I, \text{cell volume ind}^{-1} \text{d}^{-1}$) was calculated as $I = F \times C$, where C is the average algal concentration per bottle. Rates were corrected for mortality and are given as rates per surviving animal in $\text{ng C ind}^{-1} \text{h}^{-1}$. For energy budget calculation larval clearance rate was converted to energy equivalents ($1.34 \times 10^5 \mu\text{J } \mu\text{gC}^{-1}$) using $19 \mu\text{J ng}^{-1}$ *Rhodomonas* and a cell mass of $0.15 \text{ ng cell}^{-1}$ as an estimate for our strain of *Rhodomonas* sp. (Renaud et al., 2002). The *Rhodomonas* sp. Population was characterized by an average diameter of $6.38 \mu\text{m}$ and a carbon content of $0.021 \text{ ng C cell}^{-1}$.

b) Adult experiments (A2):

Feeding and fecal pellet production was monitored in the experimental setups continuously for 21 days in adult *Strongylocentrotus droebachiensis* starting a week after the sea urchins were first exposed to their experimental conditions. Experimental animals were acclimatized to *Fucus vesiculosus* for four weeks prior to the start of the experiment to ensure adequate feeding condition. To determine ingestion rate, algae were cleaned

from epibionts, dried at 10°C for 12 hours and split into servings of 8.05 ± 0.01 g. Servings were then placed into experimental units that were cleaned from all food remnants. Four separate servings per $p\text{CO}_2$ condition were incubated in urchin free tanks to determine possible effects of $p\text{CO}_2$ on the algae biomass and were used as starting amount of food for later calculation of feeding rate. Urchins were then left to feed on their algal serving for 70 hours before the remnants of food and produced fecal pellets were collected. Directly after collection, new food servings were supplied to the urchins, so that urchins were always fed *ad libitum*. Food remnants, control food servings and fecal pellets were dried at 80°C for 20 hours (dry oven U30 793 590, Memmert, Schwabach, Germany) and weighed (LC220s, Sartorius, Göttingen, Germany). Fecal pellet production is expressed in $\text{mg DM feces day}^{-1} \text{ ind}^{-1}$. Dry mass of control algae servings was used as a reference for the starting point of feeding and food intake was calculated by subtracting the food remnants from the starting quantity. Feeding rate is expressed as $\text{mg DM algae day}^{-1} \text{ ind}^{-1}$.

For organic matter absorption efficiency (AE_{OM}), food remnants and feces were ashed at 500°C for 20 hours (oven M110, Heraeus, Hanau, Germany) to determine the organic component of food and feces. Subsequently, the Conover ratio was calculated (Conover, 1966):

$$E_{\text{OM}} = (F' - E') ((1 - E') F')^{-1} \quad (2.1)$$

with F' being the ash-free dry mass to dry mass ratio of food and E' being the ash-free dry mass to dry mass ratio of feces. To calculate energy budgets for the different $p\text{CO}_2$ conditions, food intake (consumed energy C) was converted into energy equivalents using a conversion factor of $15.5 \text{ kJ g}^{-1} \text{ DM}$ determined for *Fucus serratus* (Marshall et al., 2007).

2.5.2 Routine metabolic rates (L1, A2)

a) Larval experiments (L1):

Respiration experiments were conducted every other day beginning at day 3 using *Strongylocentrotus purpuratus* larvae according to Marsh and Manahan (1999) with modifications. Briefly, respiration vials with volumes between 1624 to 1641 μl were placed in a water bath at 14°C and filled with sterile filtered seawater (0.2 μm FSW, 14°C) adjusted to control pH (pH 8.1) and low pH (pH 7.7). Larvae were washed three times with FSW of the appropriate pH of their rearing conditions to remove as much culture water as possible and were then transferred in a known volume of “transfer water” into the vials with their culture pH. Depending on stage, 48 to 724 larvae were placed into one vial. For replication, 10 vials were used for larvae of the same culture (two cultures per treatment, four cultures in total, forty vials with larvae in total per time point). Different numbers of larvae were placed into the vials for density controls as suggested by Marsh and Manahan (1999). Aerobic respiration rate increased linearly with increasing amounts of larvae in the vials. As no density effect was detected and in order to show the variability within larval cultures, we regarded each vial as a sub-replicate of each culture (true replicate) and used replicate cultures as co-variable in the statistical procedure. Several vials ($n = 4$ to 8 per measurement point) without larvae were prepared for bacterial controls. Bacterial controls were conducted according to Marsh and Manahan (1999). After addition of larvae or larval-free “transfer seawater” (bacterial control) to the vials, $p\text{O}_2$ was measured in all vials before closure with micro-optodes calibrated as suggested in the manufacturers manual (PreSens, 4-OXY Micro, Germany). Closed vials were then incubated horizontally submerged in the waterbath for 7 to 10 hours in the dark. Continuous $p\text{O}_2$ measurements ($n = 2$ to 4) were conducted additionally in order to demonstrate a linearity of $p\text{O}_2$ decline in the respiration vials during the incubation time (data not shown). No changes in oxygen consumption rates during incubations were detected. After incubation, $p\text{O}_2$ was measured again and corrected for bacterial respiration. Following $p\text{O}_2$ measurement in the vials, larvae were pelleted by hand centrifugation, removed from the bottom of the vials and fixed in 4% PFA in seawater for enumeration. Respiration in bacterial controls did not exceed 15 % of larval respiration and $p\text{O}_2$ in the vials did not drop below 80% air saturation. Larvae were counted subsequently to oxygen consumption measurements. Prior to fixation for counting, larvae

were checked for viability. Larval respiration rate was expressed as $\text{pmol O}_2 \text{ ind}^{-1} \text{ h}^{-1}$. For correction of larval growth, larval respiration was additionally normalized onto body length (BL, see publication 1 for details).

To control the effect of $p\text{CO}_2$ in respiration experiments, the pH drop due to respiratory CO_2 excretion of the larvae was measured directly in the vials before and after incubation with a pH meter (WTW 340i pH meter and Sentix 80 electrode calibrated with Radiometer NIST precision buffers) in preliminary experiments. A mean pH drop of 0.1 units (standard deviation of 0.04 units) occurred during incubation, but there was no difference between pH decreases of the two pH treatments.

b) Adult experiments (A2):

For metabolic rate determination, two sea urchins were used for one measurement. Sea urchins were starved for 12 hours and were placed in glass respiration chambers with a volume of 325 ml containing 0.2 μm filtered sea water equilibrated with the appropriate $p\text{CO}_2$ level. Respiration chambers were closed, submerged in a water bath at 10°C and oxygen saturation was measured continuously (once every 30 seconds) for 2-3 hours using non-invasive oxygen sensors connected to a OXY-4 mini multichannel fiber optic oxygen transmitter (PreSens, Regensburg, Germany), that were calibrated according to the manufacturer's instructions. Preliminary experiments demonstrated that the sea urchins could sufficiently mix the water volume without external stirrer and oxygen concentration decreased linearly (data not shown). Therefore, and in order to minimize stress, we decided to conduct the measurements without a stirrer. When oxygen concentration reached the 70% air saturation level, sea urchins were removed. The missing water volume was refilled with 0.2 μm filtered sea water, respiration chambers were closed and measured for 3 to 6 hours for detection of background respiration. Bacterial respiration never exceeded 10% of animal respiration. For calculation of oxygen consumption rates, the linear decrease in oxygen concentration during measuring intervals between 30 min and the end of the measurement period was considered. Oxygen consumption rates (MO_2) are expressed as $\mu\text{mol O}_2 \text{ g}^{-1} \text{ AFDM h}^{-1}$. Subsequently, the animal's size and total weight, as well as that of body parts was determined (WM, DM, AFDM).

2.5.3 NH_4^+ excretion rate and O:N ratio (A2)

Ammonium excretion rate was only determined in adult green sea urchin from NH_4^+ concentration measurements prior to and following incubation of sea urchins for respiration measurements. Before and after closing the respiration chambers, 1 mL sea water sample was removed and 250 μL of reagent containing orthophthaldialdehyde, sodium sulphite and sodium borate was added (Holmes et al., 1999). Samples were then incubated for 2 hours at room temperature in the dark until fluorescence was determined at an excitation and emission wavelength of 360 and 422 nm, respectively (Kontron SFM25 fluorometer). Additionally, a separate glass chamber was incubated without sea urchins to determine background readings of filtered sea water. Ammonium excretion of respiration bacterial controls was also determined. Ammonia (NH_3) was not measured as NH_3 concentrations at pH values of 8 to 7.1 are negligible (0.2-2% total ammonium/ammonia, Körner et al., 2001). Ammonium excretion rates are expressed as $\mu\text{mol NH}_4^+ \text{g}^{-1} \text{AFDM h}^{-1}$. The atomic ratio of oxygen uptake and excreted nitrogen was calculated from respiration (MO_2) and ammonium excretion rates:

$$\text{O} : \text{N} = 2 \text{MO}_2 (\text{NH}_4^+ \text{excretion})^{-1} \quad (2.2)$$

2.5.4 Energy budget calculations (L1, A2)

a) Larval experiments (L1):

For calculation of scope for growth (SfG), metabolic and feeding rates of *Strongylocentrotus purpuratus* larvae were used to estimate daily energy input and respiratory energy loss starting at 6 days post-fertilization (dpf) by conversion of metabolic and feeding rates to energy equivalents. Metabolic rates were converted to energy equivalents ($484 \mu\text{J nmol}^{-1} \text{O}_2$, Gnaiger, 1983) based on oxyenthalpic values of lipid and protein as major constituents of echinoderm larvae (Shilling and Manahan, 1994). Larval clearance rate was converted to energy equivalents ($1.34 \cdot 10^5 \mu\text{J} \mu\text{g C}^{-1}$) using $19 \mu\text{J ng}^{-1}$ *Rhodomonas* and a cell mass of $0.15 \text{ ng cell}^{-1}$ as an estimate for our strain of *Rhodomonas* sp. (Renaud et al., 2002). The *Rhodomonas* sp. population used is characterized by an average diameter of $6.38 \mu\text{m}$ and a carbon content of 0.021 ng C

cell⁻¹. SfG was then calculated from energy intake (C, consumed energy) and respiratory energy loss (R) as

$$\text{SfG} = \text{C} - \text{R}. \quad (2.3)$$

SfG is displayed as energy available for development and is thus plotted against body length as standardization for larval morphometrics. For the calculation of the energy budget model, I assumed that larvae are 8.0 % smaller under elevated $p\text{CO}_2$ conditions than under control conditions, demonstrated by the morphometric measurements in this study.

As excretion rates are difficult to determine in sea urchin larval stages, energy loss due to excretion was omitted from the analyses. One should bear in mind that this may possibly lead to an overestimation of SfG.

b) Adult experiments (A2):

A full energy budget was calculated for adult *Strongylocentrotus droebachiensis* from feeding, respiration and excretion rates. Energy deposition as somatic and gonad growth was calculated and correlated to the scope for growth. Aerobic energy loss was calculated by converting respiration and NH_4^+ excretion rates into their caloric equivalents (R and U, respectively) using $0.484 \text{ J } \mu\text{mol O}_2$ representing a mixed, but protein dominated, catabolism of hydrocarbons, lipids and proteins (Gnaiger, 1983) and $0.347 \text{ J } \mu\text{mol NH}_4^+$ (Elliott and Davison, 1975). Absorbed energy (A) was calculated using the consumed energy (C) and the Conover ratio (Conover, 1966) as an estimate of organic matter absorption efficiency multiplied by ingested energy:

$$\text{A} = \text{E}_{\text{OM}} \text{C} \quad (2.4)$$

Deposited energy into growth (G) was determined by converting absolute growth per day of body organs (gonads, test and spines, gut) over 40 days into their caloric equivalent based on biochemical constituents (lipid, carbohydrates and protein) of the respective organ using the conversion values of $4.3 \text{ kJ g}^{-1} \text{ DM}$ and $24 \text{ kJ g}^{-1} \text{ DM}$ for deposition into test and spines and deposition into gonad or gut tissue, respectively (Bishop and Watts, 1992; Fernandez, 1998). Growth of Aristotle Lantern was omitted due

to no significant differences in total dry masses of lantern of Aristotle of experimental vs. reference sea urchins.

The final energy budget was then calculated according to the following equation:

$$C = A - (R + U + G_{\text{gonad}} + G_{\text{gut}} + G_{\text{test\&spines}} + X) \quad (2.5)$$

with X the remaining energy, that is not explained by this model. SfG was determined by subtracting metabolic energy loss from the absorbed energy according to:

$$\text{SfG} = A - (R + U) \quad (2.6)$$

All energy conversions for adults are expressed in $\text{J g}^{-1} \text{DM day}^{-1}$.

2.6 Molecular techniques (L1-L2)

2.6.1 Reverse transcription quantitative polymerase chain reaction (RT qPCR, L2)

To determine energy partitioning in sea urchin larvae, transcription of genes involved in calcification, ion regulation and metabolism was quantified using quantitative real time PCR. Sampling was conducted at days 2, 4 and 7 post-fertilization in both treatments. At each time point, 20 samples of 3000 to 4000 larvae were taken from each culture, briefly concentrated in Eppendorf 1.5 mL tubes by means of hand centrifugation for 10 seconds at approximately 156 g. Excess water was discarded except for approximately 80 μl containing the larvae. Samples were then shock-frozen in liquid nitrogen. The whole sampling process took approximately 45 seconds per sample. Samples were stored at -80°C for ca. 6 months until further processing.

Total RNA was extracted from 3000 to 4000 larvae per sample using the Qiagen RNeasy Mini kit (Qiagen, Hilden, Germany) following the instruction manual. qRT-PCR analysis was carried out using the two step real-time RT-PCR method described by Vandenbrouke et al. (2001). Prior to cDNA synthesis, 3 to 10 μg total RNA (Nanodrop bioanalyzer) were treated with DNase (Ambion by Applied Biosystems, Darmstadt, Germany) to digest genomic DNA remains. For cDNA synthesis, 0.4 μg total RNA

(Nanodrop bioanalyzer) was transcribed using the Applied Biosystems High Capacity cDNA Reverse Transcriptase kit (Applied Biosystems, Darmstadt, Germany).

Primer Express Software (version 2.0 by Applied Biosystems) and sequences from the *S. purpuratus* genome were used to design primer pairs for 27 genes (publication 2). Efficiency was evaluated by applying the dilution standard curve method (dilution steps: 1:20; 1:100; 1:500; 1: 2500 and 1:12500). Primer concentrations were 300 nM. The *Taq* DNA polymerase was activated for 10 min at 95°C. Each PCR was run for 40 cycles at 95°C for 15 s and 62°C for 1 min. Subsequent to each PCR, a melting curve analysis was conducted. Each PCR of a total volume of 20 µl consisted of 2 µl template (cDNA dilution of 1:20), 3 µl of each primer (forward, reverse), 2 µl DNase free H₂O and 10 µl SYBR Green master mix (Platinum SYBR Green qPCR SuperMix-UDG with ROX, Invitrogen, Karlsruhe, Germany). Controls were conducted without template (no template control) and with RNA post DNase digestion to test for genomic DNA contamination within the cDNA. No significant DNA contamination was observed. Using LinRegPCR software version 7.4 (Ramakers et al., 2003) the PCR efficiency of each PCR reaction was determined. Efficiencies were always > 1.9. Real time qPCR measurements were conducted on a StepOnePlus real time cycler (Applied Biosystems, Darmstadt, Germany).

To identify suitable reference genes, NormFinder (Andersen et al., 2004) software was used (version 19). NormFinder uses an algorithm to estimate the overall expression variation as well as the variation between samples of subgroups of the sample set and is aiming at identifying a candidate gene with lowest intra-group variability and at the same time an inter-group variation as close to 0 as possible (Andersen et al., 2004). As data input for NormFinder, we used Ct values of all 27 gene transcripts from all treatment groups which were transformed into quantities (Q) using the appropriate PCR efficiencies as determined by LinReg PCR using formula (2.7):

$$Q = E^{(-Ct)} \quad (2.7)$$

with E being the reaction specific efficiency (maximum efficiency of 100 % would be 2, i.e. a doubling in the amount of PCR product per reaction cycle) and Ct being the Ct value as determined using StepOnePlus real time cycler software (adapted from Livak and Schmittgen, 2001). NormFinder suggested sodium bicarbonate cotransporter (NBC3, NCBI accession no: NM_001079551) to be the most stably expressed gene with an inter-

and intra-group specific variation closest to zero (NormFinder stability values for NBC 0.001 to 0.006). NBC3 was thus used as reference gene for normalization.

For statistical reasons, logarithmic Ct-values were converted into quantities (Q) using formula 1. Values were then normalized using the reference gene NBC3. A Bray-Curtis similarity analysis was conducted with square root transformed expression values (normalized quantities). From this similarity matrix, an analysis of similarity (one-way ANOSIM, two-way crossed ANOSIM using time and $p\text{CO}_2$ as factors), a Cluster analysis (principal component analysis, PCA) and a similarity of percentage analysis (SIMPER) analysis were carried out. The principal component analysis (PCA) with a cluster plot was used to determine the contribution of single genes to the observed sample pattern and test if genes from one pathway correlate in their expression behavior (e.g. ion regulation, calcification and metabolism). One-way and two-way crossed ANOSIM was chosen as non-parametric statistical method to analyze the significance in grouping elicited by the group specific gene expression patterns and determine the impact of $p\text{CO}_2$ and time on the observed pattern. A SIMPER analysis was then used to quantitatively determine the contribution of single genes to the observed similarity or dissimilarity between gene expression patterns of groups. All multivariate statistics including PCA were conducted using Primer 6 software (version 6.1.9; Primer-E Ltd.). For the evaluation of mortality and growth, t-tests and an analysis of covariance (ANCOVA) with log transformed data, respectively, were applied.

2.6.2 Immunocytochemistry (L1)

Antibody labeling was used to visualize the larval endoskeleton (Anstrom et al., 1987) and the nervous system (serotonin). At various times post-fertilization, embryos and larvae were fixed in 4% PFA in FSW for 15 min, then post-fixed with ice-cold methanol for 1 min at room temperature (RT). Fixed specimen were rinsed 3 times in phosphate-buffered saline (PBS) pH 7.4 and then blocked for 2h in 4% bovine albumin serum containing 0.1% tween-20 at RT. Anti-serotonin (Sigma) and anti-MSP130 (a gift from Dave McClay, Duke University, USA) were diluted 1:500 in PBS. After overnight incubation (RT), embryos and larvae were rinsed at least 4 times in PBS then incubated in a 1:1000 dilution of Alexa488 conjugated anti-rabbit IgG and Alexa568 conjugated anti-mouse IgG (Molecular Probes). After incubation (2h, RT), embryos and larvae were

rinsed 4 times in PBS. Specimens were mounted in PBS, examined using a Leica confocal microscope (SP5) and analyzed by collecting stacks of images and projecting them in the Y-axis.

2.7 Determination of acid-base status

2.7.1 Measurements of extracellular pH (pH_e) in sea urchin larvae (L3, L4)

To determine pH_e within the primary body cavity (PBC) and/or stomach lumen of *S. droebachiensis* larvae, two different methods were used:

- (a) selective ion electrode technique (SIET) using pH sensitive microelectrodes and
- (b) microfluorometry using the pH sensitive dye 2',7'-Bis-(carboxyethyl)-5(6)-carboxyfluoresceinacetoxymethylester (BCECF-AM).

a) Selective ion electrode technique (SIET, L4)

The SIET was used to measure H^+ concentrations in the extracellular matrix gel (ECM) of sea urchin larval primary body cavity (PBC). Glass capillary tubes (Borosilicate, inner diameter: 1.2 mm outer diameter: 1.5 mm, Hilgenberg, Germany) were pulled on a DMZ-Universal puller (Zeitz-Instruments, Munich, Germany) into micropipettes with tip diameters of 2–3 μm . These were then baked at 200°C for 4 h and vapor-silanized with dimethyl chlorosilane (Sigma- Aldrich) overnight. The micropipettes were frontloaded with a 200 μm column of liquid ion exchanger cocktail (H^+ ionophore III, Sigma-Aldrich) diluted in 2-Nitrophenyl ether at a concentration 10.5 mg mL^{-1} . Additionally, micropipettes were again frontloaded with a 100 μm column of the ionophore cocktail containing a polyvinylchloride (PVC)/tetrahydrofuran (330 mg mL^{-1}) solution in the ratio 1:3 in order to seal the opening of the electrode tip. The micropipette was backfilled with a 4 cm column of pH electrolyte (300 mM KCL, 50 mM NaPO_4 , pH 7) solution to create an ion selective microelectrode (probe). To calibrate the ion selective probe, the Nernstian property of each microelectrode was measured by placing the microelectrode in a series of FSW solutions (pH 6, 7, 8 and 9) with a reference to an Ag/AgCl electrode. By plotting the voltage output of the probe against $\log [\text{H}^+]$ values, a linear regression yielded a

Nernstian slope of 49.8 ± 2.3 mV ($n = 12$) for 1 pH unit. With this method we were able to resolve a minimum difference of 0.1 pH units. In order to determine the presence of a transepithelial potential a micropipette filled only with pH electrolyte without liquid ion exchanger cocktail was introduced into the coelomic fluid or the digestive system in the same way as the H^+ sensitive electrodes. No transepithelial potential was detected.

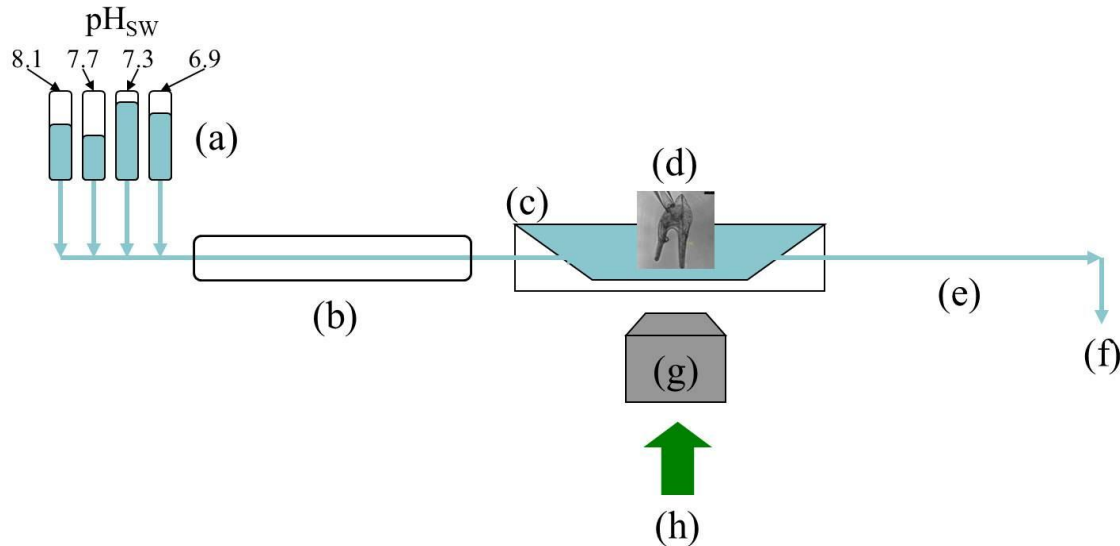


Figure 2.1: Scheme of a perfusion system mounted on an inverse microscope. Storage reservoirs (a) feed seawater with appropriate pH_{SW} through a cooling system (b) into the perfusion bath (c). A larva (d) is held in place in the perfusion bath by a glass pipette to which a slight vacuum is applied. Seawater is entering the bath via gravity feed before it is sucked out (e) of the bath by a vacuum that is applied to the waste container (f). The larvae were measured on an inverse microscope with a 20x objective (g). In micro-fluorometry measurements an Argon laser (h) excited the fluorescent dye BCECF at 488 and 458 nm and a camera recorded pictures of the emitted fluorescence intensity at 525 nm.

The electrode measurements were performed at $10^{\circ}C$ on an inverse microscope (Axiovert 135, Zeiss, Germany) equipped with a temperature-controlled perfusion system, allowing for quick exchange of different pH solutions inside the perfusion chamber (figure 2.1). The pH of the bath solutions was adjusted by equilibrating the FSW with pure CO_2 to the desired pH. The larvae was placed inside the perfusion bath and kept in position via a holding pipette (30-40 μm tip diameter) to which a slight vacuum was applied. The ion-selective probe was mounted on a remote controlled micromanipulator (Phytron GmbH, Gröbenzell, Germany) and was introduced into the PBC from the base of the arms at the oral side of the larvae (10–20 μm inside the PBC) or into the stomach through the esophagus to record the ionic activities. The epidermis and basal lamina

formed a seal around the entrance point of the electrode, preventing fluid exchange between seawater and the primary body cavity. pH_e recordings were performed on pluteus larvae (7-10 dpf) reared under control conditions which were exposed to acute changes in sea water pH ranging from 6.9 to 8.2 (PBC measurements). Furthermore, the same measurements were also performed on pluteus larvae (7-10 dpf) from the CO_2 perturbation experiment in order to address the effects of chronically elevated seawater pCO_2 on extracellular pH homeostasis (PBC and stomach lumen measurements).

b) Microfluorometry (L3)

Microfluorometry using 2',7'-Bis-(carboxyethyl)-5(6)-carboxyfluorescein-acetoxymethylester (BCECF-AM) was used as non-invasive method to measure pH_e in the larval primary body cavity to support the data obtained by microelectrode measurements. As the high pH in the digestive tract (> 8.5 pH units) exceeds the sensitivity range of BCECF, this method could not be applied to measure CO_2 induced changes in the digestive tract of sea urchin larvae.

The microfluorometry method is based on the pH dependent fluorescent intensity of BCECF. BCECF-AM is a cell-membrane permeable acetoxymethylester (AM) that is cleaved by intracellular esterases to form the fluorescent dye BCECF. BCECF is composed of two components which both emit light at 525 nm when excited, but have different excitation wavelengths. The pH sensitive component is excited at 488 nm and its fluorescence intensity increases with pH. The pH neutral component is excited at a wavelength of 458 nm, its fluorescence intensity does not change with pH and can thus be used as internal standardization for loading differences. Calculating the ratio out of the fluorescence intensities of both components (E_{488}/E_{458}) gives a measure for pH. Increases in the ratio indicate an increase in pH. To measure pH within the primary body cavity in larvae, I made use of xenobiotic transport – a mechanism usually used as a cellular defense mechanisms against toxins in aquatic organisms (multixenobiotic transport, Bard, 2000). After the export of BCECF from the cellplasma, BCECF was captured in the ECM of the body cavity and could thus be used for pH_e measurements.

The experimental protocol was conducted as follows: a BCECF-AM (Invitrogen) stock solution of 10mM in dimethyl sulfoxide (DMSO, Invitrogen) was, in a first step, diluted with filtered seawater to 100 μM (1:100). Larvae (8 to 24 days post-fertilization)

were loaded with BCECF-AM in a second dilution step by mixing 35 μ L of larval culture seawater including 5 to 6 individuals with 15 μ L of BCECF/seawater solution (100 μ M). The final working solution had a BCECF concentration of 30 μ M and a DMSO concentration of 0.3% (V:V). Animals were incubated in 30 μ M BCECF-AM for two hours at 12°C in the dark. After incubation, larvae were washed 5 times with seawater and were kept at 12°C in the dark for 60 min until fluorescent intensity in the primary body cavity was sufficient for detection. The procedure did not harm the animals: spare individuals that were not used for the pH measurements survived a minimum of 7 days following the treatment. Late larvae (24 dpf) close to settlement went through metamorphosis in the incubation tubes after the treatment with BCECF-AM.

pH_e measurements were conducted using an inverted confocal laser scanning microscope (Leica, SP5) equipped with a perfusion system (comparable to the one described for the microelectrode measurements, figure 2.1). Larvae were mounted in the perfusion bath at control $p\text{CO}_2$ conditions (pH 8.1) and held in place with a glass holding pipette to which a slight vacuum was applied. The bath (volume of 0.5 mL) was perfused at a rate of 3 mL min⁻¹ with seawater adjusted to different pHs by injection of pure CO₂ (pH 8.1, 7.7, 7.3 and 6.9, temperature of 13 \pm 0.2°C). Each larva (n=7) was left to adjust to pH 8.1 for 10 minutes before the first pH change was introduced. pH was changed in the order of 8.1, 7.7, 7.3, 6.9 and back to control pH 8.1. Each pH was applied for 10 minutes. One experiment lasted 60 to 65 minutes. The recording interval was once per minute for 5 minutes post-solution-change, one recording at 7 minutes post-solution-change and one at 10 minutes post-solution-change. The confocal laser scan settings are listed in table 2.2. With these settings, no detectible dye bleaching occurred. Two larvae exposed to the same experimental protocol, but only supplied with seawater adjusted to pH 8.1 served as control for fluorescence intensity drift over the experimental period. This way, an in- or decrease in pH_e due to potential active regulation of the larvae in response to elevated $p\text{CO}_2$ could be reliably detected. Due to high variations in fluorescence intensity ratios (ratios between 2.5 and 3.5) among individual larvae, data were normalized onto the starting fluorescence intensity ratio at pH 8.1 of the respective larva.

For calibration of BCECF fluorescence intensity ratios, it was assumed that the extracellular fluid in the primary body cavity is similar in composition to seawater.

BCECF-dextran (BCECF attached to dextran, 10 mM in dimethyl sulfoxide, Invitrogen) was used, because BCECF-AM does not fluoresce before cleavage by cellular esterases. BCECF-dextran was diluted in artificial seawater adjusted to different pH to a final concentration of 50 μ M. This concentration of BCECF-dextran yielded the same fluorescence intensity range when using the same confocal settings (table 2.2) as BCECF loaded larvae. In order to receive stable pH values in seawater, artificial seawater (400 mM NaCl, 9.6 mM KCl, 52.3 mM MgCl₂, 9.9 mM CaCl₂, 27.7 mM Na₂SO₄) was buffered with 20 mM TRIS/HCl. Measurements were conducted at 12°C. For better comparison to values obtained in larvae, normalization was conducted by dividing all ratio values by the ratio measured at pH 8.1. The normalized ratio increased linearly with increasing pH up to a pH of 7.7. Between pH 7.7 and 8.1, almost no increase in ratio could be observed. This indicated a limited BCECF sensitivity for pH measurements in seawater.

Table 2.2: Leica confocal laser scanning microscope settings for pH_e measurements using BCECF

Parameter	Setting
Scanning speed	400 Hz
Section thickness	5 to 12 μ m
Microscope objective	20x dry
Scan sequence	
Scan 1	488 laser - 9% intensity
Scan 2	458 laser - 31% intensity
PMT 1	Emission reading at 520 to 540 nm
PMT 2	Transmission image
Smart Offset	0%
Gain	400 - 700

Abbreviations: Photomultiplier tube (PMT)

2.7.2 Extracellular carbonate system speciation of perivisceral coelomic fluid (A1-A2)

Perivisceral coelomic fluid (PCF) was collected from the sea urchin coelomic cavity via a gas-tight Hamilton syringe by penetrating their perivisceral membrane at the oral surface between the two rows of their water vascular system. For coelomocyte disposal, withdrawn coelomic fluid of echinoids was centrifuged for 30 seconds (6000 rpm) using a minifuge (C1100-FIS-230-EU, Fisher Scientific, Germany). The supernatant was transferred into a new sample tube and incubated in a water bath of 10°C during C_T and pH_e measurements. Determination of pH_e was performed using a microelectrode (WTW Mic-D) and a WTW pHi 340 pH meter (precision \pm 0.01 units) that was calibrated with

Radiometer precision buffers 7 and 10 (S11M44, S11 M007). Total dissolved inorganic carbon was determined in duplicates (100 µl each) via a Corning 965 carbon dioxide analyzer (precision $\pm 0.1 \text{ mmol L}^{-1}$; Olympic Analytical Service, England) that was calibrated by generating a sodium bicarbonate (Fluka, Germany) standard curve with a fresh dilution series of 20, 10, 5, 2.5 and 1.25 mM. Carbonate system speciation (i.e. $p\text{CO}_2$, $[\text{HCO}_3^-]$) within the coelomic fluid of *S. droebachiensis* was calculated from pH_e and C_T measurements according to the Henderson-Hasselbalch equation

$$p\text{CO}_2 = C_T (\alpha (10^{(\text{pH} - pK'_1)} + 1))^{-1} \quad (2.8)$$

$$[\text{HCO}_3^-]_e = C_T - (\alpha p\text{CO}_2), \quad (2.9)$$

where α ($0.509 \text{ } \mu\text{mol L}^{-1} \text{ Pa}^{-1}$, $S=31.5$, $T=10^\circ\text{C}$, Weiss, 1974) is the solubility coefficient of CO_2 in seawater and pK'_1 the dissociation constant of carbonic acid. pK'_1 was estimated in dependency of pH_e (see below, equation 2.10).

pK'_1 and non-bicarbonate buffer (NBB) line

The dissociation constant pK'_1 in the PCF of *S. droebachiensis* was determined over a pH range of 0.9 units (pH 7.3 - 8.2). PCF of seven sea urchins was pooled, subsequently centrifuged (20 min, 4°C , 60 g, Eppendorf 5415 R, Germany) and aliquots (at least 4 x 400 µL) of the supernatant incubated for one hour in a shaking, tempered (10°C) water bath against different CO_2 - air mixtures ($p\text{CO}_2 = 0.06, 0.14, 0.4$ and 0.6 kPa). Simultaneously, $p\text{CO}_2$ values in the gas mixture used for equilibration were controlled via an infrared $p\text{CO}_2$ analyzer (GDZ 401, HTK Hamburg, Germany). After equilibration, C_T and pH_e were determined immediately (see above, carbonate system speciation). The functional pK'_1 values for the PCF of *S. droebachiensis* were calculated using the Henderson-Hasselbalch equation in the form

$$pK'_1 = \text{pH} - \log((C_T - \alpha p\text{CO}_2) \alpha p\text{CO}_2^{-1}) \quad (2.10)$$

pK'_1 values were calculated via equation 8 and were plotted against pH_e resulting in a linear relationship. For subsequent pK'_1 calculations, the following equation was used:

$$pK'_1 = -0.0876 \text{ pH}_e + 6.6596 \quad (R^2 = 0.51) \quad (2.11)$$

A non-bicarbonate buffer line (NBB) was measured from an oxygenated, pooled PCF sample from five sea urchins from our maintenance facilities. *In vitro* measurements were

performed by equilibrating samples of extracellular fluid with an air mixture of known $p\text{CO}_2$, to subsequently measure pH_e and bicarbonate $[\text{HCO}_3^-]_e$ as outlined above (see pK'_1 determination). The calculated $[\text{HCO}_3^-]_e$ values were then plotted against their extracellular pH_{NBS} resulting in a linear relationship. The negative slope of the NBB line, $-\Delta([\text{HCO}_3^-] + [\text{CO}_3^{2-}]) \Delta\text{pH}^{-1}$, is defined as β_{NB} , expressed in $\text{mEq L}^{-1} \text{pH}^{-1}$ was assessed to be -0.41 ($R^2 = 0.23$).

3 Publications and unpublished results

The following is a list of publications and declaration of my contribution to them. Experiments of first author manuscripts were designed and conducted by myself with support of the coauthors. First author manuscripts were written by myself, and revised together with the coauthors. I substantially supported the experiments of publication 4 and helped revise the manuscript, which was mainly written by the first and last authors.

- I. Stumpp, Meike; Wren, Johanna; Melzner, Frank; Thorndyke, Michael C.; Dupont, Sam (2011): *CO₂ induced seawater acidification impacts sea urchin larval development I: elevated metabolic rates decrease scope for growth and induce developmental delay*. Comparative Biochemistry and Physiology A (in press) doi:10.1016/j.cbpa.2011.06.022
- II. Stumpp, Meike; Dupont, Sam; Thorndyke, Michael C.; Melzner, Frank (2011): *CO₂ induced seawater acidification impacts sea urchin larval development II: gene expression patterns in pluteus larvae*. Comparative Biochemistry and Physiology A (in press) doi:10.1016/j.cbpa.2011.06.023
- III. Stumpp, Meike; Trübenbach, Katja; Brennecke, Dennis; Hu, Marian Y.; Melzner, Frank (2011): *Resource allocation and extracellular acid-base status in Strongylocentrotus droebachiensis in response to CO₂ induced seawater acidification*. Aquatic Toxicology (in preparation)
- IV. Dorey, Narimane; Stumpp, Meike; Thorndyke, Michael C.; Melzner, Frank; Dupont, Sam (2011): *Impact of long term and trans-life-cycle acclimation to near-*

future ocean acidification on the green sea urchin Strongylocentrotus droebachiensis. Global Change Biology (under review)

The pH_e measurements described in the discussion section of this thesis were conducted at SLC and in Markus Bleich's laboratory at CAU Kiel by myself, but with support by my supervisors. The results will be submitted as part of a publication entitled:

- V. Stumpp, Meike; Hu, Marian Y.; Dorey, Narimane; Gutowska, Magdalena A.; Dupont, Sam; Melzner, Frank; Bleich, Markus: *Acid-base control of the extracellular matrix and pH regulatory capacities of primary mesenchyme cells (PMCs) in sea urchin larvae* (manuscript in preparation)

I CO₂ induced seawater acidification impacts sea urchin larval development I: elevated metabolic rates decrease scope for growth and induce developmental delay

Stumpp, M. ; Wren, J.; Melzner, F. ; Thorndyke, M.C. ; Dupont, S.

Comparative Biochemistry and Physiology A (2011) doi:10.1016/j.cbpa.2011.06.022

CO₂ induced seawater acidification impacts sea urchin larval development I: elevated metabolic rates decrease scope for growth and induce developmental delay

Stumpp, M. ¹; Wren, J. ²; Melzner, F. ¹; Thorndyke, M.C. ³; Dupont, S. ²

1 Biological Oceanography, Leibniz-Institute of Marine Sciences (IFM-GEOMAR),
24105 Kiel, Germany

2 Department of Marine Ecology, Sven Lovén Centre for Marine Sciences, Kristineberg,
University of Gothenburg, Sweden

3 The Royal Swedish Academy of Sciences, Sven Lovén Centre for Marine Sciences,
Kristineberg, University of Gothenburg, Sweden

Corresponding author: Sam Dupont, Department of Marine Ecology, Sven Lovén
Centre for Marine Sciences, Kristineberg 566, 45034 Fiskebäckskil, Sweden,
sam.dupont@marecol.gu.se

Keywords: *Strongylocentrotus purpuratus*, larvae, pluteus, echinoderm, ocean acidification, energy budget, respiration, feeding

Abstract:

Anthropogenic CO₂ emissions are acidifying the world's oceans. A growing body of evidence is showing that ocean acidification impacts growth and developmental rates of marine invertebrates. Here we test the impact of elevated seawater *p*CO₂ (129 Pa, 1271 µatm) on early development, larval metabolic and feeding rates in a marine model organism, the sea urchin *Strongylocentrotus purpuratus*. Growth and development was assessed by measuring total body length, body rod length, postoral rod length and posterolateral rod length. Comparing these parameters between treatments suggests that larvae suffer from a developmental delay (by ca. 8%) rather than from the previously postulated reductions in size at comparable developmental stages. Further, we found maximum increases in respiration rates of +100 % under elevated *p*CO₂, while body length corrected feeding rates did not differ between larvae from both treatments. Calculating scope for growth illustrates that larvae raised under high *p*CO₂ spent an average of 39 to 45% of the available energy for somatic growth, while control larvae could allocate between 78 and 80% of the available energy into growth processes. Our results highlight the importance of defining a standard frame of reference when comparing a given parameter between treatments, as observed differences can be easily due to comparison of different larval ages with their specific set of biological characters.

1 Introduction

Anthropogenic release of atmospheric CO₂ leads to ocean warming and acidification. This has been proposed as a major threat for marine organisms, in particular calcifying organisms (Orr et al., 2006; Doney et al., 2009). However, ocean acidification research is a new field and relatively little experimental evidence is available on the potential impacts on marine biota (Kroeker et al., 2010).

Sea urchins have been used widely as model organisms in developmental biology, cell and evolutionary biology and toxicology for decades. Among the studied species, the purple sea urchin, *Strongylocentrotus purpuratus*, with a sequenced genome (The Sea Urchin Genome Sequencing Consortium, 2006), is the most widely used. Owing to the extensive knowledge accumulated on the timing of embryonic and larval development (Smith et al., 2008), as well as the underlying gene regulatory networks (Ben-Tabou de Leon and Davidson, 2007), this species is an excellent candidate to study the effects of abiotic stressors such as elevated seawater *p*CO₂ on the normal progression of larval development.

S. purpuratus is a long lived species (up to 50 years, Ebert, 1967) and an abundant and key component of the intertidal and sub-tidal zone of the Eastern Pacific coast, with a distribution range from Mexico to Alaska (Biermann et al., 2003) and an important fishery resource. It is an important grazer of macroalgae, particularly kelp, and it competes with other grazers (abalone, *Haliotis* spp., red sea urchin *Strongylocentrotus franciscanus*) and is a food source for many predators including sea otters (Steneck et al., 2002). Sea urchins are a central element in the structure of the marine benthic community. For example, a delicate balance between sea urchin grazing pressure and kelp forest productivity leads to stable states that alternate between kelp forest and sea urchin “barrens” (Pearse, 2006). In addition to competition, predation and food limitation, sea urchin abundance is heavily influenced by recruitment intensity. It is thus of primary importance to understand how climate change might impact larval recruitment in important keystone species such as *S. purpuratus* (Dupont et al., 2010c).

A growing body of evidence indicates that ocean acidification might impact growth, calcification and developmental rates in echinoderm species (Dupont et al., 2010c). While the lecithotroph echinoderm larvae *Crossaster papposus* showed elevated

growth rates (Dupont et al., 2010b) when raised under elevated $p\text{CO}_2$ (ca. 120 Pa, 1184 μatm , pH 7.7), sea urchin planktotrophic larval stages from several species appears to be smaller at a given time post-fertilization and/or grow more slowly (see Dupont et al., 2010c for review). However, it is unclear, whether observed growth reductions are due to a reduction in the ability to calcify at high rates or to other factors such as limitations in feeding ability. Although Martin et al (2011) found that *Paracentrotus lividus* larvae are characterized by a fully developed skeleton when normalized to body length, calcification of the larval skeleton, which comprises a framework of spicules made of CaCO_3 (highly soluble Mg Calcite form, Okazaki and Inoué, 1976), might be more costly due to low extracellular matrix pH and high extracellular matrix $p\text{CO}_2$. In addition, maintenance of intracellular pH and general cellular homeostasis might require additional energy (Deigweiher et al., 2010). Thus, growth reductions in larval echinoderm species might be indirect effects of an altered partitioning of the energy budget. Similar conclusions have been reached by Thomsen & Melzner (2010) where increased metabolic rates in high $p\text{CO}_2$ acclimated bivalves (blue mussel *Mytilus edulis*) were accompanied by reduced rates of calcification and growth.

Under the hypothesis that the main CO_2 effect visible on the larval organism level would be reduced speed of development, ultimately caused by energy budget constraints, investigating the impact of elevated $p\text{CO}_2$ on larval development would create a classic experimental design problem that has been poorly addressed by ocean acidification experiments on echinoderm larval stages so far: any biological parameter of interest, at a given time point in an experiment might be severely confounded by differences in development between treatment groups. For example, it is known from the extensive study of echinoderm developmental gene regulatory networks that expression patterns of genes and associated physiological function are highly variable yet precisely structured chronologically (Ben-Tabou de-Leon and Davidson, 2007). As a consequence, age or time post-fertilization would then not be the right reference scale to discuss effects of elevated seawater $p\text{CO}_2$ on biological processes of interest. Any observed effect at a given time may just be a consequence of a delay in development (Pörtner et al., 2010).

We hypothesize that elevated seawater $p\text{CO}_2$ primarily impacts the energy budget, which then leads to reduced rates of development. The aim of this paper is to test this hypothesis and investigate the impact of elevated seawater $p\text{CO}_2$ on *S. purpuratus* larval

survival, development, growth, aerobic metabolic rate and feeding rate. The data will be used to combine respiration and feeding data to calculate scope for growth (SfG), a measure of energy balance, and will be correlated and compared to the observed growth rates. In a companion paper (Stumpp et al, submitted), we use an explorative gene expression approach to analyze key physiological processes that might impact the larval energy budget.

2 Material and methods

2.1 Animal collection

Adult *Strongylocentrotus purpuratus* were collected on the Californian coast (Kerckhoff Marine Laboratory, California Institute of Technology, USA) and transferred to the Sven Lovén Centre for Marine Science (Kristineberg, Sweden). They were maintained in natural flowing seawater at 14°C and pH 8.1 on a diet of *Ulva lactuca*.

2.2 Larval culture and experimental conditions

Spawning was induced in June-July 2008 and 2009 by intra-coelomic injection of 0.5M KCl in filtered seawater (FSW). In each experiment, gametes from three males and three females were used. After fertilization, cleaving embryos (two cells stage) were placed in 5L (survival, growth and feeding) or 50L (respiration) aquaria filled with FSW at a density of 5 to 10 embryos per mL at a temperature of 14°C. Larger culture vessels for metabolic rate experiments were needed due to the high amount of larvae required for respiration trials (>2000 Larvae per time point). The FSW was continuously aerated to maintain oxygen concentrations close to air saturation and mixed by the slow convective current of a stream of single bubbles (approx. 100 bubbles per min). After 5 days, larvae were fed daily with the cryptophyte algae *Rhodomonas* sp. which were raised in B1 medium (Guillard and Ryther, 1962) at 20°C under a 12:12 h light:dark cycle. Algal strains were provided by the Marine Algal Culture Centre at Gothenburg University (GUMACC). Larvae were fed at a constant concentration of 150 µg C L⁻¹. The carbon content of the algae was estimated based on biovolume measurements as equivalent spherical diameter (ESD) with an electronic particle analyzer (Elzone 5380, Micrometrics, Aachen, Germany) and equations provided by Mullin et al. (1966). To prevent changes in food concentration, algae concentration and size were checked daily

using a coulter counter (Elzone 5380, Micrometrics, Aachen, Germany) and then adjusted in the experimental bottles to the maximum concentration of $150 \mu\text{g carbon l}^{-1}$ (~ 3000 to $6000 \text{ cells ml}^{-1}$ for diameters ranging between 6 to 8 μm). At the chosen algae concentration, seawater $p\text{CO}_2$ treatment levels and temperatures had no impact on algal growth and survival (result not shown).

Cultures were maintained at a salinity of 32‰ and a total alkalinity of $2200 \pm 30 \mu\text{mol kg}^{-1}$ as measured following Sarazin et al. (1999). The carbonate system speciation ($p\text{CO}_2$, Ω_{Ca} and Ω_{Ar}) was calculated from pH and alkalinity using CO2SYS (Lewis and Wallace, 1998, Table 1) with dissociation constants from Mehrbach et al. (1973) refitted by Dickson and Millero (1987). Our treatments were control/natural seawater (pH=8.1, $p\text{CO}_2$ 38 Pa, 375 μatm , T=14°C) and high seawater $p\text{CO}_2$ (pH=7.7, $p\text{CO}_2$ 128 Pa, 1264 μatm , T=14°C). pH was maintained in each aquarium using a computerized feedback system (AquaMedic) that regulates pH (NBS scale) by addition of pure gaseous CO_2 directly into the seawater (± 0.02 pH units). Three replicates (n=3) were used for 5L cultures (morphology) and two replicates (n=2) for the 50L cultures (respiration).

2.3 Mortality and growth

Larval cultures were monitored daily for 21 days. Each day, 3 subsamples of more than 50 larvae was removed from each culture and fixed in buffered 4% paraformaldehyde (PFA) in FSW for later analysis. Density at time t (N_t in larvae L^{-1}) was estimated by dividing the number of larvae by the corresponding volume collected. For each replicate, 10 fixed larvae were photographed every (1 to 7 days post-fertilization) or every other day (after 7 days post-fertilization) with a digital camera mounted on a dissecting microscope using polarized light to visualize the skeleton. Five morphometric parameters (body length, body rod lengths (right and left), postoral rod lengths and posterolateral rod length, Figure 1) were measured for each larva using LAS software (Leica). A symmetry index was calculated as the ratio of left to right overall length.

2.5 Antibody labeling

Antibody labeling was used to visualize the larval endoskeleton (Anstrom et al., 1987) and the nervous system (serotonin). At various times post-fertilization, embryos and larvae were fixed in 4% PFA in FSW for 15 min, then post-fixed with ice-cold methanol

for 1 min at room temperature (RT). Fixed specimen were rinsed 3 times in phosphate-buffered saline (PBS) pH 7.4 and then blocked for 2h in 4% bovine albumin serum containing 0.1% tween-20 at RT. Anti-serotonin (Sigma) and anti-MSP130 (a gift from Dave McClay, Duke University, USA) were diluted 1:500 in PBS. After overnight incubation (RT), embryos and larvae were rinsed at least 4 times in PBS then incubated in a 1:1000 dilution of Alexa488 conjugated anti-rabbit IgG and Alexa568 conjugated anti-mouse IgG (Molecular Probes). After incubation (2h, RT), embryos and larvae were rinsed 4 times in PBS. Specimen were mounted in PBS, examined using a Leica confocal microscope (SP5) and analyzed by collecting stacks of images and projecting them in the Y-axis.

2.6 Feeding

To assess the impact of elevated seawater $p\text{CO}_2$ on feeding performance, feeding rate was estimated every other day beginning at day 6 (commencement of feeding). 15 larvae each were transferred to 100 ml glass bottles (7 replicates) with food suspension (*Rhodomonas* sp. at $150 \mu\text{g C L}^{-1}$) in FSW equilibrated with the same $p\text{CO}_2$ the respective experimental animals originated from (pH 8.1 or pH 7.7). Two sets of control bottles (3 replicates for each treatment) without larvae containing the same food suspension were also prepared. The bottles were incubated on a rotating plankton wheel (0.2 rpm) at 14°C . Feeding rate was estimated as clearance rate by measuring the algal concentration ($\Delta \text{cells L}^{-1}$) at the end of the incubation (24h) in control and experimental bottles after collection of the larvae on a $50 \mu\text{m}$ sieve. As nutritional values of algae differ with size, algae cell size was simultaneously measured and feeding rate was expressed in changes in ng C L^{-1} . Feeding rate ($F, \text{ml ind}^{-1} \text{d}^{-1}$) was calculated following Frost (1972), and ingestion ($I, \text{cell volume ind}^{-1} \text{d}^{-1}$) was calculated as $I = F \times C$, where C is the average algal concentration per bottle. Rates were corrected for mortality and are given as rates per surviving animal in $\text{ng C ind}^{-1} \text{h}^{-1}$.

2.7 Aerobic metabolic rate determinations

Respiration experiments were conducted every other day beginning at day 3 according to Marsh and Manahan (1999) with modifications. Briefly, respiration vials with volumes between 1624 to 1641 μl were placed in a water bath at 14°C and filled with sterile filtered seawater ($0.2 \mu\text{m}$ FSW, 14°C) adjusted to control pH (pH 8.1) and low pH (pH

7.7). Larvae were washed three times with FSW of the appropriate pH of their rearing conditions to remove as much culture water as possible and were then transferred in a known volume of “transfer water“ into the vials with their culture pH. Depending on stage, 48 to 724 larvae were placed into one vial. For replication, 10 vials were used for larvae of the same culture (two cultures per treatment, four cultures in total, forty vials with larvae in total per time point). Different numbers of larvae were placed into the vials for density controls as suggested by Marsh and Manahan (1999). Aerobic respiration rate increased linearly with increasing amounts of larvae in the vials. As no density effect was detected and in order to show the variability within larval cultures, we regarded each vial as a sub-replicate of each culture (true replicate) and used replicate cultures as co-variable in the statistical procedure. Several vials ($n = 4$ to 8 per measurement point) without larvae were prepared for bacterial controls. Bacterial controls were conducted according to Marsh and Manahan (1999). After addition of larvae or larval-free “transfer seawater” (bacterial control) to the vials, pO_2 was measured in all vials before closure with micro-optodes calibrated as suggested in the manufacturers manual (PreSens, 4-OXY Micro, Germany). Closed vials were then incubated horizontally submerged in the waterbath for 7 to 10 hours in the dark. Continuous pO_2 measurements ($n = 2$ to 4) were conducted additionally in order to demonstrate a linearity of pO_2 decline in the respiration vials during the incubation time (data not shown). No changes in oxygen consumption rates during incubations were detected. After incubation, pO_2 was measured again and corrected for bacterial respiration. Following pO_2 measurement in the vials, larvae were pelleted by hand centrifugation, removed from the bottom of the vials and fixed in 4% PFA in seawater for enumeration. Respiration in bacterial controls did not exceed 15 % of larval respiration and pO_2 in the vials did not drop below 80% air saturation. Larvae were counted subsequently to oxygen consumption measurements. Prior to fixation for counting, larvae were checked for viability.

To control the effect of pCO_2 in respiration experiments, the pH drop due to respiratory CO_2 excretion of the larvae was measured directly in the vials before and after incubation with a pH meter (WTW 340i pH meter and Sentix 80 electrode calibrated with Radiometer NIST precision buffers) in preliminary experiments. A mean pH drop of 0.1 units (standard deviation of 0.04 units) occurred during incubation, but there was no difference between pH decreases of the two pH treatments.

2.8 Scope for growth calculations

For calculation of scope for growth (SfG), metabolic and feeding rates (regressions vs. time post-fertilization, TPF) were used to estimate daily energy input and respiratory energy loss starting at 6 days TPF by conversion of metabolic and feeding rates to energy equivalents. Metabolic rates were converted to energy equivalents ($484 \mu\text{J nmol}^{-1} \text{O}_2$, Gnaiger, 1983) based on oxyenthalpic values of lipid and protein as major constituents of echinoderm larvae (Shilling and Manahan, 1994). Larval clearance rate was converted to energy equivalents ($1.34 \cdot 10^5 \mu\text{J } \mu\text{gC}^{-1}$) using $19 \mu\text{J ng}^{-1}$ *Rhodomonas* and a cell mass of $0.15 \text{ ng cell}^{-1}$ as an estimate for our strain of *Rhodomonas* sp. (Renaud et al., 2002). Our *Rhodomonas* sp. population is characterized by an average diameter of $6.38 \mu\text{m}$ and a carbon content of $0.021 \text{ ng C cell}^{-1}$. SfG was then calculated from energy intake (I) and respiratory energy loss (R) as $\text{SfG} = \text{I} - \text{R}$.

SfG is displayed as energy available for development and is thus plotted against body length as standardization for larval morphometrics. For the calculation of the energy budget model, we assumed that larvae are 8.0 % smaller under elevated $p\text{CO}_2$ conditions than under control conditions, demonstrated by the morphometric measurements in this study.

As excretion rates are difficult to determine in sea urchin larval stages, energy loss due to excretion was omitted from the analyses. One should bear in mind that this may possibly lead to an overestimation of SfG.

2.9 Statistical analysis

Simple linear and exponential regression models were used to test the relationship type between the variables. Analysis of co-variance (ANCOVA) was used to test for $p\text{CO}_2$ effects on the tested variable using TPF or body length (BL) as co-variable. When exponential relationships were calculated, TPF and BL were logarithm transformed. For testing for different routine metabolic rates in embryonic stages (day 3 to 5 PF), a Two-way ANOVA was performed with time and pH as variables. The Shapiro–Wilk test (Shapiro and Wilk, 1965) was used to check that the data were normally distributed and the Levene test was used to check that variances were homogenous. All statistical analyses were performed using SAS/STAT® software (SAS Institute, 1990). For clarity,

regression equations, coefficients and statistics are listed in table 2. ANCOVA results are listed in table 3.

3 Results

3.1 Impact of seawater pCO_2 on larval survival

Normalized larval density in experimental cultures decreased with TPF following significant linear relationships (Figure 2A) and relative densities (RD) were estimated from the slope of the regression. Daily mortality rate (DMR) was significantly (table 3) higher under control conditions ($DMR = 2.7 \pm 0.2\% d^{-1}$) in comparison to that under high seawater pCO_2 ($DMR = 2.2 \pm 0.3\% d^{-1}$). However, when normalized against body length (BL; Figure 2B), survival was still significantly higher in the high pCO_2 treatment than that in the control treatment (table 3).

3.2 Impact of seawater pCO_2 on larval growth

Elevated seawater pCO_2 had an impact on the chronology of development. The 4-arm pluteus stage was reached (100% of the larvae) after 2 days under control conditions and after 3 days in the high pCO_2 treatment. A similar trend was observed in larval growth (BL, Figure 3A). Within the time frame of the experiment, BL growth followed a logarithmic relationship (table 2). In comparison to the control condition, increasing seawater pCO_2 had a significant negative impact on growth with no significant effects between replicates (table 3). As a consequence, at a given time, larvae were significantly different in size and larvae reached the same size at different times (Figure 3).

Similar significant relationships were also observed for other morphometric parameters (body (BRL), post-oral (POL) and posterolateral (PLL) rod lengths; Figure 4, table 2) with significant differences between pCO_2 treatments as revealed by analysis of covariance with no significant differences between replicate cultures (table 3). Differences in morphology between the pCO_2 treatments vanished when plotted against BL rather than TPF (table 3). This indicates that observed larval morphometric differences between treatments on given sampling days were a consequence of a delay in development.

Overall, the symmetry index was high (average $SI=0.97\pm 0.001$, minimum=0.90) and was not correlated to neither TPF nor BL. No difference was observed between pCO_2 treatments or replicates (Figure S1 supplementary material, TPF: $F=1.34$, $p<0.23$; BL: $F=1.38$, $p<0.22$).

3.3 Impact of seawater pCO_2 on larval morphology

The nervous system was labeled in 3 day old larvae using an anti-serotonin antibody (in red, Figure 5). The nervous system was normally developed in all treatments with regard to development stage (Bisgrove and Burke, 1986). Anti-serotonin immunoreactivity occurs in cells organized in an apical ganglion at the apical plate. In both treatments nerve cells extend fine cellular processes. Skeletal morphology was revealed by the PMC-specific cell surface marker, MSP130 (in green, Figure 5), in 3 day pluteus larvae. Skeletal rod development appeared normal in both pCO_2 treatments (Yajima and Kiyomoto, 2006).

3.4 Impact of pCO_2 on feeding

Feeding rate (FR) increased with TPF following significant linear relationships (Figure 6A, table 2). FR was significantly (table 3) higher under control conditions when compared to high pCO_2 (table 2). However, when plotted against BL (Figure 6B), FR in the high pCO_2 did not significantly differ from the control (table 3).

3.5 Impact of seawater pCO_2 on aerobic metabolic rates

Routine metabolic rates (RMR) were measured in larvae raised at pH 8.1 and 7.7. In embryonic stages (blastula, gastrula) and prism larval stages, RMR was constant, ranging from 6.9 to 10.4 $\mu\text{mol O}_2 \text{ ind}^{-1} \text{ h}^{-1}$ (Figure 7). There was no significant effect of seawater pCO_2 on RMR during embryonic development. Upon feeding (>5 days TPF), RMR increased linearly from 11.2 and 10.4 (day 7) to 29.0 and 41.9 $\mu\text{mol O}_2 \text{ ind}^{-1} \text{ h}^{-1}$ (day 21) under control conditions and elevated pCO_2 conditions, respectively (Figure 7A, table 2). No significant effect between replicate cultures was detected (table 3). The ontogenetic rate of increase in RMR under elevated pCO_2 was significantly (2 times) greater than that under control conditions when TPF was considered (table 3). When related to body length, RMR also increased linearly (Figure 7B, table 2) and the increase in respiration was significantly higher (2.1 times) under hypercapnic conditions (table 3). The

variability in RMR between low pH cultures was higher than in cultures maintained under control conditions.

3.6 Impact of seawater $p\text{CO}_2$ on scope for growth

For larval development of *S. purpuratus* under control and elevated $p\text{CO}_2$, scope for growth (SfG) was estimated using energy intake through feeding and respiratory energy loss versus larval size (body length). SfG of larvae raised under control conditions increased during larval growth from 19 μJ at a body length of 310 μm to 53 μJ at a body length of 449 μm (Figure 8A). SfG of larvae raised at elevated $p\text{CO}_2$ was reduced and showed a weaker increase during development, with values between 3 μJ at a body length of 287 μm and 13 μJ at a body length of 416 μm . SfG relative to energy input (SfG_{%I}) increased slightly in control conditions from 78% to 80 % over development. Under high $p\text{CO}_2$ conditions, SfG_{%I} was generally lower than under control conditions and decreased during development with values between 45 % to 39 % (Figure 8B). By dividing SfG by the daily growth in body length (SfG_{BL}) at a given body length), we estimated the energy that is available in *S. purpuratus* larvae to grow a certain size increment (μm) during development. SfG_{BL} increases exponentially in both treatments but steeper under control conditions: at 330 μm size larvae raised under control conditions have 30 μJ to grow another μm , while larvae under elevated $p\text{CO}_2$ only have 10 μJ . At a size of 415 μm the larvae are supplied with 110 and 50 μJ to grow one μm in length for control and elevated $p\text{CO}_2$, respectively (Figure 8C).

4 Discussion

This study revealed significant impacts of elevated seawater $p\text{CO}_2$ on the dynamic of survival, development, feeding and metabolism of *Strongylocentrotus purpuratus* larvae. Most recent studies examining sea urchin early development have focused only on development/growth and gene expression patterns in unfed larvae (Kurihara and Shirayama, 2004; Kurihara, 2008; Clark et al., 2009; Todgham and Hofmann, 2009; Brennand et al., 2010; O'Donnell et al., 2010). Here and in our companion study (Stumpp et al, submitted) we show that the impact of simulated ocean acidification on sea urchin larvae is more pronounced in feeding vs. in pre-feeding or unfed stages, resulting in a developmental delay, elevated metabolic rates and changes in gene expression patterns. Survival and feeding rate remain constant when normalized to body size (body length) as

a reference scale rather than time post-fertilization. This enables differentiation between direct effects of climate change on larval morphology and physiology and indirect effects due to delayed development. Developmental delays appear to be primarily a consequence of altered energy budgets under altered abiotic stress regimes.

4.1 Impact of $p\text{CO}_2$ on survival

Survival seemed to be positively impacted by low pH when time post-fertilization was used as a reference point. When correcting to body length, survival rate was not impacted as strongly, but was significantly higher than survival rate in control condition (by 11%). This is in contrast to larvae of the ophiuroid *Ophiotrix fragilis* which was characterized by 100% mortality at a seawater $p\text{CO}_2$ expected for the next 100-300 years (Dupont et al., 2008), but is in accordance with previous studies in a range of echinoids (*Tripneustes gratilla*, *Pseudechinus huttoni*, *Evechinus chloroticus*, *Sterechinus neumayeri*, *Echinus mathaei*, *Hemicentrotus erythrogramma*, *Hemicentrotus pulcherrimus*) where moderately elevated seawater $p\text{CO}_2$ (ca. 100-150 Pa) did not significantly alter mortality (Kurihara and Shirayama, 2004; Kurihara, 2008; Clark et al., 2009).

4.2 Impact of $p\text{CO}_2$ on growth, morphometrics and morphology

At a given time (TPF), we observed that rod and body lengths were smaller when larvae were raised under elevated $p\text{CO}_2$, compared to the control. This is in accordance with previous publications showing that an elevated $p\text{CO}_2$ resulted in smaller larvae at the same time post-fertilization (Kurihara and Shirayama, 2004; Kurihara, 2008; Clark et al., 2009; O'Donnell et al., 2010). When normalizing the different rod lengths to body length in order to correct for a potential growth delay, it became apparent that larvae raised under lower pH were not just smaller, but resemble the proportions encountered in earlier larval stages. This was confirmed by allometric comparisons. Antibody labeling of msp 130 and serotonin in 4 arm pluteus stage larvae revealed no impact of decreased seawater pH on differentiation of PMC cells or the nervous system. Development of skeletogenic cells (PMCs) and the nervous system appeared to be normal according to the 4 arm pluteus stage (Bisgrove and Burke, 1986; Yajima and Kiyomoto, 2006).

These decreased growth rates at elevated $p\text{CO}_2$ treatment in *S. purpuratus* and several other sea urchin species (*T. gratilla*, *P. huttoni*, *E. chloroticus*, *S. neumayeri*, *E.*

mathaei, *H. erythrogramma*, *H. pulcherrimus*: Kurihara and Shirayama, 2004; Kurihara, 2008; Clark et al., 2009; Brennand et al., 2010; O'Donnell et al., 2010) are very likely potentiating the susceptibility of larval stages due to the high predation pressure in the pelagic environment (Hare and Cowen, 1997; Allen, 2008; Dupont et al., 2010a) and/or have negative effect on phenology, e.g. by delaying the opportunity to settle in a favorable habitat with high quality conditions (for example seasonal feeding conditions) (Miner, 2005; Elkin and Marshall, 2007). This may influence adult recruitment and community structure of populations in the future.

4.3 Impact of pCO₂ on feeding

In sea urchin larvae, the ciliary bands running along the larval arms are the feeding structures and feeding efficiency is then directly linked to arm length. Sea urchin larvae are extremely plastic and even before the gut is fully developed and ready to digest food, larval arms grow in length depending on the environmental food conditions (Strathmann, 1971; Miner, 2005).

In our experiment, food conditions were kept constant in the two *pCO₂* treatment levels and could not alter growth of feeding structures between pH treatments. Feeding experiments revealed that when the developmental delay is ignored; feeding is apparently reduced in the high *pCO₂* treatment. When considering the developmental delay, larvae from the two *pCO₂* treatments of similar size are characterized by comparable feeding efficiency. As a consequence, the larvae are supplied with the same amount of energy for growth and maintenance under both *pCO₂* levels. A correlation between larval morphology and physiological processes in response to hypercapnia was also found in *Paracentrotus lividus*: reduced calcification rate in response to elevated *pCO₂* could be related to reduced growth rates. Skeletogenesis appeared to be normal when considering the developmental delay (Martin et al., 2011).

4.4 Impact of pCO₂ on aerobic metabolic rate and scope for growth

Routine metabolic rates increased after larvae began feeding which is in accordance with the literature for *S. purpuratus* and *Sterechinus neumayeri* (Marsh et al., 1999; Meyer et al., 2007). Our control respiration rates were in the range of published values for *S. purpuratus* (Meyer et al., 2007). Under elevated *pCO₂* larval metabolic rates increased

significantly when compared to those under control conditions (by 100%), an effect that increased in magnitude when correcting for the developmental delay. Previous studies have described a down regulation of metabolic genes in embryonic and unfed early 4-arm pluteus stages of *S. purpuratus* and *Lytechinus pictus* (Todgham and Hofmann, 2009; O'Donnell et al., 2010). In older, feeding *S. purpuratus* larvae, we found an up regulation of several metabolic genes, which is consistent with the increased metabolic rates observed in the current study (Stumpp et al. submitted).

Other studies on a range of marine invertebrates found metabolic depression under relatively high seawater $p\text{CO}_2$ values and suggested that uncompensated extracellular pH might be the trigger for these reductions (Langenbuch and Pörtner, 2002; Pörtner et al., 2004; Michaelidis et al., 2005). However, using moderate levels of acidification, metabolic rates remained unchanged or increased under CO_2 induced acidification stress in a range of species, even when extracellular pH was decreased (Gutowska et al., 2008; Wood et al., 2008; Comeau et al., 2010b; Thomsen et al., 2010; Thomsen and Melzner, 2010). An increase of metabolic rates under elevated seawater $p\text{CO}_2$ while growth and calcification rates were negatively impacted (Comeau et al., 2010b; Thomsen and Melzner, 2010) points towards higher costs for the maintenance of cellular homeostasis and calcification processes.

Deigweiher et al. (2010) investigated CO_2 induced changes in gill energy budgets in Antarctic the notothenioid fish *Gobionotothen gibberifrons* and *Notothenia coriiceps* and found that energetic demands of processes such as protein synthesis and Na^+/K^+ ATPase activity were increasing while overall metabolic rates of gill tissues remained relatively constant under hypercapnia. The Na^+/K^+ -ATPase, the main motor of cellular and extracellular acid-base balance and thus an important ion regulatory player (Melzner et al., 2009) can account for 77% of total metabolic rate in *S. purpuratus* pluteus larvae and forty percent of respiratory energy alone is needed to maintain ion balance (Leong and Manahan, (1997). As it was found that Na^+/K^+ -ATPase gene expression is upregulated under hypercapnic stress in purple sea urchin larvae (Stumpp et al submitted) it is quite likely that Na^+/K^+ -ATPase activity is increased with increasing environmental acid-base stress through CO_2 induced acidification. This could then increase routine metabolic rates under elevated $p\text{CO}_2$ conditions.

The increase in metabolic rate under elevated $p\text{CO}_2$ influences the energy balance calculated as scope for growth (SfG) in sea urchin larvae and can be correlated to the observed growth. SfG integrates physiological, cellular and biochemical changes to one response variable at the whole organism level and provides a robust tool for measuring whole animal performance under stress (Navarro et al., 2006). SfG has been shown to decrease due to a variety of stressors including temperature, salinity or pollution in a range of marine and freshwater invertebrates (Shirley and Stickle, 1982; Widdows and Johnson, 1988; Maltby et al., 1990; Gonzáles et al., 2002; Verslycke et al., 2004; Mubiana and Blust, 2007) either via decreased energy input (e.g. food intake), by increased energy loss (e.g. respiratory or excretory energy loss) or due to a combination of both. During sea urchin larval development, SfG increases exponentially with body length and in relation to the energy input SfG follows a saturation curve indicating that up to 61% of energy input can be allocated to growth/development after larvae start to feed.

Under elevated $p\text{CO}_2$, SfG is decreased by up to 50% depending on larval size. SfG follows an exponential decrease, which explains the reduced rates of development recorded. Further, the decrease in SfG during development indicates that maintenance seems to become increasingly energy consuming under hypercapnia. The energy that is supplied to grow a certain length increment increases exponentially under both conditions, which is related to rapid growth in volume. However, the energy supply to grow a defined size increment differs between treatments and highlights again, that larvae exposed to hypercapnic conditions face higher energetic demands to supply processes that are more vital on an acute basis: e.g. maintenance of cellular and extracellular homeostasis and/or maintenance of skeletal integrity. However, although gene transcription data points toward a higher need of ion regulatory activity (upregulation of Na^+/K^+ -ATPase transcripts, Stumpp et al submitted, Martin et al 2011) and possibly skeletogenesis (upregulation of calcification gene transcripts in *P. lividus*, Martin et al 2011), mechanistic data on processes that have to be fueled with additional energy is still lacking.

5 Conclusions

This study combined measurements of growth and developmental plasticity with routine metabolic and feeding rates to investigate the effects of simulated ocean acidification on *S. purpuratus* larval energy budgets. We suggest that body length is a useful scale of reference for studies in sea urchin larvae where a morphological delay in development occurs. Using time post-fertilization (TPF) as a reference may lead to misinterpretation of data. Utilizing routine metabolic and feeding rates we developed a scope for growth model (SfG) for sea urchin larvae. This is the first study that uses SfG to investigate the impact of elevated $p\text{CO}_2$ on larval energy budgets. We showed that for a given larval morphology, hypercapnia increases costs of maintenance and thus decreases SfG. However, to understand hypercapnia induced shifts in energy budgets and to pinpoint the processes that require more energy, studies focusing on ion regulatory capacity and acid-base homeostasis are needed.

6 Acknowledgements

MS and FM were funded by the DFG Excellence Cluster ‘Future Ocean’ and the German ‘Biological impacts of ocean acidification (BIOACID)’ project 3.1.4, funded by the Federal Ministry of Education and Research (BMBF, FKZ 03F0608A). SD is funded by the Linnaeus Centre for Marine Evolutionary Biology at the University of Gothenburg (<http://www.cemeb.science.gu.se/>), and supported by a Linnaeus-grant from the Swedish Research Councils VR and Formas; VR and Formas grants to MT; Knut and Alice Wallenberg’s minnen and the Royal Swedish Academy of Sciences.

7 References:

- Allen JD (2008) Size-specific predation on marine invertebrate larvae. *Biol Bull* 214:42-49
- Anstrom JA, Chin JE, Leaf DS, Parks AL, Raff RA (1987) Localization and expression of msp130, a primary mesenchyme lineage-specific cell surface protein in the sea urchin embryo. *Development* 101:255-265
- Ben-Tabou de-Leon S, Davidson EH (2007) Gene regulation: gene control network in development. *Annu Rev Biophys Biomol Struct* 36:191-212

- Biermann CH, Kessing BD, Palumbi SR (2003) Phylogeny and development of marine model species: stronglylocetrotid sea urchins. *Evol Dev* 5:360-371
- Bisgrove BW, Burke RD (1986) Development of serotonergic neurons in embryos of the sea urchin *Strongylocentrotus purpuratus*. *Develop Growth and Differ* 28:569-574
- Brennand HS, Soars N, Dworjanyn SA, Davis AR, Byrne M (2010) Impact of ocean warming and ocean acidification on larval development and calcification in the sea urchin *Tripneustes gratilla*. *Plos One* 5:e11372
- Clark D, Lamare M, Barker M (2009) Response of sea urchin pluteus larvae (Echinodermata: Echinoidea) to reduced seawater pH: a comparison among tropical, temperate, and a polar species. *Mar Biol* 156:1125-1137
- Comeau S, Jeffree R, Teyssie JL, Gattuso JP (2010) Response of the Arctic Pteropod *Limacina helicina* to projected future environmental conditions. *Plos One* 5:e11362
- Deigweier K, Hirse T, Bock C, Lucassen M, Pörtner H-O (2010) Hypercapnia induced shifts in gill energy budgets of Antarctic notothenioids. *J Comp Physiol B* 180:347-359
- Dickson AG, Millero FJ (1987) A comparison of the equilibrium constants for the dissociation of carbonic acid in seawater media. *Deep-Sea Res* 34:1733-1743. (Corrigenda. *Deep-Sea Res.* 1736, 1983)
- Doney SC, Fabry VJ, Feely RA, Kleypas JA (2009) Ocean acidification: the other CO₂ problem. *Annu Rev Marine Sci* 1:169-192
- Dupont S, Dorey N, Thorndyke M (2010a) What meta-analysis can tell us about vulnerability of marine biodiversity to ocean acidification? *Estuar Coast Shelf S* doi:10.1016/j.ecss.2010.06.013
- Dupont S, Havenhand J, Thorndyke W, Peck L, Thorndyke MC (2008) CO₂-driven ocean acidification radically affect larval survival and development in the brittlestar *Ophiotrix fragilis*. *Mar Ecol Prog Ser* 373:285-294
- Dupont S, Lundve B, Thorndyke M (2010b) Near future ocean acidification increases growth rate of the lecithotrophic larvae and juveniles of the sea star *Crossaster papposus*. *J Exp Zool B* 314B:382-389
- Dupont S, Ortega-Martínez O, Thorndyke MC (2010c) Impact of near-future ocean acidification on echinoderms. *Ecotoxicology* 19:449-462

- Ebert TA (1967) Negative growth and longevity in the purple sea urchin *Strongylocentrotus purpuratus* (Stimpson). *Science* 157:557-558
- Elkin C, Marshall DJ (2007) Desperate larvae: influence of deferred costs and habitat requirements on habitat selection. *Mar Ecol Prog Ser* 335:143-153
- Frost BW (1972) Effects of size and concentration of food particles on the feeding behaviour of the marine planktonic copepod *Calanus pacificus*. *Limnol Oceanogr* 17:805-815
- Gnaiger E (1983) Calculation of energetic and biochemical equivalents of respiratory oxygen consumption. In: Gnaiger E, Forstner H (eds) *Polarographic Oxygen Sensors: Aquatic and Physiological Applications*. Springer-Verlag, New York
- González ML, López DA, Pérez MC, Castro JM (2002) Effect of temperature on the scope for growth in juvenile scallops *Artopecten purpuratus* (Lamarck, 1819). *Aquacult Int* 10:339-349
- Guillard RRL, Ryther JH (1962) Studies of marine planktonic diatoms. I. *Cyclotella nana* Husted, and *Detonula confervacea* (Cleve). *Can J Microbiol* 8:229-239
- Gutowska MA, Pörtner H-O, Melzner F (2008) Growth and calcification in the cephalopod *Sepia officinalis* under elevated seawater $p\text{CO}_2$. *Mar Ecol Prog Ser* 373:303-309
- Hare JA, Cowen RK (1997) Size, growth, development, and survival of the planktonic larvae of *Pomatomus saltatrix* (Pisces: Pomatomidae). *Ecology* 78:2415-2431
- Kroeker KJ, Kordas RL, Crim RN, Singh GG (2010) Meta-analysis reveals negative yet variable effects of ocean acidification on marine organisms. *Ecol Lett* 13:1419-1434
- Kurihara H (2008) Effects of CO_2 -driven ocean acidification on the early developmental stages of invertebrates. *Mar Ecol Prog Ser* 373:275-284
- Kurihara H, Shirayama Y (2004) Effects of increased atmospheric CO_2 on sea urchin early development. *Mar Ecol Prog Ser* 274:161-169
- Langenbuch M, Pörtner HO (2002) Changes in metabolic rate and N excretion in the marine invertebrate *Sipunculus nudus* under conditions of environmental hypercapnia: identifying effective acid-base variables. *J Exp Biol* 205:1153-1160
- Leong PKK, Manahan DT (1997) Metabolic importance of Na^+/K^+ -ATPase activity during sea urchin development. *J Exp Biol* 200:2881-2892

- Lewis E, Wallace DWR (1998) CO₂SYN-Program developed for the CO₂ system calculations. Carbon Dioxide Inf Anal Center Report ORNL/CDIAC-105
- Maltby L, Naylor C, Calow P (1990) Effect of stress on a freshwater benthic detritivore: scope for growth in *Gammarus pulex*. *Ecotoxicol Environ Safety* 19:285-291
- Marsh AG, Leong PKK, Manahan DT (1999) Energy metabolism during embryonic development and larval growth of an antarctic sea urchin. *J Exp Biol* 202:2041-2050
- Marsh AG, Manahan DT (1999) A method for accurate measurements of the respiration rates of marine invertebrate embryos and larvae. *Mar Ecol Prog Ser* 184:1-10
- Martin S, Richier S, Pedrotti M-L, Dupont S, Castejon C, Gerakis Y, Kerros M-E, Oberhänsli F, Teyssié J-L, Gattuso JP (2011) Early development and molecular plasticity in the Mediterranean sea urchin *Paracentrotus lividus* exposed to CO₂ driven ocean acidification. *J Exp Biol* 214:1357-1368
- Mehrbach C, Culberson CH, Hawley JE, Pytkowicz RM (1973) Measurement of the apparent dissociation constants of carbonic acid in seawater at atmospheric pressure. *Limnol Oceanogr* 18:897-907
- Melzner F, Gutowska MA, Langenbuch M, Dupont S, Lucassen M, Thorndyke MC, Bleich M, Pörtner H-O (2009) Physiological basis for high CO₂ tolerance in marine ectothermic animals: pre-adaptation through lifestyle and otogeny? *Biogeosciences* 6:2313-2331
- Meyer E, Green AJ, Moore M, Manahan DT (2007) Food availability and physiological state of sea urchin larvae (*Strongylocentrotus purpuratus*). *Mar Biol* 152:179-191
- Michaelidis B, Ouzounis C, Paleras A, Pörtner H-O (2005) Effects of long-term moderate hypercapnia on acid-base balance and growth rate in marine mussels *Mytilus galloprovincialis*. *Mar Ecol Prog Ser* 293:109-118
- Miner BG (2005) Evolution of feeding structure plasticity in marine invertebrate larvae: a possible trade-off between arm length and stomach size. *J Exp Mar Biol Ecol* 315:117-125
- Mubiana VK, Blust R (2007) Effects of temperature on scope for growth and accumulation of Cd, Co, Cu and Pb by the marine bivalve *Mytilus edulis*. *Mar Environ Res* 63:219-235
- Mullin MM, Sloan PR, Eppley RW (1966) Relationship between carbon content, cell volume, and area in phytoplankton. *Limnol Oceanogr* 11:307-311

- Navarro JM, Urrutia GX, Carrasco C (2006) Scope for growth versus actual growth in the juvenile predatory gastropod *Chorus giganteus*. J Mar Biol Ass UK 86:1423-1428
- O'Donnell MJ, Todgham AE, Sewell MA, Hammond LM, Ruggiero K, Fangué NA, Zippay ML, Hofmann GE (2010) Ocean acidification alters skeletogenesis and gene expression in larval sea urchins. Mar Ecol Prog Ser 398:157-171
- Okazaki K, Inoué S (1976) Crystal property of the larval sea urchin spicule. Develop Growth and Differ 18:413-434
- Orr JC, Fabry VJ, Aumont O, Bopp L, Doney SC, Feely RA, Gnanadesikan A, Gruber N, Ishida A, Joos F, Key RM, Lindsay K, Maier-Reimer E, Matear R, Mofray P, Mouchet A, Najjar RG, Plattner G-K, Rodgers KB, Sabine CL, Sarmiento JL, Schlitzer R, Slater RD, Totterdell IJ, Weirig M-F, Yamanaka Y, Yool A (2006) Anthropogenic ocean acidification over the twenty-first century and its impact on calcifying organisms. Nature 437:681-686
- Pearse JS (2006) Ecological role of purple sea urchins. Science 314:940-941
- Pörtner H-O, Dupont S, Melzner F, Storch D, Thorndyke M (2010) Studies of metabolic rate and other characters across life stages. In: Riebesell U, Fabry VJ, Hansson L, Gattuso J-P (eds) Guide to best practices for ocean acidification research and data reporting. Publications Office of the European Union, Luxembourg, p 167-180
- Pörtner HO, Langenbuch M, Reipschläger A (2004) Biological impact of elevated ocean CO₂ concentrations: lessons from animal physiology and earth history. J Oceanogr 60:705-718
- Renaud SM, Thinh LV, Lambrinidis G, Parry DL (2002) Effect of temperature on growth, chemical composition and fatty acid composition of tropical Australian microalgae grown in batch cultures. Aquaculture 211:195-214
- Sarazin G, Michard G, Prevot F (1999) A rapid and accurate spectroscopic method for alkalinity measurements in seawater samples. Water Res 33:290-294
- SAS Institute (1990) SAS/STAT User's guide, Vol. SAS Institute
- Sea Urchin Genome Sequencing Consortium (2006) The genome of the sea urchin *Strongylocentrotus purpuratus*. Science 314:941-952
- Shapiro SS, Wilk MB (1965) An analysis of variance test for normality. Biometrika 52:591-599
- Shilling FM, Manahan DT (1994) Energy metabolism and amino acid transport during early development of antarctic and temperate echinoderms. Biol Bull 187:398-407

- Shirley TC, Stickle WB (1982) Responses of *Leptasterias hexactis* (Echinodermata: Asteroidea) to low salinity II. Nitrogen metabolism, respiration and energy budget. *Mar Biol* 69:155-163
- Smith MM, Smith LC, Cameron A, Urry LA (2008) The larval stages of the sea urchin, *Strongylocentrotus purpuratus*. *J Morph* 269:713-733
- Steneck RS, Graham MH, Bourque BJ, Corbett D, Erlandson JM, Estes JA, Tegner MJ (2002) Kelp forest ecosystems: biodiversity, stability, resilience and future. *Environ Conserv* 29:436-459
- Strathmann RR (1971) The feeding behavior of planktotrophic echinoderm larvae: mechanisms, regulation, and rates of suspension feeding. *J Exp Mar Biol Ecol* 6:109-160
- Stump M, Dupont S, Thorndyke MC, Melzner F (submitted) CO₂-induced seawater acidification impacts sea urchin larval development II: gene expression patterns in pluteus larvae. *J Comp Biochem Physiol A*
- Thomsen J, Gutowska MA, Saphörster J, Heinemann A, Fietzke J, Hiebenthal C, Eisenhauer A, Körtzinger A, Wahl M, Melzner F (2010) Calcifying invertebrates succeed in a naturally CO₂ enriched coastal habitat but are threatened by high levels of future acidification. *Biogeosciences* 7:3879-3891
- Thomsen J, Melzner F (2010) Seawater acidification does not elicit metabolic depression in the blue mussel *Mytilus edulis*. *Mar Biol* 157:2667-2676
- Todgham AE, Hofmann GE (2009) Transcriptomic response of sea urchin larvae *Strongylocentrotus purpuratus* to CO₂-driven seawater acidification. *J Exp Biol* 212:2579-2594
- Verslycke T, Roast SD, Widdows J, Jones MB, Janssen CR (2004) Cellular energy allocation and scope for growth in the estuarine mysid *Neomysis integer* (Crustacea : Mysidacea) following chlorpyrifos exposure: a method comparison. *J Exp Mar Biol Ecol* 306:1-16
- Widdows J, Johnson D (1988) Physiological energetics of *Mytilus edulis*: scope for growth. *Mar Ecol Prog Ser* 46:113-121
- Wood HL, Spicer JI, Widdicombe S (2008) Ocean acidification may increase calcification rates, but at a cost. *P Roy Soc B Bio* 275:1767-1773
- Yajima M, Kiyomoto M (2006) Study of larval and adult skeletogenic cells in developing sea urchin larvae. *Biol Bull* 211:183-192

Figure captions

Figure 1: Morphometric coordinates and morphology of a *Strongylocentrotus purpuratus* 4-arm pluteus larva. BL, body length; BRL, body rod length; PLL, posterolateral arm length; POL, post-oral rod length. Scale bar 50 μm .

Figure 2: Relative density of larvae in triplicate cultures under control (black symbols, solid regression, pH=8.1, $p\text{CO}_2$ 38 Pa) and elevated $p\text{CO}_2$ (open symbols, dashed regression, pH=7.7, $p\text{CO}_2$ 128 Pa) plotted against time post-fertilization (TPF, A) and body length (BL, B). If only two data points are visible, data points overlap. Mortality plotted against TPF and body length differs significantly between treatments (table 3). Regression equations and coefficients are listed in table 2.

Figure 3: Growth of body length (BL) of triplicate cultures (pH 8.1 black symbols and solid regression, pH 7.7 open symbols and dashed regression) plotted against time post-fertilization. Regressions differ significantly between treatments (table 3). Regression equations and coefficients are listed in table 2

Figure 4: Individual growth of 3 measured morphometric parameters in triplicate cultures (body rod length, BRL; posterolateral rod length, PLL and postoral rod length, POL, μm) plotted against time post-fertilization (A, C, E) and body length (B, D, F). See figure 1 for definition of the parameters. Significant differences between control (black symbols, solid regression) and elevated $p\text{CO}_2$ (open symbols, dashed regression) treatments were only observed, when morphometrics were plotted against time post-fertilization (table 3). For clarity reasons, regression equations and coefficients are listed in table 2.

Figure 5: Confocal laser scanning images of the larval endoskeleton (primary mesenchyme cells – PMC) and nervous system, using PMC-specific cell surface antibody, MSP130 (green), and anti-serotonin (red) antibodies, in 4-arm pluteus stage of *Strongylocentrotus purpuratus* larvae raised under control (A, dorsal view) and elevated $p\text{CO}_2$ conditions (B, left side). Scale bar for A and B with 50 μm .

Figure 6: Feeding rate (FR, $\text{ng C ind}^{-1} \text{h}^{-1}$) of larvae raised under control (black symbols, solid regression) and elevated $p\text{CO}_2$ (open symbols, dashed regression) plotted against time post-fertilization (A) and body length (B). Significant differences were observed

between treatments when plotted against time post-fertilization (table 3) but not when plotted against body length (table 3). Regression equations and coefficients are listed in table 2.

Figure 7: Routine metabolic rates in duplicate cultures (RMR, $\text{pmol O}_2 \text{ ind}^{-1} \text{ h}^{-1}$) of larvae raised under control (black symbols, solid regression) and low pH conditions (open symbols, dashed regression) plotted against time post-fertilization (A) and body length (B). Vertical line indicates start of feeding. Significant difference between treatments were observed after feeding commences when plotting RMR against time post-fertilization (table 3) as well as body length (table 3). Regression equations and coefficients are listed in table 2.

Figure 8: Scope for growth (SfG) for larvae raised under control (solid line) and elevated $p\text{CO}_2$ (dashed line) conditions. SfG was calculated from metabolic and feeding rates and were normalized onto larval size assuming a reduced size of 8% under elevated $p\text{CO}_2$ conditions in comparison to control. A SfG ($\mu\text{J ind}^{-1} \text{ h}^{-1}$). B SfG_{%I} (% energy income). C SfG_{BL} ($\mu\text{J ind}^{-1} \mu\text{m}^{-1}$).

Table captions

Table 1 Carbonate system speciation in the experimental treatments. Total dissolved inorganic carbon (C_T), $p\text{CO}_2$ and calcium carbonate saturation state for aragonite and calcite (Ω_{Ca} , Ω_{Ar}) were calculated from pH_{NBS} and A_T .

Table 2 Results of the regression analysis of measured parameters in *S. purpuratus* larvae raised under control (pH 8.1) and elevated $p\text{CO}_2$ conditions (pH 7.7): relative density (RD), larval body morphometrics (BL body length, BRL body rod length, PLL posterolateral rod length, POL postoral rod length), routine metabolic rates (RMR) and feeding rates (FR) relative to time post-fertilization (TPF) and body length (BL).

Table 3 Analysis of covariance (ANCOVA) results of measured parameters in *S. purpuratus* larvae raised under control (pH 8.1) and elevated $p\text{CO}_2$ conditions (pH 7.7): relative density (RD), larval body morphometrics (BL body length, BRL body rod length, PLL posterolateral rod length, POL postoral rod length), routine metabolic rates (RMR) and feeding rates (FR) relative to time post-fertilization (TPF) and body length (BL).

Figure 1

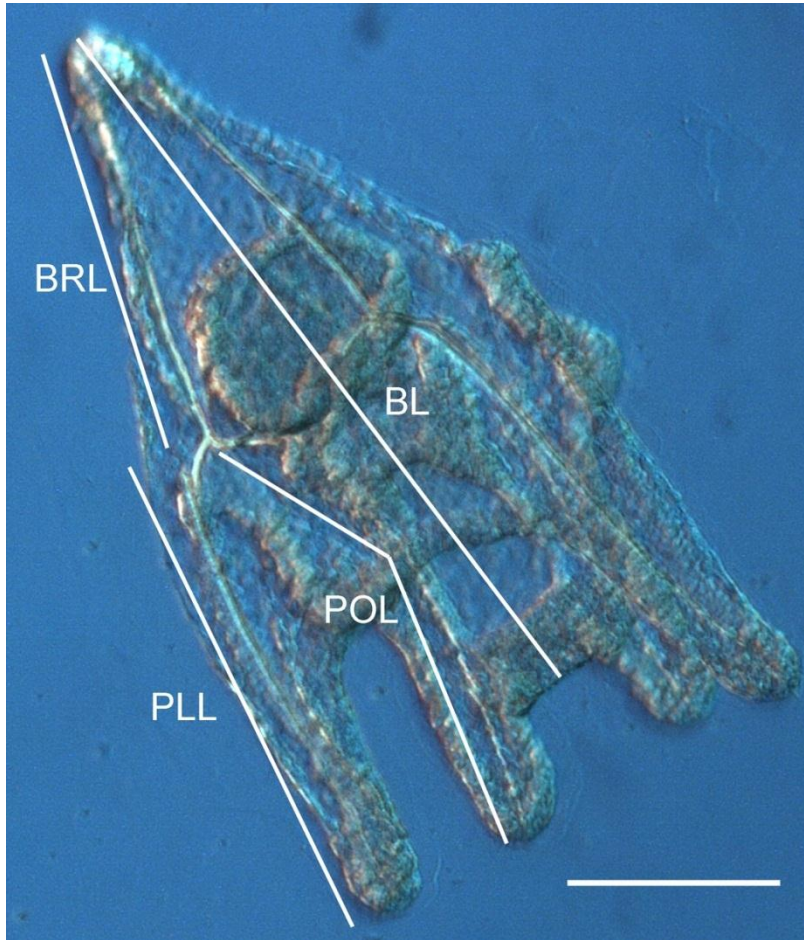
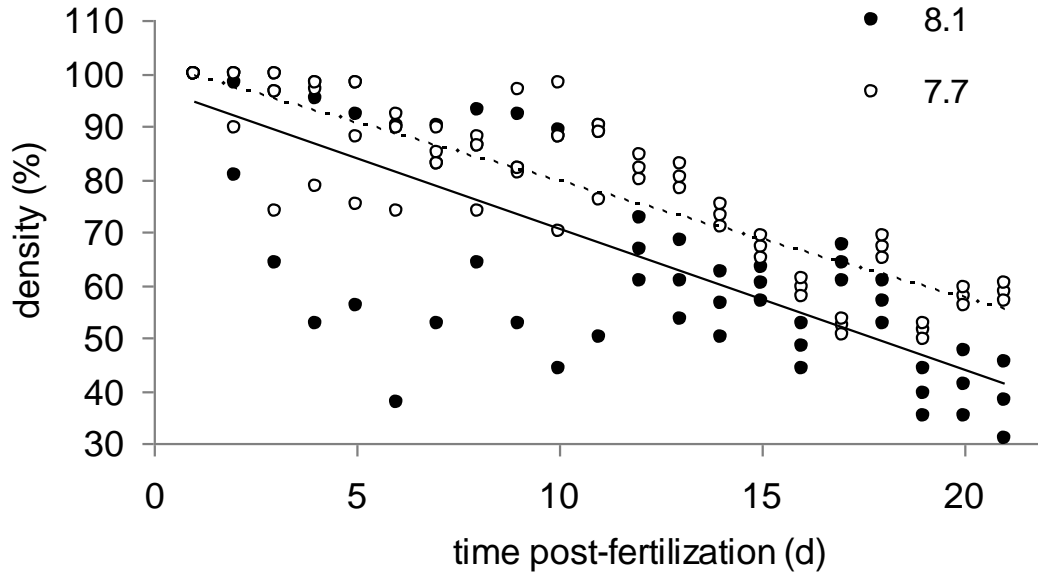


Figure 2

A



B

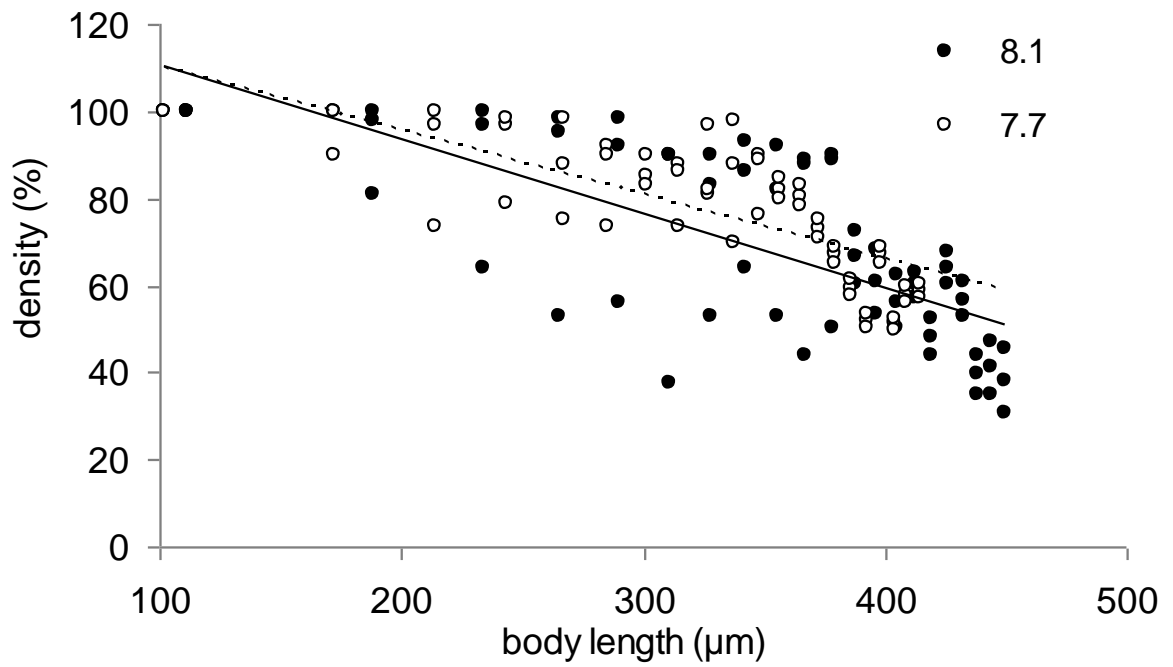


Figure 3

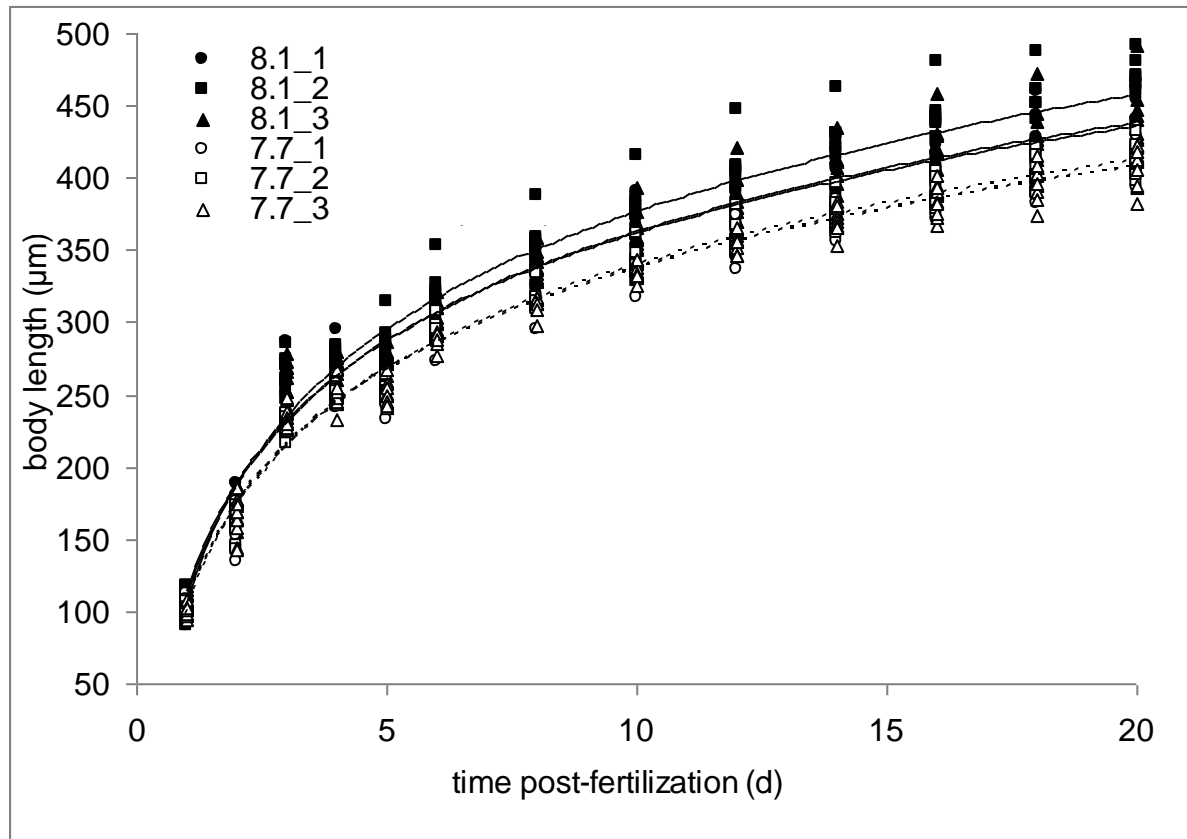
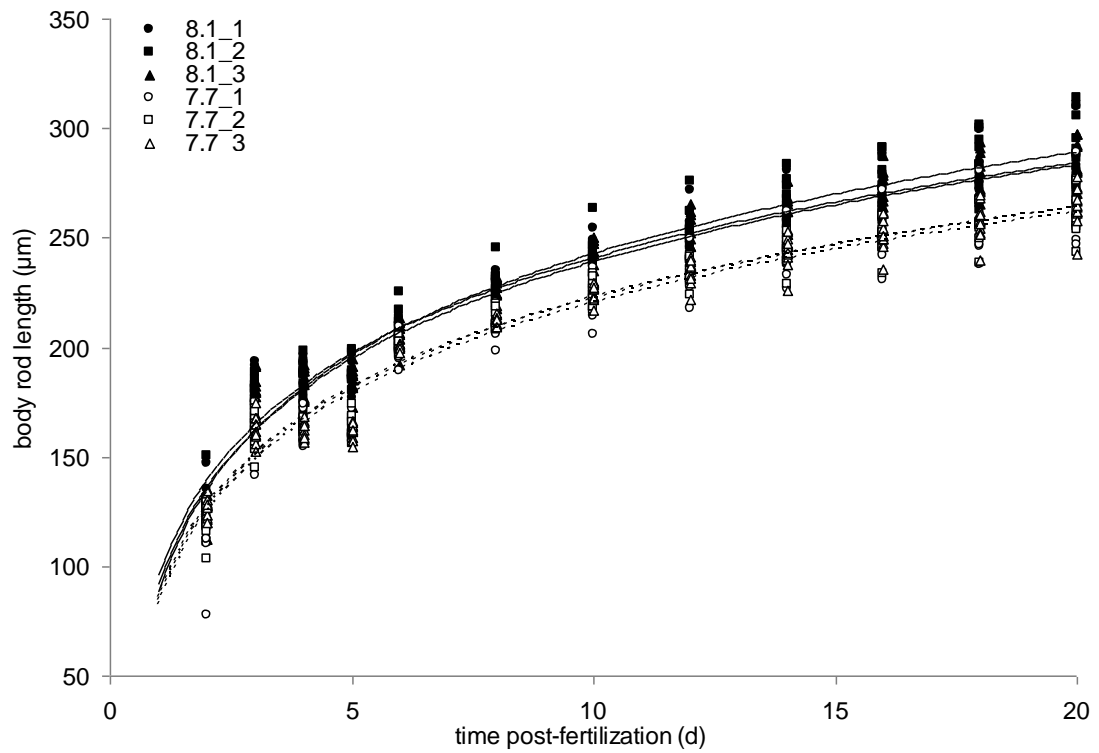
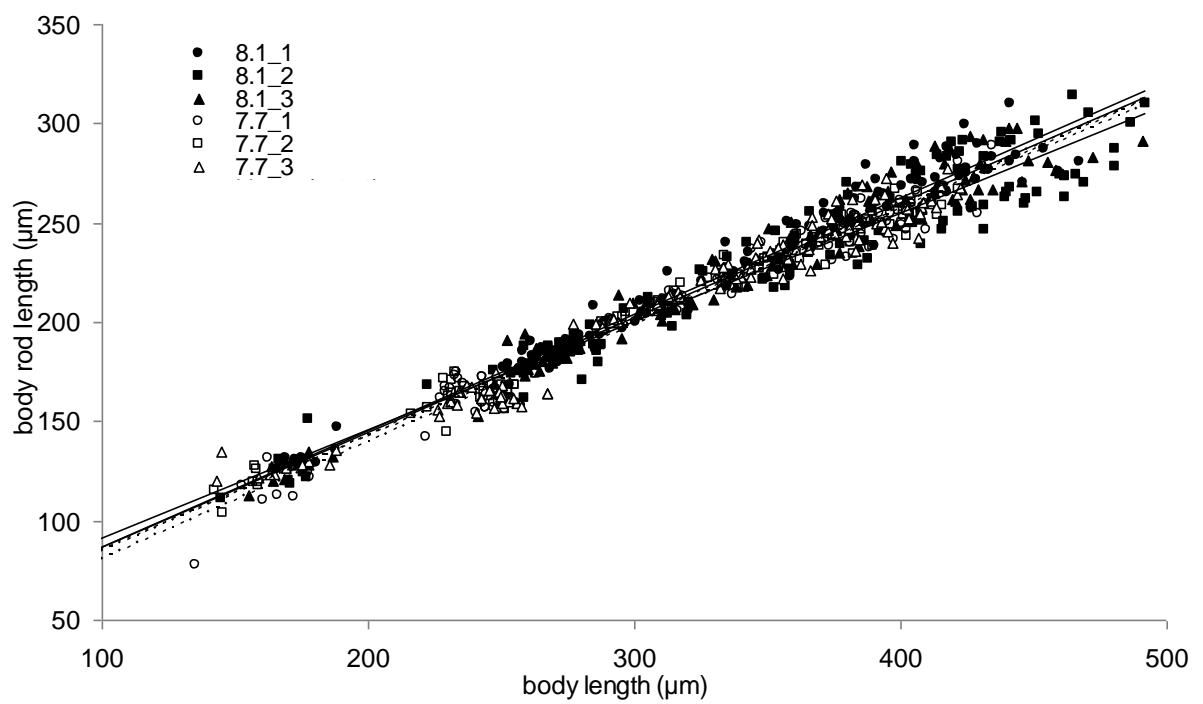


Figure 4

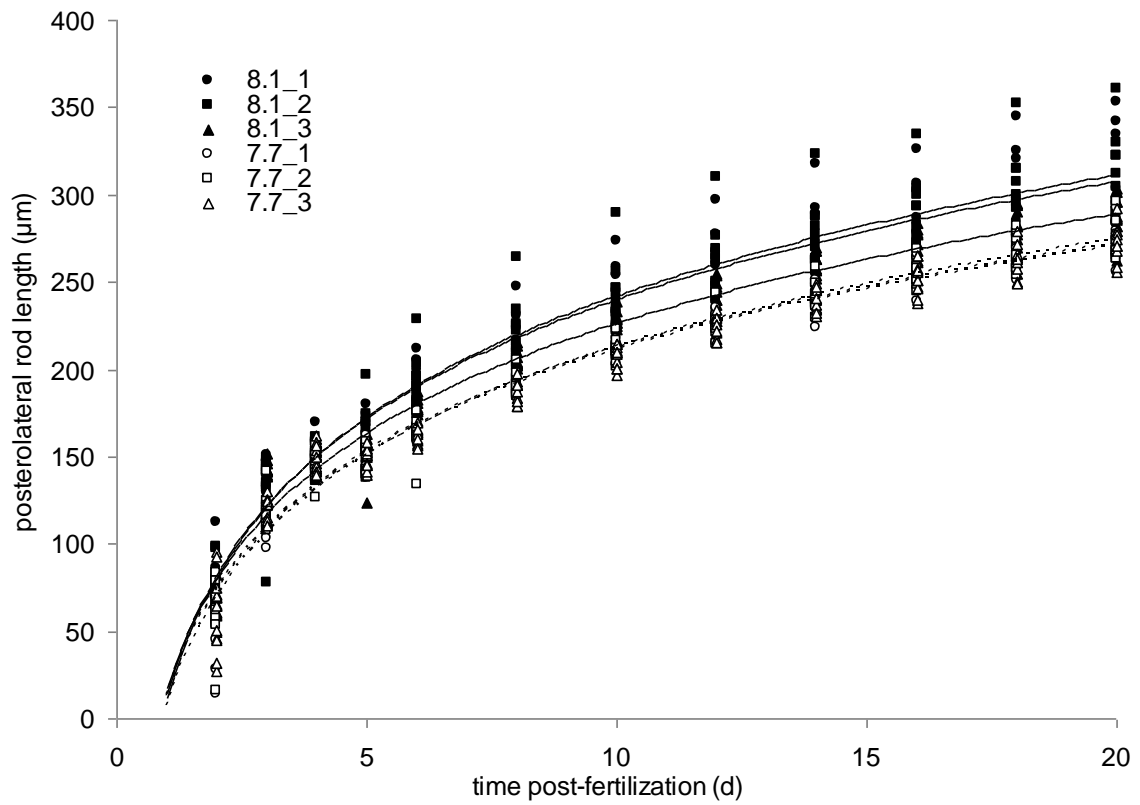
A



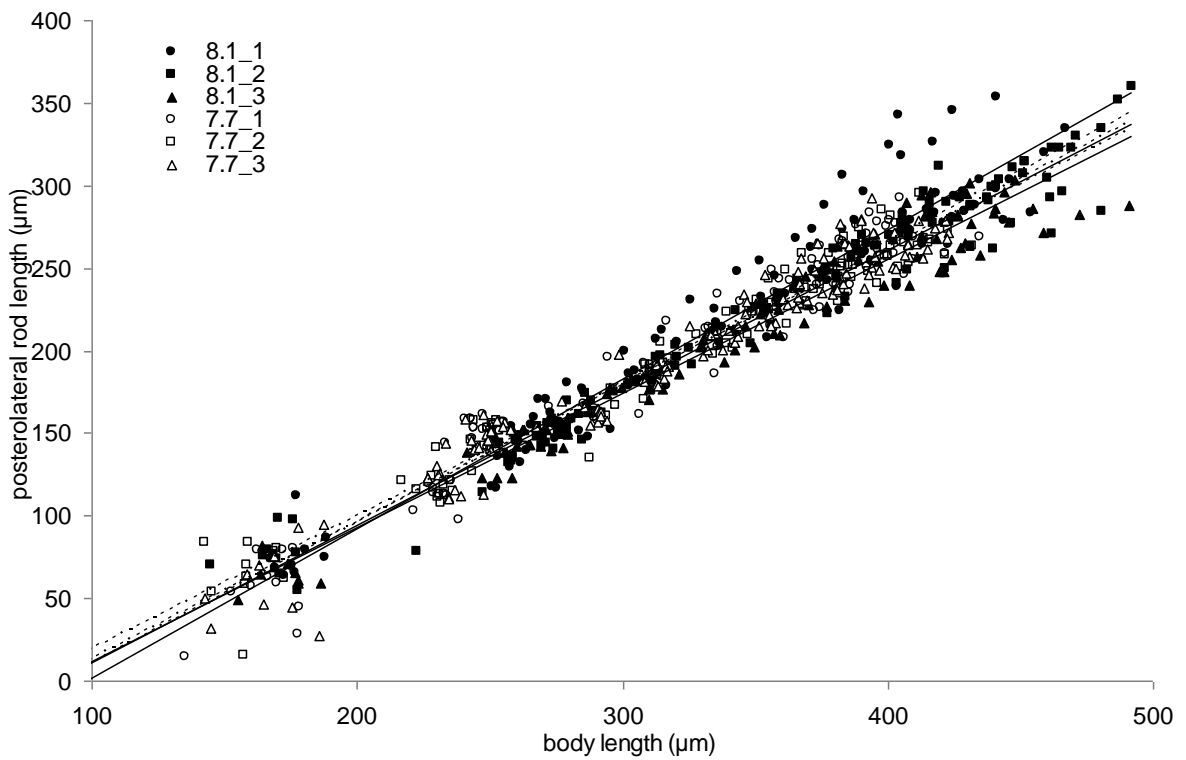
B



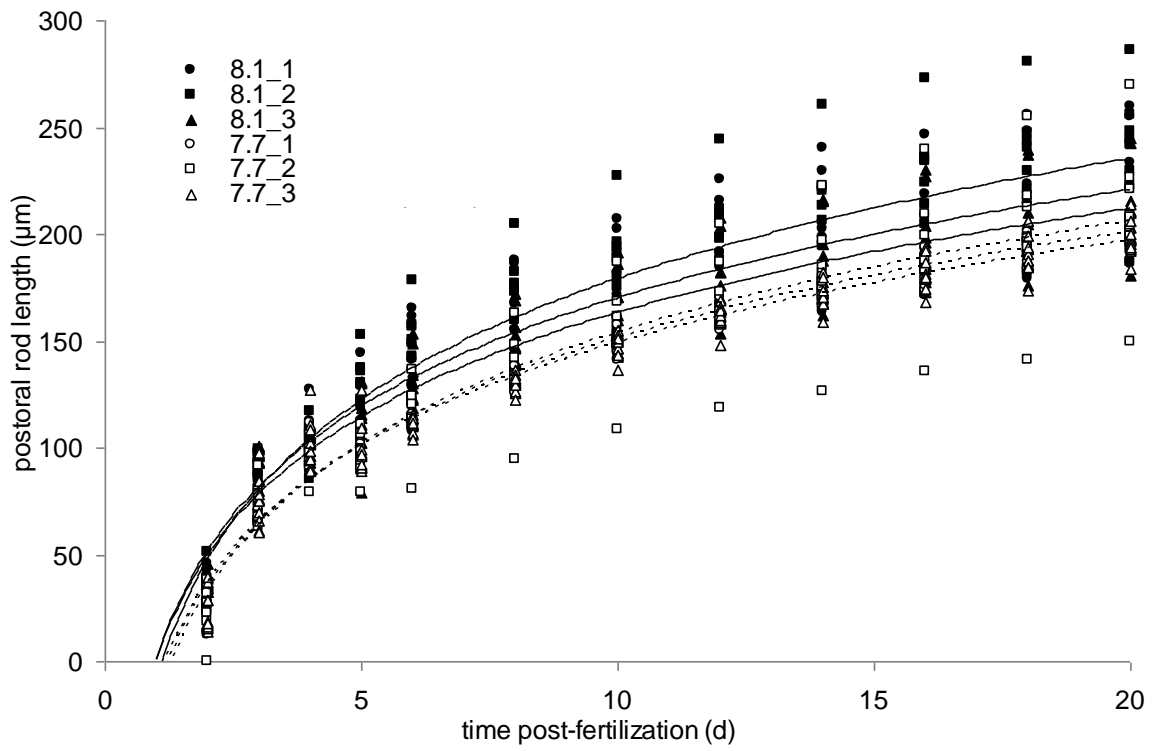
C



D



E



F

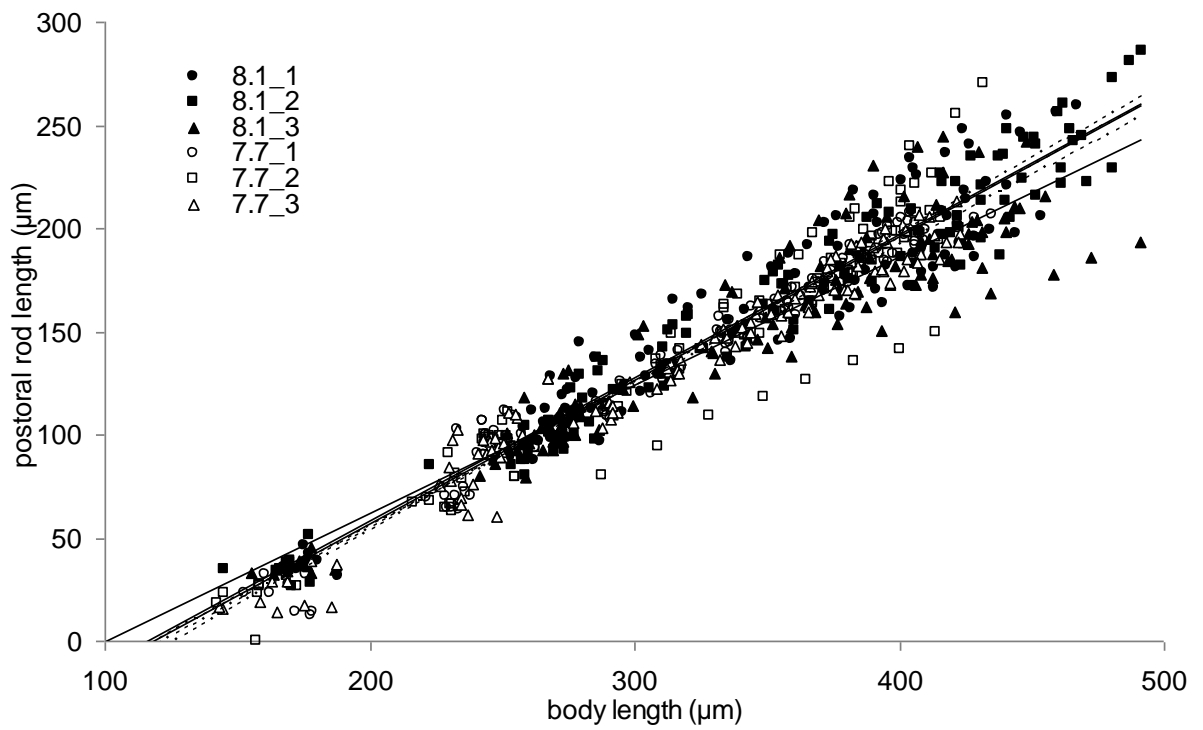


Figure 5

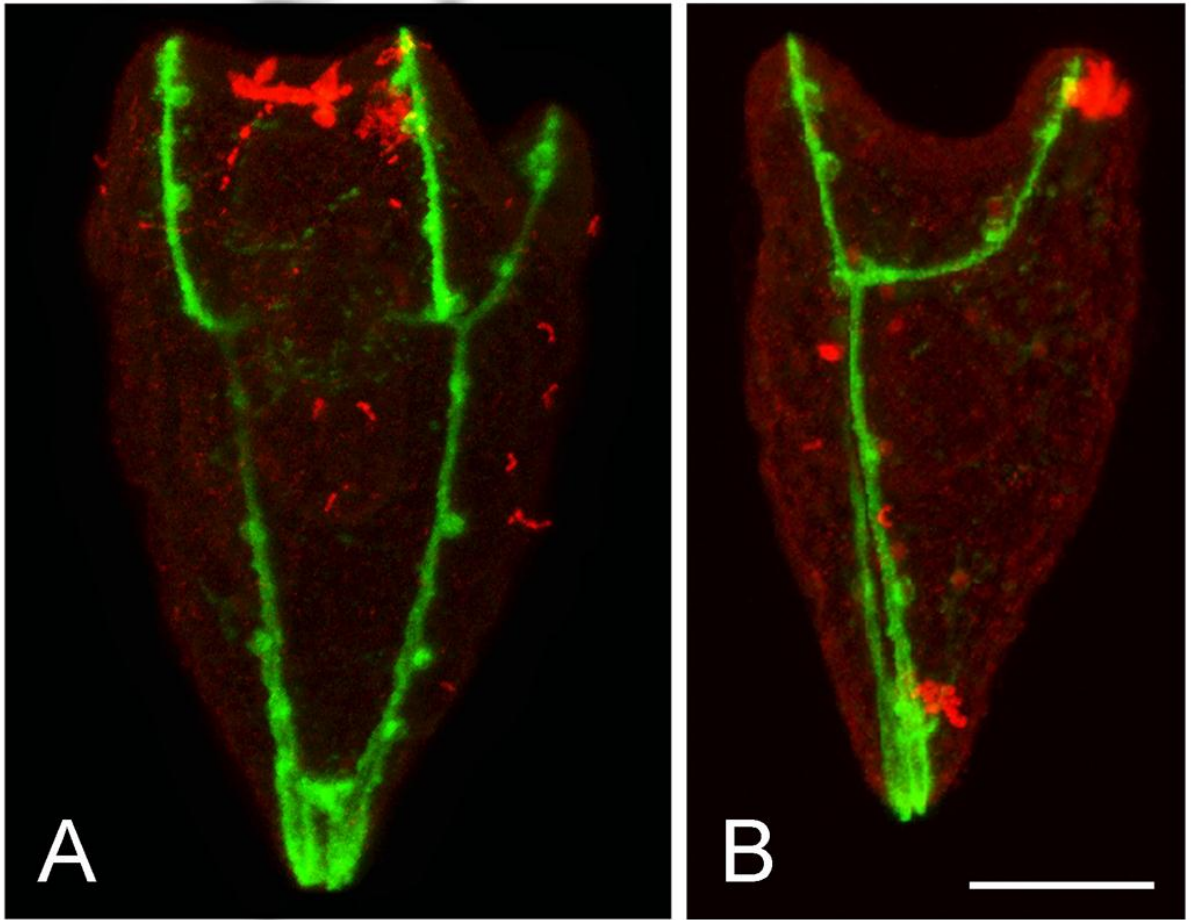
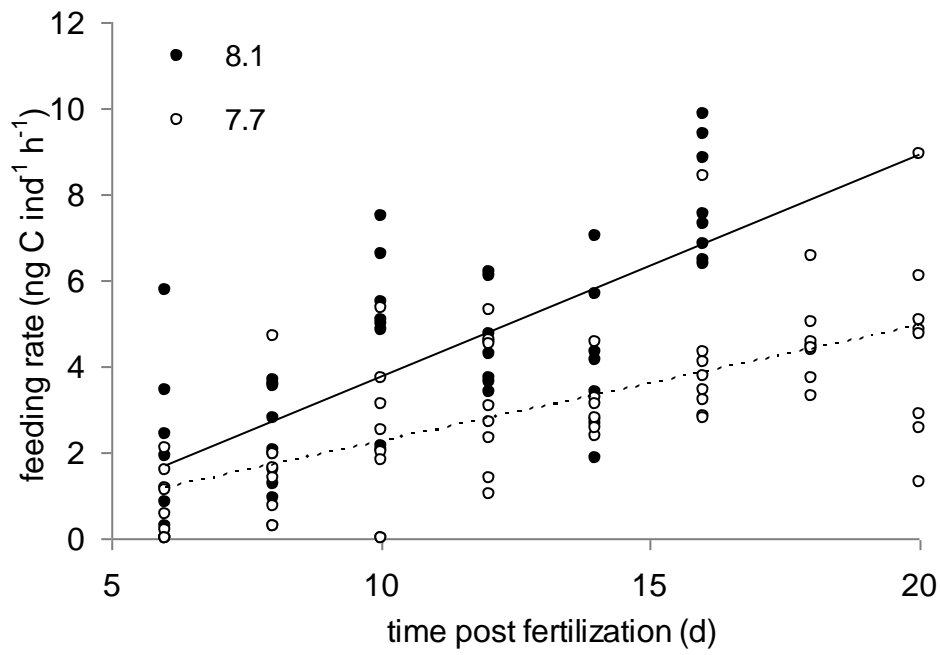
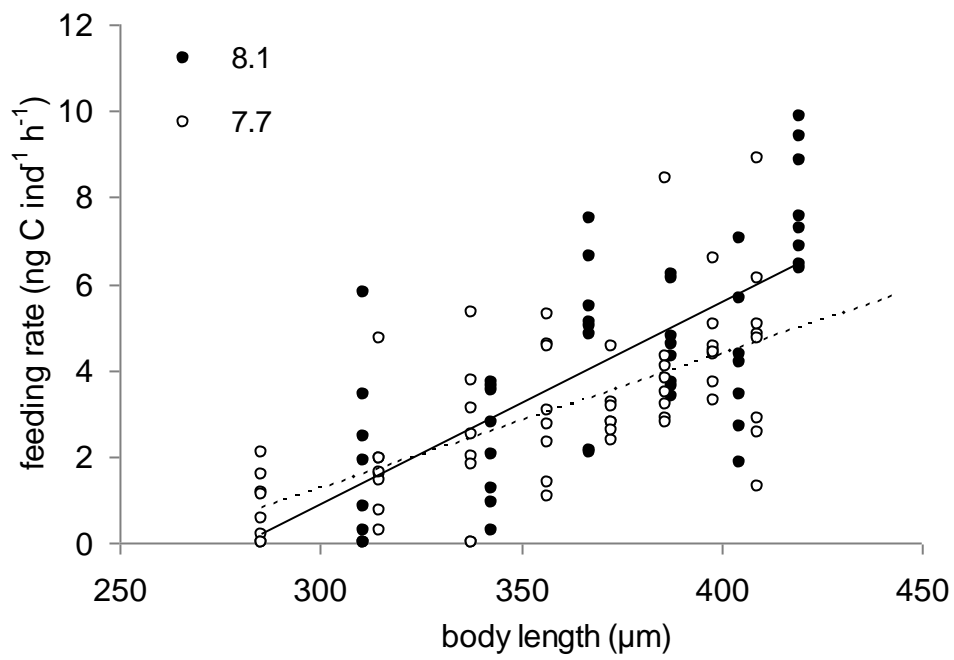


Figure 6

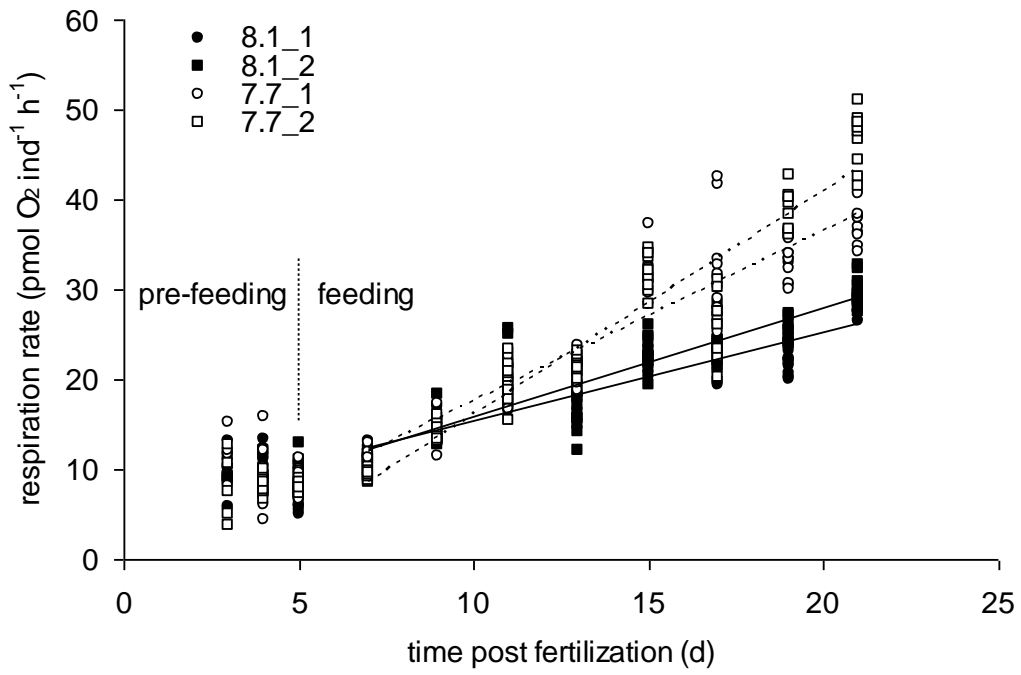


A

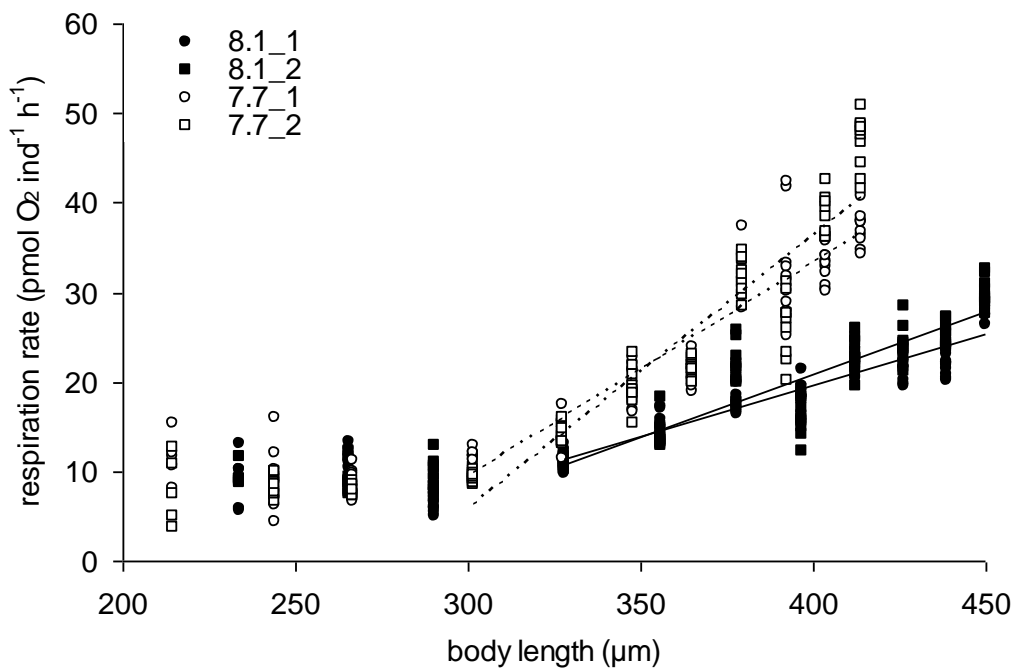


B

Figure 7

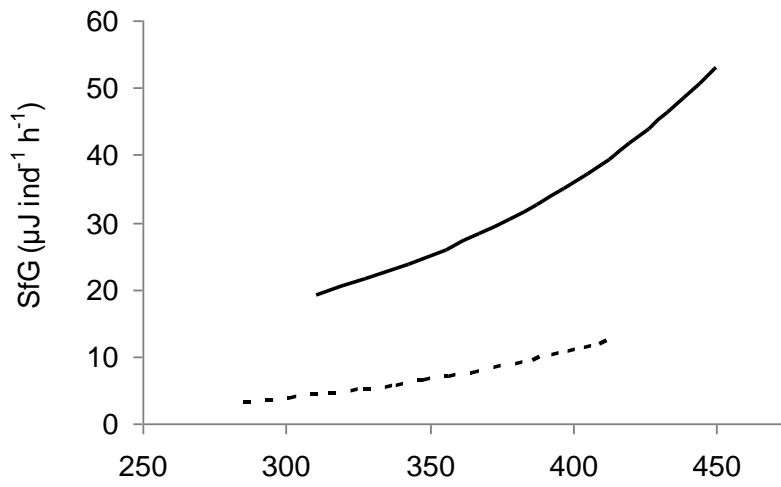


A

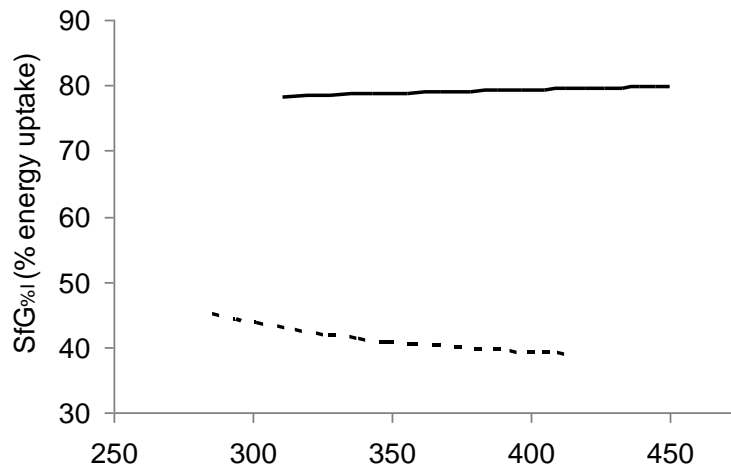


B

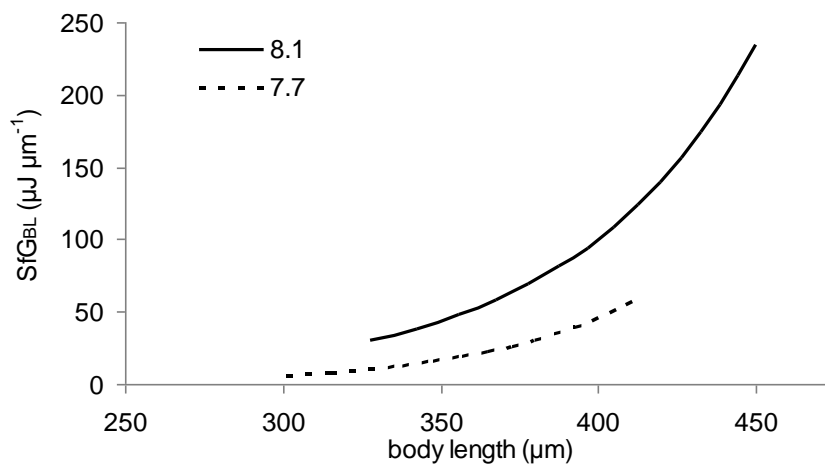
Figure 8



A



B



C

Table 1

pH_{NBS}	A_{T} ($\mu\text{mol/kg}$ SW)	S	T ($^{\circ}\text{C}$)	pCO_2 (Pa)	C_{T} ($\mu\text{mol/kg}$ SW)	Ω_{Ca}	Ω_{Ar}
8.18 ± 0.02	2200 ± 30	32	14	38 ± 3	2002 ± 37	3.42 ± 0.08	2.18 ± 0.05
7.70 ± 0.02	2200 ± 30	32	14	128 ± 8	2170 ± 36	1.27 ± 0.04	0.81 ± 0.02

Table 2

Parameter	Regression	R ²	df	F	p
RD vs TPF					
pH 8.1	RD = - 2.7 TPF + 97.2	0.58	1, 61	82.7	<0.001
pH 7.7	RD = - 2.2 TPF + 101.7	0.75	1, 61	179.2	<0.001
RD vs BL					
pH 8.1	RD = - 0.17 BL + 1.28	0.51	1, 61	63.4	<0.001
pH 7.7	RD = - 0.15 BL + 1.25	0.61	1, 61	94.7	<0.001
BL vs TPF					
pH 8.1	BL = 111.05 ln(TPF) + 111.71	0.96	1, 388	905.2	<0.001
pH 7.7	BL = 103.78 ln(TPF) + 105.05	0.96	1, 388	828.6	<0.001
BRL vs TPF					
pH 8.1	BRL = 81.96 ln(TPF) + 52.22	0.92	1, 358	1411.8	<0.001
pH 7.7	BRL = 76.92 ln(TPF) + 49.28	0.90	1, 358	1353.9	<0.001
BRL vs BL					
pH 8.1	BRL = 0.58 BL + 29.15	0.96	1, 358	6649.5	<0.001
pH 7.7	BRL = 0.58 BL + 26.28	0.96	1, 358	10949.0	<0.001
PLL vs TPF					
pH 8.1	PLL = 98.88 ln(TPF) + 8.46	0.96	1, 358	954.0	<0.001
pH 7.7	PLL = 91.87 ln(TPF) + 7.16	0.96	1, 358	624.4	<0.001
PLL vs BL					
pH 8.1	PLL = 0.81 BL - 68.74	0.96	1, 358	6333.9	<0.001
pH 7.7	PLL = 0.83 BL - 70.52	0.95	1, 358	7476.7	<0.001
POL vs TPF					
pH 8.1	POL = 74.68 ln(TPF) - 0.82	0.92	1, 358	616.6	<0.001
pH 7.7	POL = 71.55 ln(TPF) - 6.54	0.93	1, 356	575.1	<0.001
POL vs BL					
pH 8.1	POL = 0.62 BL - 62.55	0.88	1, 358	3829.5	<0.001
pH 7.7	POL = 0.68 BL - 80.66	0.96	1, 356	6175.0	<0.001
FR vs TPF					
pH 8.1	FR = 0.52 TPF - 1.38	0.50	1, 45	45.5	<0.001
pH 7.7	FR = 0.27 TPF - 0.46	0.42	1, 61	44.7	<0.001
FR vs BL					
pH 8.1	FR = 0.05 BL - 13.05	0.48	1, 45	42.1	<0.001
pH 7.7	FR = 0.03 BL - 8.12	0.43	1, 61	46.2	<0.001
RMR vs TPF					
pH 8.1	RMR = 1.09 TPF + 4.76	0.80	1, 156	639.7	<0.001
pH 7.7	RMR = 2.18 TPF - 4.98	0.87	1, 154	1074.9	<0.001
RMR vs BL					
pH 8.1	RMR = 0.13 BL - 30.38	0.80	1, 156	637.5	<0.001
pH 7.7	RMR = 0.27 BL - 73.42	0.85	1, 154	884.4	<0.001

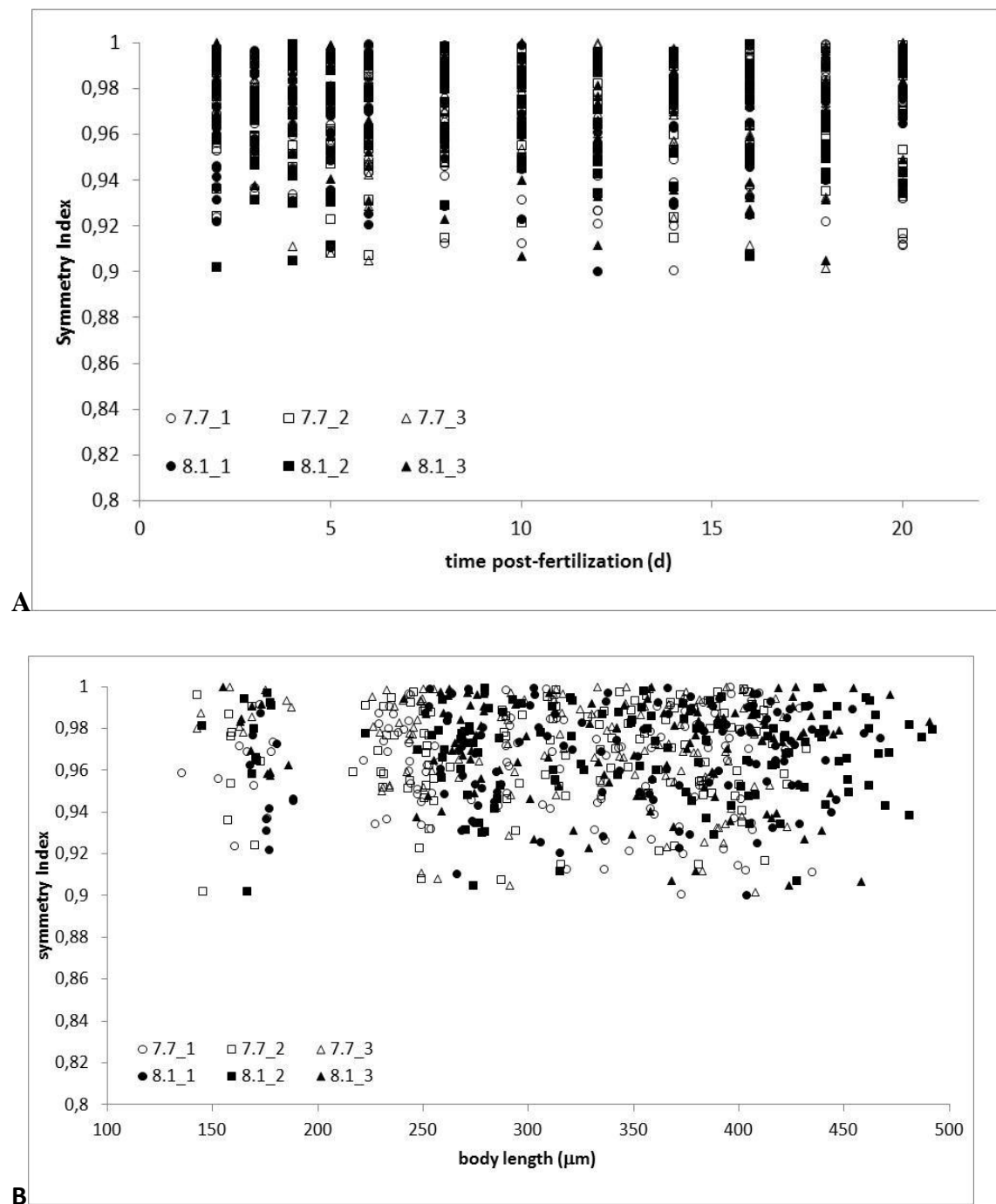
Table 3

Parameter	Source	df	F	p
RD vs TPF	Model	1, 123	115.1	<0.001
	pH	1	20.7	<0.001
	Time	1	209.4	<0.001
RD vs BL	Model	1, 123	80.92	<0.001
	pH	1	4.3	<0.05
	Time	1	209.4	<0.001
BL vs TPF ^a	Model	5, 773	292.8	<0.001
	pH	1	28.6	<0.001
	Time	1	1727.0	<0.001
	Replicate	4	0.3	= 0.87
BRL vs TPF ^a	Model	5, 713	479.7	<0.001
	pH	1	114.9	<0.001
	Time	1	2761.1	<0.001
	Replicate	4	0.6	= 0.69
BRL vs BL	Model	5, 713	2903.6	<0.001
	pH	1	1.6	= 0.12
	Time	1	16720.2	<0.001
	Replicate	4	1.0	= 0.40
PLL vs TPF ^a	Model	5, 713	261.6	<0.001
	pH	1	40.8	<0.001
	Time	1	1524.1	<0.001
	Replicate	4	1.17	= 0.32
PLL vs BL	Model	5, 713	2457.7	<0.001
	pH	1	0.96	= 0.33
	Time	1	14282.7	<0.001
	Replicate	4	1.0	= 0.41
POL vs TPF ^a	Model	5, 771	201.3	<0.001
	pH	1	39.5	<0.001
	Time	1	1166.3	<0.001
	Replicate	4	0.81	= 0.52
POL vs BL	Model	5, 771	1619.6	<0.001
	pH	1	0.27	= 0.60
	Time	1	9370.9	<0.001
	Replicate	4	2.8	= 0.06
FR vs TPF	Model	1, 107	46.1	<0.001
	pH	1	33.0	<0.001
	Time	1	78.2	<0.001
FR vs BL	Model	1, 107	49.7	<0.001
	pH	1	4.62	= 0.054
	Time	1	84.81	<0.001
RMR vs TPF	Model	3, 309	304.7	<0.001
	pH	1	142.4	<0.001
	Time	1	1073.4	<0.001
	Replicate	2	2.42	= 0.09
RMR vs TPF	Model	3, 309	253.7	<0.001
	pH	1	470.8	<0.001
	Time	1	888.8	<0.001
	Replicate	2	2.0	= 0.13

^a On log transformed data.

Supplementary material:

Figure S1: symmetry index (SI) of *Strongylocentrotus purpuratus* larvae in triplicate cultures exposed to control (pH 8.1, filled symbols) and elevated $p\text{CO}_2$ (pH 7.7, open symbols) conditions. SI was calculated as the ratio of right to left overall length. SI was not correlated to neither time post-fertilization (A) nor body length (B).



II CO₂ induced seawater acidification impacts sea urchin larval development II: gene expression patterns in pluteus larvae

Stumpp, M. ; Dupont, S. ; Thorndyke, M.C. ; Melzner, F.

Comparative Biochemistry and Physiology A (2011) doi:10.1016/j.cbpa.2011.06.023

CO₂ induced seawater acidification impacts sea urchin larval development II: gene expression patterns in pluteus larvae

Stumpp, M. ¹; Dupont, S. ²; Thorndyke, M.C. ³; Melzner, F. ¹

1 Biological Oceanography, Leibniz-Institute of Marine Sciences (IFM-GEOMAR), 24105 Kiel, Germany

2 Department of Marine Ecology, Sven Lovén Centre for Marine Sciences, Kristineberg, University of Gothenburg, Sweden

3 The Royal Swedish Academy of Sciences, Sven Lovén Centre for Marine Sciences, Kristineberg, University of Gothenburg, Sweden

Corresponding author: Meike Stumpp, Biological Oceanography, Leibniz-Institute of Marine Sciences (IFM-GEOMAR), Hohenberg Str. 2, 24105 Kiel, Germany, mstumpp@ifm-geomar.de

Keywords: *Strongylocentrotus purpuratus*, larvae, pluteus, echinoderm, growth, RT-qPCR, ocean acidification, climate change, development

Abstract

Extensive use of fossil fuels is leading to increasing CO₂ concentrations in the atmosphere and causes changes in the carbonate chemistry of the oceans which represents a major sink for anthropogenic CO₂. As a result, the oceans' surface pH is expected to decrease by ca. 0.4 units by the year 2100, a major change with potentially negative consequences for some marine species. Because of their carbonate skeleton, sea urchins and their larval stages are regarded as likely to be one of the more sensitive taxa.

In order to investigate sensitivity of pre-feeding (2 days post-fertilization) and feeding (4 and 7 days post-fertilization) pluteus larvae, we raised *Strongylocentrotus purpuratus* embryos in control (pH 8.1 and *p*CO₂ 41 Pa e.g. 399 µatm) and CO₂ acidified seawater with pH of 7.7 (*p*CO₂ 134 Pa e.g. 1318 µatm) and investigated growth, calcification and survival. At three time points (day 2, day 4 and day 7 post-fertilization), we measured the expression of 26 representative genes important for metabolism, calcification and ion regulation using RT-qPCR.

After one week of development, we observed a significant difference in growth. Maximum differences in size were detected at day 4 (ca. 10 % reduction in body length). A comparison of gene expression patterns using PCA and ANOSIM clearly distinguished between the different age groups (Two way ANOSIM: Global R=1) while acidification effects were less pronounced (Global R=0.518). Significant differences in gene expression patterns (ANOSIM R=0.938, SIMPER: 4.3% difference) were also detected at day 4 leading to the hypothesis that differences between CO₂ treatments could reflect patterns of expression seen in control experiments of a younger larva and thus a developmental artifact rather than a direct CO₂ effect. We found an up regulation of metabolic genes (between 10 to 20% in ATP-synthase, citrate synthase, pyruvate kinase and thiolase at day 4) and down regulation of calcification related genes (between 23 and 36% in *m*sp130, SM30B, SM50 at day 4). Ion regulation was mainly impacted by up regulation of Na⁺/K⁺-ATPase at day 4 (15%) and down regulation of NHE3 at day 4 (45%).

We conclude that in studies in which a stressor induces an alteration in the speed of development, it is crucial to employ experimental designs with a high time resolution

in order to correct for developmental artifacts. This helps prevent misinterpretation of stressor effects on organism physiology.

1 Introduction

Due to anthropogenic CO₂ emissions, atmospheric $p\text{CO}_2$ is expected to reach values of 70-100 Pa (ca. 700-1000 μatm) by the end of this century (Caldeira and Wickett, 2005; Cao and Caldeira, 2008). This increase in $p\text{CO}_2$ will alter ocean surface water carbonate chemistry, resulting in a reduction of ocean carbonate concentrations and a decrease in pH by up to ca. 0.4 units. It has been suggested that this progressive ocean acidification will negatively impact marine heterotrophic organisms by slowing calcification rates or even causing dissolution of carbonate shells when saturation states of calcite (Ω_{calc}) or aragonite (Ω_{arag}) drop below unity (Orr et al., 2006; Hoegh-Guldberg et al., 2007). However, recent evidence indicates that elevated seawater $p\text{CO}_2$ impacts marine ectothermic organisms through multiple processes, such as disturbances in acid-base and ion homeostasis, metabolism, somatic growth and reproduction and thus not only impacts calcification. An altered energy partitioning between different physiological processes may be a key effect of seawater acidification on heterotrophic organisms (see Fabry, 2008 ; Pörtner and Farrell, 2008; Wood et al., 2008; Melzner et al., 2009; Dupont et al., 2010c for reviews).

In echinoderms, high mortalities and morphological abnormalities were observed in ophiuroid larvae exposed to a seawater $p\text{CO}_2$ of approximately 74 Pa (Dupont et al., 2008). Studies on other echinoderm species also reported growth delays (Kurihara and Shirayama, 2004; Kurihara, 2008; Clark et al., 2009; Brennand et al., 2010; O'Donnell et al., 2010), and reduced fertilization success (Havenhand et al., 2008), but in other cases could increase developmental success (Dupont et al., 2010b) or had no measurable effect on development or fertilization (Carr et al., 2006; Byrne et al., 2009; Byrne et al., 2010a; Byrne et al., 2010b; Ericson et al., 2010) all at seawater $p\text{CO}_2$ values expected for the next century. These conflicting findings indicate high species specificity of seawater $p\text{CO}_2$ impacts on echinoderms (for review see Dupont et al., 2010c).

Because of the direct impacts of rising $p\text{CO}_2$ on the carbonate chemistry of seawater, calcification has been the primary target of previous investigations. Responses of various invertebrate taxa are diverse, ranging from reductions in calcification rates (Langdon and Atkinson, 2005; Shirayama and Thornton, 2005; Gazeau et al., 2007; Clark et al., 2009) to increases in calcification rates (Gutowska et al., 2008; Wood et al., 2008; Gutowska et al., 2010b). In sea urchin larvae, reduced growth has been observed in

several studies. Although calcification rates appeared to be normal in relation to size in *Paracentrotus lividus* larvae (Martin et al., 2011), it is unclear whether hypercapnia effects on growth are due to reductions in calcification performance or whether calcification is affected in a secondary fashion due to changes in somatic growth rate (Kurihara and Shirayama, 2004; Clark et al., 2009; Brennand et al., 2010; O'Donnell et al., 2010). The few studies examining calcification under high $p\text{CO}_2$ by means of gene expression analysis mainly observed a down regulation of genes connected with calcification in early sea urchin larval stages (Todgham and Hofmann, 2009; O'Donnell et al., 2010). In contrast, Martin et al. (2011) demonstrated that expression of calcification genes in *P. lividus* was increased in response to elevated $p\text{CO}_2$. In lecithotrophic *Crossaster papposus* larvae, no impact on calcification and a higher growth rate was detected (Dupont et al., 2010b), implying that not only calcification, but other processes such as feeding, metabolism or ion regulation are effected by elevated $p\text{CO}_2$. In fact, metabolism has been found to be up-regulated with increasing seawater $p\text{CO}_2$ in the blue mussel *Mytilus edulis* (Thomsen et al., 2010; Thomsen and Melzner, 2010) and the ophiuroid *Amphiura filiformis* (Wood et al., 2008), potentially reflecting elevated energetic costs for calcification and/or cellular homeostasis in some marine invertebrates that cannot control the carbonate system speciation in their extracellular fluids. In other invertebrate species, metabolic depression, elicited by uncompensated extracellular pH, has been suggested to occur (see Pörtner, 2008). In early sea urchin larvae, no metabolic rate measurements under acidified conditions have been performed so far, but a down-regulation of several metabolic genes (e.g. Succinyl-CoA synthetase, citrate synthase, pyruvate dehydrogenase, ATP synthase F1 complex) has been reported (Todgham and Hofmann, 2009; O'Donnell et al., 2010). This could support the metabolic depression hypothesis and explain reduced rates of growth.

In this paper, we used gene expression profiling in an explorative way to investigate, whether transcripts of genes with a crucial importance in metabolism, calcification and ion homeostasis are affected by near-future (year 2100) levels of seawater acidification in pre-feeding (day 2) and feeding (days 4 and 7) *Strongylocentrotus purpuratus* pluteus larvae. In a companion study (Stumpp et al. submitted), we investigated the effects of $p\text{CO}_2$ on larval development success, morphology, feeding and metabolic rates. Larvae were raised at two seawater $p\text{CO}_2$

values: control (40 Pa, 399 μatm , pH 8.1) and elevated $p\text{CO}_2$ (134 Pa, 1318 μatm , pH 7.7).

2 Material and Methods:

2.1 Larval cultures

Adult *S. purpuratus* were collected on the Californian coast (Kerckoff Marine Laboratory, California Institute of Technology, USA) and transferred to the Sven Lovén Center for Marine Sciences (Kristineberg, Sweden). They were fed *ad libitum* using *Ulva* spp. and kept several weeks in flow-through systems with deep-water from the Gullmarsfjord before starting the experiment. Out-flow of the tanks was sterilized using UV-light to prevent introduction of the species into the fjord. Spawning was induced by injection of 2 ml 0.5 mM KCl into the coelomic cavity. Eggs of 3 females were collected in separate 1 l beakers and were washed and fertilized by adding dry sperm (20 μl) of one male. Fertilization was followed by monitoring the fertilization-induced elevation of the oocyte membrane under a stereomicroscope (fertilization rates >95%). Zygotes were allowed to divide once before they were pooled, concentrated in 25ml and split into 50 l (1 replicate, polyethylene) and 5 l (3 replicates, Erlenmeyer flasks) culture vessels which were pre equilibrated with low (control) $p\text{CO}_2$ (ca. 40 Pa, 399 μatm) and high $p\text{CO}_2$ (ca. 134 Pa, 1318 μatm , pH 7.7; Tab 1). Larvae in 50 l cultures grew slightly slower than in 5 l cultures. The initial larval concentration in each culture was 10 larvae ml^{-1} . Larval cultures were checked daily for health i.e. vitality of larvae and mortality. Culture vessels were kept in the dark and aerated with a stream of bubbles of pressurized air (ca. 100 bubbles of 4mm diameter min^{-1}). Cultures were mixed by the slow convective current created by the motion of the bubbles in order to avoid disturbances of larvae by strong currents. Larvae of subsamples (two 10 ml samples per replicate) were enumerated daily for determination of culture densities. Larvae were collected in Eppendorf 1.5 ml tubes and fixed in 4% paraformaldehyde (PFA) in seawater pH 8.3 and stored at 4°C for later morphometric measurements and determination of growth rates. Larvae started to feed when their digestive system was fully developed at ca. day 3. Larvae were fed with *Rhodomonas* spp. raised in B1 medium (Guillard and Ryther, 1962) at 20°C under a 12:12 h light:dark cycle. Algal strains were provided by the Marine Algal Culture Centre at Gothenburg University (GUMACC). To prevent changes in food concentration, algae concentration and size were checked daily using a coulter counter (Elzone 5380,

Micrometrics, Aachen, Germany) and then adjusted in the experimental bottles to the maximum concentration of $150 \mu\text{g carbon l}^{-1}$ (~ 3000 to $6000 \text{ cells ml}^{-1}$ for diameters ranging between 7 to 9 μm). Seawater quality (e.g. presence of bacteria) was checked daily using the coulter counter and no water change was needed for the whole duration of the experiment. Samples for molecular biology were only taken from the 50 l culture replicates in order to sample sufficient amounts of larval tissue for the q RT PCR analysis.

2.2 pH regulation and carbonate chemistry measurements

Culture pH_{NBS} was kept stable (± 0.04 units) using Aqua Medic pH controllers (NBS scale, AquaMedic, Germany) that controlled valves for injection of pure CO_2 into the culture tanks once pH_{NBS} exceeded the target value by more than 0.03 units. The Aqua Medic pH electrodes were cross-calibrated regularly with a Metrohm (827 pH lab) pH_{NBS} meter in order to ensure comparability between replicates. Total alkalinity (A_{T}) measurements were conducted four times during the experiment as described by Sarazin and coworkers (1999) with an accuracy of $10 \mu\text{mol kg}^{-1}$ seawater. Total dissolved inorganic carbon (C_{T}), $p\text{CO}_2$ and calcium carbonate saturation states for calcite (Ω_{calc}) were calculated from A_{T} and pH_{NBS} using CO2SYS software (Lewis and Wallace, 1998, Tab. 1). Salinity and temperature were measured four times (Tab. 1).

2.3 Sampling

Sampling was conducted at days 2, 4 and 7 post-fertilization in both treatments. At each time point, 20 samples of 3000 to 4000 larvae were taken from each culture, briefly concentrated in Eppendorf 1.5 mL tubes by means of hand centrifugation for 10 seconds at approximately 156 g. Excess water was discarded except for approximately 80 μl containing the larvae. Samples were then shock-frozen in liquid nitrogen. The whole sampling process took approximately 45 seconds per sample. Samples were stored at -80°C for ca. 6 months until further processing.

2.4 qRT-PCR

Total RNA was extracted from 3000 to 4000 larvae per sample using the Qiagen RNeasy Mini kit (Qiagen, Hilden, Germany) following the instruction manual. qRT-PCR analysis was carried out using the two step real-time RT-PCR method described by Vandenbrouke

et al. (2001). Prior to cDNA synthesis, 3 to 10 µg total RNA (Nanodrop bioanalyzer) were treated with DNase (Ambion by Applied Biosystems, Darmstadt, Germany) to digest genomic DNA remains. For cDNA synthesis, 0.4 µg total RNA (Nanodrop bioanalyzer) was transcribed using the Applied Biosystems High Capacity cDNA Reverse Transcriptase kit (Applied Biosystems, Darmstadt, Germany).

Primer Express Software (version 2.0 by Applied Biosystems) and sequences from the *S. purpuratus* genome were used to design primer pairs for 27 genes (Table 2). Efficiency was evaluated by applying the dilution standard curve method (dilution steps: 1:20; 1:100; 1:500; 1: 2500 and 1:12500). Primer concentrations were 300 nM. The *Taq* DNA polymerase was activated for 10 min at 95°C. Each PCR was run for 40 cycles at 95°C for 15 s and 62°C for 1 min. Subsequent to each PCR, a melting curve analysis was conducted. Each PCR of a total volume of 20 µl consisted of 2 µl template (cDNA dilution of 1:20), 3 µl of each primer (forward, reverse), 2 µl DNase free H₂O and 10 µl SYBR Green master mix (Platinum SYBR Green qPCR SuperMix-UDG with ROX, Invitrogen, Karlsruhe, Germany). Controls were conducted without template (no template control) and with RNA post DNase digestion to test for genomic DNA contamination within the cDNA. No significant DNA contamination was observed. Using LinRegPCR software version 7.4 (Ramakers et al., 2003) the PCR efficiency of each PCR reaction was determined. Efficiencies were always > 1.9. Real time qPCR measurements were conducted on a StepOnePlus real time cycler (Applied Biosystems, Darmstadt, Germany).

2.5 Gene normalization and statistical analysis

To identify suitable reference genes, NormFinder (Andersen et al., 2004) software was used (version 19). NormFinder uses an algorithm to estimate the overall expression variation as well as the variation between samples of subgroups of the sample set and is aiming at identifying a candidate gene with lowest intra-group variability and at the same time an inter-group variation as close to 0 as possible (Andersen et al. 2004). As data input for NormFinder (<http://www.mdl.dk/publicationsnormfinder.htm>), we used Ct values of all 27 gene transcripts from all treatment groups which were transformed into quantities (Q) using the appropriate PCR efficiencies as determined using LinReg PCR using formula (1):

$$Q = E^{(-Ct)} \quad (1)$$

with E being the reaction specific efficiency (maximum efficiency of 100 % would be 2, i.e. a doubling in the amount of PCR product per reaction cycle) and Ct being the Ct value as determined using StepOnePlus real time cycler software (adapted from Livak and Schmittgen, 2001). NormFinder suggested sodium bicarbonate cotransporter (NBC3, NCBI accession no: [NM_001079551](#)) to be the most stably expressed gene with an inter- and intra-group specific variation closest to zero (NormFinder stability values for NBC 0.001 to 0.006). NBC3 was thus used as reference gene for normalization.

For statistical reasons logarithmic Ct-values were converted into quantities (Q) using formula 1. Values were then normalized using the reference gene NBC3. A Bray-Curtis similarity analysis was conducted with square root transformed expression values (normalized quantities). From this similarity matrix, an analysis of similarity (one-way ANOSIM, two-way crossed ANOSIM using time and $p\text{CO}_2$ as factors), a Cluster analysis (principal component analysis, PCA) and a similarity of percentage analysis (SIMPER) analysis were carried out. The principal component analysis (PCA) with a cluster plot was used to determine the contribution of single genes to the observed sample pattern and test if genes from one pathway correlate in their expression behavior (e.g. ion regulation, calcification and metabolism). One-way and two-way crossed ANOSIM was chosen as non-parametric statistical method to analyze the significance in grouping elicited by the group specific gene expression patterns and determine the impact of $p\text{CO}_2$ and time on the observed pattern. A SIMPER analysis was then used to quantitatively determine the contribution of single genes to the observed similarity or dissimilarity between gene expression patterns of groups. All multivariate statistics including PCA were conducted using Primer 6 software (version 6.1.9; Primer-E Ltd.). For the evaluation of mortality and growth, t-tests and an analysis of covariance (ANCOVA) with log transformed data, respectively, were applied.

3 Results:

Culture vessels had a salinity of 32 ± 0.7 and a temperature of 16 ± 0.8 °C. pH_{NBS} was maintained at 8.17 ± 0.04 in control and 7.70 ± 0.04 in low pH treatments. Total alkalinity (A_T) reached values of 2243 ± 40 $\mu\text{mol kg}^{-1}$ in control and 2233 ± 17 $\mu\text{mol kg}^{-1}$ in the low pH treatment. From these values a C_T of 2035 ± 38 and 2196 ± 17 $\mu\text{mol kg}^{-1}$ and a $p\text{CO}_2$ of 40 Pa and 134 Pa (i.e. 399 μatm , 1318 μatm) in control and low pH vessels respectively, were calculated. The experimental seawater was super saturated with calcite

and aragonite under control conditions (3.64 ± 0.06 and 2.33 ± 0.04 , respectively). Under low pH conditions, the experimental water was still super saturated with calcite (1.38 ± 0.01), while Ω_{arag} was <1 (0.88 ± 0.01).

As an indicator of the health of cultures and larvae, their relative density during the experimental period was determined daily while length parameters of larvae (total length, arm length, $n=20$) were measured at days 2, 4 and 7. After 7 experimental days, a decrease in relative larval density was detected in the cultures, with values of 0.94 for the control treatment and 0.86 for the acidified condition (Fig. 1 A). The difference of 0.08 between treatments was not statistically significant (ANOVA, day 7, $p<0.77$).

Growth (total length) of larvae followed a logarithmic curve for control as well as for the low pH treatment group (Fig. 1 B). Growth (total length) of larvae was significantly affected by acidification of the water (growth rate comparison on body length vs. log transformed time, ANCOVA, $p<0.001$). The smallest size difference (5.9%) was observed at culture day 7, a maximum size difference (10%) was observed at culture day 4. Proportions of larvae measured by the additional morphometric parameters that included post-oral rod and postero-lateral rod, revealed that larvae reared under elevated seawater $p\text{CO}_2$ were not only smaller, but exactly matched the morphometric parameters characteristic for earlier larval age (Stumpp et al., 2011). Thus, we used body length to normalize the detected morphological developmental delay caused by ocean acidification in order to estimate, whether changes in gene expressions are direct effects of elevated seawater $p\text{CO}_2$ or indirect effects caused by the growth delay itself.

Gene expression patterns for candidate genes involved in ion transport (8 genes), calcification (8 genes), metabolism (5 genes), the cellular stress response (2 genes) and housekeeping (4 genes) were assessed in *S. purpuratus* larvae cultured under control (pH_{NBS} : 8.2, $p\text{CO}_2$: 40 Pa, 399 μatm) and acidified (pH_{NBS} : 7.7, $p\text{CO}_2$: 134 Pa, 1318 μatm) conditions, sampled at 3 time points (2, 4, 7 days post-fertilization). Highest gene transcript levels within the 26 genes studied were those of ATP-Synthase, Na^+/K^+ -ATPase and SM30B, with values of 25.9, 17.1 and 15.6 relative to NBC, respectively (Table 3). Transcript levels of almost all genes changed strongly during the first seven days of development (except NHE3). Developmental time had a much stronger influence

on sea urchin gene expression patterns than CO₂ enrichment of the culture medium. Using principal component analysis (PCA, Fig. 3) and an analysis of similarity (ANOSIM: one-way, two-way crossed, Table 4) including the test for contribution of the genes to the similarity pattern (SIMPER, e.g. similarity percentage, Table 5), we analyzed changes in gene expression patterns overall to determine stage effects and stage independent acidification effects. Overall, the gene expression patterns (of the studied genes) of all 6 groups (day 2: pH 8.1 and 7.7; day 4: pH 8.1 and 7.7; day 7: pH 8.1 and 7.7) were characterized by a similarity of greater than 85% (based on a Bray Curtis matrix).

A principal component analysis was applied to analyze the contribution of single genes to the observed patterns (Fig. 3). Principal components (PC) 1 and 2 explain over 96% of the observed variation with PC1 being the more important component, responsible for 70.1% of the measured variation.

Calcification genes, such as SM30, SM50, msp130, CA15, MMP all contributed negatively to principal component 1 (PC1). ATP-synthase, citrate synthase and CA10 contributed positively to PC1. PC2 is not as obviously organized, with mainly Na⁺/K⁺-ATPase and HSP70 contributing negatively.

Testing all groups independently (6 groups: two CO₂ treatments, three time points) using one-way analysis of similarity (ANOSIM) (Table 4) revealed distinct differences in the gene expression patterns between culture days with R values of 1. Results for the CO₂ treatments were more variable showing no differences between treatment groups at culture day 2 with an R value of 0.084, while at culture day 4, an R value of 0.983 indicated significant differences between CO₂ treatments. This can also be seen in the distinct separation of the treatment groups at culture day 4 in the sample plot overlaying the PCA (Fig. 2). At culture day 7, the observed differences are still pronounced with an R value of 0.533, but not as clear as at culture day 4 which is also obvious in the sample plot (Fig. 2). These results were confirmed in a two-way crossed ANOSIM, which reveals that the impact of culture time on gene expression pattern and thus dissimilarity of groups is much more pronounced (R = 1) than the impact of CO₂ treatment (R = 0.518). Nevertheless, the differences between CO₂ treatments are still larger than would be expected by chance. Although CO₂ treatments/time groups are significantly different from each other (apart from CO₂ treatments at culture day 2), the

differences in gene expression patterns between the two CO₂ treatments (SIMPER analysis) are relatively small (Table 5), ranging from 2.60% difference at culture day 2 (not significant) over 3.06% at culture day 7 (significant) to 4.30% difference at culture day 4 (significant). At culture day 2 and 4, differences between treatment groups were mainly based on expression of SM30B and ATP-synthase, contributing with 15.3 % (SM30B, day 2), 8.5% (ATP-synthase, day 2), 14.6% (SM30B, day 4) and 12.7% (ATP-synthase, day 4) to the observed patterns (Fig. 2). ATP-synthase also contributed to differences between treatments at day 7 with 14.8%, with SERCA being the second most important gene at culture day 7 with a 10.6% expression level.

Taking into account that the morphological data suggest a CO₂ induced growth delay (Stumpp et al. submitted) and that developmental time has a much larger effect on gene expression patterns than seawater *p*CO₂, it becomes immediately evident that any significant differences between CO₂ treatments could reflect normal patterns of expression expected at an earlier larval stage, thus a developmental delay “artifact” rather than a ‘true’ CO₂ effect. Here, we compare expression patterns by plotting expression against body length (Fig. 4, and suppl. materials). On the one hand, significant differences between CO₂ treatments can become more obvious when correcting for larval growth as e.g. in the case of ATP-synthase (Fig 4-A) or non significant changes may become significant, as e.g. in CA15 (Fig 4-G). On the other hand, changes in expression that appeared significant by comparing them at culture time points, appear to be developmental effects, e.g. as in CA10 (Fig. 4-H at day 2). However, the differences in transcript levels of genes that contributed most to the principal components 1 and 2 (e.g. *msp130*, SM30B, SM50, ATP-synthase and Na⁺/K⁺-ATPase) were even enhanced by the (visual) analysis of expression vs. body length (Fig. 4).

4 Discussion:

This study reveals the impacts of CO₂-induced seawater acidification on gene expression on *S. purpuratus* larvae during the first week of development until the feeding pluteus larval stage. All recent studies examining gene expression pattern changes during larval development were conducted on pre-feeding or unfed larval stages (Todgham and Hofmann, 2009; O'Donnell et al., 2010). The biggest impact of *p*CO₂ on physiological processes such as metabolism was observed in sea urchin larvae once feeding had started (Stumpp et al, submitted). This study aimed at revealing changes in gene expression

patterns between pre-feeding (day 2) and feeding (day 4, 7) larval stages. The growth delay induced by elevated $p\text{CO}_2$ in *S. purpuratus* larvae was observed in a parallel study (Stumpp et al submitted). The differential regulation of genes important in calcification, metabolism and ion regulation is in accordance with results from several other recent studies (Kurihara and Shirayama, 2004; Kurihara, 2008; Clark et al., 2009; Todgham and Hofmann, 2009; Brennand et al., 2010; O'Donnell et al., 2010).

We show that in feeding pluteus larvae, a significant up-regulation of metabolic genes can be observed in response to elevated seawater $p\text{CO}_2$. These observations correlate with strongly elevated metabolic rates (ca. 2-fold) of feeding larvae from acidified treatments (Stumpp et al. submitted), which might be related to an increased energy demand for cellular homeostasis and calcification.

4.1 Mortality and growth

A slightly increased survival in response to simulated ocean acidification was observed in *S. purpuratus* larvae during the experimental period. This is in accordance with results from studies on other echinoid species, in which no increased mortality was detected (*Tripneustes gratilla*, *Pseudechinus huttoni*, *Evechinus chloroticus*, *Sterechinus neumayeri*, *Echinus mathaei*, *Hemicentrotus erythrogramma*, *Hemicentrotus pulcherrimus*) when exposed to similar levels of acidification until the four-arm pluteus stage was reached (Kurihara and Shirayama, 2004; Kurihara, 2008; Clark et al., 2009). There are no indications of increased larval mortality during sea urchin development up to the 4-arm pluteus stage in response to levels of surface ocean acidification that can be expected within the 21st century - at least with respect to average surface ocean scenarios (Caldeira and Wickett, 2003; Caldeira and Wickett, 2005). Nevertheless, CO_2 driven acidification reduced the growth rate of *S. purpuratus* larvae during the first 7 days of development. Several other studies also reported reduced larval growth in sea urchin species (*T. gratilla*, *E. chloroticus*, *S. neumayeri*, *E. mathaei*, *H. erythrogramma*, *H. pulcherrimus*, *Lytechinus pictus*, *Paracentrotus lividus*) under moderately acidified conditions (Kurihara and Shirayama, 2004; Kurihara, 2008; Clark et al., 2009; Brennand et al., 2010; O'Donnell et al., 2010; Martin et al., 2011). In our study, larvae from the acidified treatment were not only shorter, but were characterized by the same morphological proportions (body rod, posterolateral rod and postoral rod length

proportional to the body length) as control larvae at an earlier time point post fertilization (see Stumpp et al. submitted for more details).

4.2 Gene expression patterns: time vs. $p\text{CO}_2$

With increase in developmental time, expression levels of most genes changed strongly. Based on gene expression profiles of larvae, we can distinguish between different culture times using ANOSIM and PCA. The gene products most important for generation of distinct differences between groups were ATP-synthase, SM30B and Na^+/K^+ -ATPase. Na^+/K^+ -ATPase, SM30B and ATP-synthase were also the most abundant transcripts among the group of 26 assessed gene products, confirming the importance of these genes in the respective functional pathways for ion regulation, calcification and metabolism.

During the first week of development, the morphology of sea urchin larvae constantly changes. Major events are the formation of the gut, including the anus (day 2). Larval arms are formed and elongated to support feeding and motility (Smith et al., 2008). Considering these changes in larval morphology, it is not surprising that the comparison of gene expression patterns during development resulted in highly distinguishable age groups. Changes in gene expression patterns in response to high $p\text{CO}_2$ were shown to be much less pronounced. As morphological differences indicated by the difference in body length, which were greatest at culture day 4 and smallest at culture day 2, correlate with the results of the ANOSIM (e.g. highest differences in gene expression on day 4 as well), the possibility exists that these changes in gene expression may be primarily due to developmental delay (Stumpp et al. submitted) rather than a direct effect of high seawater $p\text{CO}_2$ on gene expression. Similar conclusions have also been reached in a study of gill ion transport molecule gene expression in embryonic cephalopods (Hu et al., 2011).

4.3 Seawater acidification effects on gene expression patterns

Although gene expression patterns differed more strongly in response to culture time than to CO_2 -treatment, ANOSIM demonstrated distinct changes in gene expression patterns in response to CO_2 -treatment at culture days 4 and 7, while no differences in expression patterns were found at culture day 2. This is in accordance with larval growth data, where the strongest difference in growth was observed at day 4, and a less strong effect was

found at day 7. A SIMPER analysis following the ANOSIM revealed that SM30B and ATP-synthase were contributing most to the differences in gene expression pattern between control and acidified treatment at culture day 4, while ATP-synthase and SERCA were the genes contributing most to the differences in patterns at culture day 7. ATP-synthase seems to be an important gene in the responses to hypercapnia and our results are in accordance with data from Todgham and Hofmann (2009) who also found up-regulation of this gene at a moderate $p\text{CO}_2$ of 101 Pa (997 μatm) in a microarray study at 40 hours post-fertilization. Furthermore, Todgham and Hofmann (2009) described down regulation of more than 80 genes of major functional pathways, including calcification, metabolism, ion regulation and the cellular stress response when they exposed early prism stage larvae (40 h post-fertilization) to $p\text{CO}_2$ values of ca. 55 Pa (543 μatm). At higher seawater $p\text{CO}_2$ (ca 101 Pa, 997 μatm), they still observed the majority of effected genes to be down regulated (160 of 178 differentially expressed genes). However, 18 genes, including ATP-synthase, were significantly up regulated under these conditions. These findings are in accordance with our results. A further increase in CO_2 stress (142 Pa) in our older, feeding larvae resulted in a higher proportion of up-regulated metabolic genes (i.e. up-regulation of four out of five metabolic genes), while calcification-related genes were down regulated in older larvae (culture day 4) in our study as well.

4.3.1 Skeletogenesis

Calcification in sea urchin larvae is carried out by primary mesenchyme cells (PMCs). PMCs ingress into the blastocoel during gastrulation, form a syncytium and deposit calcium carbonate to construct the larval spicules within the enclosed syncytial cavity (Okazaki, 1975; Ettensohn and Malinda, 1993; Wilt, 1999; Killian and Wilt, 2008). These spicules contain both a mineral and an organic phase. Among the about 45 discovered spicule matrix proteins expressed by PMCs, SM30E and SM50 are the most abundant water soluble proteins (Mann et al., 2008). The highest contribution to the gene pattern differences between the high $p\text{CO}_2$ and the control treatment was due to SM30B expression (SIMPER results). SM30B encodes a matrix protein occurring in concentric layers within the spicule (Wilt, 2002; Wilt, 2005; Killian and Wilt, 2008; Mann et al., 2008). This gene, along with other genes encoding proteins for larval spicule biomineralization, such as SM50, msp130 and a metalloproteinase, were down regulated

by up to 36% (msp 130) at culture day 4. When normalizing the expression data to body length (Fig. 4E-F and Fig S1E-H), it is obvious, that this effect is not a developmental artifact, but a primary effect of seawater acidification. The down regulation of msp130 is in accordance with Todgham and Hofmann (2009), who also observed a down regulation of this and other genes that code for Ca^{2+} binding proteins at $p\text{CO}_2$ of 101 Pa (997 μatm) 40 hours post-fertilization. These authors also observed a down regulation of other calcification related genes (cyclophilins, collagens, several carbonic anhydrases) that were not investigated in this study. In contrast to these results, CO_2 induced seawater acidification down to a pH of 7.5 ($p\text{CO}_2$ of 202 Pa, 2000 μatm) and 7.25 (365 Pa, 3600 μatm) caused a compensatory increase in transcript levels of a range of calcification genes (msp130, SM30) in 3 day old *P. lividus* larvae (Martin et al., 2011).

Carbonic anhydrases (CAs) catalyze the reversible hydration of CO_2 to bicarbonate and protons and play important roles in biomineralization as well as in cellular pH regulation. The most highly expressed CA in *S. purpuratus* PMCs is the CA SPU_012518 (Livingston et al., 2006). Love et al. (2007) found that CA15 is dominantly expressed in PMC cells at the growing spicule tip in *Heliocidaris tuberculata* and *H. erythrograma*, implying a function in biomineralization. There was, however, no significant effect of ocean acidification on the expression of CA15. However, when correcting for the growth delay, a trend towards down regulation of CA15 expression under elevated CO_2 conditions became apparent. This correlates with the down regulation of other calcification related genes in this study. However, in contrast to CA15, the gene coding for a carbonic anhydrase related protein (CA10) studied here does not show any impact of OA when normalized to body length. Todgham and Hofmann (2009) found an up regulation of CA15 (SPU_012518) under high seawater $p\text{CO}_2$ at 40 hours post-fertilization.

The often observed growth delay in sea urchin larvae raised under high CO_2 conditions (Kurihara and Shirayama, 2004; Kurihara, 2008; Clark et al., 2009; Brennand et al., 2010; O'Donnell et al., 2010), could so far not be causally related to reduced calcification. It was even shown, that calcification rates were not altered independently of somatic growth in response to elevated seawater $p\text{CO}_2$ (Martin et al., 2011). However, when investigating the microstructure of larval spicules, Clark et al (2009) noted eroded surface structures in two out of four sea urchin species at a $p\text{CO}_2$ of ca. 130 Pa (pH 7.7).

Considering the down regulation of matrix protein genes observed in this and other studies (Todgham and Hofmann, 2009; O'Donnell et al., 2010) and their assumed role in the stabilization of the transient ACC phase that is precipitated in intracellular compartments (Raz et al., 2003; Killian and Wilt, 2008), it is possible that disturbances in the balance between the coordinated production of mineral and organic matrix could affect the composition and mechanical properties of the skeleton.

The similar behavior of the impacted calcification genes in this study represented by the principal component analysis and the observed down regulation of transcription factors responsible for induction of calcification processes (Todgham and Hofmann, 2009; O'Donnell et al., 2010) indicates that possibly the entire biomineralization machinery is influenced by an upstream located transcription factor in *S. purpuratus* and *Strongylocentrotus franciscanus* larvae.

4.3.2 Ion regulation

Calcification and ion- and acid-base regulation are intrinsically linked via the creation of microenvironments for biomineralization using a specific set of ion regulatory proteins. Thus, proteins that transport Ca^{2+} , HCO_3^- and H^+ - besides the Na^+/K^+ -ATPase employed as the driving force for many secondary active transporters - are of special interest in this matter. We investigated transcription of eight ion regulation genes (two AE3a transcripts, lysosomal H^+ -ATPase, vacuolar H^+ -ATPase, NHE3, VSOP, SERCA and Na^+/K^+ -ATPase).

The majority of ion transport genes tested in this study were either not regulated or down regulated with the exception of an up regulation of NHE3 at culture day 2, Na^+/K^+ -ATPase and SERCA at culture day 4 and VSOP at culture day 7. Apart from down regulation of V-type H^+ -ATPase at culture day 7 and up regulation of NHE3 at culture day 2, both of which could be developmental artifacts (S3, supplementary material), the observed growth delays did not appear to impact the regulation of the other ion regulatory proteins significantly. Todgham and Hofmann (2009) found a down regulation of ion transport genes especially Na^+ -dependent transporters and primary active transporters such as H^+ -ATPases and Na^+/K^+ -ATPase. In contrast to the data of Todgham and Hofmann (2009), we show that Na^+/K^+ -ATPase and SERCA were up-regulated at culture day 4. An up regulation of Na^+/K^+ -ATPase transcripts is also in accordance with the results of Martin et al (2011).

Na^+/K^+ -ATPase activity has been proposed to require up to 77% of larval metabolism (Leong and Manahan, 1997). As an important protein also linked closely to metabolism, an up regulation of transcript levels of Na^+/K^+ -ATPase is in accordance with up regulation of metabolic gene transcription in this study. Leong and Manahan (1997) found that about half of the total Na^+/K^+ -ATPase activity is held in reserve in *S.purpuratus* larvae, but can rapidly be activated in times of higher regulatory demand, e.g. for amino acid uptake from surrounding seawater or for supporting increased cellular ion regulatory demand under acidified conditions. Apart from Na^+/K^+ -ATPase and SERCA, none of the other analyzed ion regulatory genes contributed strongly to the observed differences in gene expression patterns between the two treatment groups (SIMPER analysis).

However, a slight up regulation was observed in a voltage gated proton channel (VSOP, 16%) at day 7. Voltage gated proton channels mainly function as cost effective acid extrusion mechanisms to prevent cytosolic acidification (DeCoursey, 2008).

In contrast to Todgham and Hofmann (2009), who did not observe changes in NHE or chloride/bicarbonate exchanger (AE) transcription levels in acidified conditions, our study shows a down regulation of members from these transporter families (NHE3, SLC9A3 and AE3b, SLC4A3). However, an increased requirement for ion regulatory processes is not reflected in transcription levels of AE3b and NHE3. NHE3 is highly down regulated (45%) at culture day 4, a finding that could potentially support the “energy-turnover” model of Pörtner and coworkers (Reipschläger and Pörtner, 1996) which proposes that extracellular acidification leads to a depression of NHE due to activation of energetically more favorable transporters.

4.3.3 Metabolism

To observe whether or not ATP generating processes are impacted by increased $p\text{CO}_2$ we analyzed five genes involved in energy metabolism (e.g. ATP-synthase, CS, PK, thiolase and insulin receptor). All of them were up regulated at either culture day 4 (ATP-synthase, CS, PK, thiolase) or day 7 (insulin receptor) with ATP-synthase majorly contributing to the observed differences in gene expression patterns between treatment groups (SIMPER analysis). A growth delay dependent effect could be excluded (S3, supplementary materials). Up regulation of metabolism related genes corresponds with

the observation of elevated metabolic rates in our companion study (Stumpp et al, submitted). While sea urchin larval metabolic rates increased, it was found that growth rate decreased under acidified conditions (Stumpp et al, submitted). It seems that although metabolic rates are increasing to meet higher energetic demands, energy allocation to somatic growth is reduced in favor of other processes, possibly ion homeostasis and calcification or maintenance of skeletal integrity. It was shown in perfused teleost fish gills that, at unaltered metabolic rates (control vs. CO₂ exposure), energy budgets are shifted towards ion regulation and protein synthesis in high CO₂ treatments (Deigweier et al., 2010). In sea urchin larvae of the temperate species *Lytechinus pictus*, the cost of protein synthesis remains more or less the same regardless of physiological state, e.g. developmental stage or in fed versus non-fed larvae, and was shown to account for up to 75% of metabolic rate in feeding larvae (Pace and Manahan, 2006). Despite such a high protein synthesis rate, the deposition of protein (e.g. growth) accounted for only 21% of protein synthesis rate in 15 day pluteus larvae. Thus, protein degradation remained very high. Taking into account the high metabolic costs for ion regulation as indicated by Na⁺/K⁺-ATPase activity consuming up to 77% of metabolic rate in *S. purpuratus* larvae (Leong and Manahan, 1997), most of the energy gained from aerobic metabolism is used for the maintenance, e.g. cellular ion homeostasis and protein turnover, with comparatively little protein deposition, e.g. growth. A CO₂ induced increase in metabolic rate with equal feeding rate will therefore likely lead to a growth delay. In most organisms such as fish, crustaceans, molluscs, as well as plants, it has been shown that environmental stress usually leads to a growth delay in favor of adaptive or defense mechanisms (Sumpter, 1992; Van Weerd and Komen, 1998; Matyssek et al., 2002; Verslycke and Janssen, 2002; Verslycke et al., 2004; Voronezhskaya et al., 2004). The (potential) hypercapnia induced reallocation of energy towards vital processes such as ion homeostasis and calcification remains to be studied in future projects.

5 Conclusion

We have investigated how gene expression patterns change in response to simulated ocean acidification in pre-feeding and feeding *S. purpuratus* larvae. We showed that gene expression patterns strongly correlate with developmental stage and growth. This could lead to a misinterpretation of results should gene expression analyses be simply normalized on a temporal scale. For an adequate evaluation of gene expression patterns as

well as other physiological processes during embryonic and larval development, we conclude that it is essential to closely monitor larval morphology and increase the sampling frequency in order to be able to distinguish between effects of elevated $p\text{CO}_2$ and effects related to delayed, but otherwise normal, developmental programs. Despite the potential growth delay related effects on gene expression pattern, we found genes that were differentially regulated under acidification stress. Metabolic genes were up-regulated in order to meet the higher energetic demands, while key calcification genes were down-regulated. Nevertheless, to support and understand the present gene expression data, mechanistic studies on energy budgets, extra- and intracellular pH homeostasis and calcification in sea urchin larvae are urgently needed.

6 Acknowledgements

MS and FM are funded by the DFG Excellence cluster ‘Future Ocean’ and the German ‘Biological impacts of ocean acidification (BIOACID)’ project 3.1.4, funded by the Federal Ministry of Education and Research (BMBF, FKZ 03F0608A). SD is funded by the Linnaeus Centre for Marine Evolutionary Biology at the University of Gothenburg (<http://www.cemeb.science.gu.se/>), and supported by a Linnaeus-grant from the Swedish Research Councils VR and Formas; VR and Formas grants to MT; Knut and AliceWallenberg’s minnen and the Royal Swedish Academy of Sciences.

The authors thank T. Reusch for use of his qRT-PCR machine and we are grateful to N. Bergmann and U. Panknin for valuable advice (NB) and help with carrying out the qRT-PCR (UP).

7 References:

- Andersen CL, Jensen JL, Orntoft TF (2004) Normalization of real-time quantitative reverse transcription-PCR data: a model-based variance estimation approach to identify genes suited for normalization, applied to bladder and colon cancer data sets. *Cancer Res* 64:5245-5250
- Brennand HS, Soars N, Dworjanyn SA, Davis AR, Byrne M (2010) Impact of ocean warming and ocean acidification on larval development and calcification in the sea urchin *Tripneustes gratilla*. *Plos One* 5:e11372
- Byrne M, Ho M, Selvakumaraswamy P, Nguyen HD, Dworjanyn SA, Davis AR (2009) Temperature, but not pH, compromises sea urchin fertilization and early development under near-future climate change scenarios. *P Roy Soc B Bio* 276:1883-1888

- Byrne M, Soars N, Ho M, Wong E, McElroy D, Selvakumaraswamy P, Dworjanyn SA, Davis AR (2010a) Fertilization in a suite of coastal marine invertebrates from south east Australia is robust to near-future ocean warming and acidification. *Mar Biol*
- Byrne M, Soars N, Selvakumaraswamy P, Dworjanyn SA, Davis AR (2010b) Sea urchin fertilization in a warm, acidified and high $p\text{CO}_2$ ocean across a range of sperm densities. *Mar Environ Res* 69:234-239
- Caldeira K, Wickett ME (2003) Anthropogenic carbon and ocean pH. *Nature* 425:365-365
- Caldeira K, Wickett ME (2005) Ocean model predictions of chemistry changes from carbon dioxide emissions to the atmosphere and ocean. *J Geophys Res* 110
- Cao L, Caldeira K (2008) Atmospheric CO_2 stabilization and ocean acidification. *Geophys Res Lett* 35
- Carr RS, Biedenbach JM, Nipper M (2006) Influence of potentially confounding factors on sea urchin porewater toxicity tests. *Arch Environ ContTox* 51:573-579
- Clark D, Lamare M, Barker M (2009) Response of sea urchin pluteus larvae (Echinodermata: Echinoidea) to reduced seawater pH: a comparison among tropical, temperate, and a polar species. *Mar Biol* 156:1125-1137
- DeCoursey TE (2008) Voltage-gated proton channels. *Cell Mol Life Sci* 65:2554-2573
- Deigweier K, Hirse T, Bock C, Lucassen M, Pörtner H-O (2010) Hypercapnia induced shifts in gill energy budgets of Antarctic notothenioids. *J Comp Physiol B* 180:347-359
- Dupont S, Havenhand J, Thorndyke W, Peck L, Thorndyke MC (2008) CO_2 -driven ocean acidification radically affect larval survival and development in the brittlestar *Ophiotrix fragilis*. *Mar Ecol Prog Ser* 373:285-294
- Dupont S, Lundve B, Thorndyke M (2010a) Near future ocean acidification increases growth rate of the lecithotrophic larvae and juveniles of the sea star *Crossaster papposus*. *J Exp Zool B* 314B:382-389
- Dupont S, Ortega-Martínez O, Thorndyke MC (2010b) Impact of near-future ocean acidification on echinoderms. *Ecotoxicology* 19:449-462
- Ericson JA, Lamare MD, Morley SA, Barker MF (2010) The response of two ecologically important Antarctic invertebrates (*Sterechinus neumayeri* and *Parborlasia corrugatus*) to reduced seawater pH: effects on fertilisation and embryonic development. *Mar Biol* 157:2689-2702
- Ettensohn CA, Malinda KM (1993) Size regulation and morphogenesis: a cellular analysis of skeletogenesis in the sea urchin embryo. *Development* 119
- Fabry VJ (2008) Marine calcifiers in a high- CO_2 ocean. *Science* 320:1020-1022
- Guillard RRL, Ryther JH (1962) Studies of marine planktonic diatoms. I. *Cyclotella nana* (Husted), and *Detonula confervacea* (Cleve). *Can J Microbiol* 8:229-239
- Gutowska MA, Melzner F, Pörtner H-O, Meier S (2010) Calcification in the cephalopod *Sepia officinalis* in response to elevated seawater $p\text{CO}_2$. *Mar Biol* 157:1653-1663
- Gutowska MA, Pörtner H-O, Melzner F (2008) Growth and calcification in the cephalopod *Sepia officinalis* under elevated seawater $p\text{CO}_2$. *Mar Ecol Prog Ser* 373:303-309
- Havenhand J, Buttler FR, Thorndyke MC, Williamson JE (2008) Near-future levels of ocean acidification reduce fertilization success in a sea urchin. *Curr Biol* 18:R651-R652
- Hoegh-Guldberg O, Mumby PJ, Hooten AJ, Steneck RS, Greenfield P, Gomez E, Harvell CD, Sale PF, Edwards AJ, Caldeira K, Knowlton N, Eakin CM, Iglesias-Prieto R,

- Muthiga N, Bradbury RH, Dubi A, Hatzilios ME (2007) Coral reefs under rapid climate change and ocean acidification. *Science* 318:1737-1742
- Hu MY-A, Tseng Y-C, Stump M, Gutowska MA, Kiko R, Lucassen M, Melzner F (2011) Elevated seawater $p\text{CO}_2$ differentially affects branchial acid-base transporters over the course of development in the cephalopod *Sepia officinalis*. *Am J Physiol - Reg I* 300:R1100-R1114
- Killian CE, Wilt FH (2008) Molecular aspects of biomineralization of the echinoderm endoskeleton. *Chem Rev* 106:4463-4474
- Kurihara H (2008) Effects of CO_2 -driven ocean acidification on the early developmental stages of invertebrates. *Mar Ecol Prog Ser* 373:275-284
- Kurihara H, Shirayama Y (2004) Effects of increased atmospheric CO_2 on sea urchin early development. *Mar Ecol Prog Ser* 274:161-169
- Langdon C, Atkinson MJ (2005) Effect of elevated $p\text{CO}_2$ on photosynthesis and calcification of corals and interactions with seasonal change in temperature/irradiance and nutrient enrichment. *J Geophys Res* 110
- Leong PKK, Manahan DT (1997) Metabolic importance of Na^+/K^+ -ATPase activity during sea urchin development. *J Exp Biol* 200:2881-2892
- Lewis E, Wallace DWR (1998) CO_2SYS -Program developed for the CO_2 system calculations. Carbon Dioxide Inf Anal Center Report ORNL/CDIAC-105
- Livak KJ, Schmittgen TD (2001) Analysis of relative gene expression data using real-time quantitative PCR and the $2^{-\Delta\Delta\text{CT}}$ method. *Methods* 25:402-408
- Livingston BT, Killian C, Wilt F, Cameron A, Landrum MJ, Ermolaeva O, Sapojnikov V, Maglott DR, Buchanan AM, Ettensohn CA (2006) A genome-wide analysis of biomineralization-related proteins in the sea urchin *Strongylocentrotus purpuratus*. *Dev Biol* 300:335-348
- Love AC, Andrews ME, Raff RA (2007) Gene expression patterns in a novel animal appendage: the sea urchin pluteus arm. *Evol Dev* 9:51-68
- Mann K, Poustka AJ, Mann M (2008) The sea urchin (*Strongylocentrotus purpuratus*) test and spine proteomes. *Proteome Science* 6
- Martin S, Richier S, Pedrotti M-L, Dupont S, Castejon C, Gerakis Y, Kerros M-E, Oberhänsli F, Teyssié J-L, Gattuso JP (2011) Early development and molecular plasticity in the Mediterranean sea urchin *Paracentrotus lividus* exposed to CO_2 driven ocean acidification. *J Exp Biol* 214:1357-1368
- Matyssek R, Schnyder H, Elstner EF, Munch JC, Pretzsch H, Sandermann H (2002) Growth and parasite defence in plants; the balance between resource sequestration and retention: In lieu of a guest editorial. *Plant Biology* 4:133-136
- Melzner F, Gutowska MA, Langenbuch M, Dupont S, Lucassen M, Thorndyke MC, Bleich M, Pörtner H-O (2009) Physiological basis for high CO_2 tolerance in marine ectothermic animals: pre-adaptation through lifestyle and ontogeny? *Biogeosciences* 6:2313-2331
- O'Donnell MJ, Todgham AE, Sewell MA, Hammond LM, Ruggiero K, Fanguie NA, Zippay ML, Hofmann GE (2010) Ocean acidification alters skeletogenesis and gene expression in larval sea urchins. *Mar Ecol Prog Ser* 398:157-171
- Okazaki K (1975) Spicule formation by isolated micromeres of the sea urchin embryo. *Am Zool* 15:567-581
- Orr JC, Fabry VJ, Aumont O, Bopp L, Doney SC, Feely RA, Gnanadesikan A, Gruber N, Ishida A, Joos F, Key RM, Lindsay K, Maier-Reimer E, Matear R, Mofray P, Mouchet A, Najjar RG, Plattner G-K, Rodgers KB, Sabine CL, Sarmiento JL, Schlitzer R, Slater RD, Totterdell IJ, Weirig M-F, Yamanaka Y, Yool A (2005)

- Anthropogenic ocean acidification over the twenty-first century and its impact on calcifying organisms. *Nature* 437:681-686
- Pace DA, Manahan DT (2006) Fixed metabolic costs for highly variable rates of protein synthesis in sea urchin embryos and larvae. *J Exp Biol* 209:391-392
- Pörtner H-O (2008) Ecosystem effects of ocean acidification in times of ocean warming: a physiologist's view. *Mar Ecol Prog Ser* 373:203-217
- Pörtner H-O, Farrell AP (2008) Physiology and climate change. *Science* 322:90-92
- Ramakers C, Ruijter JM, Deprez RH, Moorman AF (2003) Assumption-free analysis of quantitative real-time polymerase chain reaction (PCR) data. *Neurosci Lett* 13:62-66
- Raz S, Hamilton PC, Wilt FH, Weiner S, Addadi L (2003) The transient phase of amorphous calcium carbonate in sea urchin larval spicules: the involvement of proteins and magnesium ions in its formation and stabilization. *Adv Funct Mater* 13:480-486
- Reipschläger A, Pörtner H-O (1996) Metabolic depression during environmental stress: the role of extracellular *versus* intracellular pH in *Sipunculus nudus*. *J Exp Biol* 199:1801-1807
- Sarazin G, Michard G, Prevot F (1999) A rapid and accurate spectroscopic method for alkalinity measurements in seawater samples. *Water Res* 33:290-294
- Shirayama Y, Thornton H (2005) Effect of increased atmospheric CO₂ on shallow water marine benthos. *J Geophys Res* 110
- Smith MM, Smith LC, Cameron A, Urry LA (2008) The larval stages of the sea urchin, *Strongylocentrotus purpuratus*. *J Morph* 269:713-733
- Stump M, Wren J, Melzner F, Thorndyke MC, Dupont S (submitted) CO₂ induced seawater acidification impacts sea urchin larval development I: elevated metabolic rates decrease scope for growth and induce developmental delay. *J Comp Biochem Physiol A*
- Sumpter JP (1992) Control of Growth of Rainbow-Trout (*Oncorhynchus mykiss*). *Aquaculture* 100:299-320
- Thomsen J, Gutowska MA, Saphörster J, Heinemann A, Fietzke J, Hiebenthal C, Eisenhauer A, Körtzinger A, Wahl M, Melzner F (2010) Calcifying invertebrates succeed in a naturally CO₂ enriched coastal habitat but are threatened by high levels of future acidification. *Biogeosciences* 7:3879-3891
- Thomsen J, Melzner F (2010) Seawater acidification does not elicit metabolic depression in the blue mussel *Mytilus edulis*. *Mar Biol* 157:2667-2676
- Todgham AE, Hofmann GE (2009) Transcriptomic response of sea urchin larvae *Strongylocentrotus purpuratus* to CO₂-driven seawater acidification. *J Exp Biol* 212:2579-2594
- Van Weerd JH, Komen J (1998) The effects of chronic stress on growth in fish: a critical appraisal. *Comp Biochem Physiol A* 120:197-112
- Vandenbroucke II, Vandesompele J, De Paepe A, Messiaen L (2001) Quantification of splice variants using real-time PCR. *Nucleic Acids Res* 29:e68
- Verslycke T, Janssen CR (2002) Effects of a changing abiotic environment on the energy metabolism in the estuarine mysid shrimp *Neomysis integer* (Crustacea : Mysidacea). *J Exp Mar Biol Ecol* 279:61-72
- Verslycke T, Roast SD, Widdows J, Jones MB, Janssen CR (2004) Cellular energy allocation and scope for growth in the estuarine mysid *Neomysis integer* (Crustacea : Mysidacea) following chlorpyrifos exposure: a method comparison. *J Exp Mar Biol Ecol* 306:1-16

- Voronezhskaya EE, Khabarova MY, Nezlin LP (2004) Apical sensory neurones mediate developmental retardation induced by conspecific environmental stimuli in freshwater pulmonate snails. *Development* 131:3671-3680
- Wilt FH (1999) Matrix and mineral in the sea urchin larval skeleton. *J Struct Biol* 126:216-226
- Wilt FH (2002) Biomineralization of the Spicules of sea urchin embryos. *Zool Sci* 19:253-261
- Wilt FH (2005) Developmental biology meets materials science: morphogenesis of biomieralized structures. *Dev Biol* 280:15-25
- Wood HL, Spicer JI, Widdicombe S (2008) Ocean acidification may increase calcification rates, but at a cost. *P Roy Soc B Bio* 275:1767-1773

Figure captions:

Fig. 1: Performance data for *Strongylocentrotus purpuratus* larval cultures. A: relative density (mean \pm SD) of larvae in control (8.1) and acidified (7.7) treatments during the experimental period (n=3). B: larval growth rate as body length (mean \pm SD; n=20) under control (8.1) and acidified (7.7) conditions (for more morphological details of larvae see also Stumpp et al. submitted).

Fig. 2: Representative pictures of *Strongylocentrotus purpuratus* larvae at day 2, 4 and 7 post-fertilization at two $p\text{CO}_2$ treatments: control (pH 8.1) and acidified condition (pH 7.7). Scale bar (100 μm) is valid for all pictures. Measurement of body length used for growth rate is indicated for a 7 day old pluteus larvae under control conditions (pH 8.1).

Fig. 3: Principal component analysis of control (pH 8.1, grey symbols) and high $p\text{CO}_2$ treated (pH 7.7, white symbols) *S. purpuratus* larvae at different time points post-fertilization (day 2 circles; day 4 triangles; day 7 squares) according to their gene expression patterns. Sample plot for the principal components PC1 and PC2 (outer axes) and superimposed loading plot (inner axes) with the relevant genes (black circles). The plot also includes R values (one way ANOSIM based on Bray-Curtis dissimilarity matrix) for differences (% , SIMPER results) in gene patterns between CO_2 treatments within each culture age group and the two genes that contribute most to these differences (SIMPER results).

Fig. 4: Transcript levels relative to NBC3 during larval growth (body length in μm) in *S. purpuratus* larvae. **A, B**: metabolism: ATP-synthase, pyruvate kinase transcript levels **C, D**: ion regulation: Na^+/K^+ -ATPase and NHE3 transcript levels. **E-H**: calcification: SM30B, msp130, CA15 and CA10 transcript levels.

Table captions:

Table 1: Experimental water chemistry. Salinity, temperature, total alkalinity (A_T) and pH were measured four times during the experimental period. Using CO2SYS software (Lewis and Wallace, 1998); C_T , calcite and aragonite saturation states and pCO_2 were calculated.

Table 2: Primer data for RT-qPCR for 27 observed genes including primer description, primer sequence (forward F, reverse R), amplicon length and PCR efficiency for the respective PCR reaction (determined by LinRegPCR).

Table 3: Gene expression data for control and low pH (e.g. pH 7.7) treatments at three time points (days 2, 4 and 7): Ct values were transformed into quantities incorporating PCR efficiencies and normalized against NBC3 as suggested by 'NormFinder'. Down regulation is highlighted in grey. The change in gene expression (% change) was calculated from control to low pH.

Table 4: Summary of ANOSIM analyses based on the Bray Curtis similarity matrix (square root transformed gene quantities). In the one way ANOSIM, the six groups were independently analyzed, while factor influence (culture time and pH treatment) was analyzed with help of two way crossed ANOSIM. Light grey shows no significant separation between groups (day 2 control vs. low pH), grey displays significant differences with some correlation between treatments, and dark grey shows high dissimilarity between groups including day 4 control vs. low pH.

Table 5: Summary of SIMPER analysis based on the Bray Curtis similarity matrix (square root transformed gene quantities) showing only results for dissimilarity between treatment groups at the three sample time points 2, 4 and 7 days post-fertilization. Only genes with a dissimilarity contribution > 5% are shown.

Figure 1

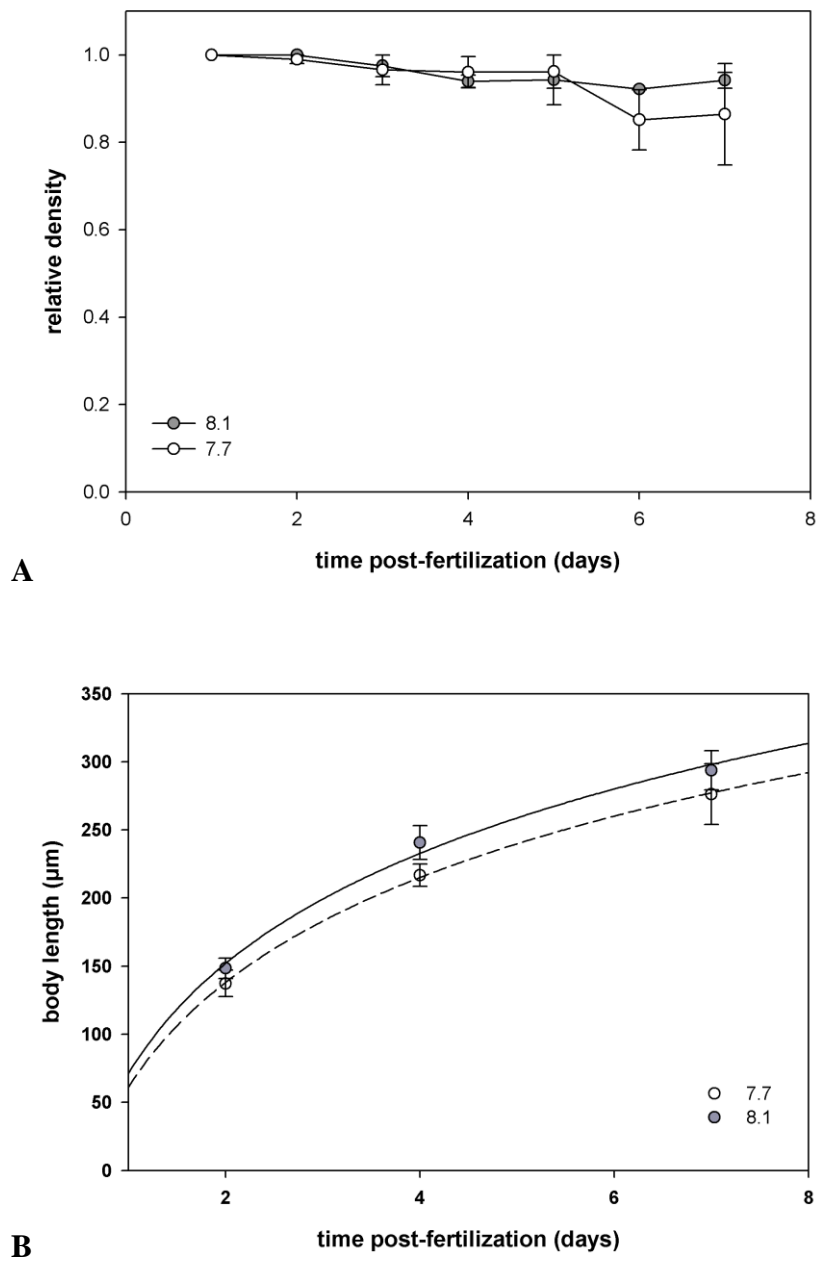


Figure 2

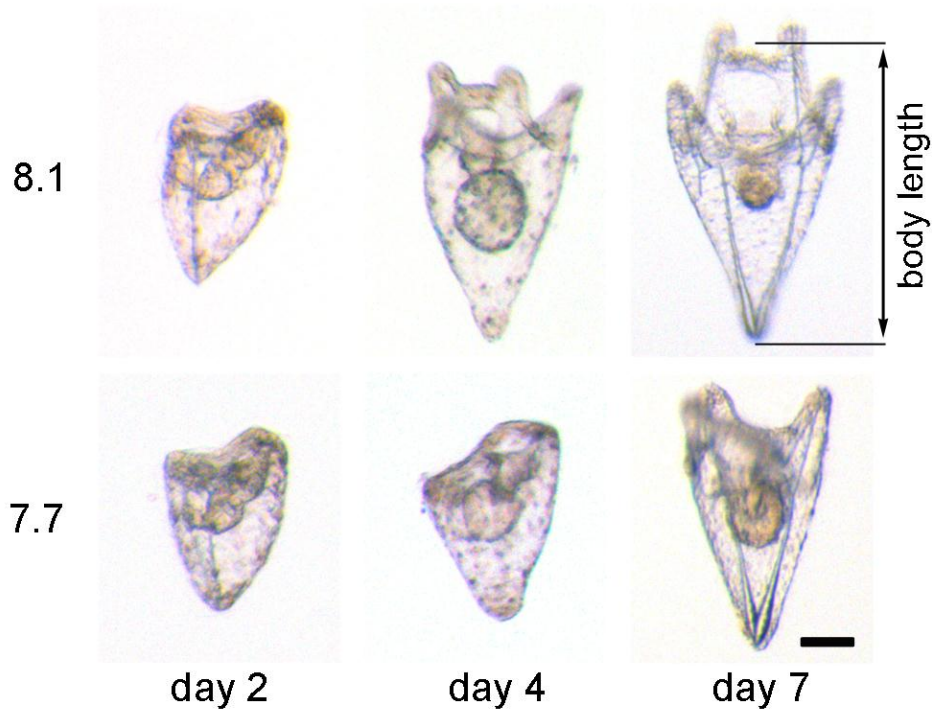


Figure 3

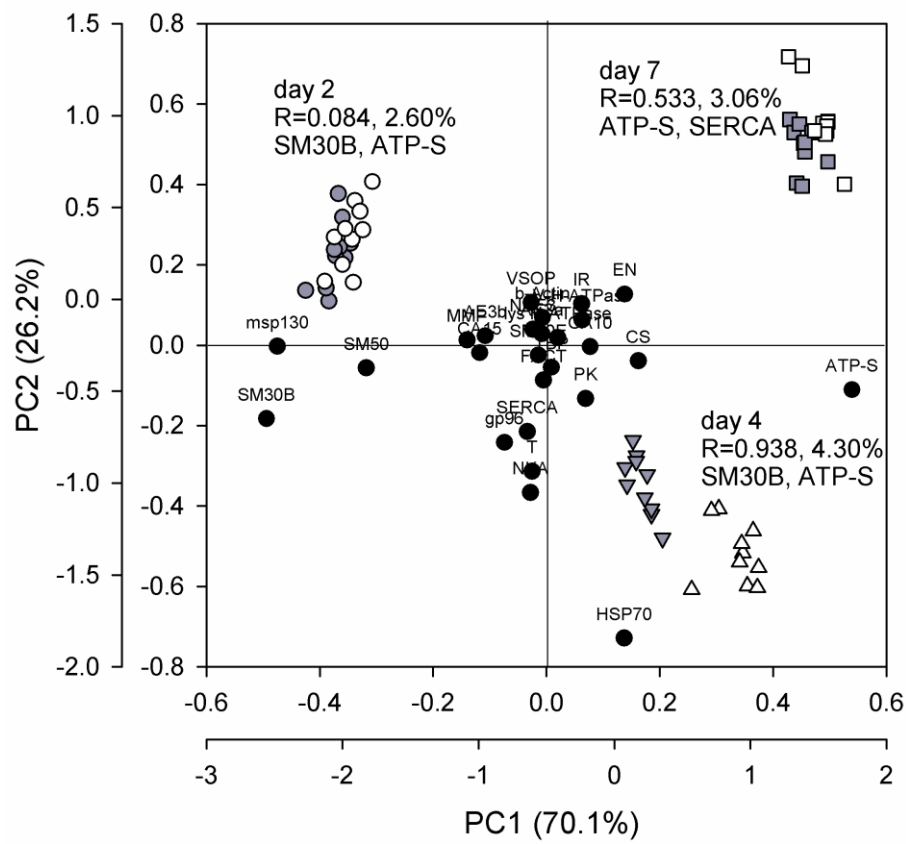


Figure 4

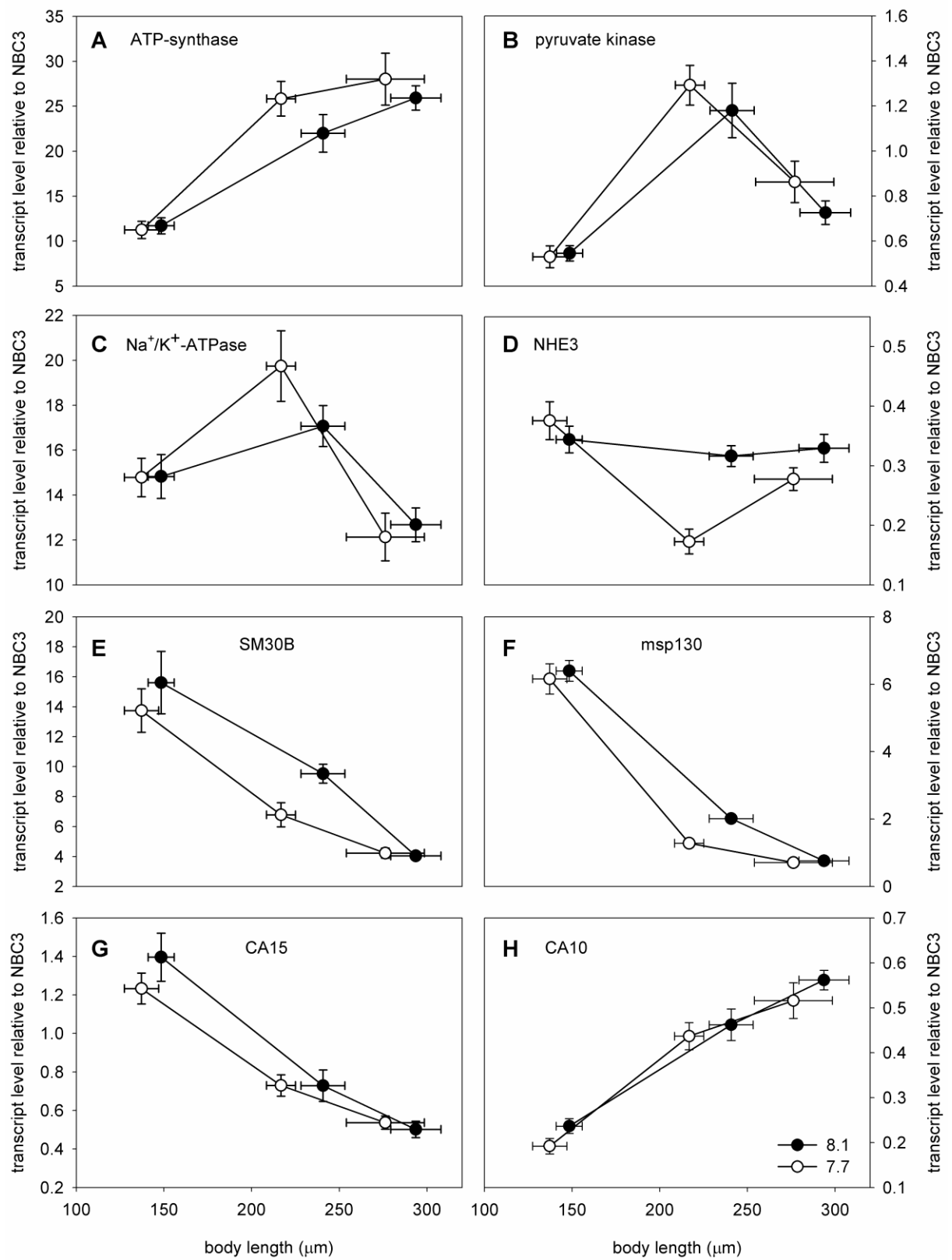


Table 1

	control pH 8.2		low pH 7.7	
measured				
salinity	32.0	± 0.7	32.0	± 0.7
temperature (°C)	16.0	± 0.8	16.0	± 0.8
A_T ($\mu\text{mol kg}^{-1}$)	2243	± 40	2233	± 17
pH_{NBS}	8.17	± 0.04	7.70	± 0.04
calculated				
C_T ($\mu\text{mol kg}^{-1}$)	2035	± 38	2196	± 17
Ω_{Ca}	3.64	± 0.06	1.38	± 0.01
Ω_{Ar}	2.33	± 0.04	0.88	± 0.01
$p\text{CO}_2$ (Pa)	40.4	± 0.7	133.5	± 1.0
$p\text{CO}_2$ (μatm)	399	± 7	1318	± 10

Table 2

ID	Primer name abbreviation /	Gene / protein description	Primer Sequence	Amplicon length (bp)	Primer Efficiency	NCBI Accession No
1	AE3a F AE3a R	Chloride/bicarbonate exchanger, Anion Exchanger 3-like protein, SLC4A3	AAGATCCCGCCGGACTCT ATGTACGGTGCCTCAAGGTACTC	71	1,96	XM_788556
2	AE3b F AE3b R	Anion exchanger 3, SLC4A3	AGGTGCCTCTAGCCGTTCTCT TCTCTACCATCTGGATACCATTGAGT	78	1,95	XM_001195823
3	ATP-S F ATP-S R	ATP-synthase β -subunit	TTCTTGTCCCAACCTTCCA TCTGCCATCGAGACGAGCTT	71	1,97	NM_001123502
4	CA15 F CA15 R	Carbonic anhydrase 15 α -subfamily (CA15)	CTTGACATGTTCCGTGAGCTTTA CGATGTGGAGCATCTCCAGTT	73	1,95	XM_001177813 SPU_012518
5	CA10 F CA10 R	Carbonic anhydrase related protein (CARP 10)	CATATCACGAGGGCCATTGAG TATTCTCCCGCCGAAGTG	71	1,97	XM_001182003.1
6	CS F CS R	Citrate synthase	CTTCCCACGTCTGCAGAT AGCGGCACTGAATTGAGACA	71	1,96	XR_026166
7	EN F EN R	(similar to) Echinonectin	AGTCAGGTGGTAACGGTTGGA GTCGCCGAGATCGACCATAA	71	1,94	XM_001184352
8	FACT F FACT R	Facilitates chromatic transcription (FACT) complex subunit SPT16	CCTGCCACCACCAGTCTA GAGCGGGATCGTTTCTCTT	71	1,96	XM_001203176
9	gp96 F gp96 R	Heat shock protein gp96	CTTTTAGCCATCGTAGGTGTTCTG CAACAATTGCCTTCCCTCATC	79	1,97	NM_214643
10	HSP70 F HSP70 R	Heat shock protein 70 kDa	GCCATGTAAGAAGGCCATTGAG CCACCGACGAGCAGAACCT	72	1,97	XM_776184
11	IR F IR R	Mannose-6-phosphate/Insulin-like growth factor II receptor	TGACACCCTGCAGCTTACGAT TGCAAACGCTTCCCCTGTA	71	1,97	XR_025889
12	lys-H ⁺ -ATPase F lys-H ⁺ -ATPase R	Lysosomal H ⁺ -ATPase	CAACGACCTGACCCAGAGTATCTA CCACTTCTTGGTGGCAGTGA	73	1,93	XR_026057
13	MMP F MMP R	Matrix-metalloproteinase 14	TCCCAAGGCCGACATCAT CAGGGCCATCGAAAGCATAA	71	1,97	XM_001175853 SPU_013670
14	msp 130 F msp 130 R	Mesenchyme-specific cell surface glycoprotein msp 130	CTTCAACGGAGCCGCATT TCGATCGCGAGTCCTTAGTCA	71	1,96	XM_001179349
15	NKA F NKA R	Sodium/potassium ATPase alpha subunit (NKA, Na ⁺ /K ⁺ -ATPase)	GGTGGTCAATTTGACAAGTCTTCA TCAGATCGGTTGCAGAGACAA	74	1,95	XM_001202868
16	NBC3 F NBC3 R	Sodium/bicarbonate cotransporter 3, SLC4A7 (NBC3)	CCAACATCCAGAACAGCCAAA CTTGCCAGGTACCAGAGT	71	1,96	NM_001079551
17	NHE3 F NHE3 R	Sodium/hydrogen exchanger 3, SLC9A3 (NHE3, Na ⁺ /H ⁺ exchanger)	CATCCGCGTGCTATCG TGCGCTGATGACTTTAGAACACA	61	1,96	XM_001178217
18	PK F PK R	(similar to) Pyruvat kinase type M2	CGCCACAGCCAACACATTTC TGCTGGACGGGATTCAAT	62	1,97	XR_025967
19	SERCA F SERCA R	Sarco/endoplasmic reticulum calcium transporting ATPase (SERCA)	ACCCTCCACAAGAGCAAGA CATCACCGTCCATAGCTGTGA	71	1,95	NM_001037630
20	SM30B F SM30B R	Spicule matrix protein 30 B	TCGACAGTGGTGTCTTCTTGA AAGGCCGTTCTCGTTGTTGA	71	1,94	XM_001175556 SPU_000826
21	SM30E F SM30E R	Spicule matrix protein 30 E	GGAAACCTTAATGCCAACCTAGTC TGGATTATGGGTCCAGTGCAA	71	1,97	XM_001177597 SPU_004867
22	SM50 F SM50 R	Spicule matrix protein 50	GGCCTCCGAATTCTGTGAAA CTGAAGCCAGAGCACCCATT	71	1,97	NM_214610 SPU_018811

23	β-Actin F	β-Actin	CGTCGTTTACATCATTCCGGACAT	71	1,96	XM_001176939.1
	β-Actin R		GACCCGTTGTCGATGACGAT			
24	TBP F	TATA-box binding protein (TBP)	AGTCCCAGCAGAGTCAGTCCTA	71	1,94	NM_214621
	TBP R		CTACCCACCGAACCAACGA			
25	T F	Thiolase: hydroxyacyl-coenzyme A dehydrogenase	AAGCCAGCACTTCCTTTGGTT	71	1,97	XM_001192117
	T R		GGCGACGTCCAGACCTACTTC			
26	V-H ⁺ -ATPase F	vacuolar (v-type) H ⁺ -ATPase B subunit, transcript variant 2 (V-type H ⁺ -ATPase)	GTCCGCTGCTCGTGAAGAAG	71	1,96	XM_001176838
	V-H ⁺ -ATPase R		TGGTTGCCAAATCAGTGACATG			
27	VSOP F	Voltage gated proton channel (VSOP)	ATCGTCGAGCTTGTCATTGACTT	71	1,96	NM_001126307
	VSOP R		TCCGTCTCTGTTGCATTGCA			

Table 3

genes	culture day 2			culture day 4			culture day 7		
	control	low pH	% change	control	low pH	% change	control	low pH	% change
Ion Transport									
AE3a	0.83 ± 0.09	0.85 ± 0.07	3.1	0.37 ± 0.02	0.33 ± 0.03	-11.3	0.34 ± 0.03	0.28 ± 0.02	-18.5
AE3b	0.11 ± 0.01	0.11 ± 0.01	-3.8	0.07 ± 0.00	0.07 ± 0.00	1.2	0.11 ± 0.01	0.10 ± 0.01	-1.7
Lys-H ⁺ -ATPase	1.29 ± 0.13	1.27 ± 0.08	-1.1	1.28 ± 0.14	1.34 ± 0.10	4.7	1.52 ± 0.09	1.44 ± 0.12	-5.3
NHE3	0.34 ± 0.02	0.38 ± 0.03	9.2	0.32 ± 0.02	0.17 ± 0.02	-45.4	0.33 ± 0.02	0.28 ± 0.02	-15.7
VSOP	0.37 ± 0.04	0.37 ± 0.03	-0.7	0.13 ± 0.01	0.13 ± 0.01	-2.4	0.31 ± 0.02	0.36 ± 0.03	16.4
V-H ⁺ -ATPase	2.53 ± 0.28	2.42 ± 0.20	-4.5	2.65 ± 0.23	2.63 ± 0.09	-0.6	3.57 ± 0.22	3.23 ± 0.19	-9.5
SERCA	4.19 ± 0.29	4.31 ± 0.14	2.7	5.10 ± 0.28	5.44 ± 0.28	6.8	3.71 ± 0.16	2.91 ± 0.16	-21.6
NKA	14.83 ± 0.98	14.78 ± 0.86	-0.3	17.08 ± 0.91	19.74 ± 1.57	15.6	12.68 ± 0.75	12.14 ± 1.06	-4.3
Calcification									
CA15	1.40 ± 0.12	1.23 ± 0.08	-11.7	0.73 ± 0.08	0.73 ± 0.06	0.2	0.50 ± 0.04	0.54 ± 0.03	7.0
CA10	0.24 ± 0.02	0.19 ± 0.02	-18.8	0.46 ± 0.04	0.44 ± 0.03	-5.4	0.56 ± 0.02	0.52 ± 0.04	-8.1
EN	0.32 ± 0.04	0.28 ± 0.02	-11.6	0.57 ± 0.05	0.46 ± 0.04	-18.8	1.26 ± 0.10	1.24 ± 0.12	-1.7
MMP	0.71 ± 0.06	0.67 ± 0.05	-5.5	0.22 ± 0.02	0.17 ± 0.01	-24.5	0.13 ± 0.01	0.12 ± 0.01	-7.5
msp130	6.40 ± 0.31	6.16 ± 0.45	-3.7	2.01 ± 0.11	1.28 ± 0.08	-36.3	0.76 ± 0.08	0.71 ± 0.05	-7.1
SM30B	15.61 ± 2.08	13.74 ± 1.46	-11.9	9.53 ± 0.63	6.79 ± 0.80	-28.8	4.05 ± 0.23	4.23 ± 0.33	4.5
SM30E	0.10 ± 0.01	0.12 ± 0.02	16.6	0.12 ± 0.01	0.11 ± 0.01	-8.9	0.06 ± 0.01	0.08 ± 0.02	41.7
SM50	5.10 ± 0.36	4.92 ± 0.46	-3.5	2.55 ± 0.12	1.96 ± 0.13	-23.2	1.27 ± 0.07	1.18 ± 0.14	-6.6
Metabolism									
ATP-synthase	11.71 ± 0.91	11.25 ± 0.96	-3.9	21.99 ± 2.10	25.84 ± 1.92	17.5	25.92 ± 1.36	28.01 ± 2.90	8.1
CS	2.75 ± 0.24	2.61 ± 0.30	-4.9	4.11 ± 0.44	4.62 ± 0.31	12.4	4.56 ± 0.25	4.91 ± 0.47	7.5
PK	0.55 ± 0.03	0.53 ± 0.05	-2.8	1.18 ± 0.12	1.29 ± 0.09	9.5	0.73 ± 0.05	0.86 ± 0.09	18.8
T	2.33 ± 0.16	2.16 ± 0.19	-7.0	3.28 ± 0.30	3.92 ± 0.24	19.7	1.48 ± 0.11	1.48 ± 0.16	-0.4
IR	0.46 ± 0.06	0.41 ± 0.03	-11.5	0.43 ± 0.04	0.44 ± 0.02	0.9	0.85 ± 0.02	0.93 ± 0.06	9.7
Heat shock proteins									
gp96	6.16 ± 0.79	5.61 ± 0.44	-9.0	6.46 ± 0.42	6.86 ± 0.21	6.2	4.32 ± 0.32	3.89 ± 0.36	-9.9
HSP70	3.54 ± 0.29	3.46 ± 0.28	-2.2	10.20 ± 0.51	12.08 ± 0.67	18.5	3.84 ± 0.28	3.40 ± 0.29	-11.6
Housekeeping genes									
FACT	0.53 ± 0.02	0.51 ± 0.03	-2.6	0.65 ± 0.05	0.74 ± 0.05	13.7	0.43 ± 0.03	0.41 ± 0.03	-4.5
β-actin	1.59 ± 0.14	1.45 ± 0.11	-8.9	1.07 ± 0.13	1.26 ± 0.06	17.4	1.42 ± 0.08	1.67 ± 0.14	17.3
TBP	0.15 ± 0.01	0.14 ± 0.01	-5.4	0.23 ± 0.02	0.24 ± 0.01	2.9	0.14 ± 0.01	0.15 ± 0.01	4.3

Table 4

ANOSIM (one way)

	day 2 control	day 2 low pH	day 4 control	day 4 low pH	day 7 control
day 2 low pH	0.084				
day 4 control	1	1			
day 4 low pH	1	1	0.938		
day 7 control	1	1	1	1	
day 7 low pH	1	1	1	1	0.533
Global R	0.91				

ANOSIM (two way crossed)

Global R _(culture time)	1
Global R _(pH treatment)	0.518

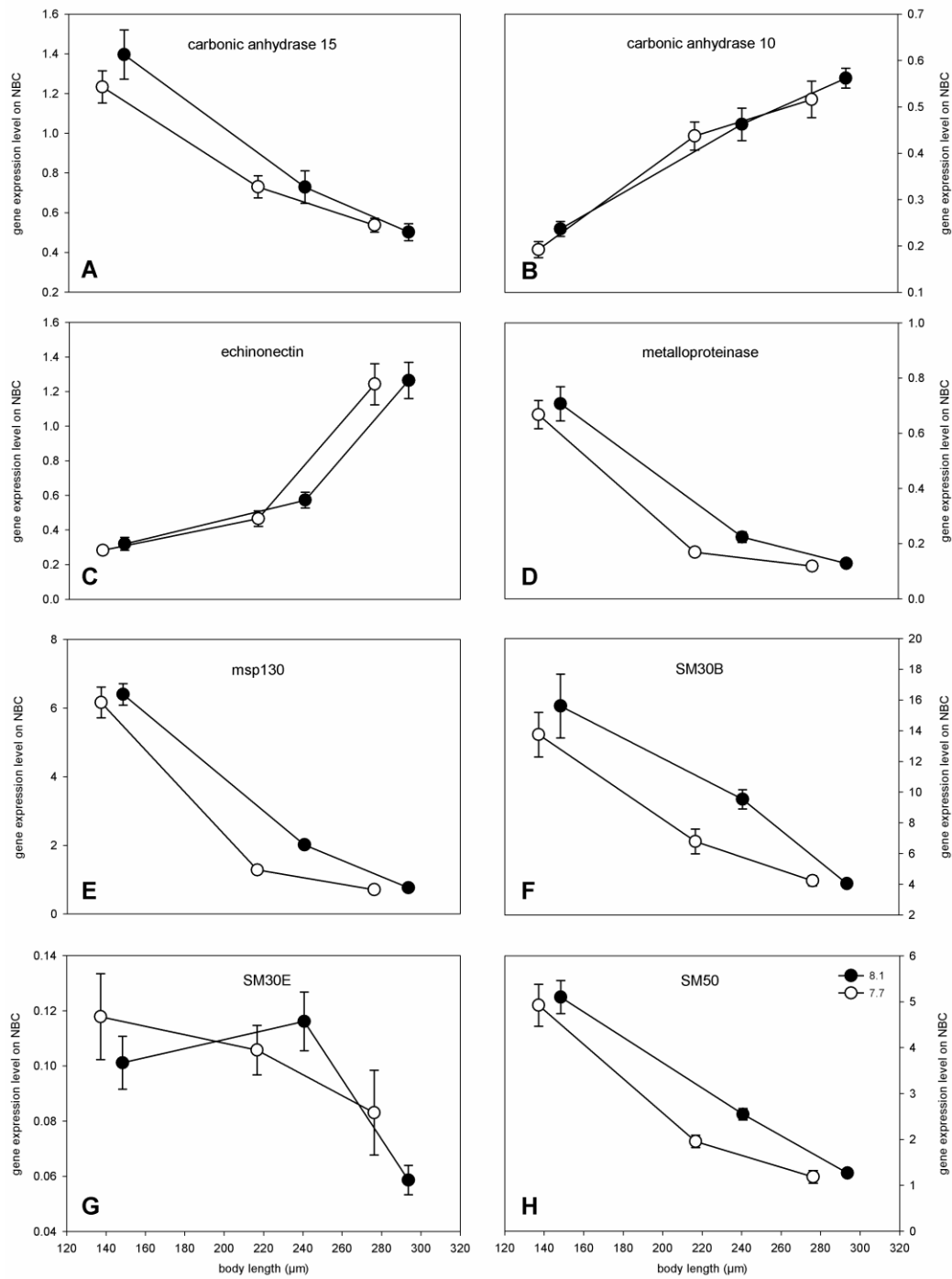
Table 5

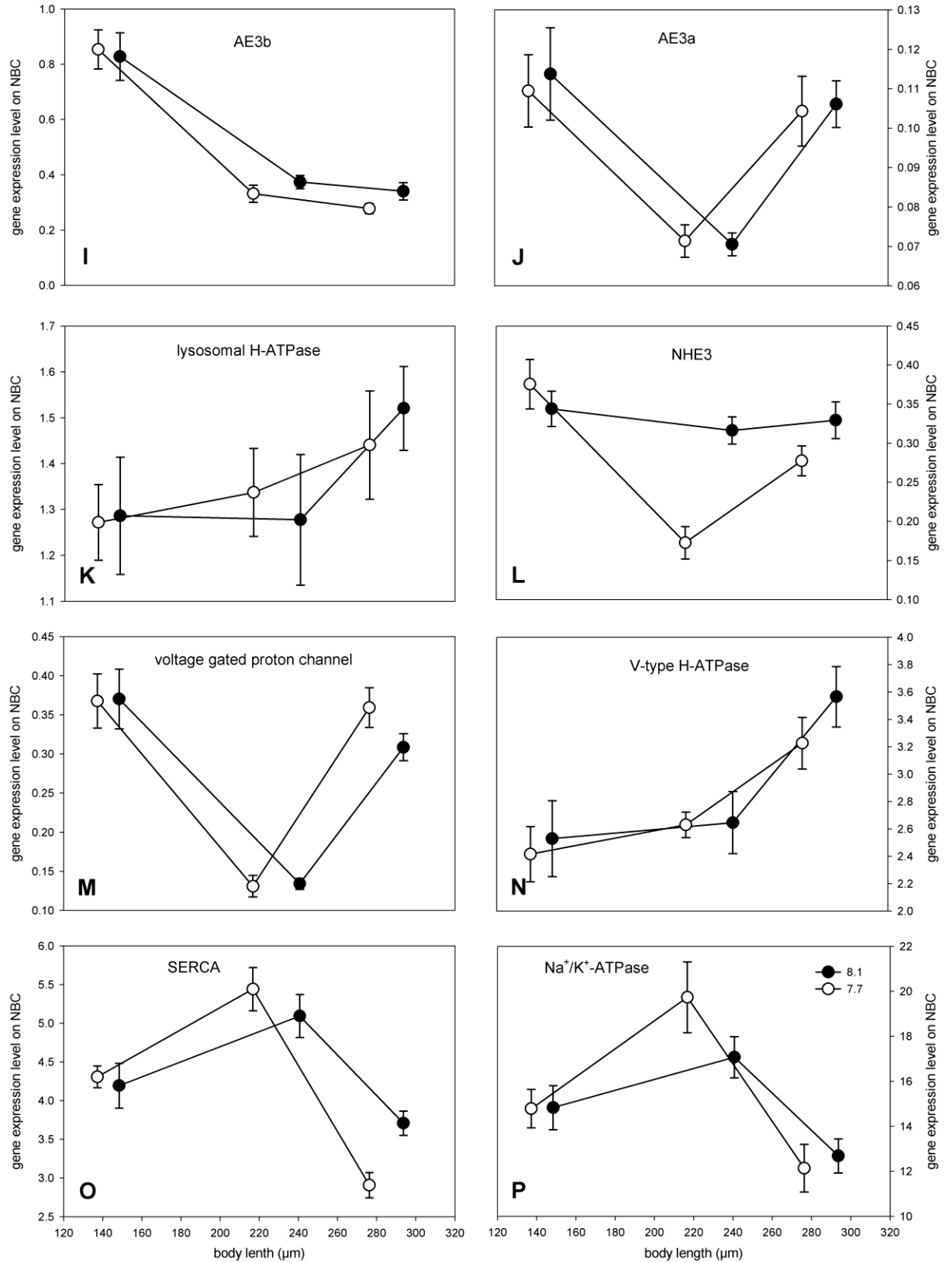
	Gene	pH 8.1 average abundance	pH 7.7 average abundance	average dissimilarity	contribution (%)
day 2 (post-fert) average dissimilarity 2.60 %	SM30B	3.94	3.7	0.4	15.26
	ATP-synthase	3.42	3.35	0.22	8.46
	gp96	2.48	2.37	0.2	7.53
	NKA	3.85	3.84	0.17	6.66
	SM50	2.26	2.22	0.14	5.31
	CS	1.66	1.61	0.13	5.08
day 4 (post-fert) average dissimilarity 4.30 %	SM30B	3.09	2.6	0.63	14.62
	ATP-synthase	4.68	5.08	0.55	12.74
	NKA	4.13	4.44	0.4	9.36
	msp130	1.42	1.13	0.37	8.63
	HSP70	3.19	3.48	0.37	8.53
	SM50	1.6	1.4	0.26	5.96
	T	1.81	1.98	0.22	5.19
day 7 (post-fert) average dissimilarity 3.06 %	ATP-synthase	5.09	5.29	0.45	14.81
	SERCA	1.93	1.7	0.32	10.58
	NKA	3.56	3.48	0.22	7.21
	HSP70	1.96	1.84	0.19	6.21
	gp96	2.08	1.97	0.19	6.19
	CS	2.14	2.21	0.17	5.5

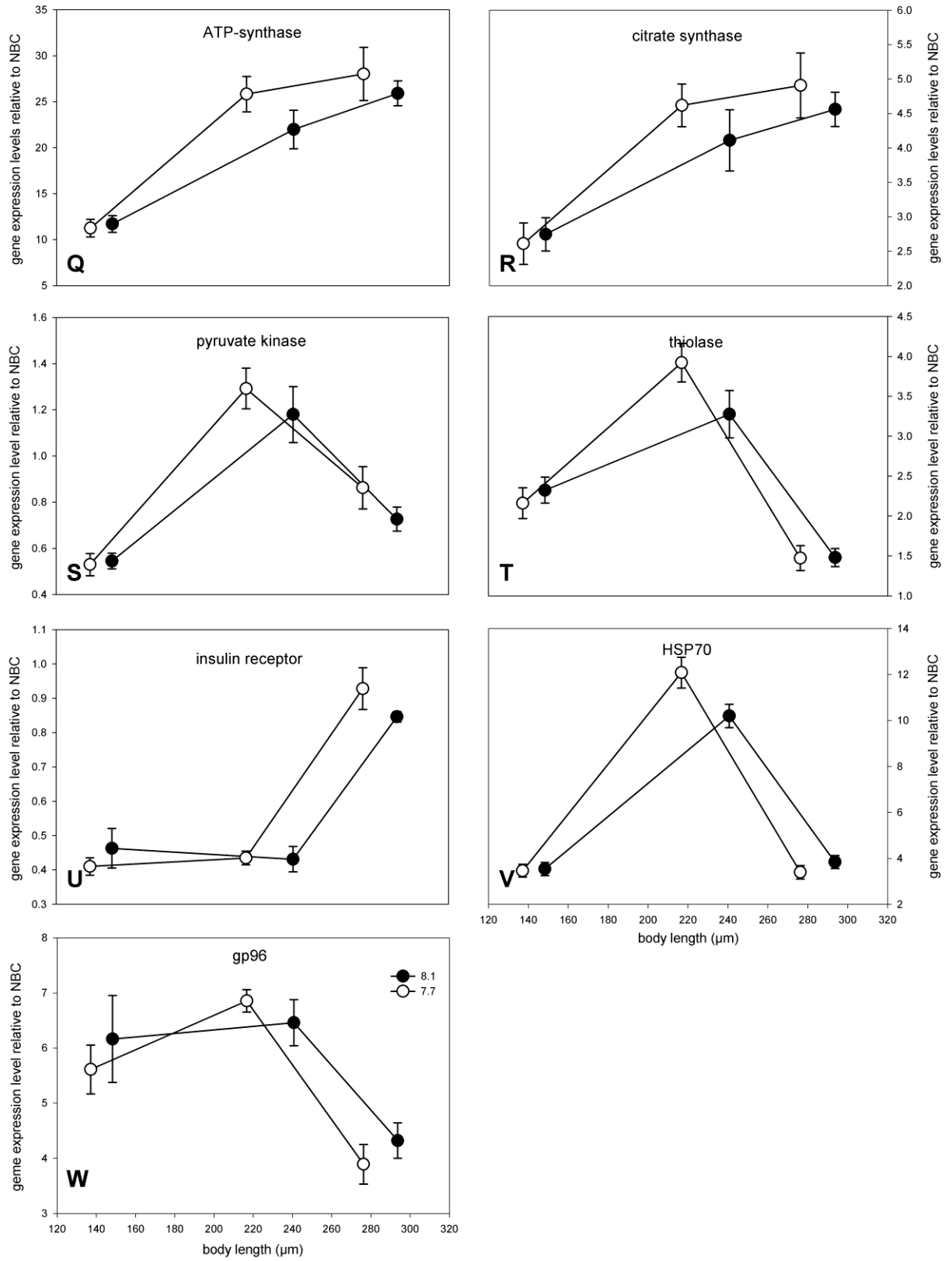
Supplementary materials

Figure S1: Transcript levels relative to NBC (NBC3) during larval development (body length in μm) to visualize real age vs. body length (stage effect) of *S. purpuratus* larvae. If no error bars (SD) are visible, error bars are smaller than data points.

Figure S1:







III Resource allocation and extracellular acid-base status in *Strongylocentrotus droebachiensis* in response to CO₂ induced seawater acidification.

Stumpp, M.; Trübenbach, K.; Brennecke, D.; Hu, M. Y.; Melzner, F.

Aquatic Toxicology (in preparation)

Resource allocation and extracellular acid-base status in the sea urchin *Strongylocentrotus droebachiensis* in response to CO₂ induced seawater acidification.

Stumpp, M.^{1,2*}; Trübenbach, K.^{1,3}; Brennecke, D.¹; Hu, M.Y.^{1,2}; Melzner, F.¹

1 Biological Oceanography, Leibniz Institute of Marine Sciences (IFM-GEOMAR), Kiel, Germany

2 Institute of Physiology, Christian-Albrechts-University Kiel (CAU), Kiel, Germany

3 Laboratório Marítimo da Guia, Centro de Oceanografia, Faculdade de Ciências da Universidade de Lisboa, Cascais, Portugal

* **Corresponding author:** Meike Stumpp, Biological Oceanography, Leibniz-Institute of Marine Sciences (IFM-GEOMAR), Hohenberg Str. 2, 24105 Kiel, mstumpp@ifm-geomar.de

Keywords: energy budget, feeding, O/N ratio, pH_e compensation, sea urchin, climate change

Abbreviations:

WM	wet mass
DM	dry mass
ASFD	ash free dry mass
MO ₂	oxygen consumption rate
RMR	routine metabolic rate
PCF	perivisceral coelomic fluid
SfG	scope for growth
pH _e	extracellular pH
ST	short term experiment (10 days)
LT	long term experiment (45 days)
OM	organic matter

Abstract

Anthropogenic CO₂ emission will lead to an increase in seawater $p\text{CO}_2$ of up to 80-100 Pa (800-1000 μatm) within this century and to an acidification of the oceans. Green sea urchins (*Strongylocentrotus droebachiensis*) occurring in the Western Baltic Sea (Kattegat) experience seasonal hypercapnic and hypoxic conditions already today. Thus, anthropogenic CO₂ emissions will add up to existing values and will lead to even higher $p\text{CO}_2$ values up to ca. 200-300 Pa (2000-3000 μatm). To estimate the green sea urchins' potential to acclimate to acidified seawater, we calculated an energy budget and determined the extracellular acid base status of adult *S. droebachiensis* exposed to moderately (102 to 145 Pa, 1007 to 1431 μatm) and highly (284 to 385 Pa e.g. 2800 to 3800 μatm) elevated seawater $p\text{CO}_2$ for 10 and 45 days.

A 45 day exposure of adult green sea urchins to elevated $p\text{CO}_2$ resulted in a shift in energy budgets, leading to reduced somatic and reproductive growth. Metabolic rates were not significantly affected by elevated $p\text{CO}_2$, but ammonium excretion increased in response to elevated $p\text{CO}_2$. This led to decreased O:N ratios. These findings suggest that protein metabolism is possibly enhanced under elevated $p\text{CO}_2$ in order to support ion homeostasis by increasing net acid extrusion. The perivisceral coelomic fluid acid-base status revealed that *S. droebachiensis* is able to fully (intermediate $p\text{CO}_2$) or partially (high $p\text{CO}_2$) compensate extracellular pH (pH_e) changes by accumulation of bicarbonate (maximum increases: +2.5 mM), albeit at a slower rate than typically observed in other taxa (10 day duration for full pH_e compensation). At intermediate $p\text{CO}_2$, sea urchins were able to maintain fully compensated pH_e for 45 days. Sea urchins from the higher $p\text{CO}_2$ treatment could be divided into two groups following long term acclimation: one group of experimental animals (29%) was characterized by remnants of food in their digestive system and was still able to maintain a partially compensated pH_e (+2.29 mM HCO_3^-), while the other group (71%) exhibited an empty digestive systems and a severe metabolic acidosis (-0.5 pH units, -2.35 mM HCO_3^-).

The results of this study suggest that *S. droebachiensis* occurring in the Kattegat might be pre-adapted to hypercapnia due to natural variability in its habitat. We show for the first time, that some echinoderm species can actively compensate extracellular pH. Environmental hypercapnia of 300 Pa or more, which could occur in the Kattegat within a century, can possibly only be endured for a short time period of a few weeks. Increases in

anthropogenic CO₂ emissions and leakages from potential sub-seabed CO₂ storage (CCS) sites thus impose a severe threat to the ecologically and economically important species *S. droebachiensis*.

1 Introduction

Anthropogenic CO₂ production will lead to an increase of $p\text{CO}_2$ up to 80-100 Pa (800 to 1000 μatm) within this century (Cao and Caldeira, 2008). Dissolution of CO₂ in seawater alters the carbonate system speciation, resulting in increased HCO₃⁻ and H⁺ and decreased CO₃²⁻ concentrations. Thus, a pH drop of up to 0.4 units in surface waters can be expected until the year 2100. Coastal benthic habitats like the Kattegat and the Baltic sea are today already experiencing seasonally elevated seawater $p\text{CO}_2$ (hypercapnia) with peak values of ca. 230 Pa (Thomsen et al., 2010) due to upwelling of deeper water masses with decreased $p\text{O}_2$ (hypoxia) and increased $p\text{CO}_2$. This is due to stratification and net heterotrophy in deeper water layers during summer months (Conley et al., 2007; Zillén et al., 2008; HELCOM, 2009; Beldowski et al., 2010; Thomsen et al., 2010). It can be expected that species living in such habitats must be adapted to seasonal hypoxic hypercapnic events. Moreover, in such habitats additional anthropogenic CO₂ will lead to much stronger increases in $p\text{CO}_2$ than expected for the average surface ocean: it has been estimated that in seasonally hypoxic habitats, $p\text{CO}_2$ values of >300 Pa (>3000 μatm) could be encountered in the summer months in benthic habitats in the Western Baltic Sea within this century (Thomsen et al., 2010). Such seawater $p\text{CO}_2$ values might deplete tolerance capacity of relatively immobile benthic invertebrates like sea urchins. Furthermore, the Skagerrak / Kattegat region is currently being examined for suitable sub-seabed carbon capture and storage (CCS) sites (Haugen et al., 2011). The associated risk of CO₂ leakage from such potential storage sites is unknown, but it is important to identify threshold $p\text{CO}_2$ values that lead to faunal changes in benthic regions. Echinoderms might develop into important indicator organisms for ecosystem monitoring, as recent community analyses in naturally acidified regions have demonstrated replacement of echinoderms by photoautotrophic communities (Hall-Spencer et al., 2008).

The green sea urchin *Strongylocentrotus droebachiensis* inhabits the shallow subtidal zone from 0 to 50 m and occurs commonly in the North-Western part of the Baltic Sea (Skagerrak and Kattegat). *S. droebachiensis* plays an important role in determining community states in the shallow rocky subtidal which alternate between seaweed beds with low abundance of sea urchins and so called sea urchin barrens, where encrusting corraline red algae replace kelp forests (Scheibling and Hatcher, 2007). It is an

important key species stabilizing either form of community states by grazing on kelp and associated epibionts and in turn forming an important prey for teleosts, crustaceans and other echinoderms (Scheibling and Hatcher, 2007).

Mechanistic studies on the effect of increased $p\text{CO}_2$ on adult sea urchin physiology are still scarce, as most research has focused on the presumably more sensitive early life stages (Dupont et al., 2010c). Somatic gonad growth of adult sea urchins *Hemicentrotus pulcherrimus* and *Echinometra mathaei* was shown to decrease under hypercapnic conditions (Shirayama and Thornton, 2005). Under very high seawater $p\text{CO}_2$ (810 Pa, 8000 μatm), food intake, feed conversion efficiency and gonad growth of *S. droebachiensis* was significantly reduced (Siikavuopio et al., 2007b). Miles et al. (2007) observed. Moreover, determinations of the extracellular acid-base status in coelomic fluids of *Psammechinus miliaris* revealed a very low capacity to compensate for disturbances in extracellular pH (pH_e) under acute exposure to hypercapnia (250 Pa, 2470 μatm , Miles et al., 2007). In fact, no study could measure significant pH_e regulatory capacity in response to environmental hypercapnia in subtidal echinoderm species so far (Melzner et al., 2009). Pörtner et al. (2004) proposed that a limited capacity to regulate pH_e might elicit metabolic depression and lead to decreased growth rates observed in several studies. However, more recent studies suggest that environmental hypercapnia primarily impacts energy budgets and partitioning, potentially due to elevated energetic demands for cellular acid-base and ion balance (Wood et al., 2008; Deigweier et al., 2010; Thomsen and Melzner, 2010; Stumpp et al., 2011a; Stumpp et al., 2011b).

We hypothesized that the energy budget in *S. droebachiensis* would be impacted by elevated $p\text{CO}_2$, resulting in decreased growth and calcification rates. In order to study energy budgets and energy partitioning, we measured food intake, excretion (fecal pellet and NH_4^+ production), food absorption efficiency, metabolic rates and growth in green sea urchins exposed to control and hypercapnic conditions for 45 days. Additionally, we estimated the capacity of *S. droebachiensis* to compensate extracellular acidosis by determining the acid-base status of the perivisceral coelomic fluid in sea urchins exposed to acute (<10 days) and long-term hypercapnia (45 days). By using two hypercapnic levels of intermediate (102-145 Pa, 1010-1430 μatm) and high $p\text{CO}_2$ (284-385 Pa, 2800-3800 μatm) we tried to estimate adaptation of *S. droebachiensis* to a seasonally high

$p\text{CO}_2$ in their benthic habitat and to $p\text{CO}_2$ values that might be encountered within this century.

2 Material & Methods

2.1 Animal collection and maintenance

Green sea urchins (*S. droebachiensis*) were collected on a cruise with FK Littorina in April 2008 for short-term (ST) experiments and in June 2010 for long-term (LT) experiments at subtidal depths (17.7 ± 0.2 m) in the Kattegat, Western Baltic Sea ($56^\circ 21' \text{N}$, $11^\circ 19' \text{E}$). Sea urchins were immediately transported to the aquarium of the Leibniz-Institute of Marine Sciences (IFM-GEOMAR, Kiel) and maintained in a recirculation aquaculture system (20m³ volume, protein skimmers, nitrification and denitrification filters). Seawater (salinity 29.4 ± 0.6) was adjusted in equilibrating tanks by mixing Baltic seawater from Kiel Fjord with a SeequaSal salt mixture (Münster, Germany). The composition of SeequaSal corresponds to that of normal seawater. The physiochemical parameters of the seawater (i.e. pH, temperature, salinity and ammonia) were controlled regularly and sea urchins were fed *ad libitum* with fresh *Fucus vesiculosus* collected in Kiel Fjord.

Short term (ST) experiments were conducted at the facilities of the IFM-GEOMAR in Kiel in summer 2008. Long term (LT) experiments were performed on the island Sylt at the Wadden Sea Station Sylt of the Alfred Wegener Institute for Polar and Marine Research in October 2010.

2.2 Experimental setups (ST and LT experiment)

For ST experiments, a salinity of 31.5 was created by mixing distilled water with synthetic sea salt (SeequaSal). For LT experiments, North Sea water (average salinity 29.5) was used in the cooling chambers of the AWI facilities. A storage tank was used in both experiments for thermal equilibration and aeration with pressurized air. Water was distributed to the experimental units (ST n=4, LT n=6) via a pump (ST) or via gravity feed (LT). To avoid bacterial infections, seawater was continuously passed over a 15 Watt UV sterilizer (HW-Aquaristik, Germany). In order to avoid alterations of the seawater carbonate system by biological activity of experimental animals and microorganisms, we used flow-through systems in 10°C climate chambers with flow rates

adjusted to a minimum twofold water exchange per tank per day (Table 1). A light regime with a 12 h:12 h light:dark cycle was chosen. For both experiments, three different $p\text{CO}_2$ levels (a control, an intermediate and a high $p\text{CO}_2$ level, see table 1) were used by equilibrating experimental aquaria with an air/ CO_2 gas mixture generated by a central automatic gas mixing-facility (Linde Gas, HTK Hamburg, Germany). The gas mixture (0.8 l min^{-1}) was introduced into the experimental aquaria using diffusor stones (Dohse, Grafenschaft-Gelsdorf, Germany). All sea urchins were incubated under control conditions for at least one week and morphometric parameters (i.e. live wet weight (in g ind^{-1}) and individual test diameter (in mm) were quantified at the start and end of the experiments. Exposure times were 10 days for the ST incubation (acid-base status) and up to 45 days for the long-term incubation (growth, feeding, respiration, excretion and acid-base status, summarized in figure 1). In the ST experiment, a time-series was performed with additional subsamples at day 2, 4 and 7. In both experiments, sea urchins were fed daily with fresh, epibiont-free brown algae *F. vesiculosus ad libitum*. Faeces were removed prior to feeding. For ST experiments, 4 sea urchins were placed in one experimental unit (4 replicate aquaria, 3 $p\text{CO}_2$ levels, 4 sea urchins each, 48 sea urchins in total), for LT experiments, 10 urchins were placed together in one experimental unit (6 replicate aquaria, 3 $p\text{CO}_2$ levels, 10 urchins each, 180 urchins in total). Due to time management constraints, feeding and fecal pellet production in the LT experiment were measured between days 10 and 35 of the experiment. Aerobic metabolic rates, ammonium excretion rates and growth were measured on days 36 to 42. Subsequently, acid-base status was determined in the remaining animals on days 43 to 48. An experimental time schedule is depicted in figure 1.

2.3 Carbonate system characterization (ST and LT experiment)

In the ST experiment, the seawater carbonate system speciation was calculated from three total alkalinity (A_T) and total dissolved inorganic carbon (C_T) measurements (taken on days 0, 4, 10) and from C_T and pH_T measurements (weeks 1, 3, 6) in the LT experiment using CO2SYS software (Lewis and Wallace, 1998), with dissociation constants from Mehrbach et al. (1973) as refitted by Dickson and Millero (1987). A 500 ml water sample was taken for C_T/A_T or C_T/pH_T determinations and immediately poisoned with 100 μl of saturated HgCl_2 solution. C_T was measured according to Dickson et al. (2007) using either a SOMMA (Marianda, Kiel, Germany) coulometric auto analyzer or an AIRICA

(Marianda, Kiel, Germany) analyzer, which is based on infrared-detection of CO₂ purged from an acidified sample. A_T was determined according to Dickson et al. (2007) by means of potentiometric open-cell titration with hydrochloric acid that was performed with a VINDTA (Marianda, Kiel, Germany) auto analyzer. Reference material was used according to Dickson et al. (2007). pH_T measurements were conducted with a Metrohm pH meter (826 pH mobile, Metrohm, Filderstadt, Germany) and a glass electrode calibrated with sea water buffers based on TRIS/HCl and 2-aminopyridine/HCl according to (Dickson et al., 2007). Daily, seawater salinity and temperature were measured (precision ± 0.1 g/kg respectively °C) with a salinometer (WTW cond 315i, WTW TETRACON 325-measuring chain). Additionally, seawater pH_{NBS} was controlled daily with a pH meter (WTW 340i pH-analyzer, WTW SenTix 81-measuring chain, precision 0.01 units) that was calibrated with Radiometer IUPAC precision pH buffers 7.00 and 10.00 (S11M44, S11 M007). Ammonia concentrations ($[NH_4^+]$) were detected via the salicylat method (Reardon et al., 1966) and values ranged between 0-0.3 mg L⁻¹ in experimental aquaria.

2.4 Biometric measurements and growth determinations (LT experiment)

Sea urchins used for this study had a fresh mass between 7 and 12 g. Growth of sea urchins in the LT experiment was analyzed using wet mass (WM), dry mass (DM), ash-free dry mass (AFDM) and ash content (ash dry mass) of several body parts (Lantern of Aristotle, gonads, gut and test including spines). A random sample of 18 urchins was taken as a reference group at the beginning of the experiment (prior to CO₂ incubation) and randomly grouped into 6 replicates. The diameter (to the nearest 0.1 cm) was recorded using a caliper. Test diameter was recorded before and after experimental incubation. In order to determine the masses of body organs, urchins were dissected (Aristotle Lantern, gonads, gut, test and spines) and organs / body parts blotted dry on paper towels. Wet masses were determined using a precision scale (LC220s, Sartorius, Göttingen, Germany, 1 mg resolution). Organs were dried at 80°C for 20 hours (U30 793 590 Memmert, Schwabach, Germany) and masses were determined again. Ash dry mass of body organs was determined by placing organs in a drying oven at 500°C for 20 hours (M110, Heraeus, Hanau, Germany) prior to mass determination. AFDM was then calculated by subtracting ash dry mass from dry mass of the respective organ. Detailed biometric measurements were conducted with urchins that were used for respiration and

ammonium excretion trials after the physiological measurements were completed. Urchins that were used for extracellular acid-base status determinations were only visually inspected for health (outer appearance, feeding state, gonad development, coelomic fluid color and behavior, for details see 2.10). Four urchins from each replicate aquarium were used to determine growth. For statistical analyses, values of single individuals (four per replicate) were averaged and the n=6 experimental aquaria per CO₂ level were considered the unit of replication.

2.5 Feeding and fecal pellet production (LT experiment)

Feeding and fecal pellet production was monitored in the experimental setups continuously for 21 days starting a week after urchins were first exposed to their experimental conditions. In preliminary studies, preference for different algae types (*Fucus vesiculosus* and *Ulva lactuca*) was tested and experimental animals were acclimatized to their preferred food choice for four weeks prior to the start of the experiment to ensure adequate condition. To determine ingestion rate, algae were cleaned from epibionts dried at 10°C for 12 hours and split into servings of 8.05 ± 0.01 g. Servings were then placed into experimental units that were cleaned from all food remnants. Four separate servings per pCO₂ condition were incubated in urchin free tanks to determine possible effects of pCO₂ on the algae biomass. Urchins were then left to feed on their algal serving for 70 hours before the remnants of food and produced fecal pellets were collected. Directly after collection, new food servings were supplied to the urchins, so that urchins were always fed *ad libitum*. Food remnants, control food servings and fecal pellets were dried at 80°C for 20 hours (dry oven U30 793 590, Memmert, Schwabach, Germany) and weighed (LC220s, Sartorius, Göttingen, Germany). Fecal pellet production is expressed in mg DM faeces day⁻¹ ind⁻¹. Dry mass of control algae servings was used as a reference for the starting point of feeding and food intake was calculated by subtracting the food remnants from the starting quantity. For statistical analysis, repeated measures of feeding rate and fecal pellet production (6 subsequent experiments per aquarium in three weeks) were averaged per replicate aquarium and means over time of each aquarium (6 per pCO₂ level) was treated as unit of replication (n=6). Feeding rate is expressed as mg DM algae day⁻¹ ind⁻¹.

For organic matter absorption efficiency, food remnants and faeces were ashed at 500°C for 20 hours (oven M110, Heraeus, Hanau, Germany) to determine the organic component of food and faeces. Subsequently, the Conover ratio was calculated (Conover, 1966):

$$E_{OM} = (F' - E') ((1 - E') F')^{-1} \quad (1)$$

with F' being the ash-free dry mass to dry mass ratio of food and E' being the ash-free dry mass to dry mass ratio of faeces.

To calculate energy budgets for the different pCO_2 conditions, food intake (consumed energy C) was converted into energy equivalents using a conversion factor of 15.5 kJ g DM determined for *Fucus serratus* (Marsham et al., 2007).

2.6 Respiration (LT experiment)

For metabolic rate determination, two sea urchins were used for one measurement. Sea urchins were starved for 12 hours and were placed in glass respiration chambers with a volume of 325 ml containing 0.2 μ m filtered sea water equilibrated with the appropriate pCO_2 level. Respiration chambers were closed, submerged in a water bath at 10°C and oxygen saturation was measured continuously (once every 30 seconds) for 2-3 hours using non-invasive oxygen sensors connected to a OXY-4 mini multichannel fiber optic oxygen transmitter (PreSens, Regensburg, Germany), that were calibrated according to the manufacturer's instructions. Preliminary experiments demonstrated that the sea urchins could sufficiently mix the water volume without external stirrer and oxygen concentration decreased linearly (data not shown). Therefore, and in order to minimize stress, we decided to conduct the measurements without a stirrer. When oxygen concentration reached the 70% air saturation level, sea urchins were removed. The missing water volume was refilled with 0.2 μ m filtered sea water, respiration chambers were closed and measured for 3 to 6 hours for detection of background respiration. Bacterial respiration never exceeded 10% of animal respiration. For calculation of oxygen consumption rates, the linear decrease in oxygen concentration during measuring intervals between 30 min and the end of the measurement period was considered. Oxygen consumption rates (MO_2) are expressed as μ mol O_2 g⁻¹ AFDM h⁻¹. Subsequently, the

animal's size and total weight, as well as that of body parts was determined (WM, DM, ASDM).

2.7 NH_4^+ excretion (LT experiment)

Ammonium excretion rates were determined from NH_4^+ concentration measurements prior to and following incubation of sea urchins for respiration measurements. Before and after closing the respiration chambers, a 1 mL seawater sample was removed and 250 μL of reagent containing orthophthaldialdehyde, sodium sulphite and sodium borate was added (Holmes et al., 1999). Samples were then incubated for 2 hours at room temperature in the dark until fluorescence was determined at an excitation and emission wavelength of 360 and 422 nm, respectively (Kontron SFM25 fluorometer). Additionally, a separate glass chamber was incubated without sea urchins to determine background readings of filtered sea water and ammonium excretion of respiration bacterial controls was also determined. Ammonia (NH_3) was not measured as NH_3 concentrations at pH values of 8 to 7.1 are negligible (0.2-2% of total ammonium/ammonia, Körner et al., 2001). Ammonium excretion rates are expressed as $\mu\text{mol NH}_4^+ \text{g}^{-1} \text{AFDM h}^{-1}$.

2.8 Calculation of O:N ratio and energy budgets

The atomic ratio of oxygen uptake and excreted nitrogen was calculated from respiration and ammonium excretion rates:

$$\text{O} : \text{N} = 2 \text{MO}_2 (\text{NH}_4^+ \text{excretion})^{-1} \quad (2)$$

Aerobic energy loss was calculated by converting respiration (R) and NH_4^+ excretion (U) rates into their caloric equivalents using 0.484 J $\mu\text{mol O}_2$ representing a mixed, but protein dominated, catabolism of hydrocarbons, lipids and proteins and 0.347 J $\mu\text{mol NH}_4^+$ (Elliott and Davison, 1975; Gnaiger, 1983). Absorbed energy (A) was calculated using the consumed energy (C) and the Conover ratio (Conover, 1966) as an estimate of organic matter absorption efficiency (E_{OM}) multiplied by ingested energy:

$$A = E_{\text{OM}} C \quad (3)$$

Deposited energy into growth (G) was determined by converting absolute growth per day of body organs (gonads, test and spines, gut) over 40 days into caloric equivalents based on biochemical constituents (lipid, carbohydrates and protein) of the respective organ

using the conversion values of 4.3 kJ g⁻¹ DM and 24 kJ g⁻¹ DM for deposition into test and spines and deposition into gonad or gut tissue, respectively (Bishop and Watts, 1992; Fernandez, 1998). Growth of Aristotle Lantern was omitted due to non significant differences in dry mass of this organ in experimental vs. reference urchins.

The final energy budget was then calculated according to the following equation:

$$C = A - (R + U + G_{\text{gonad}} + G_{\text{gut}} + G_{\text{test\&spines}} + X) \quad (4)$$

with X being the unexplained energy fraction.

Scope for growth (SfG) was determined by subtracting metabolic energy loss from the absorbed energy according to:

$$\text{SfG} = A - (R + U) \quad (5)$$

All energy conversions are expressed in J g⁻¹ DM day⁻¹.

2.9 Extracellular (perivisceral coelomic fluid) acid-base status

2.9.1 Carbonate system speciation

Perivisceral coelomic fluid (PCF) was collected from the sea urchin coelomic cavity via a gas-tight Hamilton syringe by penetrating their perivisceral membrane at the oral surface between the two rows of their water vascular system. For coelomocyte disposal, withdrawn coelomic fluid of echinoids was centrifuged for 30 seconds (6000 rpm) using a minifuge (C1100-FIS-230-EU, Fisher Scientific, Germany). The supernatant was transferred into a new sample tube and incubated in a water bath of 10°C during C_T and pH measurements. Determination of pH_e was performed using a microelectrode (WTW Mic-D) and a WTW pHi 340 pH meter (precision ± 0.01 units) that was calibrated with Radiometer precision buffers 7 and 10 (S11M44, S11 M007). Total dissolved inorganic carbon was determined in duplicates (100 μl each) via a Corning 965 carbon dioxide analyzer (precision ± 0.1 mmol L⁻¹; Olympic Analytical Service, England) that was calibrated by generating a sodium bicarbonate (Fluka, Germany) standard curve with a fresh dilution series of 20, 10, 5, 2.5 and 1.25 mM. Carbonate system speciation (i.e. pCO_2 , $[\text{HCO}_3^-]$) within the coelomic fluid of *S. droebachiensis* was calculated from extracellular pH (pH_e) and total dissolved inorganic carbon (C_T) measurements according to the Henderson-Hasselbalch equation

$$p\text{CO}_2 = C_T (\alpha (10^{(\text{pH} - pK'_1)} + 1))^{-1} \quad (6)$$

$$[\text{HCO}_3^-]_e = C_T - (\alpha p\text{CO}_2) \quad (7)$$

where α (0.509 $\mu\text{mol}/(\text{L Pa})$) at a salinity of 31.5, and a temperature of 10°C; Weiss, 1974) is the solubility coefficient of CO_2 in seawater and pK'_1 the dissociation constant of carbonic acid. pK'_1 was estimated in dependency of pH_e (see below, Equ. 9).

2.9.2 pK'_1 and non-bicarbonate buffer (NBB) line

The dissociation constant pK'_1 in the PCF of *S. droebachiensis* was determined over a pH range of 0.9 units (pH 7.3 - 8.2). PCF of seven sea urchins was pooled, subsequently centrifuged (20 min, 4°C, 60 g, Eppendorf 5415 R, Germany) and aliquots (at least 4 x 400 μL) of the supernatant incubated for one hour in a shaking, tempered (10°C) water bath against different CO_2 - air mixtures ($p\text{CO}_2 = 0.06, 0.14, 0.4$ and 0.6 kPa). Simultaneously, $p\text{CO}_2$ values in the gas mixture used for equilibration were controlled via an infrared $p\text{CO}_2$ analyzer (GDZ 401, HTK Hamburg, Germany). After equilibration, C_T and pH_e were determined immediately (see above, carbonate system speciation). The functional pK'_1 values for the PCF of *S. droebachiensis* were calculated using the Henderson-Hasselbalch equation in the form

$$pK'_1 = \text{pH} - \log ((C_T - \alpha p\text{CO}_2) / \alpha p\text{CO}_2^{-1}) \quad (8)$$

pK'_1 values were calculated via equation 8 and were plotted against pH_e resulting in a linear relationship. For subsequent pK'_1 calculations, the following equation was used:

$$pK'_1 = -0.0876 \text{ pH}_e + 6.6596 \quad (R^2 = 0.51) \quad (9)$$

A non-bicarbonate buffer line (NBB) was measured from an oxygenated, pooled PCF sample from five sea urchins from our maintenance facilities. *In vitro* measurements were performed by equilibrating samples of extracellular fluid with an air mixture of known $p\text{CO}_2$, to subsequently measure pH_e and bicarbonate $[\text{HCO}_3^-]_e$ as outlined above (see pK'_1 determination). The calculated $[\text{HCO}_3^-]_e$ values were then plotted against their extracellular pH_{NBS} resulting in a linear relationship. The negative slope of the NBB line, $-\Delta([\text{HCO}_3^-] + [\text{CO}_3^{2-}]) / \Delta\text{pH}^{-1}$, is defined as β_{NB} , expressed in $\text{mEq L}^{-1} \text{ pH}^{-1}$ was assessed to be -0.41 ($R^2 = 0.23$).

2.10 General observations

Animal behavior was noted throughout the experiment (LT). During the last experimental week (falling together with acid-base status measurements) we noticed a decreasing health status of urchins exposed to 284 Pa with increasing mortality towards the end of experiment. Dead sea urchins were excluded from measurements. Sea urchins used for determination of acid-base status (LT experiment) were therefore additionally characterized according to their health status. This was defined using (i) outer appearance (categories: a = healthy, b = infected with bacteria, i.e. black epidermal lesions on the test (Gilles & Pearse 1989), C = stressed, i.e. non- erect spines or visible decrease in spine density), (ii) PCF color, which is mostly characterized by the content of red spherule cells (visual analysis: red, light red and colorless, Johnson, 1969; Matranga et al., 2006) and (iii) by determining the digestive status (categories: a = completely filled gut, b = filled hind gut, c = empty digestive system) and (iv) state of gonads (categories: a = big gonads filling 30-50% of the coelomic cavity volume, b = gonads present but filling less than 30% of the coelomic cavity volume, c = no visible gonad tissue present) and (v) by analyzing the inner test surface (which is covered by the peritoneum) for visible signs of bacterial infection. Black lesions on the test's inner or outer side are characteristic for bacterial infections in echinoids (Gilles & Pearse 1989). As digestive status correlated with acid base status of sea urchins, sea urchins used for acid-base status measurements were divided into animals containing food in their digestive tract (high $p\text{CO}_2$ and food: h_F) and animals not containing food in their digestive system (high $p\text{CO}_2$ and empty digestive system: h_E). All control (47 Pa) and 102 Pa $p\text{CO}_2$ animals contained food in their digestive system and were not divided into subgroups. Although these features were characterized subjectively, some points hold interesting information for further research.

2.11 Statistics

For each measurement, several urchins from each of the six experimental units per treatment were used and averaged. Normality of distributions was assessed via the Kolmogorov-Smirnov test. Differences between hypercapnia treatment groups were analyzed using one-factorial ANOVA followed by *post hoc* Tukey tests using STATISTICA 8 (StatSoft, Tulsa, USA). Percentage values of absorption efficiencies

were arcsine transformed prior to statistical analysis. The threshold for significance was $p < 0.05$. The data in the text and figures are presented as the mean \pm standard deviation (SD).

3. Results

3.1 Survival and general observations (LT experiment)

Survival rates over the whole experimental period were 95% under control, 100% under moderately and 95% under highly increased seawater $p\text{CO}_2$. However, within the last week of the experimental period, the health status of individuals exposed to 284 Pa CO_2 decreased (table 2) and 66% of the overall mortality in this treatment occurred within the last week of the experiment. In contrast, the observed mortality of 5% in the control treatment occurred only in the initial phase of the experiment. After 40 days of exposure, animals from the high $p\text{CO}_2$ treatment started to show a strong tendency to maintain positions close to the surface of the experimental aquaria. At exposure day 44, 81% of all observed high $p\text{CO}_2$ animals were located within 2 cm of the aquarium surface while most of control and intermediate $p\text{CO}_2$ animals remained on the bottom of the aquaria between algae (90% control animals and 71% intermediate $p\text{CO}_2$ animals) (table 2). Analysis of digestive tract contents revealed that 71 % of sea urchins in all replicate tanks exposed to 284 Pa over 40 days did not contain any food particles in their digestive system (table 2) and some even contained air within their digestive system.

3.2 Somatic and gonadal growth (LT experiment)

Body organ masses under the different $p\text{CO}_2$ treatments are provided in table 3. During 40 days of exposure to different seawater $p\text{CO}_2$, only sea urchins incubated under ambient and intermediate $p\text{CO}_2$ significantly increased in test diameter from 2.79 ± 0.02 and 2.78 ± 0.02 cm to 2.93 ± 0.05 and 2.89 ± 0.05 cm, respectively (table 3). Total and test dry mass of control urchins increased significantly from 1.67 ± 0.16 g and 1.80 ± 0.05 g to 2.06 ± 0.18 g and 2.38 ± 0.07 g, respectively. Animals incubated in intermediate and high $p\text{CO}_2$ seawater did not significantly increase in total and test drymass. However, gonad and gut tissue dry mass significantly increased in all $p\text{CO}_2$ treatments in relation to the reference group by an average of 104 and 62 mg in control animals, by 73 and 56 mg under moderately elevated $p\text{CO}_2$ and 51 and 45 mg under high $p\text{CO}_2$ in gonad and gut,

respectively. Aristotle Lantern dry mass did not significantly change in any treatment over the experimental period. After 40 days of exposure to the various seawater $p\text{CO}_2$ s, total dry mass, test dry mass, gonad dry mass and gut dry mass was significantly larger in control animals than in high $p\text{CO}_2$ treatment animals (table 3). Gonad dry mass of control animals was also significantly higher than gonad dry mass of animals exposed to the intermediate level of 102 Pa CO_2 . Ash-free dry mass of total body and body organs showed the same pattern as dry mass in terms of statistically significant changes due to $p\text{CO}_2$ treatments.

The test CaCO_3 content, measured as ash dry mass of tests, did not significantly differ between the reference urchin group and any CO_2 treatment, but a significant difference was detected between control and high $p\text{CO}_2$ animals with values of 1.58 ± 0.04 g and 1.39 ± 0.09 g, respectively. The CaCO_3 content of tests (87-88%) was not significantly different between treatments (table 3).

3.3 Ingestion, fecal production and absorption efficiencies (LT experiment)

The food ingestion rate was observed to be highly variable over the time period of the LT experiment, ranging between 27.5 and 82.0 mg DM algae $\text{day}^{-1} \text{ind}^{-1}$ (figure 2). Averaged over the whole experimental time there was a significant decrease in ingestion rates between control (47 Pa) and high $p\text{CO}_2$ (284 Pa) with a mean of 59.6 ± 11.6 mg $\text{day}^{-1} \text{ind}^{-1}$ under control conditions and 55.1 ± 4.1 and 42.0 ± 7.3 mg $\text{day}^{-1} \text{ind}^{-1}$ under medium and high $p\text{CO}_2$, respectively (Fig. 3A white bar, ANOVA, $F=7.38$, $p<0.01$). Fecal pellet production over time was significantly lower at high $p\text{CO}_2$ than under intermediate and control $p\text{CO}_2$ (Fig. 3A black bar, ANOVA, $F=34.85$, $p<0.01$). There was no significant difference between the organic matter absorption efficiency among the different treatments (Fig. 3B, One-way ANOVA, $F=0.09$, $p=0.91$).

3.4 Routine metabolic rates, ammonium excretion and O:N ratio (LT experiment)

Routine metabolic rates tended towards lower values with increasing $p\text{CO}_2$ (Fig. 4A), ranging from 14.2 ± 2.4 to 12.6 ± 1.6 $\mu\text{mol O}_2 \text{ h}^{-1} \text{g}^{-1}$ AFDM (ANOVA, $F=1.136$ $p=0.347$). Ammonium excretion rates significantly increased with increasing $p\text{CO}_2$ from 1.05 ± 0.22 $\mu\text{mol NH}_4^+ \text{ h}^{-1} \text{g}^{-1}$ AFDM under control conditions to 1.70 ± 0.47 $\mu\text{mol NH}_4^+ \text{ h}^{-1} \text{g}^{-1}$ AFDM at high $p\text{CO}_2$ (Fig. 4B, ANOVA, $F=7.704$, $p<0.01$). Accordingly, the O:N

ratio decreased significantly with increasing $p\text{CO}_2$ from 28.5 ± 5.6 at 47 Pa CO_2 to 17.4 ± 7.0 at 284 Pa CO_2 (Fig. 4C, ANOVA, $F=5.787$, $p<0.05$).

3.5 Energy budget (LT experiment)

Energy budgets for urchins exposed to three different $p\text{CO}_2$ treatments were calculated from ingestion, organic matter absorption efficiency, respiration, ammonium excretion and growth of gonad, gut and test including spines (table 4).

The energy assimilated (absorbed energy, A) was significantly higher in sea urchins exposed to control $p\text{CO}_2$ with $204 \pm 33 \text{ J day}^{-1} \text{ g}^{-1} \text{ DM}$ than in urchins exposed to high $p\text{CO}_2$ conditions with $166 \pm 15 \text{ J day}^{-1} \text{ g}^{-1} \text{ DM}$ (table 4). The energy used for aerobic metabolism and ammonium excretion did not significantly differ between treatments (table 4). Scope for growth (SfG), defined as energy not used in oxidative phosphorylation and lost as NH_4^+ excretion, was significantly higher (table 4) in sea urchins exposed to control $p\text{CO}_2$ ($166 \pm 32 \text{ J day}^{-1} \text{ g}^{-1} \text{ DM}$) than in animals exposed to high $p\text{CO}_2$ ($134 \pm 13 \text{ J day}^{-1} \text{ g}^{-1} \text{ DM}$).

Under control conditions, most energy available for growth was channeled into gonad production followed by gut growth and by test and spine growth (table 4). In sea urchins exposed to intermediate and high $p\text{CO}_2$ significantly less energy was deposited into gonad tissue (ANOVA, $F=10.525$, $p<0.01$) and test growth (ANOVA, $F=9.938$, $p<0.01$). Energy deposition into gut growth did not differ between CO_2 treatments (ANOVA, $F=1.954$, $p=0.176$).

The energy balance was positive in all $p\text{CO}_2$ treatments with values between $56.9 \pm 8.9\%A$ under control conditions and $66.4 \pm 6.3\%A$ at high $p\text{CO}_2$.

3.6 Extracellular acid-base status (ST and LT experiment)

Extracellular acid-base status in coelomic fluid of sea urchins kept under elevated $p\text{CO}_2$ was assessed in two separate experiments: one short-term experiment with acute exposure to two elevated $p\text{CO}_2$ levels (145 Pa and 385 Pa) and repeated measurements (0, 2, 4, 7 and 10 days) to evaluate the time course of potential pH_e regulatory reactions and a long-term experiment (102 Pa and 284 Pa) to observe the capacity to regulate pH_e after 40 to 45 days of exposure. Differences in PCF $[\text{HCO}_3^-]_e$ of control sea urchins between short

term and long term experiments are due to differences in sea water alkalinity (artificial sea water in short term experiments vs. natural seawater in long term experiments). The magnitude of bicarbonate accumulation was not influenced by the type of sea water used for the respective experiments.

Acute exposure to moderately elevated $p\text{CO}_2$ resulted in a significant drop in PCF pH_e of -0.31 units over the first 4 days below the non-bicarbonate buffer line (figure 5A, ANOVA, $F= 8.656$, $p<0.01$) and then in a complete compensation of pH at day 10 of exposure. $[\text{HCO}_3^-]_e$ remained almost unchanged with a slight drop at day 4 of exposure and then increased significantly between day 4 and day 10 (ANOVA, $F=6.437$, $p<0.01$) with a total $[\text{HCO}_3^-]_e$ accumulation of +2.1 mM.

Under acute exposure to 385 Pa CO_2 , a significant mean pH_e drop of -0.39 units in the coelomic fluid was observed until day 4 of exposure (ANOVA, $F=21.430$, $p<0.01$) with partial pH compensation at day 10 (-0.19 units, figure 5B). Bicarbonate concentrations started to increase at day 4 of exposure and a total accumulation of 2.2 mM bicarbonate was achieved by day 10 (ANOVA, $F=8.712$, $p=0.001$).

After 40 days exposure (figure 6), full pH_e compensation was observed in animals kept at 102 Pa and partial compensation in animals with food in their gastric system (h_F) at 284 Pa (-0.28 pH_e units, ANOVA, $F=46.201$, $p<0.01$). Sea urchins with empty guts (h_E) showed no compensation with a mean drop in extracellular pH of -0.53 units compared to control animals. A compensation of pH_e was accompanied by a significant increase in $[\text{HCO}_3^-]_e$ in sea urchins exposed to 102 Pa and 284 Pa sea urchins with food present in the digestive by +2.5 and +2.3 mM, respectively (ANOVA, $F=56.923$, $p<0.01$). $[\text{HCO}_3^-]_e$ in high $p\text{CO}_2$ urchins with empty digestive tracts dropped significantly below the non-bicarbonate buffer line with -2.35 mM when compared to control animals.

PCF calcium carbonate saturation state for calcite was <1 at exposure day 4 in the intermediate and high $p\text{CO}_2$ treatment (PCF Ω_{Ca} 69 Pa = 2.2 ± 0.5 , PCF Ω_{Ca} 145 Pa = 0.8 ± 0.4 and PCF Ω_{Ca} 384 Pa = 0.8 ± 0.3). After 10 and 45 days of exposure, animals of all treatments were characterized by calcite supersaturation (PCF Ω_{Ca} 47 Pa = 3.0 ± 0.6 , PCF Ω_{Ca} 102 Pa = 4.0 ± 0.9 and PCF h_F Ω_{Ca} 284 Pa = 2.3 ± 0.9). Only in sea urchins with empty digestive systems and highly acidified PCF, extracellular calcite saturation state dropped below unity (Ω_{Ca} for h_E = 0.49 ± 0.15).

4 Discussion

4.1 Ingestion rate, absorption efficiency and absorbed energy (LT experiment)

Ingestion and egestion rates of green sea urchins were highly variable over time in the present study, which matches previous studies conducted on *Strongylocentrotus droebachiensis* (Mamelona and Pelletier, 2005; Christiansen and Siikavuopio, 2007; Siikavuopio et al., 2007a; Siikavuopio et al., 2007b) and other sea urchin species (Beddingfield and McClintock, 1998; Lawrence et al., 2003; Otero-Villanueva et al., 2004). Ingestion rates decreased by 8% (102 Pa) and 30% (284 Pa) in response to elevated $p\text{CO}_2$, which corresponds to results from Siikavuopio and coworkers (2007b) who noted a significant, 17% decrease in feeding rate when they exposed *S. droebachiensis* to much higher $p\text{CO}_2$ values of 810 Pa. Elevated $p\text{CO}_2$ did not significantly influence organic matter absorption efficiency in this experiment. Reduced food intake as a response to environmental stress was also observed in green sea urchins in response to hypoxia (Siikavuopio et al., 2007a), that commonly occurs simultaneously with hypercapnia in the field (Brewer and Peltzer, 2009), suggesting that the combined effects of hypoxia and hypercapnia might even stronger impact energy acquisition.

4.2 Resource allocation and energy budget: somatic and gonad growth (LT experiment)

Sea urchins exhibit a great plasticity in terms of growth in response to different environmental stressors. Food limitation or food of low quality affects growth of sea urchins the most (Edwards and Ebert, 1991; Russell, 1998; Lau et al., 2009). Sea urchin gonads serve as nutrient storage as well as reproduction organs (Hughes et al., 2006) and were shown to respond strongly to different food regimes, as reflected in changes in mass and maturity state (Beddingfield and McClintock, 1998; Meidel and Scheibling, 1999; Lyons and Scheibling, 2007). We demonstrated that *S. droebachiensis* allocated less energy into somatic or gonad growth when they were exposed to elevated $p\text{CO}_2$. This was previously also observed in *Hemicentrotus pulcherrimus* and *Echinometra mathaei* exposed to 55 Pa CO_2 for six months (Shirayama and Thornton, 2005). Dorey et al. (submitted) conducted 4 and 16 month long acclimation experiments with *S. droebachiensis* using a $p\text{CO}_2$ of 123 Pa (1217 μatm) and observed a 5 time reduction in egg abundance of sea urchins exposed to elevated $p\text{CO}_2$ for 4 months. In contrast, an incubation time of 16 months was sufficient for *S. droebachiensis* to compensate egg

production (Dorey et al. submitted). This suggests that 6 weeks of $p\text{CO}_2$ incubation may not be sufficiently long of an acclimation interval to draw conclusions from gonad growth to fertility. Energy budgets of urchins exposed to long term incubations would be necessary to reliably predict sea urchins reproductive response to elevated $p\text{CO}_2$.

4.3 Energy budget: metabolism (LT experiment)

Six weeks acclimation of *S. droebachiensis* to elevated $p\text{CO}_2$ resulted in slightly decreased, yet not significantly reduced metabolic rates. Unaltered or even elevated metabolic rates were previously observed in response to hypercapnia in an ophiuroid echinoderm, teleost fish, a cephalopod, the bivalve *Mytilus edulis* and sea urchin larvae (Gutowska et al., 2008; Wood et al., 2008; Munday et al., 2009; Thomsen and Melzner, 2010; Stumpp et al., 2011b). Metabolic depression – especially at higher hypercapnic levels - was observed in *Mytilus galloprovincialis* (Michaelidis et al., 2005) and the sipunculid worm *Sipunculus nudus* (Langenbuch and Pörtner, 2002). Our control respiration and NH_4^+ excretion rates correspond to previously published results on echinoid species fed an algal diet (Giese et al., 1966; Johansen and Vadas, 1967; Miller and Mann, 1973; Greenwood, 1980; Sabourin and Stickle, 1981; Propp et al., 1983; Otero-Villanueva et al., 2004; Hill and Lawrence, 2006). Energy losses due to respiration and NH_4^+ excretion amount to values between 17 and 20 % of absorbed energy. Similar values were recorded for *P. miliaris* (Otero-Villanueva et al., 2004). The energy balance of animals in all treatments was positive. The remaining unexplained energy ranged between 56% in control urchins and 66% in the high $p\text{CO}_2$ treatment which is in agreement with the energy budgets calculated previously for *S. droebachiensis* and *P. miliaris* (Miller and Mann, 1973; Otero-Villanueva et al., 2004). Several studies on echinoids also noted that the energy budget overestimated the energy supplied for growth (Moore and McPherson, 1965; Miller and Mann, 1973; Hollertz, 2002; Otero-Villanueva et al., 2004) which could be due to dissolved organic matter (DOM) production that was not considered in the energy budgets. Carefoot (1967) suggested that DOM production leads to underestimation of respiration rates in *Aplysia punctata*. Similarly, it is not fully known, how much energy is lost via DOM production in sea urchins, but was estimated to significantly minimize the gap of energy in the budget of *S. droebachiensis* (Miller and Mann, 1973). Another explanation for the unaccounted energy could be that anaerobic metabolism either by the sea urchin itself or by microorganisms populating the digestive

system of the animals was not taken into account in this energy budget study. It was found that microorganisms in the sea urchin digestive system, which is entirely anaerobic (Thorsen, 1998), significantly contribute to digestive efficiency, thus contributing to anaerobic energy metabolism (Guerinot and Patriquin, 1981; Sawabe et al., 1995; Thorsen, 1999). Furthermore, high rates of anaerobic metabolism have been measured in gonad tissue (Bookbinder and Shick, 1986). Bookbinder and coworkers (1986) found that anaerobiosis accounts for 76 to 92% of the total heat dissipation in isolated ovaries and for 20% in isolated cleaned gut tissues of *S. droebachiensis*. Considering that gonad and gut tissue of our control animals constitutes approximately 25 and 23% of the metabolically active tissue (organic matter as AFDM), respectively, we calculated an energy contribution of $9 \text{ J d}^{-1} \text{ g}^{-1} \text{ DM}$ of gonad and $8.25 \text{ J d}^{-1} \text{ g}^{-1} \text{ DM}$ for gut tissue of total respired energy. Data from experimental animals with similar gonad indices published by Bookbinder and Shick (1986) suggest contribution of anaerobic metabolism of 77% for gonad (conversion factor anaerobic to aerobic MR of 2.3) and 21% (conversion factor of 0.27) for cleaned gut tissue. Thus, anaerobic metabolism would provide additional 20.7 ($2.3 * 9 \text{ J d}^{-1} \text{ g}^{-1} \text{ DM}$) and 2.2 $\text{J d}^{-1} \text{ g}^{-1} \text{ DM}$ ($0.27 * 8.25$) in gonad and gut tissue, respectively. However, exhaustion of glucose via a anaerobic pathway is much more inefficient than providing energy via citric acid cycle and the respiratory chain. Compared to aerobic metabolism that yields 30 to 32 moles ATP per mole glucose (Lehninger xxx), fermentation of glucose to succinate, propionate or acetate only yields between 4 and 6 moles ATP per mole glucose (Hochachka & Somero, 2002). Thus, the provision of a certain energy amount via anaerobic pathways requires 5 to 8 times more glucose than the same amount of energy provided by aerobic metabolism. Therefore, the supply of $22.9 \text{ J d}^{-1} \text{ g}^{-1} \text{ DM}$ via anaerobic pathways would require energy equivalents in the range between $114.5 \text{ J d}^{-1} \text{ g}^{-1} \text{ DM}$ and $183.2 \text{ J d}^{-1} \text{ g}^{-1} \text{ DM}$. The unaccounted energy in the individual energy balance amounts to $118 \text{ J d}^{-1} \text{ g}^{-1} \text{ DM}$. Assuming that this energy is exclusively fuelling anaerobiosis, an “efficiency” factor of 5.3 (energy input vs. energy output) could be calculated. This value is thus in the range of the “efficiency” values calculated between aerobic vs. anaerobic pathways via different anaerobic end products.

In response to environmental conditions, anaerobiosis in ovaries exhibited a high seasonal variation (changes of two fold) and was shown to increase with decreasing environmental and PCF $p\text{O}_2$ (Bookbinder and Shick, 1986). Thus, anaerobiosis, which

possibly accounts for 39% of metabolic activity (without bacterial metabolic activity in the gut) in the sea urchin *S. droebachiensis*, seems to be an important pathway in response to hypoxia or hypoxia coupled hypercapnia. This could potentially explain the 10% difference in the energy balance between control and high $p\text{CO}_2$ treated animals. However, as experimental data for anaerobic metabolic rates under hypercapnic conditions are still lacking in echinoids, we could not reliably estimate anaerobic metabolic rates for elevated $p\text{CO}_2$ treated animals. Detection of a slight increase in acetate, fumarate and succinate/lactate levels in coelomic fluid of *E. esculentus* suggests that anaerobic metabolism is up regulated in response to emersion (Spicer et al 1995). An increase in lactate dehydrogenase and malate dehydrogenase activity in response to hypercapnia in muscle tissue of *Sparus aurata* is also indicating an up regulation of anaerobic metabolism (Michaelidis et al 2007). However, the question, whether environmental hypercapnia induces an up regulation of anaerobic metabolism in *S. droebachiensis* could not be answered in this study.

4.4 O:N ratio and ammonium excretion as acid extrusion mechanism (LT experiment)

In animals exposed to high $p\text{CO}_2$ we observed a significant increase in NH_4^+ excretion. Higher NH_4^+ excretion rates in response to exposure to elevated $p\text{CO}_2$ significantly decreased the O:N ratio from control to high $p\text{CO}_2$ treatments. Measured O:N ratios are comparable to published values for the sea urchins *Psammechinus miliaris* (Otero-Villanueva et al., 2004) and *Sterechinus neumayeri* (Hill and Lawrence, 2006). O:N ratios of over 400 correspond to lipid metabolism, protein metabolism would result in O:N ratios of 7 and a ratio between 25 and 60 represents a mixed diet of protein and carbohydrate (Ikeda, 1977). Otero-Villanueva and coworkers (2004) measured an O:N ratio of 37 in *P. miliaris* maintained on an algal diet, while urchins fed with mussel or salmon tissue were characterized by a ratio of 29 and 12, respectively. This indicates that *S. droebachiensis*, when exposed to elevated $p\text{CO}_2$, metabolized more protein than under control conditions. A decreased O:N ratio based on elevated NH_4^+ excretion rates in response to short term exposure to elevated $p\text{CO}_2$ (between 100 and 5000 Pa) has already been observed in marine bivalves (Lindinger et al., 1984; Michaelidis et al., 2005; Thomsen and Melzner, 2010) and a sipunculid worm (Langenbuch and Pörtner, 2002). It has been hypothesized that secretion of NH_4^+ derived from protein catabolism serves as an additional acid extrusion mechanism in the mussel *Mytilus edulis* (Thomsen and

Melzner, 2010). The involvement of the acid-equivalent NH_4^+ in regulating extracellular pH has been recently described on a mechanistic basis for marine teleost fish (Nawata et al., 2010; Wu et al., 2010). These studies demonstrated the extrusion of NH_4^+ from gill and skin ionocytes by rhesus proteins (e.g. Rhcg) and Na^+/H^+ -exchangers (NHE) or V-type- H^+ -ATPases located in apical membranes. The current models propose that NH_4^+ enters from the basolateral side and is deprotonated to NH_3 and exported by the Rhcg protein. NH_3 combines again with H^+ , which is secreted via apical NHE-like proteins or V-type H^+ -ATPases to form NH_4^+ (Gruswitz et al., 2010; Wu et al., 2010). Interestingly, ammonium excretion only increased significantly in the green sea urchin during exposure to the high $p\text{CO}_2$ level. Accordingly, we suggest that proton extrusion mechanisms via increased protein degradation and NH_4^+ excretion become more important when the capacity for extracellular bicarbonate accumulation to compensate extracellular pH changes might be reaching its upper limit.

4.4 Extracellular acid-base status (ST, LT experiment)

S. droebachiensis could fully compensate hypercapnia induced extracellular (coelomic fluid) acidosis in response to 145 Pa $p\text{CO}_2$ within 10 days of incubation by means of substantial accumulation of $[\text{HCO}_3^-]_e$. *S. droebachiensis* could maintain compensated pH_e for an incubation period of 45 days to 100 Pa $p\text{CO}_2$. This is the first study that reports persistent (>10 days of exposure) pH_e compensation in an echinoderm. Partial pH_e compensation was also achieved in animals exposed to higher $p\text{CO}_2$ levels of 385 Pa after 10 days. However, $[\text{HCO}_3^-]_e$ accumulation of +2.1 to +2.5 mM above control concentrations seems to be the maximum regulatory effort that *S. droebachiensis* can accomplish in response to hypercapnic stress. Bicarbonate accumulation in order to regulate pH_e in response to hypercapnia is a well-known response in a range of animals including cephalopods (Gutowska et al., 2010a), decapod crustaceans (Pane and Barry, 2007) and fish (Larsen et al., 1997; Michaelidis et al., 2007). In contrast to invertebrates like bivalves and echinoderms, animals with higher ion regulatory capacity such as crustaceans and fish are far more efficient in $[\text{HCO}_3^-]_e$ accumulation and are able to fully or partially compensate pH_e under much higher $p\text{CO}_2$ conditions (table 5, see Melzner et al. 2009 for a discussion).

In a short term study with the sea urchin *Psammechinus miliaris* (Miles et al., 2007), it was demonstrated that *P. miliaris* was not able to compensate its pH_e at the chosen $p\text{CO}_2$ (0.25 to 5.2 kPa $p\text{CO}_2$). Merely animals exposed to the highest $p\text{CO}_2$ level (5.2 kPa, 51333 μatm) significantly accumulated bicarbonate - which might be primarily related to test dissolution. In the lower $p\text{CO}_2$ treatments, *P. miliaris* did not accumulate $[\text{HCO}_3^-]_e$ and the observed buffering reaction of +1.5 mM $[\text{HCO}_3^-]_e$ was due to non-bicarbonate buffers in the PCF (Miles et al., 2007). In response to very short emersion experiments (24 hours), a full pH_e compensation using a substantial $[\text{HCO}_3^-]_e$ accumulation of 1 and approximately 2.8 mM was demonstrated in *P. miliaris* and *Echinus esculentus*, respectively (Spicer et al., 1988), while no accumulation could be observed in *Strongylocentrotus purpuratus* during an eight hour exposure experiment (Burnett et al., 2002). Additionally, exposure to hypercapnia, hypoxia or air resulted in higher extracellular Mg^{2+} and Ca^{2+} concentrations in the coelomic fluid (Spicer et al., 1988; Spicer, 1995; Miles et al., 2007) indicating that elevated $[\text{HCO}_3^-]_e$ in *P. miliaris* and *E. esculentus* might be due to shell dissolution as the PCF is most likely undersaturated with respect to calcium carbonate. PCF calcium carbonate saturation state for calcite was <1 at exposure day 4 in the intermediate and high $p\text{CO}_2$ treatment, suggesting that test dissolution might initially contribute to pH_e compensation. However, after 10 and 45 days of exposure, animals of all treatments were characterized by calcite supersaturation. Only in sea urchins with empty digestive systems and highly acidified PCF, extracellular calcite saturation state dropped below unity. As a significant increase in test diameter was observed in animals exposed to the intermediate $p\text{CO}_2$ treatment, and test dry weight did not decrease in response to elevated $p\text{CO}_2$, it seems unlikely that the green sea urchin uses dissolution of its test to compensate pH_e . However, the timing of the pH_e compensation reaction is much slower than typically observed in mobile marine ectotherms, which usually compensate pH_e in response to abrupt changes in seawater $p\text{CO}_2$ within <1 day (Pane and Barry, 2007; Gutowska et al., 2010a). Furthermore, the acid-base regulatory capacity seems to be closely linked to the general condition in *S. droebachiensis*, as a strong extracellular metabolic acidosis, indicated by a strong drop in PCF pH_e and PCF $[\text{HCO}_3^-]_e$ below the non-bicarbonate buffer line could be correlated to a cessation of feeding observed in 71% of experimental animals exposed to high $p\text{CO}_2$ values for 45 days. It is unclear, whether an inability to control extracellular acid-base status is causally related to physiological deterioration or whether these conditions are merely correlated.

The indication of metabolic acidosis and a significant, but weak accumulation of anaerobic metabolites (e.g. lactate/succinate, acetate and fumarate) detected in PCF of *P. miliaris* or *E. esculentus* exposed to emersion (Spicer et al., 1988), supports the suggestion of increased anaerobic metabolic rates in response to elevated $p\text{CO}_2$. However, the participation of anaerobiosis in the physiological response to hypercapnia still needs to be confirmed.

In contrast to the more intertidal *P. miliaris*, which seems not to be adapted to seasonally elevated $p\text{CO}_2$, Western Baltic *S. droebachiensis* can maintain compensated pH_e in response to moderately elevated $p\text{CO}_2$. The animals in this study were collected in the Kattegat and encounter seasonally elevated $p\text{CO}_2$ already today, as their habitats are seasonally hypoxic (Conley et al., 2007; HELCOM, 2009). However, if the anthropogenic dissolved inorganic carbon adds up to dissolved organic carbon produced during seasonal hypoxic phases, it can be expected that $p\text{CO}_2$ in green sea urchin habitats in the Western Baltic exceeds values at which *S. droebachiensis* is able to fully compensate its extracellular pH in response to hypercapnia induced acidosis (e.g. Thomsen et al. 2010). Our observation of an increased mortality towards the end of our experiment (after 45 days of incubation) in response to 300 Pa is in accordance with high mortalities observed in *P. miliaris* after eight days exposure to 5.2 kPa (Miles et al., 2007). Although *S. droebachiensis* is able to survive short periods (a few weeks) of highly elevated $p\text{CO}_2$ (up to 284 Pa), longer periods (more than six weeks) of continuous seawater acidification may exceed the green sea urchin's tolerance capacity.

5 Conclusion

The results of this study suggest that *S. droebachiensis* has at least two acid-base regulatory mechanisms to overcome environmentally induced acidosis. Minor acid-base disturbances (102-144 Pa) can be fully compensated by means of $[\text{HCO}_3^-]_e$ accumulation, which enables the sea urchins to grow and mature albeit more slowly. However, major acid-base disturbances shift the sea urchins energy budget and lead towards higher rates of protein catabolism that support additional acid extrusion through NH_4^+ excretion. Growth and maturation of gonads is then compromised in favor of acid-base regulation. Furthermore, we conclude that the green sea urchin *S. droebachiensis* is already adapted to seasonal hypercapnia in the range up to 145 Pa for a longer period of time. This is also

supported by Dorey et al. (submitted), who demonstrated a profound potential of *S. droebachiensis* adults to acclimate to 120 Pa CO₂ if sufficient time is given. However, the results of our acid-base study suggest that highly elevated seawater *p*CO₂, which are likely to occur in the Kattegat in the future, might exceed the acclimation capacity of this species and can possibly only be endured for a short time period of a few weeks. Increases in anthropogenic CO₂ emissions thus impose a severe threat to the ecologically and economically important species *S. droebachiensis*. Future studies should determine, whether [HCO₃⁻]_e accumulation is achieved by passive shell dissolution or by active processes. This promises interesting results which will lead to a better understanding of sea urchin physiology in response to abiotic stressors and will thus help to estimate the impacts of climate change on *S. droebachiensis*.

Acknowledgements

This study was funded by the DFG Excellence Cluster ‘Future Ocean’, the German ‘Biological impacts of ocean acidification (BIOACID)’ project 3.1.4, funded by the Federal Ministry of Education and Research (BMBF, FKZ 03F0608A) and the EU FP7 project ECO2 (project number 265847). The authors would like to thank Ragnhild Asmus and her staff for the provision of laboratory, cold room and office facilities and general support at the Wadden Sea Station Sylt (Alfred Wegener Institute for Polar and Marine Research) and Ulrike Panknin for help with sea water chemistry measurements.

References

- Beddingfield, S. D., McClintock, J. B., 1998. Differential survivorship, reproduction, growth and nutrient allocation in the regular echinoid *Lytechinus variegatus* (Lamarck) fed natural diets. *J Exp Mar Biol Ecol.* 226, 195-215.
- Beldowski, J., Löffler, A., Schneider, B., Joensuu, L., 2010. Distribution and biogeochemical control of total CO₂ and total alkalinity in the Baltic Sea. *J Marine Syst.* 81, 252-259.
- Bishop, C. D., Watts, S. A., 1992. Biochemical and morphometric study of growth in the stomach and intestine of the echinoid *Lytechinus variegatus* (Echinodermata). *Mar. Biol.* 114, 459-467.
- Bookbinder, L. H., Shick, J. M., 1986. Anaerobic and aerobic energy metabolism in ovaries of the sea urchin *Strongylocentrotus droebachiensis*. *Mar. Biol.* 93, 103-110.
- Brewer, P. G., Peltzer, E. T., 2009. Limits to marine life. *Science.* 324, 347-348.
- Burnett, L., Terwilliger, N., Carroll, A., Jorgensen, D., Scholnick, D., 2002. Respiratory and acid-base physiology of the purple sea urchin, *Strongylocentrotus purpuratus*, during air exposure: presence and function of a facultative lung. *Biol. Bull.* 203, 42-50.

- Cao, L., Caldeira, K., 2008. Atmospheric CO₂ stabilization and ocean acidification. *Geophys. Res. Lett.* 35, doi:10.1029/2008GL035072.
- Carefoot, T. H., 1967. Growth and nutrition of *Aplysia punctata* feeding on a variety of marine algae. *J Mar Biol Ass U.K.* 47, 565-589.
- Christiansen, J. S., Siikavuopio, S. I., 2007. The relationship between feed intake and gonad growth of single and stocked green sea urchin (*Strongylocentrotus droebachiensis*) in a raceway culture. *Aquaculture.* 262, 163-167.
- Conley, D. J., Carstensen, J., Aertebjerg, G., Christensen, P. B., Dalsgaard, T., Hansen, J. L. S., Josefson, A. B., 2007. Long-term changes and impacts of hypoxia in danish coastal waters. *Ecol. Appl.* 17 Supplement, S165-S184.
- Conover, R. J., 1966. Assimilation of organic matter by zooplankton. *Limnol. Oceanogr.* 11, 338-345.
- Deigweier, K., Hirse, T., Bock, C., Lucassen, M., Pörtner, H.-O., 2010. Hypercapnia induced shifts in gill energy budgets of Antarctic notothenioids. *J. Comp. Physiol. B.* 180, 347-359.
- Dickson, A. G., Millero, F. J., 1987. A comparison of the equilibrium constants for the dissociation of carbonic acid in seawater media. *Deep-Sea Res.* 34, 1733-1743. (Corrigenda. *Deep-Sea Res.* 36, 983).
- Dickson, A. G., Sabine, C. L., Christian, J. R., 2007. Guide to best practices for ocean CO₂ measurements. *PICES Special Publication.* 3, 191 pp.
- Dupont, S., Ortega-Martínez, O., Thorndyke, M. C., 2010. Impact of near-future ocean acidification on echinoderms. *Ecotoxicology.* 19, 449-462.
- Edwards, P. B., Ebert, T. A., 1991. Plastic responses to limited food availability and spine damage in the sea urchin *Strongylocentrotus purpuratus* (Stimpson). *J Exp Mar Biol Ecol.* 145, 205-220.
- Elliott, J. M., Davison, W., 1975. Energy equivalents of oxygen-consumption in animal energetics. *Oecologia.* 19, 195-201.
- Fernandez, C., 1998. Seasonal changes in the biochemical composition of the edible sea urchin *Paracentrotus lividus* (Echinodermata: Echinoidea) in a lagoonal environment. *PSZN Mar Ecol.* 19, 1-11.
- Giese, A. C., Farmanfarmaian, A., Hilden, S., Doezema, P., 1966. Respiration during the reproductive cycle in the sea urchin, *Strongylocentrotus purpuratus*. *Biol. Bull.* 130, 192-201.
- Gnaiger, E., Calculation of energetic and biochemical equivalents of respiratory oxygen consumption. In: E. Gnaiger, H. Forstner, Eds.), *Polarographic Oxygen Sensors: Aquatic and Physiological Applications.* Springer-Verlag, New York, 1983.
- Greenwood, P. J., 1980. Growth, respiration and tentative energy budgets for two populations of the sea urchin *Parechinus angulosus* (Leske). *Estuar. Coast. Mar. S.* 10, 347-367.
- Gruswitz, F., Chaudhary, S., Ho, J. D., Schlessinger, A., Pezeshki, B., Ho, C. M., Sali, A., Westhoff, C. M., Stroud, R. M., 2010. Function of human Rh based on structure of RhCG at 2.1 Å. *PNAS.* 107, 9638-9643.
- Guerinot, M. L., Patriquin, D. G., 1981. The association of N₂-fixing bacteria with sea urchins. *Mar. Biol.* 62, 197-207.
- Gutowska, M. A., Melzner, F., Langenbuch, M., Bock, C., Claireaux, G., Pörtner, H.-O., 2010. Acid-base regulatory capacity in the cephalopod *Sepia officinalis* exposed to environmental hypercapnia. *J. Comp. Physiol. B.* 180, 323-335.

- Gutowska, M. A., Pörtner, H.-O., Melzner, F., 2008. Growth and calcification in the cephalopod *Sepia officinalis* under elevated seawater $p\text{CO}_2$. *Mar. Ecol. Prog. Ser.* 373, 303-309.
- Hall-Spencer, J. M., Rodolfo-Metalpa, R., Martin, S., Ransome, E., Fine, M., Turner, S. M., Rowley, S. J., Tedesco, D., Buia, M.-C., 2008. Volcanic carbon dioxide vents show ecosystem effects of ocean acidification. *Nature.* 454, 96-99.
- Haugen, H. A., Aagaard, P., Thyberg, B., Kjärstad, J., Langlet, D., Melaaen, M. C., Liljemark, S., Bergmo, P., Skagestad, R., Mathisen, A., Jarsve, E. M., Faleide, J. I., Bjornsen, D., 2011. CCS in the Skagerrak/Kattegat area. *Energ. Proc.* 4, 2324-2331.
- HELCOM, 2009. Eutrophication in the Baltic Sea - An integrated thematic assessment of the effects of nutrient enrichment and eutrophication in the Baltic Sea region. *Bal. Sea Environ. Proc.* 115B.
- Hill, S. K., Lawrence, J. M., 2006. Interactive effects of temperature and nutritional condition on the energy budgets of the sea urchins *Arbacia punctulata* and *Lytechinus variegatus* (Echinodermata: Echinoidea). *J. Mar. Biol. Ass. U.K.* 86, 783-790.
- Hollertz, K., 2002. Feeding biology and carbon budget of the sediment-burrowing heart urchin *Bryopsis lyrifera* (Echinoidea: Spatangoida). *Mar. Biol.* 140, 959-969.
- Holmes, R. M., Aminot, A., Kerouel, R., Hooker, B. A., Peterson, B. J., 1999. A simple and precise method for measuring ammonium in marine and freshwater ecosystems. *Can. J. Fish. Aquat. Sci.* 56, 1801-1808.
- Hughes, A. D., Kelly, M. S., Barnes, D. K. A., Catarino, A. I., Black, K. D., 2006. The dual functions of sea urchin gonads are reflected in the temporal variations of their biochemistry. *Mar. Biol.* 148, 789-798.
- Ikeda, T., 1977. The effect of laboratory conditions on the extrapolation of experimental measurements to the ecology of marine zooplankton. IV. Changes in respiration and excretion rates of Boreal zooplankton species maintained under fed and starved conditions. *Mar. Biol.* 41, 241-252.
- Johansen, K., Vadas, R. L., 1967. Oxygen uptake and responses to respiratory stress in sea urchins. *Biol. Bull.* 132, 16-22.
- Johnson, P. T., 1969. The coelomic elements of sea urchins (*Strongylocentrotus*) I. The normal coelomocytes; their morphology and dynamics in hanging drops. *J Invertebr Pathol.* 13, 25-41.
- Körner, S., Das, S. K., Veenstra, S., Vermaat, J. E., 2001. The effect of pH variation at the ammonium/ammonia equilibrium in wastewater and its toxicity to *Lemna gibba*. *Aquat. Bot.* 71, 71-78.
- Langenbuch, M., Pörtner, H. O., 2002. Changes in metabolic rate and N excretion in the marine invertebrate *Sipunculus nudus* under conditions of environmental hypercapnia: identifying effective acid-base variables. *J. Exp. Biol.* 205, 1153-1160.
- Larsen, B. K., Pörtner, H. O., Jensen, F. B., 1997. Extra- and intracellular acid-base balance and ionic regulation in cod (*Gadus morhua*) during combined and isolated exposures to hypercapnia and copper. *Mar. Biol.* 128, 337-346.
- Lau, D. C. C., Lau, S. C. K., Qian, P. Y., Qiu, J. W., 2009. Morphological plasticity and resource allocation in response to food limitation and hyposalinity in a sea urchin. *J Shellfish Res.* 28, 383-388.

- Lawrence, J. M., Plank, L. R., Lawrence, A. L., 2003. The effect of feeding frequency on consumption of food, absorption efficiency, and gonad production in the sea urchin *Lytechinus variegatus*. *Comp. Biochem. Physiol. A.* 134, 69-75.
- Lewis, E., Wallace, D. W. R., 1998. CO2SYS-Program developed for the CO₂ system calculations. Carbon Dioxide Inf. Anal. Center. Report ORNL/CDIAC-105.
- Lindinger, M. I., Lauren, D. J., McDonald, D. G., 1984. Acid-base-balance in the sea mussel, *Mytilus edulis*. 3. Effects of environmental hypercapnia on intracellular and extracellular acid-base-balance. *Mar. Biol. Lett.* 4, 371-381.
- Lyons, D. A., Scheibling, R. E., 2007. Differences in somatic and gonadic growth of sea urchins (*Strongylocentrotus droebachiensis*) fed kelp (*Laminaria longicruris*) or the invasive alga *Codium fragile* ssp. *tomentosoides* are related to energy acquisition. *Mar. Biol.* 152, 285-295.
- Mamelona, J., Pelletier, É., 2005. Green urchin as a significant source of fecal particulate organic matter within nearshore benthic ecosystems. *J Exp Mar Biol Ecol.* 314, 163-174.
- Marsham, S., Scott, G. W., Tobin, M. L., 2007. Comparison of nutritive chemistry of a range of temperate seaweeds. *Food Chem.* 100, 1331-1336.
- Matranga, V., Pinsino, A., Celi, M., Di Bella, G., Natoli, A., 2006. Impacts of UV-B radiation on short-term cultures of sea urchin coelomocytes. *Mar. Biol.* 149, 25-34.
- Mehrbach, C., Culbertson, C. H., Hawley, J. E., Pytkowicz, R. M., 1973. Measurement of the apparent dissociation constants of carbonic acid in seawater at atmospheric pressure. *Limnol. Oceanogr.* 18, 897-907.
- Meidel, S. K., Scheibling, R. E., 1999. Effects of food type and ration on reproductive maturation and growth of the sea urchin *Strongylocentrotus droebachiensis*. *Mar. Biol.* 134, 155-166.
- Melzner, F., Gutowska, M. A., Langenbuch, M., Dupont, S., Lucassen, M., Thorndyke, M. C., Bleich, M., Pörtner, H.-O., 2009. Physiological basis for high CO₂ tolerance in marine ectothermic animals: pre-adaptation through lifestyle and otogeny? *Biogeosciences.* 6, 2313-2331.
- Michaelidis, B., Ouzounis, C., Paleras, A., Pörtner, H.-O., 2005. Effects of long-term moderate hypercapnia on acid-base balance and growth rate in marine mussels *Mytilus galloprovincialis*. *Mar. Ecol. Prog. Ser.* 293, 109-118.
- Michaelidis, B., Spring, A., Pörtner, H. O., 2007. Effects of long-term acclimation to environmental hypercapnia on extracellular acid-base status and metabolic capacity in Mediterranean fish *Sparus aurata*. *Mar. Biol.* 150, 1417-1429.
- Miles, H., Widdicombe, S., Spicer, J. I., Hall-Spencer, J., 2007. Effects of anthropogenic seawater acidification on acid-base balance in the sea urchin *Psammechinus miliaris*. *Mar. Pollut. Bull.* 54, 89-96.
- Miller, R. J., Mann, K. H., 1973. Ecological energetics of the seaweed zone in a marine bay on the Atlantic coast of Canada. III. Energy transformations by sea urchins. *Mar. Biol.* 18, 99-114.
- Moore, H. B., McPherson, B. F., 1965. A contribution to the study of the productivity of the urchins *Tripneustes esculentus* and *Lytechinus variegatus*. *B Mar Sci.* 15, 855-871.
- Munday, P. L., Crawley, N. E., Nilsson, G. E., 2009. Interacting effects of elevated temperature and ocean acidification on the aerobic performance of coral reef fishes. *Mar. Ecol. Prog. Ser.* 388, 235-242.

- Nawata, C. M., Hirose, S., Nakada, T., Wood, C. M., Kato, A., 2010. Rh glycoprotein expression is modulated in pufferfish (*Takifugu rubripes*) during high environmental ammonia exposure. *J. Exp. Biol.* 213, 3150-3160.
- Otero-Villanueva, M. M., Kelly, M. S., Burnell, G., 2004. How diet influences energy partitioning in the regular echinoid *Psammechinus miliaris*; constructing an energy budget. *J Exp Mar Biol Ecol.* 304, 159-181.
- Pane, E. F., Barry, J. P., 2007. Extracellular acid-base regulation during short-term hypercapnia is effective in a shallow-water crab, but ineffective in a deep-sea crab. *Mar. Ecol. Prog. Ser.* 334, 1-9.
- Pörtner, H. O., Langenbuch, M., Reipschläger, A., 2004. Biological impact of elevated ocean CO₂ concentrations: lessons from animal physiology and earth history. *J. Oceanogr.* 60, 705-718.
- Propp, M. V., Ryabushko, V. I., Zhuchikhina, A. A., Propp, L. N., 1983. Seasonal changes in respiration, ammonia and phosphate excretion, and activity of carbohydrate-metabolism enzymes in four echinoderm species from the sea of Japan. *Comp. Biochem. Physiol. B.* 75, 707-711.
- Reardon, J., Foreman, J. A., Searcy, R., 1966. New reactants for the colourimetric determination of ammonia. *Clin. Chim. Acta.* 39, 403-405.
- Russell, M. P., 1998. Resource allocation plasticity in sea urchins: rapid, diet induced, phenotypic changes in the green sea urchin, *Strongylocentrotus droebachiensis* (Müller). *J Exp Mar Biol Ecol.* 220, 1-14.
- Sabourin, T. D., Stickle, W. B., 1981. Effects of salinity on respiration and nitrogen excretion in two species of echinoderms. *Mar. Biol.* 65, 91-99.
- Sawabe, T., Oda, Y., Shiomi, Y., Ezura, Y., 1995. Alginate degradation by bacteria isolated from the gut of sea urchins and abalones. *Microb. Ecol.* 30, 193-202.
- Scheibling, R. E., Hatcher, B. G., Ecology of *Strongylocentrotus droebachiensis*. In: J. M. Lawrence, (Ed.), *Edible Sea Urchins Biology and Ecology*. Elsevier, Amsterdam, 2007, pp. 353-382.
- Shirayama, Y., Thornton, H., 2005. Effect of increased atmospheric CO₂ on shallow water marine benthos. *J. Geophys. Res.* 110.
- Siikavuopio, S. I., Dale, T., Mortensen, A., Foss, A., 2007a. Effects of hypoxia on feed intake and gonad growth in the green sea urchin, *Strongylocentrotus droebachiensis*. *Aquaculture.* 266, 112-116.
- Siikavuopio, S. I., Mortensen, A., Dale, T., Foss, A., 2007b. Effects of carbon dioxide exposure on feed intake and gonad growth in green sea urchin, *Strongylocentrotus droebachiensis*. *Aquaculture.* 266, 97-101.
- Spicer, J. I., 1995. Oxygen and acid-base status of the sea urchin *Psammechinus miliaris* during environmental hypoxia. *Mar. Biol.* 124, 71-76.
- Spicer, J. I., Taylor, A. C., Hill, A. D., 1988. Acid-base status in the sea urchins *Psammechinus miliaris* and *Echinus esculentus* (Echinodermata: Echinoidea) during emersion. *Mar. Biol.* 99, 527-534.
- Stumpp, M., Dupont, S., Thorndyke, M., Melzner, F., 2011a. CO₂ induced seawater acidification impacts sea urchin larval development II: gene expression patterns in pluteus larvae. *Comp. Biochem. Physiol.* (under review).
- Stumpp, M., Wren, J., Melzner, F., Thorndyke, M., Dupont, S., 2011b. CO₂ induced seawater acidification impacts sea urchin larval development I: elevated metabolic rates decrease scope for growth and induce developmental delay. *Comp. Biochem. Physiol.* (under review).

- Thomsen, J., Gutowska, M. A., Saphörster, J., Heinemann, A., Fietzke, J., Hiebenthal, C., Eisenhauer, A., Körtzinger, A., Wahl, M., Melzner, F., 2010. Calcifying invertebrates succeed in a naturally CO₂ enriched coastal habitat but are threatened by high levels of future acidification. *Biogeosciences*. 7, 3879-3891.
- Thomsen, J., Melzner, F., 2010. Seawater acidification does not elicit metabolic depression in the blue mussel *Mytilus edulis*. *Mar. Biol.* 157, 2667-2676.
- Thorsen, M. S., 1998. Microbial activity, oxygen status and fermentation in the gut of the irregular sea urchin *Echinocardium cordatum* (Spatangoida: Echinodermata). *Mar. Biol.* 132, 423-433.
- Thorsen, M. S., 1999. Abundance and biomass of the gut-living microorganisms (bacteria, protozoa and fungi) in the irregular sea urchin *Echinocardium cordatum* (Spatangoida: Echinodermata). *Mar. Biol.* 133, 353-360.
- Weiss, R. F., 1974. Carbon dioxide in water and seawater: the solubility of a non-ideal gas. *Mar. Chem.* 2, 203-215.
- Wood, H. L., Spicer, J. I., Widdicombe, S., 2008. Ocean acidification may increase calcification rates, but at a cost. *P. Roy. Soc. B Bio.* 275, 1767-1773.
- Wu, S. C., Horng, J. L., Liu, S. T., Hwang, P. P., Wen, Z. H., Lin, C. S., Lin, L. Y., 2010. Ammonium-dependent sodium uptake in mitochondrion-rich cells of medaka (*Oryzias latipes*) larvae. *Am. J. Physiol. Cell. Physiol.* 298, C237-C250.
- Zillén, L., Conley, D. J., Andrén, T., Andrén, E., Björck, S., 2008. Past occurrences of hypoxia in the Baltic Sea and the role of climate variability, environmental change and human impact. *Earth-Sci. Rev.* 91, 77-92.

Figure captions:

Figure 1: experimental design summary: overview of measurements conducted at specific time points/frames in short term (ST) and long term (LT) experiments.

Figure 2: Variance in daily ingestion rate (mean \pm SD) of *Strongylocentrotus droebachiensis* monitored over a time period of three weeks during exposure to three different $p\text{CO}_2$ values (47 Pa, 102 Pa and 284 Pa, n=6). Sea urchins were fed *ad libitum* with *Fucus vesiculosus*.

Figure 3: Feeding and excretion rates of *Strongylocentrotus droebachiensis* in response to three different $p\text{CO}_2$ levels (47 Pa, 102 Pa, 284 Pa) averaged over 3 weeks of experimental time (n = 6). (A) ingestion (black bar) and egestion rate (white bar), (B) organic matter (OM) absorption efficiency (Conover ratio). All values are given as means \pm SD. Different letters indicate statistically significant differences between treatments (One-Way-ANOVA, $p < 0.05$, n=6), lower case letters are for comparison of ingestion and capital letters for comparison of egestion rate between treatment groups.

Figure 4: Routine metabolic rates (RMR) and NH_4^+ excretion rates in *Strongylocentrotus droebachiensis* exposed to three different $p\text{CO}_2$ levels (control = 47 Pa, 102 Pa, 284 Pa). (A) routine metabolic rate, (B) NH_4^+ excretion rate and C O:N ratio. Values are given as means \pm SD. Significant differences between treatments are presented by different letters (One-Way-ANOVA, $p < 0.05$, n=6)

Figure 5: pH-bicarbonate (Davenport) diagram showing the time course of acid-base compensation (mean \pm SD) during 10 days of hypercapnic exposure in perivisceral coelomic fluid (PCF) of *Strongylocentrotus droebachiensis* ((A): 143 Pa $p\text{CO}_2$, (B): 380 Pa $p\text{CO}_2$, n=4 at all treatments and exposure times). The non-bicarbonate buffer line is delineated with a dashed line (NBB). The solid curved lines represent $p\text{CO}_2$ isopleths. Numbers in brackets represent the sampling days.

Figure 6: pH-bicarbonate (Davenport) diagram showing end points of PCF acid-base compensation (mean \pm SD) following 40 days of hypercapnic exposure in *Strongylocentrotus droebachiensis*. The non-bicarbonate buffer line (NBB) is delineated with a dashed line. The solid curved lines represent $p\text{CO}_2$ isopleths. Letters in brackets represent: c=control 46 Pa, i=intermediate $p\text{CO}_2$ of 102 Pa, h=high $p\text{CO}_2$ of 284 Pa, subscripts in the high treatments F=filled digestive system, E=empty digestive system, n=6 in all treatments, except h_F n=4)

Table captions:

Table 1: Seawater physiochemical parameters in all of the experimental setups for the control and hypercapnic treatments (intermediate and high $p\text{CO}_2$). Flow rate (flow, mL seawater min^{-1}) is the rate with which fresh seawater entered each aquarium. Salinity, temperature and pH_{NBS} (pH NBS scale) was measured daily in each tank and averaged per replicate aquarium over the whole experimental period. pH_{T} (pH total scale) was measured simultaneously with C_{T} for long term (LT) experiments (see material and methods for details). The combination of A_{T} and C_{T} and combination of C_{T} and pH_{T} were used to calculate the carbonate system parameters $p\text{CO}_2$, Ω_{Ca} and Ω_{Ar} in short term (ST) and LT experiments, respectively. Values are represented as means \pm SD. Average $[\text{NH}_4^+]$ values ranged between 0-0.3 mg L^{-1} .

Table 2: General observations and characterization of health status of *Strongylocentrotus droebachiensis* adults in response to exposure to three different $p\text{CO}_2$ values (control = 47 Pa, 102 Pa and 284 Pa) over 42 to 45 days. The high $p\text{CO}_2$ (284 Pa) group was divided into two subgroups with respect to their feeding status (h_{F} = filled digestive system, h_{E} = empty digestive system). Behavioral observations (position of sea urchins in the tanks, for details see material and methods) was conducted on day 44 of the experimental incubation independently from the other parameters.

Table 3: Biometric data (short term experiment $n = 4$; long term experiment, $n = 6$). Growth of body parts (total body, test including spines, Lantern of Aristotle, gonads and gut) during long term exposure to three different $p\text{CO}_2$ levels (control = 47 Pa, 102 Pa and 284 Pa), wet mass (WM), dry mass (DM), ash-free dry mass (AFDM) and ash dry mass (ADM). Values are given as means \pm SD. For carbonate system speciation see table 1. Different letters indicate statistically significant differences between treatments ($n=6$).

Table 4: Energy partitioning in *Strongylocentrotus droebachiensis* exposed to three different $p\text{CO}_2$ levels (control = 47 Pa, 102 Pa and 284 Pa). Absorption efficiency was estimated using the Conover ratio (Conover, 1966). The lantern of Aristotle was omitted from the calculation as no significant change in dry weight was detected over the exposure time in any of the treatments (see table 2). Values are given in $\text{J d}^{-1} \text{g}^{-1}$ dry mass urchin (or % where stated) as mean \pm SD. Values with different letters in each row are statistically different (one-way ANOVA, $n=6$).

Table 5: Changes in extracellular acid-base parameters expressed as mean (SD) of selected marine organisms in response to acute hypercapnia (modified after Gutowska et al. 2010).

Figure 1:

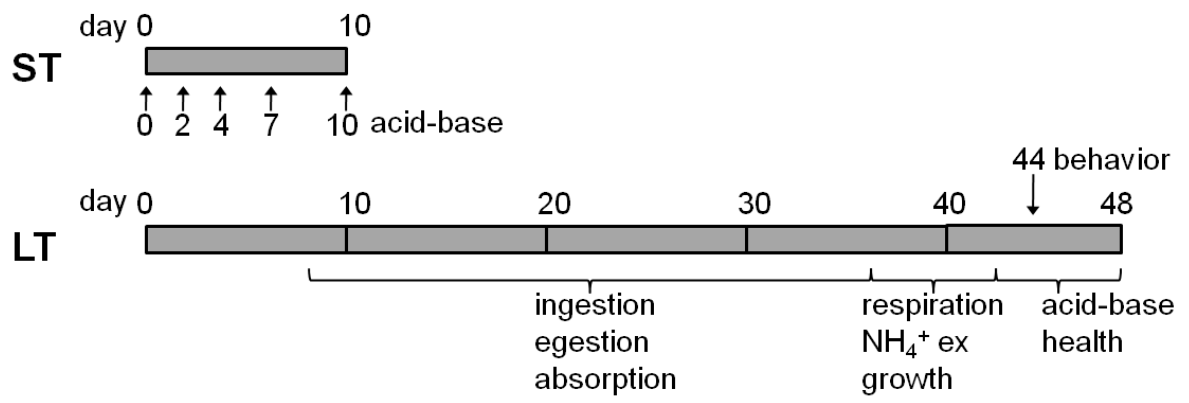


Figure 2:

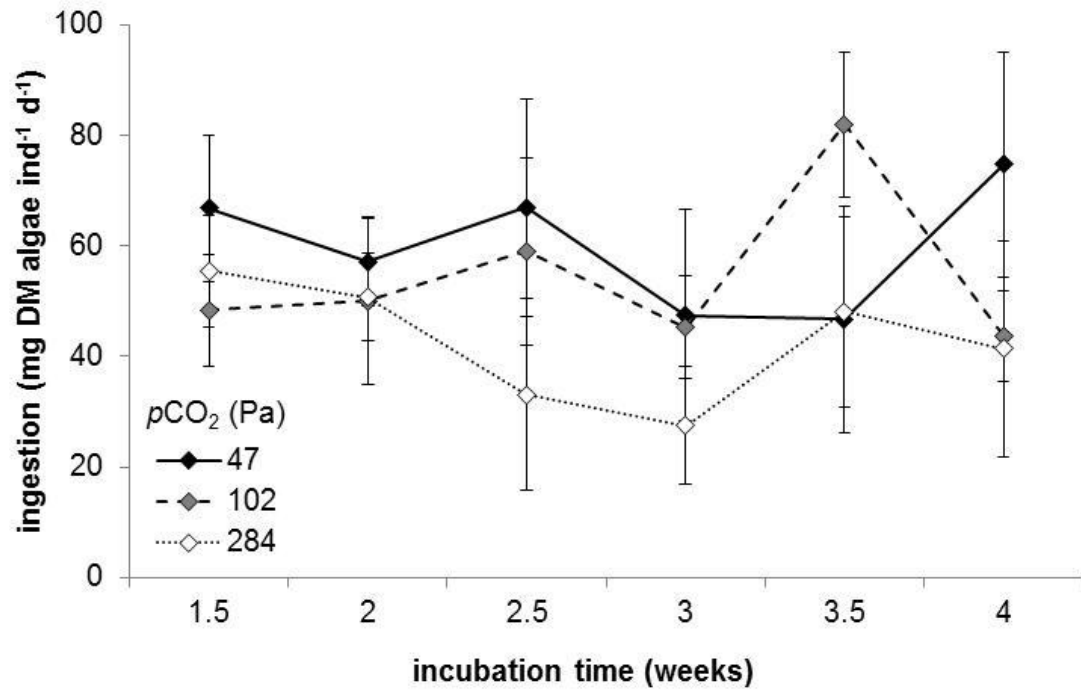


Figure 3

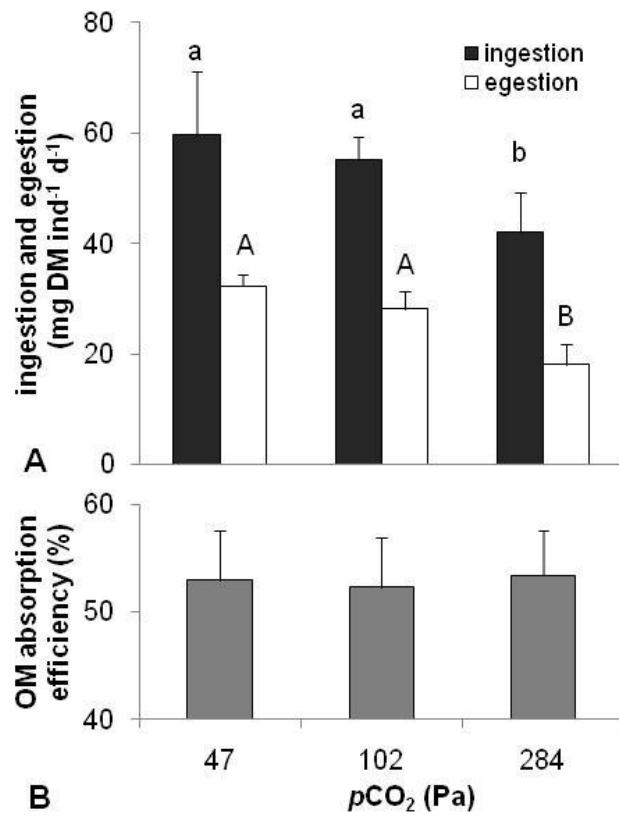


Figure 4

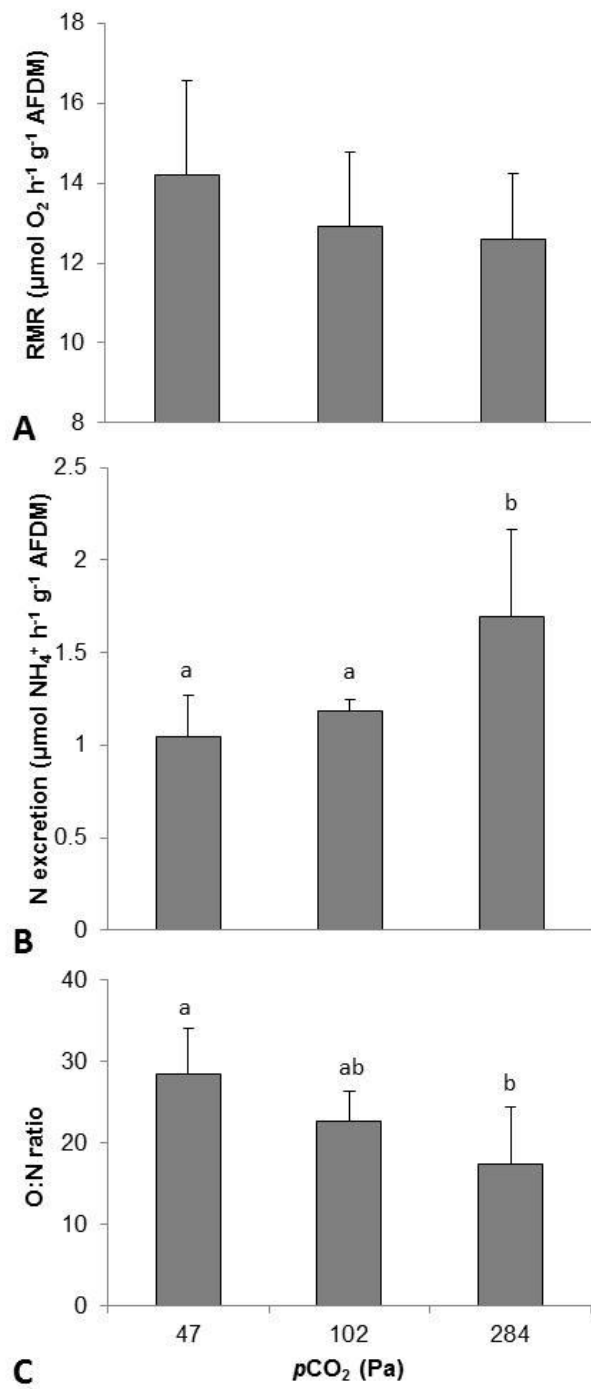


Figure 5

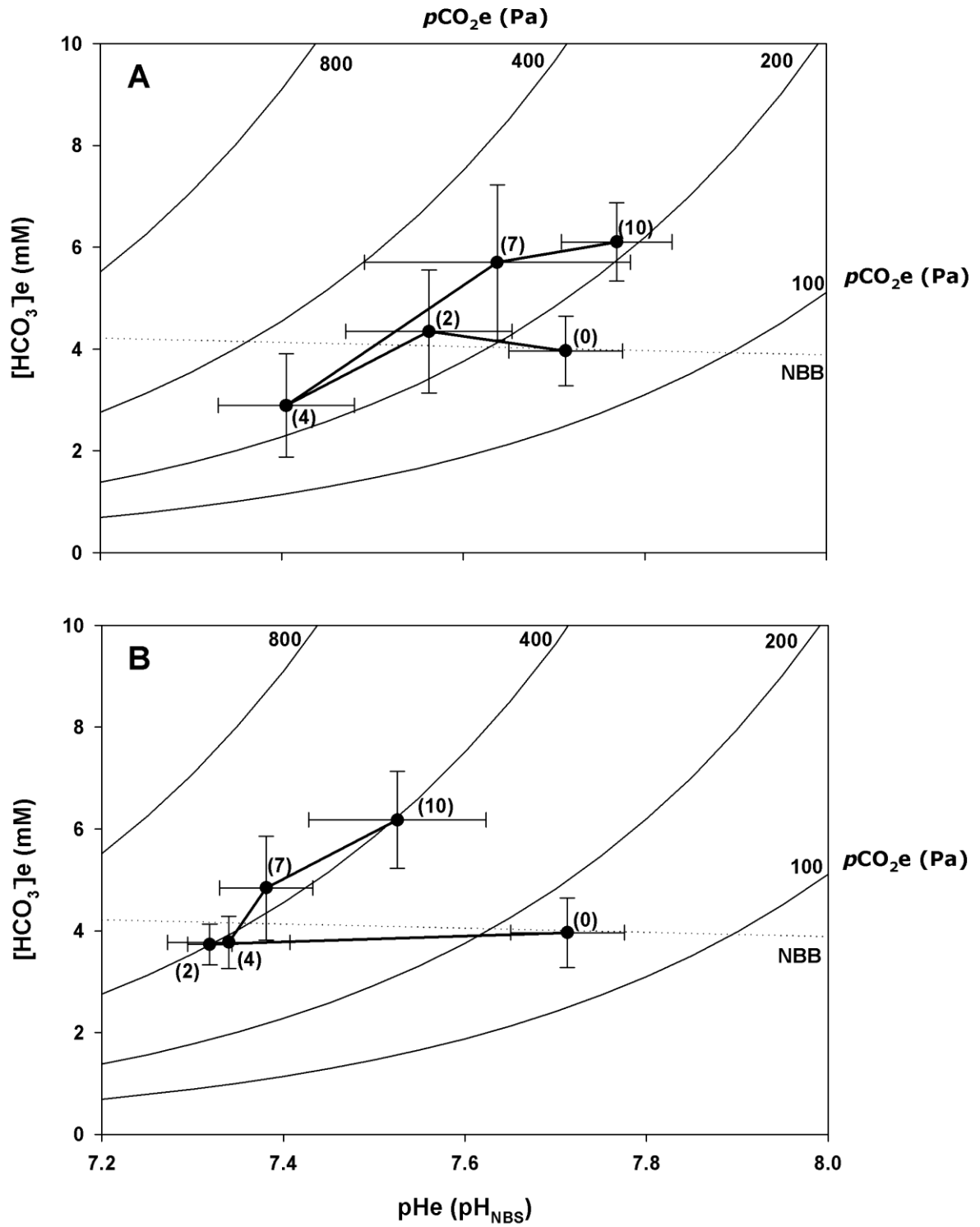


Figure 6

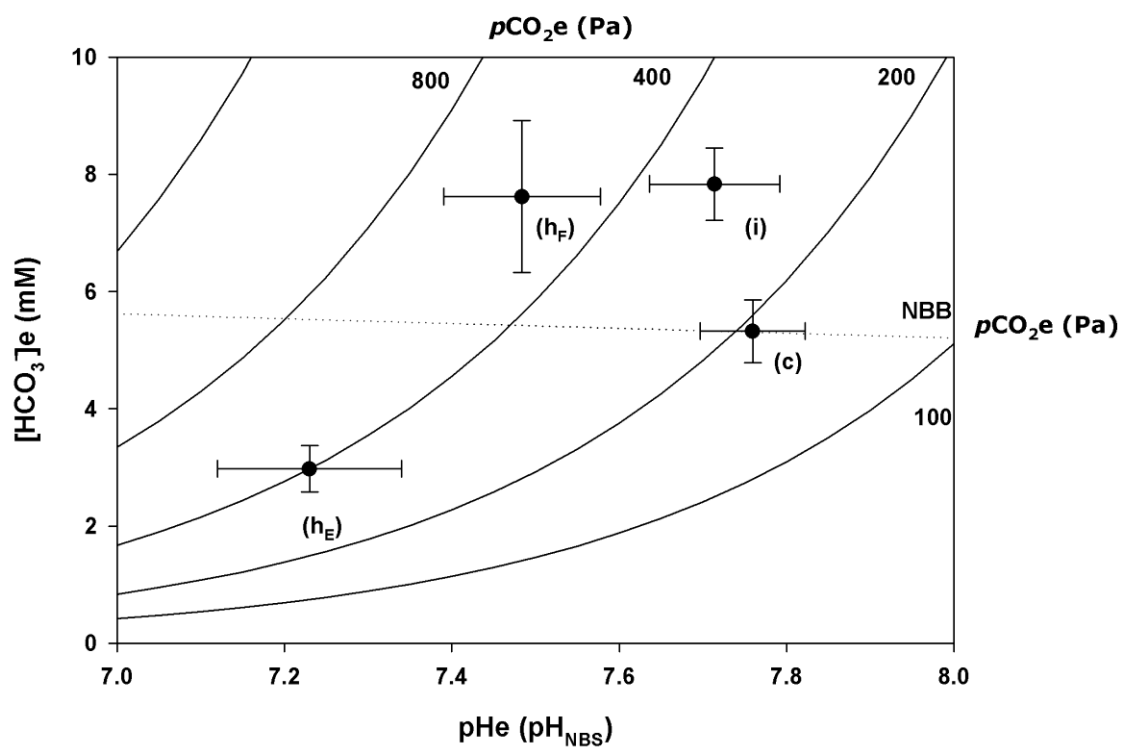


Table 1

	ST experiment (10 days)						LT experiment (45 days)					
	control $p\text{CO}_2$		intermediate $p\text{CO}_2$		high $p\text{CO}_2$		control $p\text{CO}_2$		intermediate $p\text{CO}_2$		high $p\text{CO}_2$	
<i>measured</i>	n		n		n		n		n		n	
flow rate (ml min^{-1})	28.0 \pm 0.8		28.0 \pm 0.8		28.0 \pm 0.8		27.6 \pm 0.8		27.7 \pm 0.8		27.7 \pm 0.9	
temperature ($^{\circ}\text{C}$)	10.5 0.60		10.3 0.30		10.4 0.20		10.4 \pm 0.2		10.4 \pm 0.2		10.4 \pm 0.2	
salinity	31.3 0.2		31.4 0.1		31.3 0.1		29.5 \pm 0.0		29.6 \pm 0.0		29.5 \pm 0.0	
pH_{NBS}	8.02 \pm 0.02		7.55 \pm 0.01		7.13 \pm 0.03		8.00 \pm 0.03		7.66 \pm 0.01		7.19 \pm 0.02	
pH_{T}	-		-		-		7.98 \pm 0.04 4		7.67 \pm 0.01 4		7.25 \pm 0.02 4	
A_{T} ($\mu\text{mol kg}^{-1} \text{SW}$)	2024 \pm 65 3		2092 \pm 46 3		2124 \pm 46 3		-		-		-	
C_{T} ($\mu\text{mol kg}^{-1} \text{SW}$)	1950 \pm 90 3		2098 \pm 17 3		2268 \pm 65 3		2016 \pm 17 4		2109 \pm 21 4		2286 \pm 16 4	
<i>calculated</i>												
$p\text{CO}_2$ (Pa)	69.1 \pm 19.3 3		145.2 \pm 41.0 3		385.3 \pm 41.0 3		46.5 \pm 4.8 4		102.2 \pm 4.1 4		284.3 \pm 12.0 4	
pH_{T}	7.80 \pm 0.09 3		7.51 \pm 0.10 3		7.10 \pm 0.03 3		-		-		-	
A_{T} ($\mu\text{mol kg}^{-1} \text{SW}$)	-		-		-		2147 \pm 12 4		2156 \pm 10 4		2195 \pm 10 4	
Ω_{Ca}	1.61 \pm 0.25 3		0.90 \pm 0.25 3		0.36 \pm 0.02 3		2.45 \pm 0.18 4		1.26 \pm 0.03 4		0.51 \pm 0.02 4	
Ω_{Ar}	1.02 \pm 0.16 3		0.57 \pm 0.16 3		0.23 \pm 0.01 3		1.55 \pm 0.11 4		0.79 \pm 0.02 4		0.32 \pm 0.01 4	

Table 2

parameter (% all individuals)	$p\text{CO}_2$			
	47 Pa (control)	102 Pa	284 Pa	
	n=18	n=18	h_F (n=15) 29%	h_E (n=6) 71%
<i>outer appearance</i>				
infections	0	6	0	7
stressed	0	0	0	13
healthy	100	94	100	80
<i>feeding state</i>				
full gut system	72	67	50	0
full hind gut system	28	33	50	0
empty gut system	0	0	0	100
<i>gonad development</i>				
full	61	39	0	0
medium	39	61	100	80
no gonads	0	0	0	20
<i>coelomic fluid color</i>				
red	61	67	33	0
light red	39	33	0	33
colorless	0	0	67	67
<i>behaviour</i>				
water surface	5	8		81
bottom	5	20		0
bottom between algae	90	71		5

Table 3

short term experiment	reference group (pre-incubation)		$p\text{CO}_2$			One-Way-ANOVA	
			69 Pa (control)	145 Pa	384 Pa	F	p
test diameter (cm)	-	-	3.27 ± 0.06	3.22 ± 0.07	3.26 ± 0.03	0.091	0.914
long term experiment			47 Pa (control)	102 Pa	284 Pa		
test diameter start (cm)	2.80 ± 0.06		2.79 ± 0.02	2.78 ± 0.02	2.80 ± 0.04	0.223	0.879
test diameter end (cm)	-	-	2.93 ± 0.05 a	2.89 ± 0.05 a	2.80 ± 0.03 b	14.392	<0.01
wet mass							
total (g)	4.07 ± 0.33 a		5.56 ± 0.15 b	5.17 ± 0.26 bc	4.70 ± 0.43 c	25.622	<0.01
test (g)	3.17 ± 0.28 ad		3.76 ± 0.10 b	3.56 ± 0.19 bc	3.27 ± 0.29 cd	8.462	<0.01
Lantern of Aristotle (mg)	451 ± 42 a		561 ± 26 b	553 ± 43 b	518 ± 41 b	10.028	<0.01
gonad (mg)	176 ± 42 a		627 ± 74 b	507 ± 62 c	429 ± 82 c	49.138	<0.01
gut (mg)	281 ± 12 a		613 ± 58 b	557 ± 37 bc	505 ± 58 c	60.880	<0.01
dry mass							
total (g)	2.06 ± 0.18 a		2.38 ± 0.07 b	2.26 ± 0.11 abc	2.07 ± 0.13 ac	8.655	<0.01
test (g)	1.67 ± 0.16 ab		1.80 ± 0.05 a	1.72 ± 0.08 ab	1.59 ± 0.11 b	4.288	0.017
Lantern of Aristotle (mg)	281 ± 37		299 ± 12	296 ± 25	275 ± 19	1.278	0.309
gonad (mg)	39 ± 14 a		143 ± 22 b	112 ± 16 c	90 ± 15 c	39.184	<0.01
gut (mg)	76 ± 6 a		138 ± 10 b	132 ± 7 bc	121 ± 12 c	61.001	<0.01
ash-free dry mass							
total (mg)	369 ± 72 a		527 ± 36 b	483 ± 34 bc	422 ± 35 ac	12.898	<0.01
test (mg)	198 ± 10 a		225 ± 10 b	215 ± 14 ab	193 ± 15 c	8.784	<0.01
Lantern of Aristotle (mg)	37 ± 7		48 ± 5	46 ± 9	43 ± 5	2.903	0.060
gonad (mg)	37 ± 13 a		132 ± 22 b	104 ± 15 c	82 ± 13 c	36.974	<0.01
gut (mg)	69 ± 4 a		123 ± 10 b	118 ± 8 bc	108 ± 11 c	49.321	<0.01
ash dry mass							
total (g)	1.72 ± 0.17 ab		1.85 ± 0.04 a	1.78 ± 0.08 ab	1.65 ± 0.10 b	3.931	0.023
test (g)	1.47 ± 0.17 ab		1.58 ± 0.04 a	1.51 ± 0.06 ab	1.39 ± 0.09 b	3.225	0.044
Lantern of Aristotle (mg)	234 ± 20		251 ± 11	250 ± 19	232 ± 15	2.194	0.12
gonad (mg)	2 ± 1 a		10 ± 2 b	8 ± 2 b	8 ± 3 b	19.275	<0.01
gut (mg)	7 ± 2 a		16 ± 2 b	14 ± 3 b	12 ± 2 b	17.575	<0.01
test ash DM / test DM	88.3 ± 3.8		87.5 ± 0.2	87.5 ± 0.3	87.8 ± 0.5		

Table 4:

	$p\text{CO}_2$			One-way ANOVA		conversion (unit)	Ref.
	47 Pa (control)	102 Pa	284 Pa	F	p		
provided energy							
consumed C	388.9 ± 79.6	377.2 ± 24.1	314.4 ± 50.1	3.070	0.076	15.5 (kJ g ⁻¹ dry algae)	a
absorption efficiency (%)	53.0 ± 4.6	52.3 ± 4.6	53.4 ± 4.1				
absorbed A	204.0 ± 33.4 ab	197.1 ± 17.5 a	166.3 ± 14.7 b	4.401	<0.05		
used energy							
respired R	36.3 ± 5.1	31.7 ± 4.1	29.8 ± 5.1	2.818	0.091	0.48 (J μmol ⁻¹ O ₂)	b
excreted U	1.92 ± 0.37 a	2.11 ± 0.15 ab	2.82 ± 0.74 b	5.749	<0.05	0.35 (J μmol ⁻¹ NH ₄ ⁺)	c
R + U	38.2 ± 5.1	33.9 ± 4.0	32.7 ± 5.1	2.210	0.144		
R + U (% of A)	19.0 ± 3.1	17.3 ± 2.7	19.6 ± 2.5				
Scope for Growth (SfG)	165.8 ± 31.6 ab	163.3 ± 18.1 a	133.7 ± 12.8 b	3.851	<0.05		
deposited in growth over 40 days							
test & spines	6.0 ± 2.1 a	2.6 ± 3.5 a	-4.2 ± 5.7 b	9.938	<0.01	4.3 (kJ g ⁻¹ dry tissue)	d
gut	15.6 ± 2.1	14.8 ± 1.4	12.9 ± 3.3	1.954	0.176	24 (kJ g ⁻¹ dry tissue)	d,e
gut (% of A)	7.8 ± 1.6	7.6 ± 1.1	7.7 ± 1.6				
gonad	26.1 ± 5.0 a	19.4 ± 3.9 b	14.7 ± 4.1 b	10.252	<0.01	24 (kJ g ⁻¹ dry tissue)	d
gonad (% of A)	13.2 ± 3.7	9.8 ± 1.6	8.9 ± 2.8				
total deposition	47.7 ± 6.9 a	36.8 ± 7.4 a	23.4 ± 8.9 b	14.722	<0.01		
total deposition (% of A)	24.1 ± 6.1	18.7 ± 3.5	13.9 ± 5.0				
total deposition (% of SfG)	30.0 ± 8.7	22.6 ± 4.0	17.4 ± 6.6				
remaining energy (% of A)	56.9 ± 8.9	64.0 ± 3.5	66.4 ± 6.3				

References: (a) Marsham et al. 2007, (b) Gnaiger 1983, (c) Elliot and Davidson 1975, (d) Fernandez 1998, (e) Bishop & Watts 1992

Table 5:

Species	control extracellular values			hypercapnic extracellular values					Ref
	pH (NBS)	[HCO ₃] (mM)	pCO ₂ (kPa)	seawater pCO ₂ (kPa)	exposure (days)	maximum ΔpH	final ΔpH	Δ[HCO ₃] (mM)	
<i>Strongylocentrotus droebachiensis</i>	7.76 (0.06)	3.96 (0.68)	0.16 (0.02)	0.14	10	-0.31	0.06	+2.14	a
				0.40	10	-0.39	-0.19	+2.21	a
	7.76 (0.05)	5.33 (0.54)	0.19 (0.02)	0.10	43	-	-0.05	+2.51	a
				0.28 F	43	-	-0.28	+2.29	a
			0.28 E	43	-	-0.53	-2.35	a	
<i>Psammechinus miliaris</i>	7.40 (0.05)*	1.80 (0.20)	0.13 (x)*	0.25	8	-0.55	-0.55	+1.50	b
<i>Mytilus edulis</i>	7.59 (0.16)	1.77 (0.15)	0.17 (0.08)	0.14	14	-	-0.23	-0.13	c
				0.40	14	-	-0.43	-0.04	c
<i>Sepia officinalis</i>	7.67 (0.05)	3.38 (0.12)	0.22 (0.03)	0.60	2	-0.18	-0.18	+6.70	d
<i>Cancer magister</i>	7.81 (x)*	6.50 (x)*	0.28 (x)*	1.10	1	-0.41	-0.07	+12.0	e
<i>Sparus aurata</i>	7.65 (0.03)	7.34 (0.54)	0.34 (0.04)	0.51	10	-0.24	-0.06	+19.2	f
<i>Gadus morhua</i>	7.90 (x)*	10.5 (x)*	0.43 (x)*	1.10	1	-0.18	0.02	+21.0	g

References: (a) this study, (b) Miles et al 2007, (c) Thomsen et al 2010, (d) Gutwoska et al. 2009, (e) Pane and Barry 2007, (f) Michaelidis et al. 2007, (g) Larsen et al. 1997

maximum ΔpH maximum pH decrease measured in the respective study; final ΔpH and Δ[HCO₃-] values reported for the endpoint measurement in each study

* values read from figures, x SD < minimum readable from figure

IV Impact of long term and trans-life-cycle acclimation to near-future ocean acidification on the green sea urchin *Strongylocentrotus droebachiensis*.

Dorey, N.; Stumpp, M.; Thorndyke, M. C.; Melzner, F.; Dupont, S.

Global Change Biology (under review)

Impact of long term and trans-life-cycle acclimation to near-future ocean acidification on the green sea urchin *Strongylocentrotus droebachiensis*

Running title: Long-term impact of ocean acidification

Narimane Dorey¹, Meike Stumpp², Michael Thorndyke³, Frank Melzner² and Sam Dupont^{1,*}

¹ Department of Marine Ecology, University of Gothenburg, The Sven Lovén Centre for Marine Sciences, Kristineberg 45034, Sweden

² Biological Oceanography, Leibniz-Institute of Marine Sciences (IFM-GEOMAR), 5 24105 Kiel, Germany

³ The Royal Swedish Academy of Sciences, The Sven Lovén Centre for Marine Sciences, Kristineberg 45034, Sweden

* Corresponding author: phone: +46 523 18534; fax:+46 523 18501; sam.dupont@marecol.gu.se

Keywords: Ocean acidification – Sea urchin – Acclimation – Long term – Carry-over

Abstract:

Atmospheric carbon dioxide partial pressure is increasing due to anthropogenic carbon emissions. A significant part of this CO₂ is taken up by the oceans, changing carbonate chemistry speciation and decreasing pH. This phenomenon, known as ocean acidification, is expected to have serious consequences for the marine biota by the end of the present century. To allow for any large-scale biological prediction, it is important to have accurate data on species-sensitivity or -resilience to these near-future climate change stressors. However, a vast majority of previous experiments demonstrating impacts of ocean acidification on marine invertebrates have been short-term (a vast majority less than 2 weeks and always less than 30 weeks) and did therefore not consider (i) acclimation time allowing expression of individual plasticity and (ii) life as a cycle, including several subsequent life-history stages. In this study, we highlight the importance of long-term and trans- generation studies by exposing different life stages (adults, larvae and juveniles) of the ecologically and economically key sea urchin species *Strongylocentrotus droebachiensis* to long term (4 or 16 months) near future CO₂-driven ocean acidification conditions (control pH_{NBS}=8.1, pCO₂~401 μatm vs. acidic pH_{NBS}=7.7, pCO₂~1217 μatm). We show that after 4 months, low pH decreased female fecundity by 4-5 times while no difference was observed after 16 months. On the other hand, adult pre-exposure to low pH had a strong negative impact on subsequent larval settlement success while pH experienced during development had no significant direct impact on settlement. Juvenile mortality was not increased in low pH conditions except when both larvae and juvenile were raised in low pH. These two results highlight the importance of “carry-over” effects between subsequent life stages and identify settlement and early juvenile development as key bottlenecks in sea urchin development (25 times decrease in number of eggs reaching the 3 months juvenile stage).

Key-Words: Ocean acidification, echinoderm, life-cycle, acclimation, carry-over effects, long term

Introduction:

As a consequence of anthropogenic carbon emissions, atmospheric pressures of CO₂ have been dramatically rising in the past century and, global models predict *p*CO₂ to rise at even higher rates in the next decades (IPCC 2007). These emissions are not without consequences on marine chemistry (Sabine *et al.* 2004), shifting the carbonate system and lowering the pH at rates that have not been documented since 450 000 years. In the last 150 years, average surface ocean pH has dropped by ~0.1 units, which is equivalent to a 25% increase in acidity. Modeling predicts the pH of the oceans to drop of 0.2 to 0.4 units in less than a century (Caldeira and Wickett 2005). This phenomenon, known as ocean acidification (OA), is predicted to have large impacts on marine biota and marine ecosystems (Fabry *et al.* 2008). However, in temperate coastal systems, much higher changes in pH and *p*CO₂ can be expected. Seasonal hypoxia can enrich such systems with CO₂ and future *p*CO₂ of >2000 µatm (pH<7.5) are realistic, particularly in the Western Baltic Sea (HELCOM 2009, Thomsen *et al.* 2010).

Marine calcifying organisms both benthic – such as coralline algae, bryozoans, corals, echinoderms, and bivalves - and planktonic – foraminifera, pteropods or larval stages of benthic invertebrates- are predicted to be primarily impacted by changes in carbonate system speciation (Orr *et al.* 2005). Ocean acidification will decrease the carbonate ion concentration (CO₃²⁻), which can eventually lead to external and internal dissolution of carbonate shells (Feely *et al.* 2004, Thomsen *et al.* 2010). Changes in extracellular acid-base status that go along with ocean acidification influence the carbonate system speciation at the calcification front and potentially alter calcification dynamics (e.g. Gutowska *et al.* 2010).

In consequence, marine invertebrate calcifying organisms have been the focus of considerable research effort (Kleypas *et al.* 2006, Doney *et al.* 2009). However, physiology and individual ability to buffer or regulate these changes are often underestimated (Pörtner and Farrell 2008, Melzner *et al.* 2009) and an increasing amount of data show unpredicted resilience in marine calcifiers (*e.g.* Ries *et al.* 2009, Gutowska *et al.* 2010, Dupont *et al.* 2010b). Observed effects on organisms are often contrasting, showing specific and even contradictory responses within major groups (see review by Doney *et al.* 2009). Even looking only within one taxonomic group, the echinodermata,

Dupont *et al.* (2010a) highlighted variable responses as a function of taxonomic group, studied processes, life-history stage and population history. For example, under acidified conditions, calcification is significantly decreased in the adult sea urchin *Eucidaris tribuloides* but is increased 4.5 fold in the adult sea urchin *Arbacia punctulata* (Ries *et al.* 2009). It is therefore difficult to make any generalization or any predictions on future ecosystem changes (Blackford *et al.* 2010). Other parameters largely ignored at present, such as carry-over effects between different life-history stages and acclimation potential, additionally complicate the picture.

Most experiments have traditionally focused on only one life-history stage. However, many benthic marine invertebrates develop by means of a free-living dispersive planktonic larval stage and go through several major ontogenetic shifts including larval metamorphosis and settlement. Moreover, significant but less conspicuous ecological shifts can also occur during postmetamorphic life (Fig. 1; Gosselin 1997). Each life stage (larvae, juveniles, adults) could differ in form and function with various degrees of autonomy and thus could have differing sensitivities to environmental stressors. However, these different life-stages are a continuum and the consequences of an environmental change leading to a disturbance in one stage can then “carry over” into following stages and be detrimental by altering the performance and selection of those that follow (Podolsky and Moran 2006).

One of the most documented carry over effect is the maternal effect. It has been shown in plants (review by Roach and Wulff 1987), arthropods (review on insects by Mousseau and Dingle 1991), mollusks (*e.g.* Lacoue-Labarthe *et al.* 2008), fish (*e.g.* Mc Cormick 1998), birds (Norris 2005, Sorensen *et al.* 2009) and mammals (*e.g.* Robinson 1981), including humans (Zdravkovic *et al.* 2005), that egg quality and subsequent offspring fitness are dependent on diet quality, life style, temperature or O₂ concentrations experienced by the mothers.

Carry-over effects are also observed between other life-history stages: from eggs to larvae (Marshall *et al.* 2002, Marshall and Keough 2003), from embryo to larva and juvenile (Moran and Emlet 2001, Giménez and Anger 2003) and latent effects from larva to juvenile or adults (Marshall *et al.* 2003, Pechenik 2006). For example, experiences during the pelagic period can determine phenotypic traits (*e.g.* larval size) or post-

settlement probability and performance, and for competent larvae, delays in metamorphosis can reduce juvenile performance (Emlet and Sadro 2006; Hamilton *et al.* 2008).

Another gap in knowledge is related to the fact that we know almost nothing about how marine species will be able to acclimate or adapt to predicted changes. Time of exposure to a stressor is a well known parameter modulating a species response. For example, meta-analysis of echinoderms reveals a greater impact following long term exposure (6 months) compared to shorter term (<2 weeks) (Dupont *et al.* 2010a). A review of the available literature on invertebrates reveals that of the 131 published perturbation experiments studied so far, 71% had an exposure time less than 6 weeks and 92% of less than 10 weeks and the longest exposure time used to date was only 30 weeks. Organisms have the ability to adjust to changes in their environment and available studies have largely ignored plasticity potential. For example, it was shown that the sea urchin *Strongylocentrotus purpuratus* is extremely plastic and is able to go through major changes including a drastic deformation of its morphology (including shape of the skeleton) and modified behavior in a matter of 8-20 weeks when exposed to a different habitat structure (Hernández and Russell 2010). These changes are associated with transient energetic costs that could have consequences for other processes.

In summary, most published studies so far have focused on a single life-history stage, single generation and short exposure time which may both under- and over-estimate the real impact of ocean acidification.

In this study, we aimed to investigate (i) the impact of long term acclimation (up to 16 months) and (ii) carry-over effects between life-history stages on fitness related parameters of the green sea urchin *Strongylocentrotus droebachiensis*. This should allow us to provide insights into the time course of potential plasticity responses and to identify bottlenecks in the life-cycle.

The green sea urchin *Strongylocentrotus droebachiensis* is a keystone calcifier determining the structure of coastal ecosystems of Nordic European coastal waters (Norderhaug and Christie 2009) and therefore a relevant organism for ocean acidification investigations, both ecologically, as a major regulator of kelp forests due to its high grazing activity and economically, as a food resource.

Egg production, larval and juvenile growth and survival were studied in response to moderate near-future ocean acidification (0.4 unit pH decrease). Female fertility was assessed under two different time scales of exposure (4 months and 16 months). Carry over effects were also investigated between adults, larvae and juveniles (parental effect) and between larvae and juveniles (latent effect).

Material and methods:

(a) Animal handling

In December 2008 (experiment 1) and March 2010 (experiment 2), specimens of the green sea urchin *Strongylocentrotus droebachiensis* were collected from two populations along the thermal gradient from Skagerrak to the Barent Sea: (i) individuals in sea urchin dominated barren near Hammerfest (“Norway”) and (ii) a stone reef at Anholt (“Denmark”). Individuals were subsequently maintained in natural flowing seawater [12°C, pH_{NBS} 8.1 ± 0.1 units (control), salinity 32‰ and alkalinity of 2.16 ± 0.02 mM (measured following Sarazin *et al.* 1999)] for 2 weeks prior to the experiment. Other parameters ($p\text{CO}_2$, saturation states for calcite (Ω_{ca}) and aragonite (Ω_{ar})) were calculated from measured pH (measured with a Metrohm (827 pH lab) pH electrode calibrated with NIST or total (TS) scale buffers, Dickson *et al.* 2007) and total alkalinity (method by Sarazin *et al.* 1999) using sea water CO_2 (SW CO_2) with dissociation constants from Mehrbach *et al.* (1973), refitted by Dickson and Millero (1987). The sea urchins from each population were then transferred into separate 400L basins (open system with a water replacement rate of 1L min⁻¹) allowing a minimum volume of 10L per individual. For the experimental manipulation we selected a seawater pH, predicted to occur by the year 2100 ($\Delta\text{pH} \approx -0.4$ units to a pH of 7.7; Caldeira and Wickett, 2003). pH was maintained in each basin using a computerized control system (AquaMedic) that regulated pH by the addition of pure gaseous CO_2 directly into the experimental tank and mixed with Eheim 600 submersible pumps at a rate of 300 L h⁻¹.

S. droebachiensis were either used immediately to collect gametes (n=2x10 individuals; experiment 2; 2010) or exposed to natural seawater (control, pH_{NBS}=8.1, $p\text{CO}_2=401\mu\text{atm}$, $\Omega_{\text{ca}}=2.96$, $\Omega_{\text{ar}}=1.88$) and to acidified sea water (pH_{NBS}=7.7, $p\text{CO}_2=1217\mu\text{atm}$, $\Omega_{\text{ca}}=1.18$, $\Omega_{\text{ar}}=0.75$) for a total period of either 4 months or 16 months (experiment 1; n=15 individual in 2009; n=7 individuals in 2010). The adult sea urchins

were fed *ad libitum* with *Ulva* spp. twice a week. The diameter of the sea urchins used for the experiment ranged between 4.5 and 5cm.

(b) Experiment 1: Effect of adult acclimation on fertility and settlement success

After 4 (Denmark and Norway populations, April 2009) or 16 months (Denmark population, April 2010) of exposure to control or low pH conditions, spawning of 4 to 11 females and 4 males in each treatment was induced by two intracoelomic injections with 1 ml of 0.5M KCl in FSW. Females were separately placed in 1L beaker filled with FSW during spawning. Sperm were collected dry using a pipette and kept on ice until use. The collected eggs were used to assess fecundity (number of eggs per female, estimated as the average 5 sub-samples of 50 μ L and then fertilized with collected sperm to evaluate further settlement success (number of larvae reaching the juvenile stage).

The impact of adult acclimation on larval settlement success was measured for the Denmark population after a 4 month acclimation period. Eggs from the different females were pooled and concentrated into 1L FSW at the relevant pH (control, $\text{pH}_{\text{NBS}}=8.1$ or acidified, $\text{pH}_{\text{NBS}}=7.7$). Sperm stock solution (mix of 4 males) in filtered sea water (FSW) was added to each dish to a final concentration of ~ 1000 sperm ml^{-1} . After 15 min, fertilized eggs (mixed females and males, $>95\%$ fertilization success) were rinsed in filtered seawater (FSW) at the appropriate pH and at the two-cell stage were transferred to 5L aquaria at a density of 10 embryos per ml. The different culture treatments (control, $\text{pH}_{\text{NBS}}=8.1$, $p\text{CO}_2=432\mu\text{atm}$, $\Omega_{\text{ca}}=2.64$, $\Omega_{\text{ar}}=1.68$ or acidified, $\text{pH}_{\text{NBS}}=7.7$, $p\text{CO}_2=1177\mu\text{atm}$, $\Omega_{\text{ca}}=1.14$, $\Omega_{\text{ar}}=0.72$) were set up as a 2 x 2 experimental design: 2 acclimation pH treatments (pH of the basin in which the adults were kept 4 months prior to spawning) x 2 larval culture pH treatments (Fig. 2). pH was maintained in each aquarium using a computerized control system as described above. Cultures were maintained at 12 °C, a salinity of 32‰ and alkalinity of 2.09 ± 0.02 mM. The experiment was replicated 4 times using the same batch of parental animals. After Day 4, larvae were fed daily with the cryptophyte *Rhodomonas* sp. at a concentration of 150 $\mu\text{g C L}^{-1}$. Food concentration was estimated using an Elzone 5380 particle sizing and counting analysis system and corrected daily (at this concentration, the pH had no impact on algal growth and/or survival; SD personal observation). Settlement success was measured after 28 days as the number of larvae reaching the juvenile stage.

(c) Experiment 2: Effect of larval exposure on juvenile growth and survival

Gametes from freshly collected sea urchins from both Denmark and Norway populations were collected, fertilized and cultured using a full-cross design experiment (2 populations x 2 females x 4 males x 2 nominal pH (8.1 and 7.7) for a total of 64 cultures) according to the methods described above. Juveniles were then collected, measured (diameter of the test), pooled to ensure the highest genetic variability representative of the species along the geographical distribution and cultured for 3 months in a 5L system identical to that used for the larvae. pH was maintained in each aquarium using a computerized control system as described above. The different culture treatments (control, $\text{pH}_{\text{TS}}=8.07$, $p\text{CO}_2=361\mu\text{atm}$, $\Omega_{\text{ca}}=3.09$, $\Omega_{\text{ar}}=1.96$ or acidified, $\text{pH}_{\text{TS}}=7.69$, $p\text{CO}_2=942\mu\text{atm}$, $\Omega_{\text{ca}}=1.46$, $\Omega_{\text{ar}}=0.92$) were set up as a 2 x 2 experimental design: 2 larval culture pH x 2 juvenile culture pH. Cultures were maintained at 12 °C, a salinity of 32‰ and alkalinity of 2.17 ± 0.06 mM. The entire experiment was replicated 2 times using different parental animals. The juveniles were fed *ad libitum* with small pieces of *Ulva* spp. Juvenile survival (%) and growth ($\text{mm}\cdot\text{mo}^{-1}$, calculated as the difference between average size after 3 months and at the beginning of the exposure) were estimated after 3 months. It is important to notice that because of the high mortality in one of the treatment, juvenile growth may be biased due to size-dependent sensitivity (e.g. see Green *et al.* 2004).

(d) Statistical analyses

Each mean value is expressed with its standard error of the mean (mean \pm SEM). One way analysis of variance (ANOVA) was used to test the impact of the treatment (pH 7.7 and 8.1) on fecundity. Two- and three factors mixed model ANOVA with the treatments (fixed, pH treatment and pH acclimation) and experiment (random) were used to test the impact of pH on settlement success. The normality and variance homogeneity data were tested before data was entered for the ANOVA. All data were analysed using SAS/STAT software.

Results:*(a) Experiment 1: Effect of adult acclimation on fertility and settlement success*

After 4 months, the number of eggs per female was 4 to 5 time smaller in females acclimated in low pH water (nominal 7.7) compared to control (nominal 8.1) in both

tested populations (Fig. 3; ANOVA, Denmark: $F=9.82$, $p<0.0086$; Norway: $F=19.50$, $p<0.0022$). In striking contrast, no differences between pH treatments were observed after 16 months of acclimation (Fig. 3; ANOVA, Norway; $F=0.77$, $p<0.7663$).

Impact of pH during both adult acclimation (4 months, Norway population), larval development (28 days) and on settlement success was investigated. Five to 9 times less eggs reached the juvenile stage in cultures from gametes collected from adults acclimated in low pH conditions (ANOVA II, $F=4.87$, $p<0.0306$; acclimation pH: $F=9.71$, $p<0.0098$). On the other hand, the settlement success was the same whatever the pH experienced by the larvae (Fig. 4; larval culture pH: $F=0.03$, $p<0.8775$).

It is important to notice that no mortality was recorded in adults during the whole experimental period.

(b) Experiment 2: Effect of larval exposure on juvenile growth and survival

46% to 67% of the newly settled juveniles survived for the 3 first months of their development with the exception of juveniles from larvae raised at pH 7.7 and maintained in pH 7.7 where 95% mortality was observed (Fig. 5).

However, the pH during larval development does not explain the differences in juvenile growth rate (ANOVA 2: $F=29.27$, $p<0.0001$; pH development: $F=3.72$, $p>0.0539$). The main differences were observed between pH exposure during juvenile growth (pH juvenile: $F=6.89$, $p<0.0088$) and the interaction of pH during larval development and juvenile growth (pH development x pH juvenile: $F=58.13$, $p<0.0001$). Juveniles grew significantly faster when they were kept in the same pH conditions during both larval development and the first 3 months of the juvenile life (Fig. 6).

Discussion:

Our results highlight the importance of including long-term and multi-stage exposures in ocean acidification research. We show that short term and single stage exposure can both under- and over-estimate the real impact of near-future ocean acidification and potentially lead to faulty conclusions regarding species-sensitivity and the identification of CO₂ dependent bottlenecks in ontogeny.

What is a relevant exposure time?

Considerations have to be taken regarding the exposure time of the organisms in ocean acidification perturbation experiments. In our first experiment, fecundity is dramatically decreased when adult sea urchins are exposed to low pH during 4 months prior to spawning but no difference is observed after a 16 months exposure. This observation can be related to the high degree of phenotypic plasticity found in sea urchins (Russell 1998), 16 months being enough time to reach a new physiological steady-state that permits allocation of similar fractions of the energy budget into gonad maturation as found under control conditions. As adults, the green sea urchin *S. droebachiensis* lacks fast escape or migratory abilities and therefore needs to be able to cope with any change in its environment. For example, it was shown that sea urchins can modulate their body size or shape, and/or shift the energy allocated to growth between different compartments depending on food availability (*e.g.* Levitan 1991), competitor density (*e.g.* Levitan 1989, Fernandez and Bouderesque 1997), predator cues (*e.g.* Selden *et al.* 2009), prey morphology (*e.g.* Hagen 2008), salinity (*e.g.* Lau *et al.* 2009) or even habitat structure (*e.g.* Hernández and Russell 2010). These morphological and underlying physiological changes can take place within relatively short-time periods during one individual lifetime and are reversible. Hernández and Russel (2010) showed in the sea urchin *S. purpuratus* that 8 to 20 weeks were needed to fully express their plasticity when transferred into a new habitat. This “phenotypic flexibility” is an advantage in terms of survival and reproduction success, “flexibility” therefore being an important adult life history trait to consider (Piersma and Drent 2003). Gonads can be regarded as the most plastic body components in echinoderms, as they are essentially storage energy compartments that can be filled or depleted depending on conditions (Russell 1998). We hypothesized that the differences in fertility observed between individuals exposed to ocean acidification for 4 and 16 months exposure could be attributed to a transient change in energy budget to invest energy in the observed morphological and underlying physiological re-organization. In the first months of exposure, energy could have been re-allocated from gonadic storage to energy for physiological acclimation, which would explain the drop in egg number after a few months. Once new, potentially cost neutral, equilibria have been achieved, energy could be re-invested in egg production and would enable the full compensation of egg production after 16 months.

Our results strengthen the recommendations to conduct long-term perturbation experiments (Widdicombe et al. 2010) avoiding short-term transient negative effects due to plasticity responses. On the other hand, some negative effects may only be revealed after long term exposure. For example, juvenile and adult mortality was only observed after 7 to 18 weeks exposure to low pH in a range of invertebrates including echinoderms (Langenbuch and Pörtner 2004, Shirayama and Thornton 2005 *et al.* 2008).

Single vs. multiple life-history stages: carry-over effects

Podolsky and Moran (2006) stressed the importance of considering life as a cycle since every life-history stage has very different traits and does not live in complete autonomy from the others. This is illustrated by the result of our second experiment. Considering only isolated life stages, we could not identify negative impacts of ocean acidification on larval settlement success and juvenile survival. This is in agreement with previous studies on the impact of ocean acidification on echinoderm early life stages (reviewed by Dupont *et al.* 2010a). When exposed to near-future ocean acidification, the vast majority of studied species (but see 100% mortality during the development of the brittlestar *Ophiothrix fragilis*, Dupont *et al.* 2008) only show sublethal effects.

However, such conclusions should be reconsidered in the light of the present results which suggest strong carry-over effects. When two subsequent life-stages were considered (from adult to larvae and from larvae to juvenile), very strong negative impacts of ocean acidification and a clear bottleneck in the life-cycle were observed (a 5 time decrease in settlement success and juvenile survival over the first 3 months). In sea urchin species, conditions experienced by a female have been shown to influence egg quality, gonad weight, and offspring quality (maternal effect, *e.g.* Russell 1998, Garrido and Barber 2001). This is mainly linked to parental diet, but also to abiotic parameters such as the seawater oxygen partial pressure (Burnett *et al.* 2002). We hypothesize that an additional energy cost to adults during the first month of exposure (see previous discussion on plasticity) may not only impact fertility but also egg quality with negative consequences for larvae, significantly reducing their settlement success.

In our study, we also showed that juveniles experienced 5 times increased mortality when both larvae and juveniles were kept at low pH. This additive effect could not be explained by a maternal effect but rather by energy budget considerations: gaps in

the energy budget at one stage cannot be fulfilled by the subsequent stage therefore increasing the negative effects on offspring fitness.

Consequence for the green sea urchin

Adult sea urchins appeared to be resilient to long term ocean acidification with no mortality recorded and a maintained fertility over 16 months. This is surprising since results from another sea urchin species, *Psammechinus miliaris*, (Miles *et al.* 2007) showed an accumulation of CO₂ and a significant reduction in pH in coelomic fluid in all low pH treatments compared with controls. Based on this inability to compensate acid-base balance following short-term exposure to low pH ($\Delta\text{pH}_{\text{NBS}}=0.5$ for 7 days), the authors predicted severe impacts on echinoids. Similar results were recently observed in the seastar *Asterias rubens* with a persistent lack of compensation of coelomic fluid pH under low pH conditions ($\Delta\text{pH}_{\text{NBS}}=0.4$ for 6 months) but without direct consequences for survival but significant consequences for immunology (Hernroth *et al.* 2011). This long term survival also contrasts with the high mortality observed during long term exposure of sea urchins by Shirayama and Thornton (2005); however, their experiment was performed on sea urchin juveniles that also appeared to be quite sensitive in our experiment. Several hypotheses could be used to explain these differences. First, *S. droebachiensis* is more efficient at regulating coelomic fluid pH than other tested species: Stumpp *et al.* (submitted) found fully compensated coelomic fluid pH by means of bicarbonate accumulation in this species following > 2 week exposure to a pCO₂ of 1400 μatm / pH 7.7. On the other hand, it may also be possible that sea urchins are able to survive this disturbance in acid-base balance with only sub-lethal consequences (e.g. reduced immune response, Hernroth *et al.* 2011; reduced growth, Appelhans *et al.* submitted). It can be speculated in this context that *S. droebachiensis* might be exposed to frequent hypoxia, which is always coupled to high pCO₂ and low pH, in its natural habitat, particularly in the Western Baltic population (Diaz and Rosenberg 2008). This population may therefore be genetically adapted to a high variability in carbonate system speciation in the contemporary ocean already.

We were able to identify a clear bottleneck in the *S. droebachiensis* life-cycle. Under realistic experimental conditions (long term exposure, several life-cycle stages, etc.), low pH has a dramatic impact on *S. droebachiensis* early development where a 5

time decrease in settlement success and a 5 time increased mortality over the last 3 months of juvenile growth is observed. This 25 time decrease in egg number reaching the 3 month juvenile stage could have dramatic consequences for population sustainability.

Echinoderms are among the most abundant and ecologically successful groups of marine organisms and of tremendous ecological and economical importance. They are among the most familiar seashore organisms and are also widely distributed in all oceans at all depths. They occupy keystone positions in many of the ocean's most vulnerable ecosystems worldwide. They are often important ecosystem engineers and bioturbators as well as being an important part of the food chain as prey for carnivorous fish and crustaceans. Sub littoral starfish and sea urchins represent an important grazing community while in many areas urchins and sea cucumbers are exploited for food (Micael *et al.* 2009). In particular, *S. droebachiensis* is widely distributed and plays a key ecological role in determining the distribution and abundance of benthic macroalgae. Consequently, it has been considered a pest in areas where intensive grazing destroys kelp habitat and limits production of commercial species such as cod. On Nordic coasts, grazing by the green sea urchin is central for structuring marine benthic communities leading to two "stable" states: luxuriant kelp forests and species-depleted sea urchin barrens (Norderhaug and Christie 2009). This balance is in some areas determined by recruitment intensity and supply of sea urchin larvae (Pearse 2006). On the other hand, urchins have become a valued commodity and are now extensively fished and cultured for roe in the Northwest Atlantic and Northeast Pacific. Major changes in *S. droebachiensis* populations may then have positive (e.g restoration of the kelp habitat) and negative (e.g. economic cost) consequences.

It is also important to remember that any experiment is an abstraction of reality. Many relevant parameters at the ecosystem level were not considered in our experiment including the natural variability of environmental parameters, the synergy with other stressors such as temperature, ecological interactions, selection, etc. In consequence, we have to be cautious with any ecological extrapolation. However, the observed decrease in settlement success and juvenile survival combined with other sublethal effects observed (e.g. delay in development, Dupont *et al.* 2010a) suggest a very strong potential impact of ocean acidification on green sea urchin populations.

Conclusions

S. droebachiensis adults and gametes appeared to be relatively resistant to simulated ocean acidification. On the other hand, larval settlement and juvenile survival can be drastically decreased with potential consequences for population sustainability. This draws attention to the value of juveniles in ocean acidification predictions, their current under-valuation and the importance to place them in a global cyclic and ecosystemic view. Only integration across marine life-cycles into experimental design will allow realistic predictions on the maintenance of populations or species.

Acknowledgement:

SD is funded by the Linnaeus Centre for Marine Evolutionary Biology at the University of Gothenburg (<http://www.cemeb.science.gu.se/>), and supported by a Linnaeus-grant from the Swedish Research Councils VR and Formas; VR and Formas grants to MT; Knut and Alice Wallenberg's minnen and the Royal Swedish Academy of Sciences. MS and FM were funded by the DFG Excellence Cluster „Future Ocean“ and the German „Biological impacts of ocean acidification (BIOACID)“ project 3.1.4, funded by the Federal Ministry of Education and Research (BMBF, FKZ 03F0608A).

References:

- Blackford JC (2010) Predicting the impacts of ocean acidification: Challenges from an ecosystem perspective. *Journal of Marine Systems*, **81**, 12-18.
- Burnett L, Terwilliger N, Carroll A, Jorgensen D, Scholnick S (2002) Respiratory and Acid-Base Physiology of the Purple Sea Urchin, *Strongylocentrotus purpuratus*, During Air Exposure: Presence and Function of a Facultative Lung. *Biological Bulletin*, **203**, 42-50.
- Caldeira K, Wickett M (2005) Ocean model predictions of chemistry changes from carbon dioxide emissions to the atmosphere and ocean. *Journal of Geophysical Research C: Oceans*, **110**, 1-12.
- Diaz RJ, Rosenberg R (2008) Spreading Dead Zones and Consequences for Marine Ecosystems. *Science*, **321**, 926-929.

- Dickson AG, Millero FJ (1987) A comparison of the equilibrium constants for the dissociation of carbonic acid in seawater media. *Deep Sea Research*, **34**, 1733-1743.
- Dickson AG, Sabine CL, Christian JR (2007) Guide to best practices for ocean CO₂ measurements. PICES Special Publications 191 p.
- Doney SC, Fabry VJ, Feely RA, Kleypas JA (2009) Ocean Acidification: The Other CO₂ Problem. *Annual Review of Marine Science*, **1**, 169-192.
- Dupont S, Dorey N, Thorndyke M (2010b) What meta-analysis can tell us about vulnerability of marine biodiversity to ocean acidification? *Estuarine, Coastal and Shelf Science*, **89**, 182-185.
- Dupont S, Havenhand J, Thorndyke W, Peck L, Thorndyke M (2008) Near-future level of CO₂-driven ocean acidification radically affects larval survival and development in the brittlestar *Ophiothrix fragilis*. *Marine Ecology Progress Series*, **373**, 285–294.
- Dupont S, Ortega-Martínez O, Thorndyke M (2010a) Impact of near-future ocean acidification on echinoderms. *Ecotoxicology*, **19**, 449-462.
- Emllet RB, Sadro SS (2006) Linking stages of life history: How larval quality translates into juvenile performance for an intertidal barnacle (*Balanus glandula*). *Integrative and Comparative Biology*, **46**, 334-346.
- Fabry VJ, Seibel BA, Feely RA, Orr JC (2008) Impacts of ocean acidification on marine fauna and ecosystem processes. *ICES Journal of Marine Science*, **65**, 414-432.
- Feely RA, Sabine CL, Lee K, Berelson W, Kleypas J, Fabry VJ, Millero FJ (2004) Impact of anthropogenic CO₂ on the CaCO₃ system in the oceans. *Science*, **305**, 362-366.
- Fernández C, Boudouresque C (1997) Phenotypic plasticity of *Paracentrotus lividus* (Echinodermata: Echinoidea) in a lagoonal environment. *Marine Ecology Progress Series*, **152**, 145-154.
- Garrido CL, Barber BJ (2001) Effects of temperature and food ration on gonad growth and oogenesis of the green sea urchin, *Strongylocentrotus droebachiensis*. *Marine Biology*, **138**, 447-456.

Giménez L, Anger K (2003) Larval performance in an estuarine crab, *Chasmagnathus granulata*, is a consequence of both larval and embryonic experience. *Marine Ecology Progress Series*, **249**, 251–264.

Gosselin LA (1997) An ecological transition during juvenile life in a marine snail. *Marine Ecology Progress Series*, **157**, 185-194.

Green MA, Jones ME, Boudreau CL, Moore RL, Westman BA (2004) Dissolution Mortality of Juvenile Bivalves in Coastal Marine Deposits. *Limnology and Oceanography*, **49**, 727-734

Gutowska MA, Melzner F, Langenbuch M, Bock C, Claireaux G, Pörtner, HO (2010) Acid–base regulatory ability of the cephalopod (*Sepia officinalis*) in response to environmental hypercapnia. *Journal of Comparative. Physiology part B*, **180**, 323–335.

Hagen NT (2008) Enlarged lantern size in similar-sized, sympatric, sibling species of Strongylocentrotid sea urchins: from phenotypic accommodation to functional adaptation for durophagy. *Marine Biology*, **153**, 907-924.

Hamilton SL, Regetz J, Warner RR (2008) Postsettlement survival linked to larval life in a marine fish. *Proceedings of the National Academy of Sciences*, **105**, 1561-1566.

HELCOM (2009) Biodiversity in the Baltic Sea – An integrated thematic assessment on biodiversity and nature conservation in the Baltic. *Sea. Balt. Sea Environ. Proc.* **116B**.

Hernández JC, Russell MP (2010) Substratum cavities affect growth-plasticity, allometry, movement and feeding rates in the sea urchin *Strongylocentrotus purpuratus*. *Journal of Experimental Biology*, **213**, 520-525.

Hernroth B, Baden S, Thorndyke M, Dupont S (2011) Immune suppression of the echinoderm *Asterias rubens* (L.) following long-term ocean acidification. *Aquatic toxicology*, doi:10.1016/j.aquatox.2011.03.001.

IPCC (2007). Climate change 2007: the physical science basis. Contribution of Working Group I to the Fourth Assessment Report of the Intergovernmental Panel on Climate Change. Cambridge University Press, Cambridge.

Kleypas JA, Feely RA, Fabry VJ, Langdon C, Sabine CL, Robbins LL (2006) Impact of ocean acidification on coral reefs and other marine calcifiers: a guide for future research. Report of a workshop held 18-20 April 2005. FL, sponsored by NSF, NOAA, and the US Geological Survey, St Petersburg, 88 pp.

Kurihara H, Asai T, Kato S, Ishimatsu A (2008) Effects of elevated pCO₂ on early development in the mussel *Mytilus galloprovincialis*. *Aquatic Biology*, **4**, 225–233.

Lacoue-Labarthe T, Warnau M, Oberhänsli F, Teyssié J-L, Jeffree R, Bustamante P (2008) First experiments on the maternal transfer of metals in the cuttlefish *Sepia officinalis*. *Marine Pollution Bulletin*, **57**, 826–831.

Langenbuch M, Pörtner HO (2002) Changes in metabolic rate and N excretion in the marine invertebrate *Sipunculus nudus* under conditions of environmental hypercapnia: identifying effective acid–base variables. *Journal of Experimental Biology*, **205**, 1153–1160.

Lau DCC, Lau SCK, Qian P-Y, Qiu J-W (2009) Morphological plasticity and resource allocation in response to food limitation and hyposalinity in a Sea Urchin. *Journal of Shellfish Research*, **28**, 383–388.

Levitan DR (1989) Density-dependent size regulation in *Diadema antillarum*: Effects on fecundity and survivorship. *Ecology*, **70**, 1414–1424.

Levitan DR (1991) Skeletal changes in the test and jaws of the sea urchin *Diadema antillarum* in response to food limitation. *Marine Biology*, **111**, 431–435.

Marshall DJ, Bolton TF, Keough MJ (2003) Offspring size affects the post-metamorphic performance of a colonial marine invertebrate. *Ecology*, **84**, 3131–7.

Marshall DJ, Keough MJ (2003) Sources of variation in larval quality for free-spawning marine invertebrates: egg size and the local sperm environment. *Invertebrate Reproduction and Development*, **44**, 63–70.

Marshall DJ, Styan CA, Keough MJ (2002) Sperm environment affects offspring quality in broadcast spawning marine invertebrates. *Ecology Letters*, **5**, 173–6.

McCormick MI (1998) Behaviorally induced maternal stress in a fish influences progeny quality by a hormonal mechanism. *Ecology*, **79**, 1873–1883.

Mehrbach C, Culberson CH, Hawley JE, Pytkowicz RM (1973) Measurement of the apparent dissociation constants of carbonic acid in seawater at atmospheric pressure. *Limnology and Oceanography*, **18**, 897-907.

Melzner F, Gutowska MA, Langenbuch M, Dupont S, Lucassen M, Thorndyke MC, Bleich M, Pörtner H-O (2009) Physiological basis for high CO₂ tolerance in marine ectothermic animals: pre-adaptation through lifestyle and ontogeny? *Biogeosciences*, **6**, 1-19.

Micael J, Alves MJ, Costa AC, Jones MB (2009) Exploitation and conservation of echinoderms. *Oceanography and Marine Biology*, **47**, 191-208.

Miles H, Widdicombe S, Spicer JJ, Hall-Spencer J (2007) Effects of anthropogenic seawater acidification on acid-base balance in the sea urchin *Psammechinus miliaris*. *Marine Pollution Bulletin*, **54**, 89-96.

Moran AL, Emlet RB (2001) Offspring size and performance in variable environments: field studies on a marine snail. *Ecology*, **82**, 1597–1612.

Mousseau TA, Dingle H (1991) Maternal effects in insects: examples, constraints, and geographic variation. In: *The unity of evolutionary biology, Vol. II*, Dudley EC, (ed.), Dioscorides Press, Portland, pp. 745–61.

Norderhaug KM, Christie HC (2009) Sea urchin grazing and kelp re-vegetation in the NE Atlantic. *Marine Biology Research*, **5**, 515-528.

Norris DR (2005) Carry-over effects and habitat quality in migratory populations. *Oikos*, **109**, 178-186.

Orr JC, Fabry VJ, Aumont O *et al.* (2005) Anthropogenic ocean acidification over the twenty-first century and its impact on calcifying organisms. *Nature*, **437**, 681-686.

Pearse JS (2006) Ecological role of purple sea urchins. *Science*, **314**, 940-941.

Pechenik JA (2006) Larval experience and latent effects—metamorphosis is not a new beginning. *Integrative and Comparative Biology*, **46**, 323–333.

- Piersma T, Drent J (2003) Phenotypic flexibility and the evolution of organismal design. *Trends in Ecology and Evolution*, **18**, 228-233
- Podolsky RD, Moran, AL (2006) Integrating function across marine life cycles. *Integrative and Comparative Biology*, **46**, 577–586.
- Pörtner H.O, Farrell AP (2008) Physiology and climate change. *Science*, **322**, 690-692.
- Ries J, Cohen A, McCorkle D (2009) Marine calcifiers exhibit mixed responses to CO₂-induced ocean acidification. *Geology*, **37**, 1131–1134.
- Roach DA, Wulff RD (1987) Maternal effects in plants. *Annual Review of Ecology and Systematics*, **18**, 209-235.
- Robinson OW (1981) The influence of maternal effects on the efficiency of selection; a review. *Livestock Production Science*, **8**, 121-137
- Russell MP (1998) Resource allocation plasticity in sea urchins: rapid, diet induced, phenotypic changes in the green sea urchin, *Strongylocentrotus droebachiensis* (Müller). *Journal of Experimental Marine Biology and Ecology*, **220**, 1–14.
- Sabine CL, Feely RA, Gruber N *et al.* (2004) The oceanic sink for anthropogenic CO₂. *Science*, **305**, 367-371.
- Sarazin G, Michard G, Prevot F (1999) A rapid and accurate spectroscopic method for alkalinity measurements in sea water samples. *Water Research*, **33**, 290-294.
- Selden R, Johnson AS, Ellers O (2009) Waterborne cues from crabs induce thicker skeletons, smaller gonads and size-specific changes in growth rate in sea urchins. *Marine Biology*, **156**, 1057-1071.
- Shirayama Y, Thornton H (2005) Effect of increased atmospheric CO₂ on shallow water marine benthos. *Journal of Geophysical Research*, **110**, C09-S08.
- Sorensen MC, Hipfner JM, Kyser TK, Norris DR (2009) Carry-over effects in a Pacific seabird: stable isotope evidence that pre-breeding diet quality influences reproductive success. *Journal of Animal Ecology*, **78**, 460–467.

Thomsen J, Gutowska MA, Saphrster J *et al.* (2010) Calcifying invertebrates succeed in a naturally CO₂-rich coastal habitat but are threatened by high levels of future acidification. *Biogeosciences*, **7**, 3879–3891.

Widdicombe S, Dupont S, Thorndyke M (2010) Laboratory experiments and benthic mesocosm studies. In: Riebesell U, Fabry VJ, Hansson L, Gattuso JP (editors). Guide to best practices in ocean acidification research and data reporting, p.113-122.

Zdravkovic T, Genbaceva O, McMastera MT, Fisher SJ (2005) The adverse effects of maternal smoking on the human placenta: A review. *Placenta*, **26**, S81-S86.

Figure legends:

Figure 1: Life cycle of the sea urchin *Strongylocentrotus droebachiensis*. Benthic adults live on the substrate and release eggs and sperm in the water, in spring, where fertilization occurs. Pelagic embryo develops into feeding larvae (few weeks) that feed in the water column for a few more weeks before acquiring the ability to settle and metamorphose into a benthic exotrophic juvenile on the adequate substrate.

Figure 2: Experimental design summary. Grey urchins represent adults coming from 'Norway' and black ones adults from 'Denmark'. Parameters measured during the experiment are shown in italic. Durations of each phase within each experiment are described above the thick horizontal arrows (d: days, mo: months).

Figure 3: Fecundity (eggs.female⁻¹) of females collected in two populations (Hammerfest ("Norway") and Anholt ("Denmark")) and acclimated for either 4 or 16 months to control (8.1) or low (7.7) pH conditions.

Figure 4: Impact of pH during adult acclimation and larval development on settlement success (number of juvenile per culture 28 days post-fertilization).

Figure 5: Impact of pH during larval and juvenile development on juvenile survival 3 months after settlement.

Figure 6: Impact of pH during larval and juvenile development on juvenile growth over the first 3 months after settlement.

Figure 1

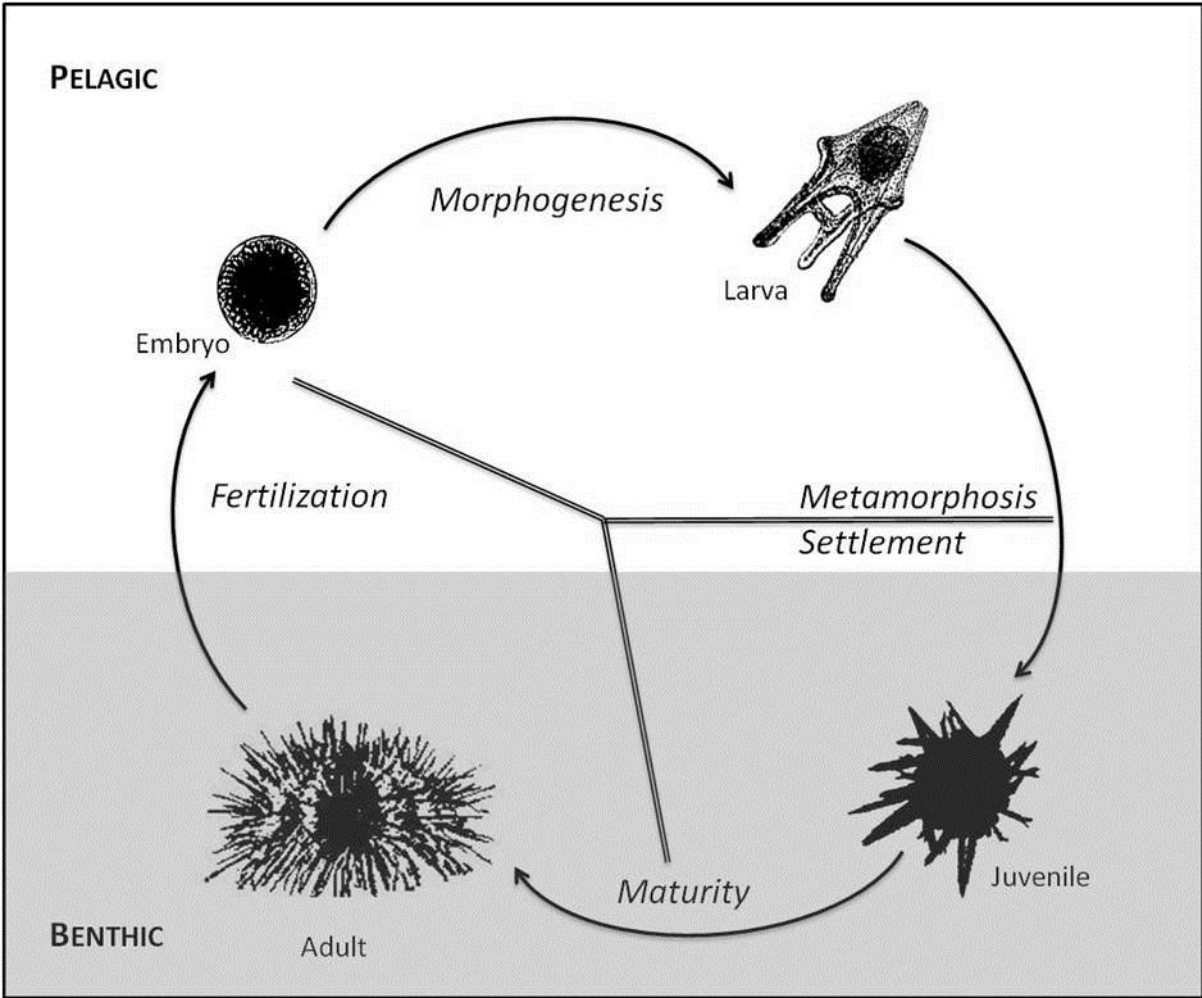


Figure 2

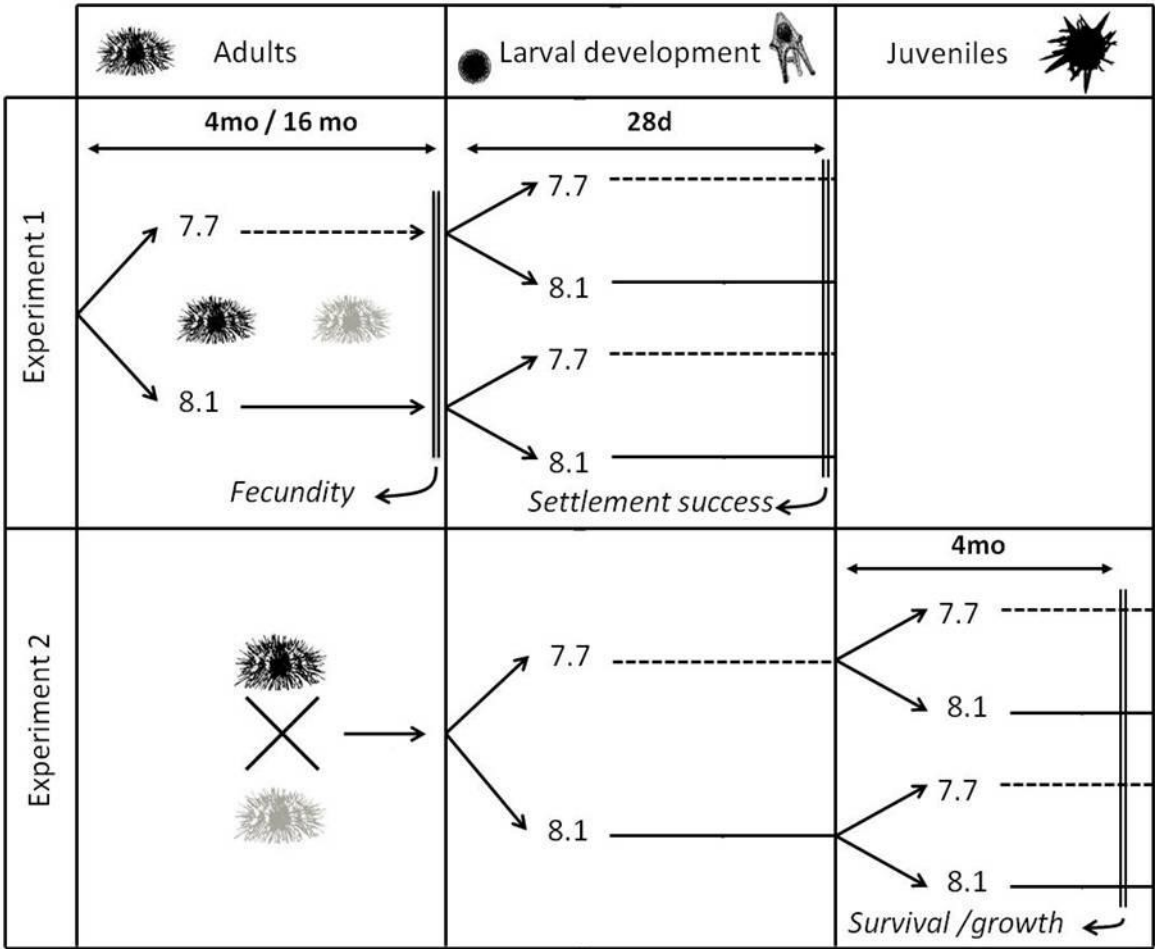


Figure 3:

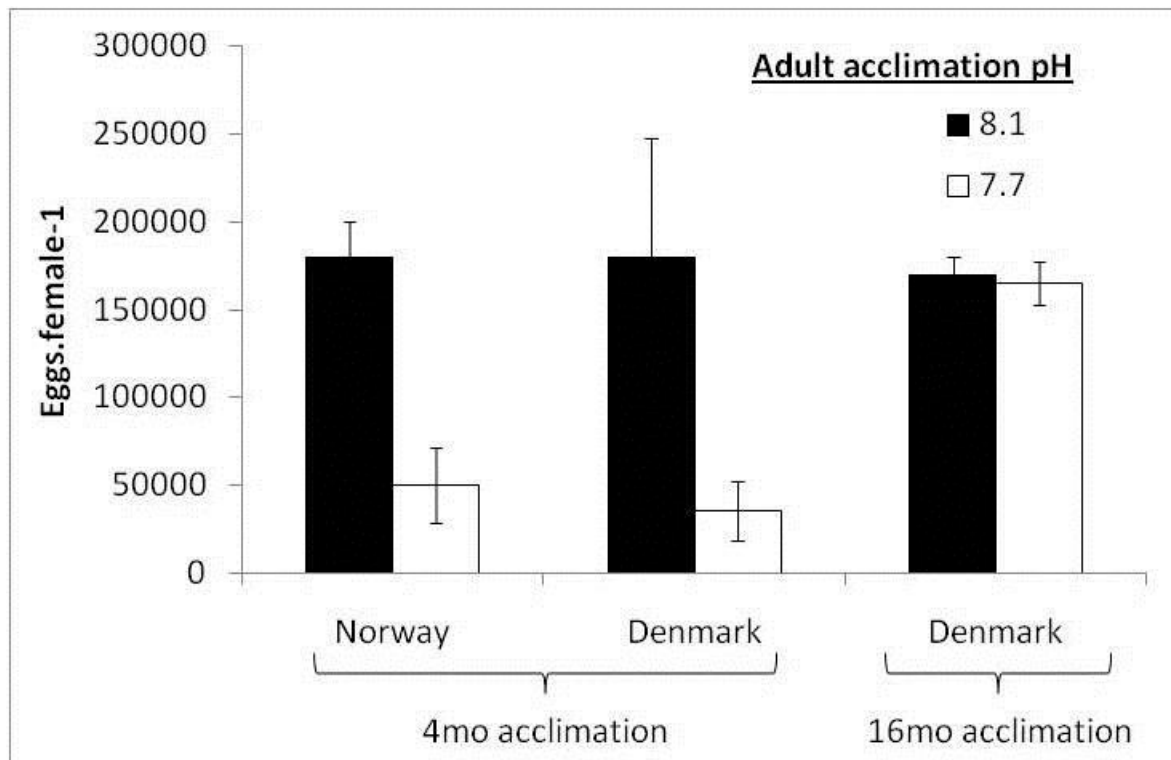


Figure 4:

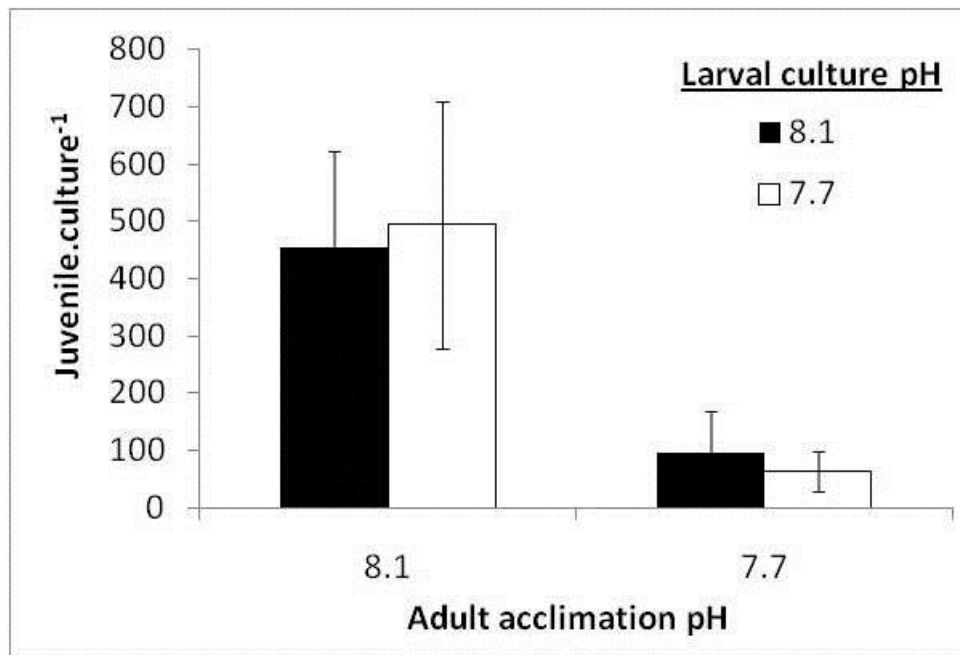


Figure 5:

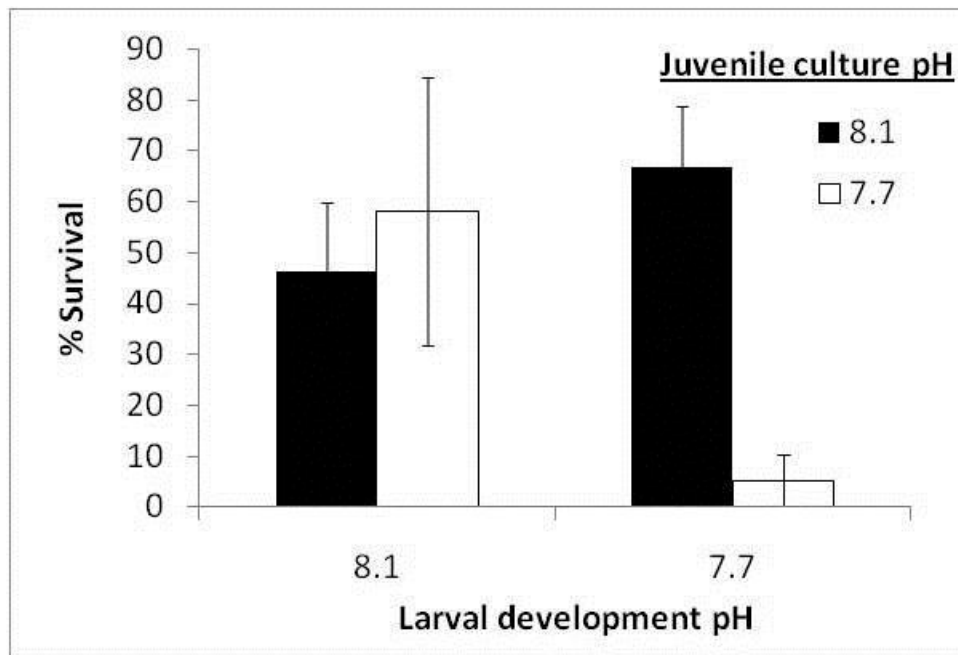
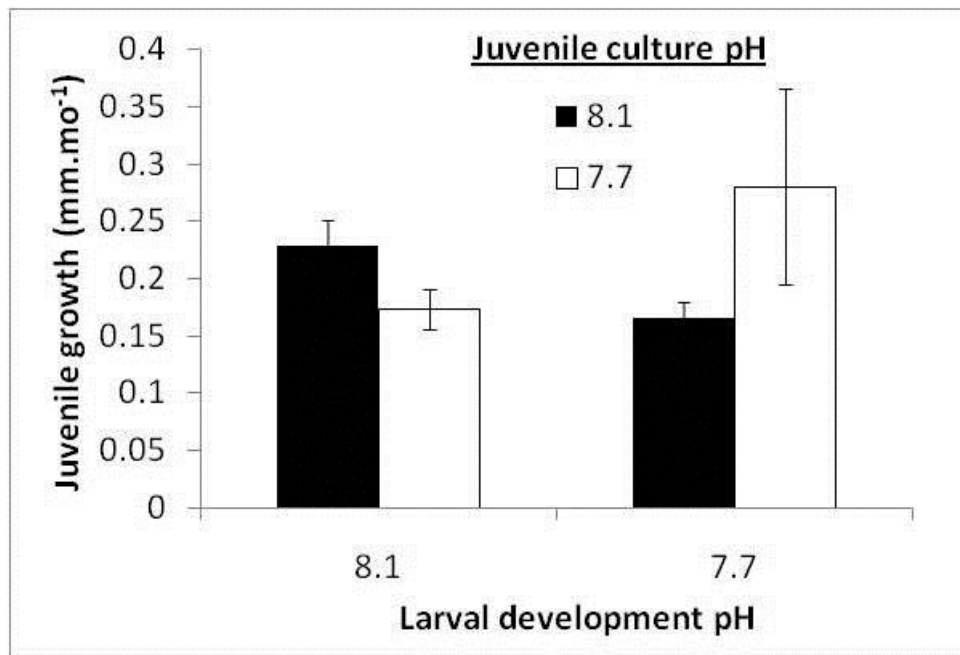


Figure 6



4 Discussion

In this study I have investigated the effects of simulated ocean acidification on physiology and energy budget allocation decisions in two sea urchin species, *S. droebachiensis* and *S. purpuratus*. Due to their calcified skeleton in both, larval and adult stages, echinoids were identified early on as one of the particularly sensitive taxa when exposed to increased seawater $p\text{CO}_2$ (Kurihara and Shirayama, 2004; Shirayama and Thornton, 2005). The main responses observed in adult, juvenile as well as larval sea urchins in response to elevated surface seawater $p\text{CO}_2$ expected to be reached by the year 2300 (appr. 100-200 Pa, 1000-2000 μatm , Caldeira & Wickett 2005) were reduced growth or slowed development (Shirayama and Thornton, 2005; Dupont et al., 2010c; Byrne et al., 2011; Yu et al., 2011). There are several hypotheses on the impact of elevated $p\text{CO}_2$ on the physiology of metazoans and related growth declines.

One idea is, that reduced growth rates in calcifying organisms are related to an impairment of calcification performance or dissolution of already existing calcified structures (Riebesell et al., 2000; Orr et al., 2006; Comeau et al., 2009; Comeau et al., 2010a; Lischka et al., 2011). These particular responses were demonstrated in a range of different molluscs species. For example, exposure of the marine snail *Nucella lamellosa* to elevated $p\text{CO}_2$ for 8 days led to a linear decrease of shell gain per day with increasing $p\text{CO}_2$ (Nienhus et al., 2010). Similarly, acute exposure (2h) of the bivalves *Mytilus edulis* and *Crassostrea gigas* to hypercapnia caused a linear reduction of calcification rates with

increasing $p\text{CO}_2$ (Gazeau et al., 2007). In the polar pteropod *Limacina helicina*, strong increases in shell degradation and external shell dissolution in response to elevated $p\text{CO}_2$ could be observed. Acidification induced reductions in net shell growth was apparently accompanied with the animals' effort to "repair" sites of increased external shell dissolution (Lischka et al., 2011). Findings from naturally CO_2 enriched tropical and subtropical habitats indicate progressive displacement of calcifying marine invertebrates at pH values of 7.7-7.8 in favor of non-calcifying photoautotrophic communities (Hall-Spencer et al., 2008; Fabricius et al., 2011).

This is thus leading to the next hypothesis on CO_2 induced acidification responses: Increases in calcification and/or ion regulatory costs are leading to elevated energy demands. Increased metabolic rates measured in *Limacina helicina* in response to hypercapnia (Comeau et al., 2010b) could be related to the increased costs of repair mechanisms due to external shell dissolution additionally to the elevated costs of calcification itself. Consequently, less energy is available for somatic growth. Such conclusions have been reached for long-term acclimated bivalves *Mytilus edulis* where increased metabolism and higher ammonium excretion rates were measured following 8-week exposure to hypercapnic conditions (Thomsen and Melzner, 2010).

Similar to the responses in mussels, echinoderms have been observed to exhibit reduced growth (Shirayama and Thornton, 2005) and calcification rates (Ries et al., 2009) in response to seawater acidification. Embryonic responses of echinoderms to hypercapnia appear to be more diverse, ranging from high mortalities in the ophiuroid *Ophiotrix fragilis* (Dupont et al., 2008) over developmental retardation in echinoid larvae (Brennand et al., 2010; Dupont et al., 2010c; Martin et al., 2011) to enhanced developmental speed in the lecithotroph asteroid *Crossaster papposus* larvae (Dupont et al., 2010b). Interestingly, so far echinoid (sea urchin) larvae seem to be uniform in their response of decreased developmental rates without increased mortalities (Clark et al., 2009; Todgham and Hofmann, 2009; O'Donnell et al., 2010) or deformations during early development exposed to $p\text{CO}_2$ s expected to occur during the next decades to centuries (up to 100-200 Pa). Nevertheless, detrimental effects on sea urchin larval development cannot be excluded, yet, since all present studies followed sea urchin larval development for only a few days. So far, only one study observed the impacts of seawater acidification on newly metamorphosed juveniles of the lecithotrophic sea urchin *Heliocidaris*

erythrogramma. In this study, a reduced calcification performance, evaluated as the number of adult spines developed at 5 days post-settlement, could be observed (Byrne et al., 2011). However, these authors did not report if settlement success was affected by elevated seawater $p\text{CO}_2$ in *H. erythrogramma*, nor did they monitor, whether the juveniles exposed to the high $p\text{CO}_2$ treatment reached the same calcified state as control larvae at a later time point (Byrne et al., 2011). Despite the great body of literature presently available examining the effect of seawater acidification on somatic growth and development in sea urchin larvae and adults, the underlying mechanisms responsible for the observed reductions in sea urchin development or growth are still unknown.

Extensive cDNA microarray studies observing changes in transcript abundance of several hundreds of genes in 40 to 142 hours post-fertilization *Lytechinus pictus* and *S. purpuratus* larvae suggest that those coding for calcification and metabolic pathways are down regulated - with the exception of 2 genes for ion- and acid-base homeostasis that were up regulated in *L. pictus* larvae (Todgham and Hofmann, 2009; O'Donnell et al., 2010). In contrast to these studies, transcript abundance of Na^+/K^+ -ATPase and several biomineralization genes were up regulated in a compensatory fashion in *Paracentrotus lividus* larvae raised at an increasing range of different $p\text{CO}_2$ levels up to 350 Pa (Martin et al., 2011). A drop in gene transcript levels was only observed at the highest $p\text{CO}_2$ condition of 660 Pa. Calcification rates at all $p\text{CO}_2$ levels appeared to be normal when corrected for the CO_2 induced developmental delay (Martin et al., 2011). Consequently, this and other recent studies suggest that growth reductions are not only due to impaired calcification rates and increased dissolution pressure, but are possibly related to a shift in energy partitioning, withdrawing energy from growth and development in order to fuel more essential processes such as acid-base regulation and calcification (Findlay et al., 2009; Thomsen and Melzner, 2010). As mentioned before, decreases of growth rate in bivalves and pteropods were observed to be accompanied by increases in routine metabolic rates when exposed to elevated seawater $p\text{CO}_2$ indicating a higher cost for maintenance processes (Beniash et al., 2010; Comeau et al., 2010b; Lanning et al., 2010; Thomsen and Melzner, 2010; Cummings et al., 2011). No such measurements were conducted with echinoid adults or larvae in response to environmental hypercapnia so far.

Energy budgets for sea urchin larvae and adults in response to CO_2 induced seawater acidification were constructed in the present thesis in order to observe if change

in energy partitioning occurs and to examine the mechanisms underlying the observed sensitivity of echinoids towards environmental hypercapnia (publication 1 and 3). The results were set in context with observed CO₂ driven “carry-over” effects (publication 4) between echinoid life cycle stages. In order to determine if ion regulatory or calcification processes could be the sink for increased energy demands, extracellular pH homeostasis was studied in larval and adult sea urchins (publication 2, 3, and unpublished results discussed in part 4.2.2).

4.1 CO₂ induced changes in growth and energy budgets

Growth and development was significantly decreased in *S. purpuratus* larvae and *S. droebachiensis* adults in response to elevated *p*CO₂ (publication 1 and 3). This is in accordance with previous studies observing negative *p*CO₂ induced effects on echinoid larval, juvenile and adult growth rates (Shirayama and Thornton, 2005; Brennan et al., 2010; Dupont et al., 2010c; Martin et al., 2011).

4.1.1 Growth and energy budgets of larval sea urchins

Larval growth in echinoderms is extremely plastic and depends to a high degree on environmental conditions. Planktotrophic echinoderm larvae feed by creating currents with ciliary bands running along their body and appendages (larval arms) and capture food particles in their mouth (Strathmann, 1971). The larval arms function primarily as feeding structure. Pluteus larvae alter their arm length in response to the feeding conditions they encounter. The more abundant the food in the environment is, the shorter the larval appendages are grown (George, 1999; Miner, 2005; Podolsky and McAlister, 2005) and the less energy is used for growing the feeding structures. The morphometric analysis of *S. purpuratus* larval shape (e.g. arm length relative to body length) over 20 days post-fertilization revealed that CO₂ exposed larvae are not just smaller but are characterized by the same morphological proportions as control larvae at earlier points in development (publication 1, figure 3 and 4). A CO₂ - induced developmental delay of two days could be observed at 8 days post-fertilization. This developmental delay increased with developmental time, e.g. a delay of 6 days was observed at 20 days post-fertilization.

Since growth and feeding are intrinsically linked in pluteus larvae (Strathmann, 1971), larval particle ingestion was decreased in response to elevated $p\text{CO}_2$ when comparing larvae of the same age (time post-fertilization). When larvae of the same body dimensions i.e. with similar arm and thus, ciliary band, lengths were compared, the remaining decrease of particle ingestion (by 40%) under elevated $p\text{CO}_2$ appeared to be statistically insignificant (publication 1, table 3 and figure 6). Thus, given that the digestive efficiency was not influenced by environmental hypercapnia, larval feeding provided the almost the same amount of energy at comparable larval dimensions.

An increase in energetic demands for maintenance processes could be detected when comparing routine metabolic rates in feeding *S. purpuratus* larvae. In hypercapnic larvae, the slope of respiration rate increase after commencement of feeding was 2.1 times higher than the routine metabolic rate increase in control larvae (publication 1, figure 7). This indicates that the costs for maintenance processes are increased in response to seawater acidification. Elevated metabolic rates in response to hypercapnia were recently also demonstrated for other marine invertebrates (Wood et al., 2008; Beniash et al., 2010; Comeau et al., 2010b; Lanning et al., 2010; Thomsen and Melzner, 2010; Wood et al., 2010; Cummings et al., 2011; Wood et al., 2011). The twofold increase in routine metabolic rates in response to elevated $p\text{CO}_2$ eventually decreased scope for growth (SfG) – the fraction of total energy assimilation available for growth and development – by up to 50% (figure 4.1, publication 1, figure 8B). However, the observed growth reductions of approximately 10% are in contrast to the observed decreases in scope for growth by 50% due to elevated metabolic rates in 320 to 420 μm long larvae. On the one hand, this discrepancy is partially due to three - dimensional growth of the larvae and the one - dimensional measurement scale used to assess growth (body length). On the other hand, echinoid larvae are able to take up dissolved organic matter from surrounding seawater (Manahan and Crisp, 1982; Shilling and Manahan, 1990; Hoegh-Guldberg, 1994; Shilling and Bosch, 1994; Shilling and Manahan, 1994), but it was not measured to what extent DOM fostered larval nutrition in the current experiments. Thus, other parameters potentially altering the larval energy budget (e.g. DOM uptake and NH_4^+ excretion, figure 4.1) still need to be determined to fully understand the larval energy balance. However, acidification induced changes in the energy budget neither increased mortality, nor the number of deformed or asymmetric larvae (publication 1, figure 2B and S1), which stands

in contrast to the ophiuroid *Ophiotrix fragilis* exhibiting a high degree of body deformations and 100% mortality after 8 days post-fertilization when exposed to elevated $p\text{CO}_2$ (130 Pa, Dupont et al., 2008). Although echinoid larval development doesn't seem to be corrupted by CO_2 induced seawater acidification, the observed developmental delay may still have negative impacts on recruitment success. Decreased growth could potentially result in a higher mortality due to predatory pressure in the pelagic environment (Hare and Cowen, 1997; Allen, 2008; Dupont et al., 2010a). Furthermore, the developmental delay may induce a shift in metamorphosis timing and could result in later settlement. A change in settlement conditions (e.g. change in food availability, predator density or seasonal abiotic conditions) will thus likely alter recruitment of sea urchin populations and community structure (Miner, 2005; Elkin and Marshall, 2007).

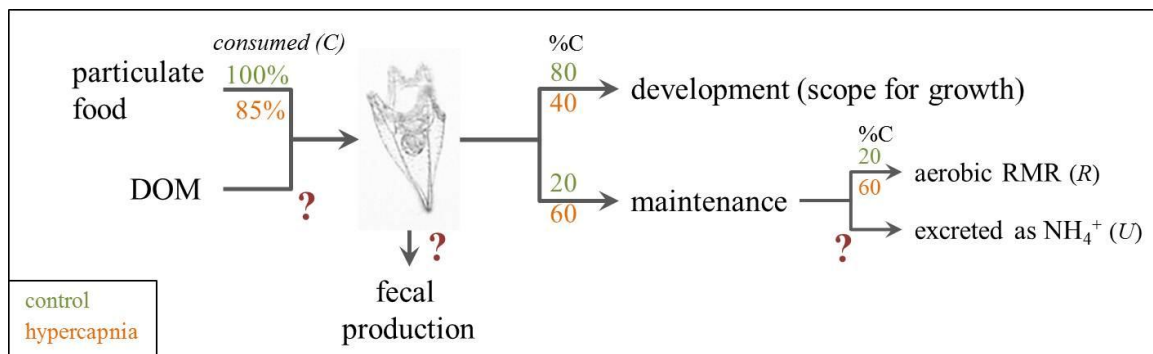


Figure 4.1: Schematic representation of the energy budget for *Strongylocentrotus purpuratus* echinopluteus larvae (360 μm body length). Control values are presented in green (38 Pa CO_2), the hypercapnic treatment is presented in orange (128 Pa CO_2). Values are calculated by converting feeding rates and routine metabolic rates (RMR) into energy equivalents ($\mu\text{J ind}^{-1} \text{h}^{-1}$, see section 2.5.4/a for details). Feeding rate did not differ statistically between treatments, but appeared to be reduced by 15% under hypercapnic conditions. Feeding rates are relative to control feeding rates. Scope for growth and routine metabolic rates are expressed as per cent of consumed energy (i.e. SfG: 40% of 85% and maintenance: 60% of 85% for elevated $p\text{CO}_2$). Unknown variables (i.e. uptake of dissolved organic matter (DOM) and excretion rates) are indicated by a red question mark.

Furthermore a shift in the larval energy budget may also influence post-larval or juvenile fitness. During the larval planktotrophic phase (30 days) of *Heliocidaris erythrogramma*, approximately 50% of the energy provided by aerobic metabolism is channeled towards maintenance and growth of the larval feeding apparatus, while the other 50% of energy is channeled into the development of the future juvenile (Hoegh-Guldberg and Emlet, 1997). Given that the animals need to provide more energy to development and maintenance of larval feeding structures, then less energy is available for the development of the rudiment. Although a delay of larval development was

observed in *S. purpuratus*, settlement success and timing was independent from larval culture $p\text{CO}_2$ in *S. droebachiensis* larvae (publication 4, figure 4). In both treatments (44 Pa and 119 Pa CO_2) the same number of larvae had undergone metamorphosis after 28 days post-fertilization (publication 4, figure 4). Nevertheless, juvenile mortality was extremely high (95% compared to 48% under control conditions) when both larvae and juveniles were exposed to elevated $p\text{CO}_2$ (publication 4, figure 5). This suggests that energetic disadvantages at the planktotrophic larval stage translate directly into juvenile performance. Several studies reported so called latent effects – “effects that have their origins in early development but that are first exhibited in juveniles or adults” (Pechenik, 2006) – for a range of meroplanktonic organisms (reviewed by Pechenik, 2006). The observation of reduced juvenile fitness of marine meroplanktonic invertebrates in response to (i) delayed metamorphosis (sea urchin *Paracentrotus lividus*, *Dendraster excentricus* and *Echinarachnius parma*, Highsmith and Emlet, 1986; Vaitilingon et al., 2001), (ii) food limitation during larval development (sea urchins *P. lividus*, *Strongylocentrotus franciscanus* and *S. purpuratus*, Miller and Emlet, 1999; Vaitilingon et al., 2001) and (iii) increased larval swimming activity (ascidian *Diplosoma listerianum*, Marshall et al., 2003) suggest that latent effects are connected to changes in the larval energy budget (Pechenik, 2006). Furthermore, it could be observed that planktotrophic larvae of the sea urchin *Tripneustes gratilla* accumulate lipids in stomach cells during larval development, which are later incorporated into the juvenile during metamorphosis (Byrne et al., 2008). These energy reserves are essential during the first two weeks after metamorphosis until the mouth and after open and the digestive system is fully developed (Miller and Emlet, 1999; Vaitilingon et al., 2001). Thus, even if echinoid larvae appear to be relatively robust to moderate levels of CO_2 induced seawater acidification, environmental hypercapnia potentially causes latent effects and thus negatively impacts recruitment success in the sea urchins *S. droebachiensis* and *H. erythrogramma* (publication 4, Byrne et al., 2011).

4.1.2 Growth and energy budgets of adult sea urchins

Growth of adult sea urchins was similarly impacted by elevated $p\text{CO}_2$. Although growth rates were decreased in response to hypercapnia, sea urchins exposed to 102 Pa CO_2 still exhibited a net increase of test diameter over the experimental time

(publication 3, table 3). The greatest difference between $p\text{CO}_2$ treatments was observed in gonad weight gain. During the incubation period of 6 weeks, gonads of control animals increased significantly more in mass than gonads of sea urchins exposed to 102 or 284 Pa CO_2 . Dry mass increase of other body parts (i.e. gut and test) as well as increase of total dry mass differed significantly between control and high $p\text{CO}_2$ treatments, but not between control and intermediate $p\text{CO}_2$ treatments (publication 3, table 3). Reduced growth rates in response to environmental hypercapnia is in accordance with findings by Shirayama & Thornton (2005) who observed reduced wet mass gain in juveniles and young adults of *Hemicentrotus pulcherrimus* and *Echinometra mathaei* exposed for 26 weeks to 57 Pa CO_2 .

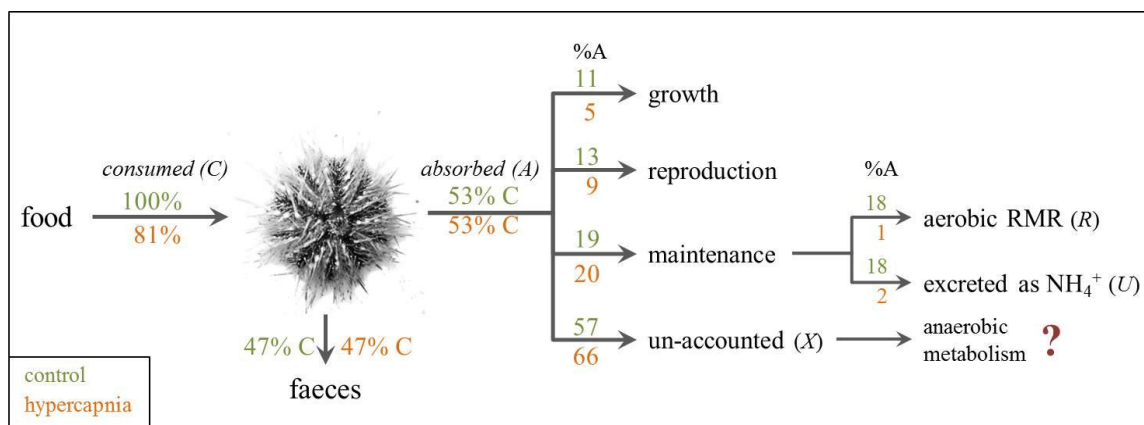


Figure 4.2: Schematic representation of the energy budget for adult *Strongylocentrotus droebachiensis*. Control values are presented in green (47 Pa CO_2), hypercapnic treatment is presented in orange (284 Pa CO_2). Values are calculated by converting feeding rates, aerobic routine metabolic rates (RMR) and growth rates into energy equivalents ($\text{J d}^{-1} \text{g}^{-1}$ animal dry mass, see section 2.5.4/b for details). Reproduction stands for gonad growth, growth stands for gut and test growth. Feeding rate values are relative to the control feeding rates. Thus, hypercapnia treated animals fed 19% less than control animals. Other values are expressed as either % of consumed energy (% C) or as % of absorbed energy (% A). Processes with unknown contribution are indicated by a red question mark.

In contrast to the larval energy budget that was altered by increased metabolic rates, adult sea urchins exhibited reduced feeding rates in response to elevated $p\text{CO}_2$ (figure 4.2; publication 3, figure 3; Siikavuopio et al., 2007b), which also translated into a decreased scope for growth (publication 3, table 4). Aerobic metabolic rates decreased slightly, but not significantly, in response to elevated $p\text{CO}_2$ (publication 3, figure 4). The energy balance calculated from absorbed energy and the energy channeled into different processes like growth, reproduction and maintenance revealed that 57% to 66% of the absorbed energy could not be linked to any of the above mentioned processes (figure 4.2). This corresponds to previous energy budget calculations conducted for *S. droebachiensis*

and *Psammechinus miliaris* (Miller and Mann, 1973; Otero-Villanueva et al., 2004). Similar to these and other studies (Moore and McPherson, 1965; Miller and Mann, 1973; Hollertz, 2002; Otero-Villanueva et al., 2004), a simple calculation of scope for growth based on feeding rates, aerobic metabolic rates and NH_4^+ -excretion rates overestimated the amount of energy supplied for growth. Hence, there are two possible explanations for the incidence of unaccounted energy. First, the production of dissolved organic matter (DOM) was not measured in this study and was demonstrated to significantly reduce the gap in the energy budget calculation for the gastropod mollusc *Aplysia punctata* and *S. droebachiensis* adults (Carefoot, 1967; Miller and Mann, 1973). Secondly, anaerobic metabolism by sea urchin tissues itself or through associated digestive system microorganisms were equally not taken into account. Microorganisms populating the digestive tract contribute significantly to digestive efficiency in echinoids (Guerinot and Patriquin, 1981; Sawabe et al., 1995; Thorsen, 1999), and thus possibly to anaerobic metabolism. Furthermore, anaerobiosis was measured to account for 77% of gonad and 21% of gut metabolic rates (Bookbinder and Shick, 1986). Due to the fact that anaerobic pathways are 5 to 16 times more inefficient than aerobic metabolism (depending on the species of end-product formed), the remaining energy could potentially be used to fuel anaerobiosis by gonads and gut (see publication 3 for details on calculation). The slight increase in acetate, fumarate and succinate/lactate levels in coelomic fluid of *S. droebachiensis* and *Echinus esculentus* in response to hypercapnia and emersion, respectively (Spicer, 1995; Spicer et al., 2011), as well as the increases in enzymatic activities of anaerobic pathways (malate and lactate dehydrogenase) in muscle tissue of the teleost fish *Sparus aurata* in response to hypercapnia (Michaelidis et al., 2007) supports the hypothesis of a general CO_2 induced up regulation of anaerobic metabolism. Nevertheless, the interesting question, whether the large fraction of unaccounted energy and its increase in response to hypercapnia is related to anaerobic metabolic rate could not be answered by this study.

In accordance with the observed CO_2 induced reductions in gonad growth over 6 weeks of acclimation, an incubation of 4 months to a $p\text{CO}_2$ of 119 Pa resulted in a decreased fertility of *S. droebachiensis* (measured as number of eggs per female, publication 4, figure 3). In contrast to these findings, a 16 - months acclimation period diminished the differences between treatments. Sea urchins are well known to exhibit a

high degree of morphological plasticity towards a great range of stressors like predatory pressure (Selden et al., 2009), food availability (Levitan, 1991), habitat structure (Hernandez and Russell, 2010) and salinity (Lau et al., 2009) and were observed to require up to 20 weeks to fully exhibit the new morphological and physiological state (Hernandez and Russell, 2010). Hence, exposure periods between 6 weeks and 4 months seem not to be a long enough time for *S. droebachiensis* to fully acclimate to new environmental conditions and to replenish energy stores for successful reproduction. Nevertheless, adult acclimation to elevated $p\text{CO}_2$ induced a strong negative maternal effect on larval settlement success. Settlement success of larvae from adults exposed to elevated $p\text{CO}_2$ was reduced by 80% (publication 4, figure 4).

This study revealed so far that a change in energy allocation (larvae) or a decrease in energy uptake at certain life cycle stages can cause negative effects on the subsequent developmental stage. The high susceptibility of post-larvae and juveniles towards CO_2 induced seawater acidification is indicating a clear bottleneck at post-settlement in *S. droebachiensis*.

4.2 Energy partitioning

4.2.1 Calcification, ion regulation and metabolism: changes in larval gene transcript levels

The examination of energy budgets of *S. purpuratus* larvae in response to elevated $p\text{CO}_2$ revealed that elevated metabolic rates decreased the amount of energy available for growth. Thus, it remained to be established which physiological processes are favored for a sacrifice in developmental speed. In order to develop hypotheses, transcript levels of several genes relevant for ion regulation, calcification and metabolism were measured and larval gene expression patterns were compared via a principle component analysis with respect to developmental time (2, 4 and 7 dpf old larvae) and $p\text{CO}_2$ (40 Pa vs. 134 Pa) in the sea urchin *S. purpuratus* (publication 2).

Generally, an analysis of similarity (ANOSIM) revealed that developmental time had a far greater impact on gene expression patterns than elevation of $p\text{CO}_2$. However,

the impact of $p\text{CO}_2$ was still greater than would be expected by chance (publication 2, table 4). The greatest difference between gene expression patterns with respect to acidification treatment was observed at culture day 4 and coincided with the time point of greatest larval size difference of 10% (publication 2, figure 2 and 3). This led to the assumption that the observed differences in gene expression patterns could be related to comparing larvae of different size classes and developmental stages. In order to distinguish between such developmental artifacts and true $p\text{CO}_2$ impacts, transcript levels were plotted against larval body length (publication 2, figure 4 and supp. mat.), which had been confirmed to be a suitable reference scale for *S. purpuratus* pluteus larvae up to 20 days post-fertilization (publication 1, discussion 4.1.1). Greatest impacts on gene expressions on larvae at culture day 4 are summarized in figure 4.3.

Since CO_2 induced seawater acidification is directly changing the seawater carbonate chemistry, calcification related processes have been suggested as the most sensitive processes in response to hypercapnia (Fabry, 2008). Many previous studies have therefore focussed on the impacts of elevated $p\text{CO}_2$ on calcification performance of several marine invertebrates finding a great variety of responses (Langdon and Atkinson, 2005; Wood et al., 2008; Ries et al., 2009; Gutowska et al., 2010b; Thomsen et al., 2010). Calcification in sea urchin larvae is a relatively well studied process (Wilt et al., 2008). The high-magnesium calcite spicules of sea urchin larvae are formed via the production of a transient amorphous calcium carbonate (ACC) phase (Beniash et al., 1997; Beniash et al., 1999; Raz et al., 2003; Politi et al., 2004; Politi et al., 2008) that is precipitated within vesicles in primary mesenchyme cells (PMCs) and stabilized by matrix proteins and Mg^{2+} ions. Vesicles are then transported through the PMC syncytium to the site of calcification, where CaCO_3 is thought to be exocytosed and incorporated into the growing spicule (Wilt et al., 2008). Calcium derived from the surrounding sea water (Nakano et al., 1963) is accumulated in PMCs. Using Ca^{2+} channel and secretory pathway inhibitors, Hwang and Lennarz (1993) demonstrated that both play a role in the provision of Ca^{2+} for spicule formation. As inorganic carbon source for calcification, sea urchin embryos use both, metabolically derived CO_2 and bicarbonate (HCO_3^-) from the surrounding sea water (Sikes et al., 1981). Despite the surrounding PMC syncytium, the spicules appear to be in direct contact with the extracellular matrix and the embedded fluid within the primary body cavity via small openings in the plasmatic sheaths (Decker et al., 1987). Thus, the

calcification process itself and calcified structures of sea urchin larvae may be vulnerable to increases in extracellular $p\text{CO}_2$ driven by environmental hypercapnia. Compensatory efforts, either by increased calcification or by up regulation of ion regulatory activity necessary for the establishment of microenvironments and supply of ions (e.g. Ca^{2+} , HCO_3^-) to the calcification site, could then lead to increased aerobic metabolic rates.

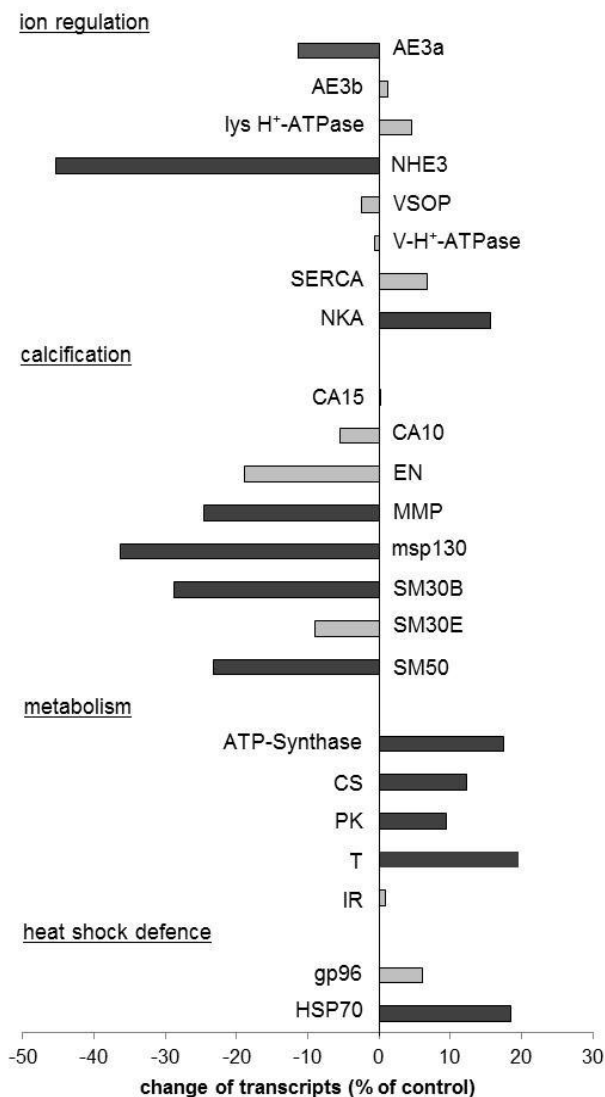


Figure 4.3: Overview of change in transcript abundance (relative to NBC3, RT-qPCR) of selected genes relevant for ion regulation, calcification, metabolism and heat shock defence in 4 dpf old *Strongylocentrotus purpuratus* pluteus larvae. Larvae were exposed to 134 Pa CO_2 . Values are given in % transcripts of larvae raised under control conditions (40 Pa CO_2). Larval size independent differences in transcript levels are indicated in black (see publication 2 for details). Differences that are not significant or potential developmental artifacts are depicted in grey. Abbreviations: AE3: anion exchanger 3, lys H⁺-ATPase: lysosomal H⁺-ATPase, NHE3: Na⁺/H⁺ exchanger 3, VSOP: voltage gated proton channel, V-H⁺-ATPase: V-type H⁺-ATPase, SERCA: sarco-endoplasmatic reticulum Ca²⁺-ATPase, NKA: Na⁺/K⁺-ATPase, CA15: carbonic anhydrase 15, CA10 carbonic anhydrase 10, EN: echinonectin, MMP: metalloproteinase, msp130: mesenchyme specific cell surface protein 130 kDa, SM30B: spicule matrix protein 30B, SM30E: spicule matrix protein 30E, SM50: spicule matrix protein 50, CS: citrate synthase, PK: pyruvate kinase, T: thiolase, IR: insulin receptor, gp96: heat shock protein gp96, HSP70: heat shock protein 70 kDa. For more details on gene sequences, primers and methods see publication 2 and section 2.6.1.

Calcification related genes such as msp130, SM30B and SM50 were down regulated in *S. purpuratus* larvae exposed to environmental hypercapnia (figure 4.3). This is in accordance with a microarray study of Todgham and Hofmann (2009), who observed a down regulation of a great range of calcification related genes in CO_2 exposed *S.*

purpuratus larvae (40h post-fertilization, 101 Pa CO₂). A CO₂ induced down regulation of calcification related genes could possibly influence either calcification rate or the integrity of the mineral and matrix composition of the larval skeleton. Larval exposure of four sea urchin species to 130 Pa CO₂ resulted a lowered percentage of inorganic material per dry mass in all observed species (*Pseudechinus huttoni*, *Evechinus chloricus*, *Tripneustes gratilla* and *Sterechinus neumayeri*) and in eroded surface structures of the larval skeleton in both temperate species *P. huttoni* and *E. chloricus* (Clark et al., 2009). However, the decreased inorganic mass to dry mass ratio could potentially be related to a decreased developmental speed, because only one time point was considered for the analysis. In contrast to these studies, calcification related genes (msp130 and SM30) were up regulated in a compensatory fashion in *Paracentrotus lividus* (Martin et al., 2011) in response to increasing *p*CO₂ levels (up to 200 Pa for msp130 and 365 Pa for SM30). A drop in transcript levels could only be observed in the higher *p*CO₂ treatments (365/669 Pa for msp130 and 669 Pa for SM30). Furthermore, calcification rates in *P. lividus* appeared to be normal, when normalized to developmental speed (Martin et al., 2011).

Closely linked to the calcification processes are ion regulatory processes, which are important for creating microenvironments and the supply of ions to the calcification site. Most studied ion regulatory genes were not differentially regulated in response to environmental hypercapnia (figure 4.3). Down regulation of the anion exchanger 3 (AE3a) and the Na⁺/H⁺-exchanger 3 (NHE3) are in accordance with the down regulation of Na⁺-dependent transporters found by Todgham and Hofmann (2009). Although AE3 and NHE3 were found to be down regulated, indicating a decrease in ion regulatory capacity, this study cannot exclude that possibly other more energy efficient transporters are up regulated in response to elevated *p*CO₂. In contrast to the data of Todgham and Hofmann (2009), who also found down regulation of Na⁺/K⁺-ATPase (NKA), is the up regulation of NKA found in this study and the recent study by Martin and colleagues (2011). Larval NKA is not only the driving force for secondary active transporters needed for pH and ion homeostasis, but is also establishing the electrochemical gradient for DOM uptake from the surrounding seawater (Leong and Manahan, 1999)), an important support of nutrient acquisition in echinoderm larvae (Manahan and Crisp, 1982; Manahan, 1990; Hoegh-Guldberg, 1994). Larval NKA activity required for maintaining ion balance is using 40% of aerobic metabolism under normal conditions in *S.*

purpuratus, but can be rapidly increased at times with elevated needs for nutrient uptake (Leong and Manahan, 1997) or potential increased needs for cellular ion regulation due to environmental acidification. Addition of the amino acid alanine to the culture medium led to a rapid increase of NKA activity to 94% of metabolic rate, likely due to activation of inactive reserve NKA (Leong and Manahan, 1997). Increases in transcript levels of genes related to metabolism (e.g. ATP-synthase, citrate synthase, pyruvate kinase and thiolase, figure 4.3) are in accordance with up regulation of NKA transcripts and confirm the results of elevated larval aerobic metabolic rates under acidification stress (publication 1).

4.2.2 Extracellular pH homeostasis in *S. droebachiensis* larvae

Echinoderm larvae are characterized by an extensive cell free gelatinous material occupying the primary body cavity and surrounding the calcifying primary mesenchyme cells (PMCs) in echinopluteus larvae (Strathmann, 1989). The gel like compounds of the primary body cavity are extremely flexible and the larval body is able to rebound to its original shape following muscle contraction (e.g. during swallowing of food particles). Thus, it is a highly energy saving system for larval movement, allowing for large larvae with relatively little cellular material, a situation not unlike that in many scyphomedusae (Strathmann, 1989; Crawford, 1990). The larval spicules combined with the gelatinous material support the larval form (Strathmann, 1989; Crawford, 1990) and orientation of the larvae in the water column (Pennington and Strathmann, 1990).

Microelectrode and micro-fluorescence measurements of extracellular pH (pH_e) within the primary body cavity of *S. droebachiensis* pluteus larvae revealed that the fluid of the primary body cavity is pH conform to the surrounding seawater (figure 4.4). Given that the fluid composition of the primary body cavity is similar to seawater this would indicate that extracellular $p\text{CO}_2$ is similar to that of seawater $p\text{CO}_2$. This result is surprising, since it would imply that sea urchin larvae do not have an outward directed CO_2 diffusion gradient due to metabolic CO_2 production. Usually, extracellular $p\text{CO}_2$ of adult, heterotrophic metazoans is at least 100 Pa higher than the seawater $p\text{CO}_2$ in order to establish a CO_2 diffusion gradient away from the organism (Melzner et al., 2009). The observed high pH_e within the body cavity could have several reasons: (i) the extracellular matrix of the primary body cavity could have a high non-bicarbonate buffer capacity to enable higher extracellular $p\text{CO}_2$ than seawater, (ii) the outer epithelial cells as well as the

inner endodermal cells could be capable of an outward directed secretion mechanisms to channel metabolically derived CO_2 or H^+ either directly to the seawater (ectodermal epithelium) or into the gastric tract (endodermal epithelium) or (iii) active accumulation of $[\text{HCO}_3^-]_e$ in the extracellular space could stabilize pH_e at elevated extracellular $p\text{CO}_2$. In these cases, primary mesenchyme cells would strongly benefit from such mechanisms in terms of facilitated calcification processes due to increased calcite saturation states at the site of calcification. Another possibility is that the ectodermal epithelium and the gel filled body cavity are extremely leaky for ions and small molecules to allow rapid equilibration of body fluids with the surrounding seawater. Diffusion processes would be sufficient to drive CO_2 from the site of production (i.g. epithelial cells and PMCs) to the seawater.

During acute exposure of larvae to elevated seawater $p\text{CO}_2$, pH_e decreased linearly with pH_{sw} (figure 4.4 B and E). A histological study examining the composition of extracellular body cavity matrix materials in asteroid and echinoid larval stages revealed fibrillar structures (Burke and Tamboline, 1990; Crawford, 1990) similar to the extracellular matrix structures filling the gastrocoel and blastocoel of echinoids and asteroids (Crise-Benson and Benson, 1979; Katow and Solursh, 1979; Kawabe et al., 1981; Cherr et al., 1992) and to the mesoglea known from scyphozoan (Barzansky and Lenhoff, 1974; Schmid et al., 1991; Shaposhnikova et al., 2005). This is suggesting that the later larval stages' extracellular matrix consists of collagen and glycoproteins - the same materials as in blastula and gastrula stages (Crise-Benson and Benson, 1979) and as in the cnidarian mesoglea (Hausman and Burnett, 1969; Barzansky et al., 1975; Shimizu et al., 2008). For example Type I and small amounts of type IV collagen was found in the interstitial extracellular matrix – the mesoglea – while type IV collagen is mainly colocalized with laminin in the basal membrane of *Hydra vulgaris* and *Hydra magnipapillada* (Sarras et al., 1991; Deutzmann et al., 2000; Shimizu et al., 2008). Type IV collagen is the typical collagen isoform of vertebrate basal laminae (Timpl et al., 1979). Non-bicarbonate buffer substances, however, usually consist of proteins with partially protonated amino acid side chains (cysteine and histidine), N-terminal amino groups or inorganic/organic phosphate groups (Melzner et al., 2009), none of which were predominantly found in the mesoglea of cnidarians or in blasto- and gastrocoelic matrix

of echinoderm embryos. An exceptional high non-bicarbonate buffer capacity of the matrix constituents thus seems rather unlikely.

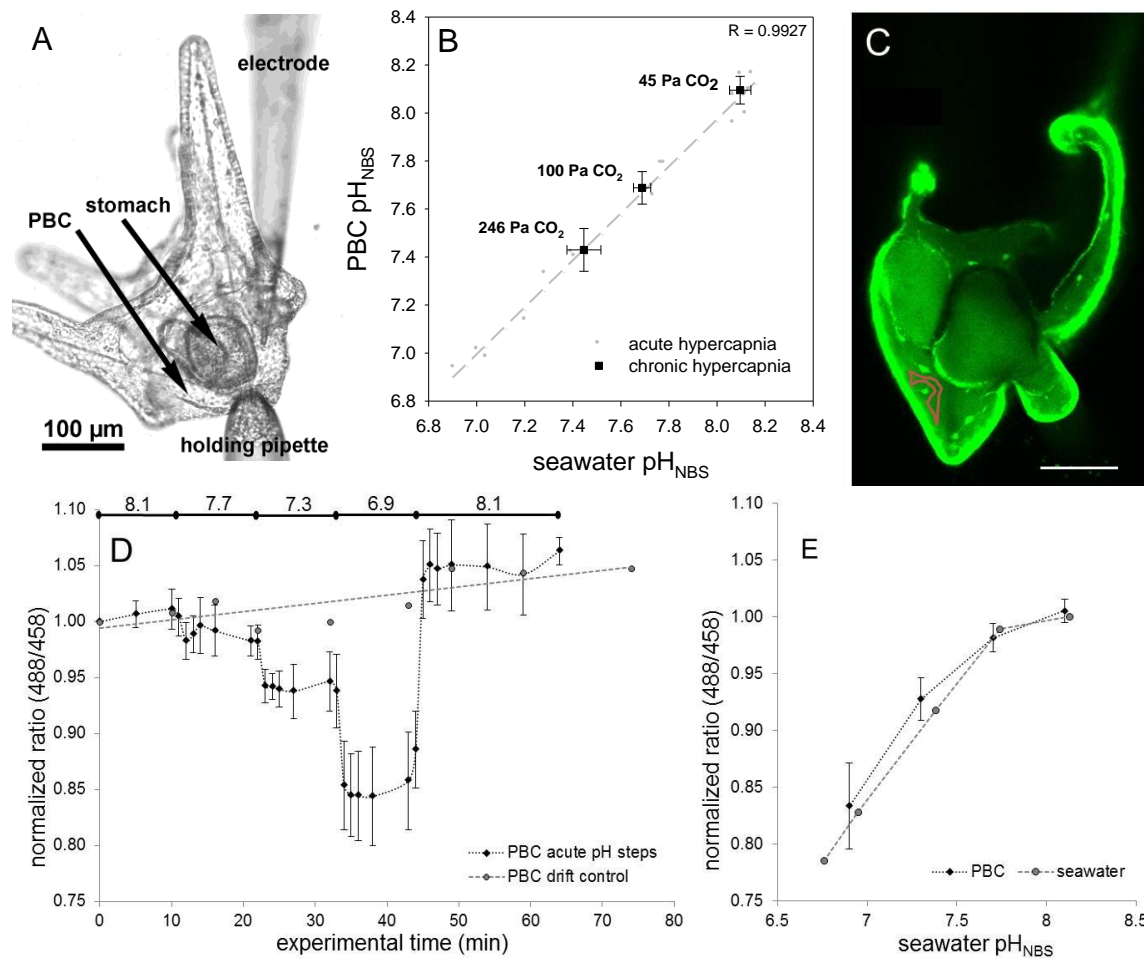


Figure 4.4: pH_e measurements in the primary body cavity (PBC) of *Strongylocentrotus droebachiensis* echinopluteus larvae using an invasive method via microelectrodes (A, B) and a non-invasive method via microfluorometry (C, D, E) both conducted using microscopes equipped with perfusion systems (figure 2.1). A: Transmission light picture of a pluteus larva held in the perfusion bath with injected pH microelectrode. B: pH_e microelectrode measurements of larva exposed to acute (grey symbols) and chronic (black symbols) hypercapnia. Acute hypercapnia was applied to larvae raised at 40 Pa CO_2 via solution change of the perfusion system during measurements (duration of 8 min per solution change). For pH_e measurements during chronic hypercapnia, larvae were raised at three different $p\text{CO}_2$ s (45 Pa, 100 Pa and 246 Pa) and measured at the respective culture $p\text{CO}_2$ / pH . C: fluorescence image of a larva loaded with BCECF-AM (488 nm excitation, 525 nm emission) with an example of measured region of interest (red). Scale bar is 75 μm . D: Normalized fluorescence emission ratio of BCECF loaded larvae during acute $p\text{CO}_2$ exposure experiments (black symbols). Two larvae were measured over an experimental time course of 75 minutes at control $p\text{CO}_2$ conditions (40 Pa) to determine background ratio drift (grey symbols and dashed line). Bars and values above the measurement indicate duration and seawater pH and times of bath exchanges. E: BCECF-dextran calibration curve in pH adjusted seawater (grey symbols) and summarized larval measurements (black symbols). Please refer to part 2.7.1 for details on methods.

Epithelia in echinoid larvae are single layered, but of different structure and thickness. The outer ectodermal epithelium is comprised of broad and thin (of 1 to 2 μm height) squamous cells covering the mesoglea-like matrix (Burke, 1981; Strathmann, 1989). This epithelium is similar in structure to the exumbrellar epithelium covering the mesoglea of hydromedusae (Josephson and Schwab, 1979). A transepithelial potential (measured with a KCl electrode; 300 mM KCL, 50 mM NaPO_4 , pH 7) of 0 mV of the ectodermal epithelium suggests that the epithelium is not an electrogenic transporting epithelium (see part 2.7.1 for details). A transepithelial resistance was not measured in this study and further studies on the permeability of ions or molecules through epithelia of echinoderm larvae have not been conducted so far. The exumbrellar epithelium of the hydromedusa *Euphysa japonica* has a very low transepithelial resistance of $7.5 \Omega\text{cm}^2$ (Josephson and Schwab, 1979) similar to the low resistance of the oral epithelium of *Anemonia viridis* tentacles ($23 \Omega\text{cm}^2$, Bénazet-Tambutté et al., 1996). In comparison, a tight non - transporting epithelium, such as the mammalian urinary bladder exhibits a transepithelial resistance above $1000 \Omega\text{cm}^2$ and a tight transporting epithelium such as the rabbit colon has a transepithelial resistance around $300 \Omega\text{cm}^2$ (Powell, 1981; Schneeberger and Lynch, 1984). In both cases where cnidarian epithelia were studied, no transepithelial resting potential could be detected (Josephson and Schwab, 1979; Bénazet-Tambutté et al., 1996). This indicates similarly to the outer epithelium of *S. droebachiensis* echinoplutei that the exumbrellar as well as the oral epithelial layers are not characterized by high transport rates of molecules. Furthermore, small molecules such as Ca^{2+} , Na^+ , Cl^- and dissolved inorganic carbon (C_T) species were detected to move passively via paracellular pathways in the cnidarians *Anemonia viridis* and *Heliofungia actiniformis* (Bénazet-Tambutté et al., 1996; Furla et al., 1998). An efficient pH_e regulating machinery of the larval outer epithelium compensating for pH_e changes is thus rather improbable. Furthermore, considering that the mesoglea of *Hydra* spp. is a porous structure with multiple trans-matrix pores (Shimizu et al., 2008) and that basal membranes in general – apart from a few very specialized cases – are regarded as leaky structures (Williams, 1994), it also seems unlikely that the echinoplutei mesoglea-like structure itself forms an efficient diffusion barrier for large molecules.

In contrast to the thin squamous epidermal cell layers, the echinopluteus' stomach epithelium consists of simple columnar cells (of 10 to 15 μm height) with microvilli

extending into the stomach lumen (Burke, 1981). At least two cell types are present in the stomach epithelium. Type I cells are characterized by a variety of different vacuoles and are expected to function in absorption and storage of nutrients as well as the secretion of digestive enzymes (Burke, 1981). Type II cells are assumed to phagocytose and digest whole algal cells (Burke, 1981). Although this epithelium appears much more active, no electrical transepithelial resting potential between the stomach lumen and surrounding seawater could be detected in this study (see part 2.7.1 for details). This can, however, also be due to a methodological constraint since the KCl-electrode was introduced through the esophagus into the stomach lumen and was thus not sealed from the surrounding seawater by epithelial layers. The luminal pH in the stomach increased after feeding commenced from pH 8.9 at 5 days post-fertilization to pH 9.5 at 9 days post-fertilization (figure 4.5). This is the first study reporting an alkaline pH in the gastric tract of echinoderm larvae. Alkaline gastric pHs are known to occur in a range of insect larvae and adults, for example in lepidopteran (Dow, 1984) and dipteran larvae (Boudko et al., 2001), as well as in adult termites (Brune and Köhl, 1996) and also the marine copepod *Calanus helgolandicus* (Pond et al., 1995). The mechanism of midgut alkalization is studied best in lepidopteran and dipteran insect larvae (reviewed by Linser et al., 2009; Onken and Moffett, 2009). However, the insect gut alkalization model is based on rather uncommon principles (apical but not basolateral occurrence of NKA, the major driving force of $V\text{-H}^+\text{-ATPase}$ for the alkalization and the absence of high intracellular carbonic anhydrase activity) compared to the widely distributed mechanisms found in ion regulatory epithelia of for example fish gills (Linser et al., 2009; Onken and Moffett, 2009). In these more general model systems, acid-base regulation is driven by the basolateral NKA establishing the electrochemical gradient for secondary active transporter such as NHE3 and $\text{Na}^+/\text{HCO}_3^-$ -cotransporter 1 (NBC1) (Evans et al., 2005). An intracellular carbonic anhydrase (CAII) facilitates the reaction of CO_2 with H_2O to H^+ and HCO_3^- . H^+ is then secreted via an apical NHE3 to the seawater while the basolateral located NBC1 carries HCO_3^- and Na^+ to the basolateral side, the blood (Claiborne et al., 2002; Evans et al., 2005). The cellular principles of gut alkalization in sea urchin larvae have not been investigated so far, but this would be an interesting topic also possibly in respect to evolution of ion regulatory mechanism due to the echinoderms evolutionary position as basic deuterostomians.

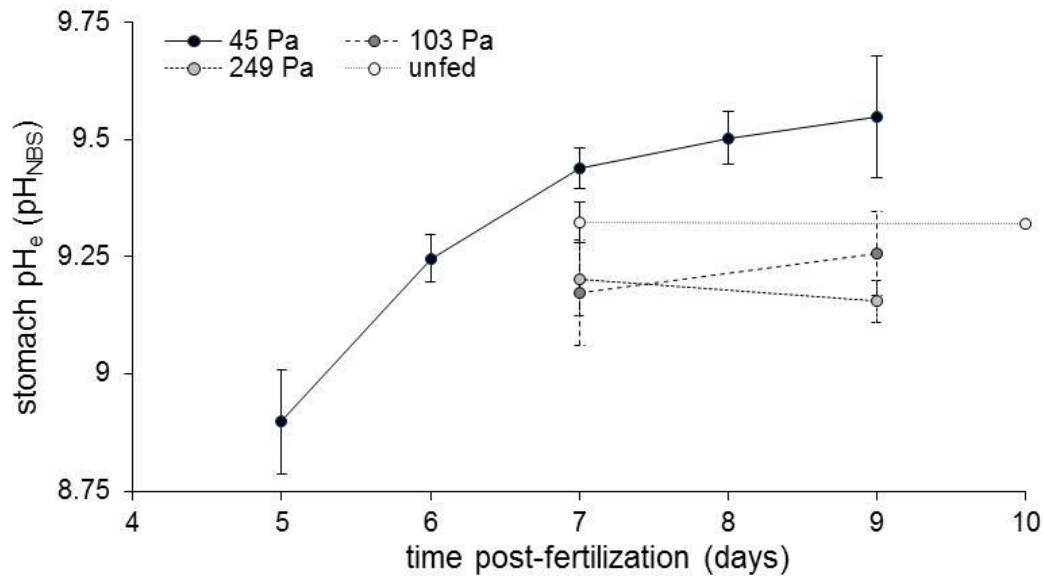


Figure 4.5: pH_e microelectrode measurements in stomach lumen of *Strongylocentrotus droebachiensis* larvae. Larvae were raised at three different $p\text{CO}_2$ levels (control 45 Pa, 103 Pa and 249 Pa). Unfed larvae were raised at control conditions of 45 Pa CO_2 .

Chronic exposure of larvae to elevated $p\text{CO}_2$ (103 Pa and 249 Pa) led to the same decrease in primary body cavity pH_e as acute exposure of larvae (figure 4.4B). This indicates that no re-structuring of extracellular matrix components during development occurred in order to compensate for pH_e changes. Furthermore, chronic exposure of larvae to elevated $p\text{CO}_2$ resulted in a lower stomach lumen pH at 7 and 9 days post-fertilization in both CO_2 treatments (figure 4.5). The data suggest that the environmental CO_2 induced acidification is exceeding the larval capacity of fully alkalize the stomach lumen to control or unfed larval levels (figure 4.5). The drop in stomach pH of 0.25 and 0.4 pH units at the high $p\text{CO}_2$ level (at 7 and 9 dpf, respectively) is, however, much smaller than the environmental pH_{SW} drop of 0.67 pH units, possibly indicating an activation of compensatory mechanisms. The observed elevated transcript levels of NKA (publication 2) and aerobic metabolic rates (publication 1) could be due to increased demands of ion regulation for alkalization of the stomach lumen. It is, however, unclear whether excess protons are secreted into the primary body cavity or possibly across stomach and intestinal epithelia into the intestinal lumen. Since no elevated acidification of the primary body cavity could be detected in this study (figure 4.4 B), it seems unlikely that excess protons are introduced into the gel-filled body cavity. A more acidic pH towards the end of digestive system was observed in mosquito larvae (Boudko et al., 2001). Similarly, a net excretion of H^+ from the primary body cavity into the gut system

especially the intestine could thus be accomplished. But this question remains a topic for future studies.

Nevertheless, a lowered stomach pH might have negative consequences for larval energy acquisition. Digestive enzymes secreted into the gut to hydrolyze nutrients usually exhibit specific pH optima at which the enzymes are most efficient. Digestive proteases of insects that exhibit a high alkaline pH in their midgut often have an activity pH optimum at pH 8 to 10 (Wolfson and Murdock, 1990). Furthermore, digestive enzymes commonly have a rather narrow pH optimum i.e. enzyme activity is significantly decreasing within 0.5 pH units from their pH optimum (Klinger, 1984; Wolfson and Murdock, 1990). Thus, a decrease in 0.4 pH units in the stomach lumen may have severe impacts on the digestive efficiency of sea urchin larvae, reducing the energy assimilation and subsequently, negatively impacting the energy budget. Studies on the digestive efficiency and enzyme activity pH optima of planktotrophic echinoid larvae could yield interesting information about larval energy acquisition under elevated seawater $p\text{CO}_2$.

4.2.3 Extracellular pH homeostasis in *S. droebachiensis* adults

Short term exposure (ST, 10 days) of adult *S. droebachiensis* to 145 and 385 Pa CO_2 led to an initial perivisceral coelomic fluid (PCF) pH_e drop within 2 days (publication 3, figure 5). In the intermediate $p\text{CO}_2$ level (145 Pa), 10 days were sufficient for the animals to fully compensate the acidosis by accumulation of $[\text{HCO}_3^-]_e$ (publication 3, figure 5A). Animals exposed to the high $p\text{CO}_2$ level also substantially accumulated $[\text{HCO}_3^-]_e$ but only a partial pH_e compensation could be achieved (publication 3, figure 5B). Animals of both treatments (i.e. 102 and 284 Pa CO_2), could sustain full and partial compensation, respectively, during an incubation period of 45 days (publication 3, figure 6). However, a $[\text{HCO}_3^-]_e$ accumulation of 2.1 to 2.5 mM above control conditions seemed to be the maximum regulatory capacity in *S. droebachiensis* in response to environmental hypercapnia. This is the first study reporting significant and persistent pH_e compensation in an echinoid. A pH_e compensation could not be observed in *Psammechinus miliaris* exposed to $p\text{CO}_2$ levels ranging 0.25 to 5.2 kPa for 8 days (Miles et al., 2007) or in *S. droebachiensis* exposed to elevated $p\text{CO}_2$ (137, 275 and 662 Pa) for 5 days (Spicer et al., 2011). *P. miliaris* exposed to the highest $p\text{CO}_2$ level (5.2 kPa), however, significantly accumulated $[\text{HCO}_3^-]_e$ (Miles et al., 2007). Since Mg^{2+} and Ca^{2+} concentrations increased

in the PCF in parallel with $[\text{HCO}_3^-]_e$, the observed $[\text{HCO}_3^-]_e$ accumulation could be primarily related to test dissolution in *P. miliaris* (Miles et al., 2007). Short exposure (24 hours) of *P. miliaris* and *Echinus esculentus* to air also resulted in significant $[\text{HCO}_3^-]_e$ accumulation of 1 and 2.8 mM, respectively, but this accumulation was also accompanied with increases in Mg^{2+} and Ca^{2+} concentrations in the PCF (Spicer et al., 1988). No $[\text{HCO}_3^-]_e$ accumulation could be observed in *S. purpuratus* in response to 8 hour emersion (Burnett et al., 2002). However, since net growth in shell diameter and shell weight could be detected in this study in response to the intermediate $p\text{CO}_2$ treatment (publication 3, table 3) an accumulation of $[\text{HCO}_3^-]_e$ due to test dissolution seems unlikely. On the other hand, the rate of $[\text{HCO}_3^-]_e$ accumulation is much slower than the rate observed in more active marine ectotherms that are able to compensate a hypercapnia induced acidosis within <1 day (Pane and Barry, 2007; Gutowska et al., 2010a). Interestingly, the sea urchins capacity to sustain high $[\text{HCO}_3^-]_e$ levels in response to the high $p\text{CO}_2$ treatment was correlated with the animals' feeding state. Sea urchins with empty digestive systems exhibited a strong extracellular metabolic acidosis as indicated by the PCF $[\text{HCO}_3^-]_e$ below the non-bicarbonate buffer line and the accompanied strong drop in pH_e (publication 3, figure 6). However, it remains to be determined, whether the ability of $[\text{HCO}_3^-]_e$ accumulation is causally related to the animals physiological condition or if both conditions are merely correlated.

The green sea urchins used for this study were collected in the Kattegat at the border of the Western Baltic Sea. The Kattegat and the Western Baltic are characterized by a seasonal occurring hypoxia induced hypercapnia (Conley et al., 2007; HELCOM, 2009). Thus, the capacity of *S. droebachiensis* to fully compensate pH_e in response to moderately elevated seawater $p\text{CO}_2$ of up to 145 Pa which is in the range of current seasonal events (Thomsen et al., 2010) could indicate that this species is already adapted to increases of seawater $p\text{CO}_2$. This is further supported by the observation that *S. droebachiensis*' fertility fully recovers at elevated $p\text{CO}_2$ conditions (138 Pa) when enough time for acclimation is allowed (publication 4). However, if anthropogenic CO_2 is adding up to already high seawater $p\text{CO}_2$, it can be expected that future $p\text{CO}_2$ conditions exceed the value at which *S. droebachiensis* is able to fully compensate an hypercapnia induced extracellular acidosis (Thomsen et al., 2010). And although *S. droebachiensis* was able to survive a few weeks of highly elevated seawater $p\text{CO}_2$ (up to 284 Pa), longer

exposure would likely lead to increased mortality (publication 3; Miles et al., 2007). Together with the increased mortality of juveniles after larval exposure to hypercapnia, elevated seawater $p\text{CO}_2$ has the potential to negatively impact recruitment success and can thus be regarded a serious threat to echinoids. Nevertheless, further studies on the acclimation and adaptation potential of sea urchins to elevated seawater $p\text{CO}_2$, possibly combined with elevated temperatures as an additive stressor, are urgently needed.

5 Conclusion

Based on the experimental results of the present thesis I can now address the research hypotheses formulated in the introduction:

a) Growth reductions in sea urchin larval and adult stages are related to a decrease in scope for growth which is either caused by elevated metabolic rates or decreased feeding rates.

The energy budgets constructed for both, larval and adult, echinoids revealed that in both cases, scope for growth was reduced in response to elevated $p\text{CO}_2$. This is in accordance with real growth and development declines observed in echinoids. Decreased feeding rates in response to hypercapnia were observed to be the primary factor reducing the scope for growth in adult *S. droebachiensis*. In contrast to adult sea urchins, *S. purpuratus* echinoplutei responded with highly elevated metabolic rates (up to 100%) towards elevated seawater $p\text{CO}_2$.

b) Larval stages are not able to actively buffer extracellular acid-base disturbances in order to support calcification by PMCs. Calcification and ion regulatory processes are up regulated in order to sustain growth and development.

Extracellular pH of the primary body cavity appeared to be pH conform to the surrounding seawater pH in *S. droebachiensis* larvae exposed to, both, acute and chronically elevated $p\text{CO}_2$ conditions. This suggests that a strong acid base regulatory machinery for pH homeostasis in the primary body cavity in order to support calcification by primary mesenchyme cells does not exist. In contrast, a strong acid-base regulatory capacity could be observed in the larval stomach epithelium that alkalized the lumen to a pH of 9.5 after feeding commenced. Chronic exposure of larvae to CO_2 induced seawater acidification (249 Pa CO_2) lowered the stomach lumen pH significantly by up to 0.4 pH units. This may have negative impacts on the digestive efficiency of the larval gastric system. The genetic approach supported the observed up regulation of aerobic metabolism in *S. purpuratus* revealing an up regulation of genes relevant for metabolism. Most genes relevant for calcification and ion regulation – apart from NKA – were, however, down regulated in *S. purpuratus* larvae exposed to environmental hypercapnia. Nevertheless, an up regulation of NKA supports the hypothesis of increased ion regulatory demands for important processes e.g. the alkalization of stomach lumen.

c) Sea urchins are regarded as weak acid-base regulators and are using test dissolution in order to buffer excess protons within the perivisceral coelomic fluid during exposure to high seawater $p\text{CO}_2$.

Adult green sea urchins could be observed to significantly accumulate $[\text{HCO}_3^-]_e$ in their perivisceral coelomic fluid and to fully compensate CO_2 induced acid-base disturbances at environmental seawater $p\text{CO}_2$ s up to 145 Pa and for an exposure period of 45 days. Higher seawater $p\text{CO}_2$ (290 to 390 Pa) resulted in a partial pH_e compensation revealing the same $[\text{HCO}_3^-]_e$ accumulation capacity of maximal 2.5 mM above control values. Due to the slow reaction of $[\text{HCO}_3^-]_e$ accumulation (appr. 10 days), it cannot be fully excluded that some $[\text{HCO}_3^-]_e$ for pH_e compensation derives from shell dissolution. Nevertheless, a net test growth (i.e. calcification) of sea urchins exposed to 102 Pa CO_2 for 45 days suggests that long term $[\text{HCO}_3^-]_e$ accumulation is not derived by test dissolution. The

strong metabolic acidosis elicited by sea urchins exposed to 284 Pa CO₂ with empty digestive systems suggests rather that the capacity to sustain high [HCO₃⁻]_e is linked to the sea urchins physiological status and thus to the animals' energy budget.

d) The green sea urchin has a potential to adapt to environmental hypercapnia, because it occurs in areas with seasonally hypercapnic conditions. Nevertheless, a further increase in seawater pCO₂ may severely threaten echinoids.

This study demonstrated that the green sea urchin was able to overcome prolonged periods (up to 16 months) of environmental hypercapnia (up to 145 Pa CO₂). Especially the long term incubation of 16 months highlighted that *S. droebachiensis* has a potential to acclimate to moderately elevated pCO₂. This could be due to an adaptation of this sea urchin species to current events of seasonal hypercapnia. Nevertheless, the dominant metabolic acidosis in *S. droebachiensis* adults exposed to 284 Pa CO₂ for 6 weeks – a realistic scenario for future seasonal hypercapnic events – suggests that a few weeks of such high seawater pCO₂ may exceed the green sea urchins acclimation potential and may severely impact the sea urchin population in future. Furthermore, the observed high mortalities in the juvenile stages after larval exposure to elevated pCO₂ demonstrated that the transition from larva to juvenile appears to be a serious life cycle “bottle neck” in response to hypercapnia. Further studies on acclimation/adaptation potential of sea urchins to hypercapnia are urgently needed to reliably predict echinoids fate in future oceans.

Concluding, it can be said, that echinoids generally belong to the more sensitive taxa with respect to CO₂ induced seawater acidification than for example cephalopods surviving much higher pCO₂ levels (Gutowska et al., 2008; Gutowska et al., 2010a). But although severe impacts of elevated seawater pCO₂ could be detected in some life cycle stages in this study, this work and another study examining phenotypic and genetic plasticity of *S. franciscanus* larvae (Sunday et al., 2011) also demonstrated some acclimation and adaptation potential in stronglyloentrotid echinoids. An extrapolation to other echinoid species or to echinoderms in general remains to be difficult also because a high species specificity in hypercapnia responses has been observed within this phylum (Dupont et al., 2010c). Generally it should be mentioned that echinoderms are an old

phylum that already survived other periods of rapid climate change, such as the end-Permian mass extinction event (Knoll et al., 2007). Thus, it seems rather unlikely that anthropogenic CO₂ emissions will lead to a complete extinction of this phylum. Nevertheless, it can be expected that several species of this phylum will be severely threatened by ocean acidification and may not survive such a rapid climate change which has not been encountered on earth for the last 450 thousand years (Petit et al., 1999) and this will inevitably lead to a reorganization of today's ecosystems.

6 References

- Allen, J. D., 2008. Size-specific predation on marine invertebrate larvae. *Biol Bull.* 214, 42-49.
- Andersen, C. L., Jensen, J. L., Orntoft, T. F., 2004. Normalization of real-time quantitative reverse transcription-PCR data: a model-based variance estimation approach to identify genes suited for normalization, applied to bladder and colon cancer data sets. *Cancer Res.* 64, 5245-5250.
- Anstrom, J. A., Chin, J. E., Leaf, D. S., Parks, A. L., Raff, R. A., 1987. Localization and expression of msp130, a primary mesenchyme lineage-specific cell surface protein in the sea urchin embryo. *Development.* 101, 255-265.
- Bard, S. M., 2000. Multixenobiotic resistance as a cellular defense mechanism in aquatic organisms. *Aquat Toxicol.* 48, 357-389.
- Barzansky, B., Lenhoff, H. M., 1974. On the chemical composition and developmental role of the mesoglea of hydra. *Am Zool.* 14, 575-581.
- Barzansky, B., Lenhoff, H. M., Bode, H., 1975. Hydra mesoglea - similarity of its amino acid and neutral sugar composition to that of vertebrate basal lamina. *Comp Biochem Physiol B.* 50, 419-424.
- Bathmann, U. V., Noji, T. T., von Bodungen, B., 1991. Sedimentation of pteropods in the Norwegian Sea in autumn. *Deep-Sea Res.* 38, 1341-1360.
- Beaufort, L., Probert, I., de Garidel-Thoron, T., Bendif, E. M., Ruiz-Pino, D., Metzl, N., Goyet, C., Buchet, N., Coupel, P., Grelaud, M., Rost, B., Rickaby, R. E., de Vargas, C., 2011. Sensitivity of coccolithophores to carbonate chemistry and ocean acidification. *Nature.* 476, 80-3.
- Beddingfield, S. D., McClintock, J. B., 1998. Differential survivorship, reproduction, growth and nutrient allocation in the regular echinoid *Lytechinus variegatus* (Lamarck) fed natural diets. *J Exp Mar Biol Ecol.* 226, 195-215.
- Beldowski, J., Löffler, A., Schneider, B., Joensuu, L., 2010. Distribution and biogeochemical control of total CO₂ and total alkalinity in the Baltic Sea. *J Marine Syst.* 81, 252-259.
- Ben-Tabou de-Leon, S., Davidson, E. H., 2007. Gene regulation: gene control network in development. *Annu Rev Biophys Biomol Struct.* 36, 191-212.
- Bénazet-Tambutté, S., Allemand, D., Jaubert, J., 1996. Permeability of the oral epithelial layers in cnidarians. *Mar Biol.* 126, 43-53.

- Beniash, E., Addadi, L., Weiner, S., 1999. Cellular control over spicule formation in sea urchin embryos: a structural approach. *J Struct Biol.* 125, 50-62.
- Beniash, E., Aizenberg, J., Addadi, L., Weiner, S., 1997. Amorphous calcium carbonate transforms into calcite during sea urchin larval spicule growth. *P Roy Soc Lond B Bio.* 264, 461-465.
- Beniash, E., Ivanina, A., Lieb, N. S., Kurochkin, I., Sokolova, I. M., 2010. Elevated level of carbon dioxide affects metabolism and shell formation in oysters *Crassostrea virginica*. *Mar Ecol Prog Ser.* 419, 95-108.
- Biermann, C. H., Kessing, B. D., Palumbi, S. R., 2003. Phylogeny and development of marine model species: stronglyloacetrotid sea urchins. *Evol. Dev.* 5, 360-371.
- Bisgrove, B. W., Burke, R. D., 1986. Development of serotonergic neurons in embryos of the sea urchin *Strongylocentrotus purpuratus*. *Dev Growth Diff.* 28, 569-574.
- Bishop, C. D., Watts, S. A., 1992. Biochemical and morphometric study of growth in the stomach and intestine of the echinoid *Lytechinus variegatus* (Echinodermata). *Mar. Biol.* 114, 459-467.
- Bookbinder, L. H., Shick, J. M., 1986. Anaerobic and aerobic energy metabolism in ovaries of the sea urchin *Strongylocentrotus droebachiensis*. *Mar. Biol.* 93, 103-110.
- Bottjer, D. J., 2006. Paleogenomics of echinoderms. *Science.* 314, 956-960.
- Boudko, D. Y., Moroz, L. L., Harvey, W. R., Linser, P. J., 2001. Alkalinization by chloride/bicarbonate pathway in larval mosquito midgut. *P Natl Acad Sci USA.* 98, 15354-15359.
- Brennand, H. S., Soars, N., Dworjanyn, S. A., Davis, A. R., Byrne, M., 2010. Impact of ocean warming and ocean acidification on larval development and calcification in the sea urchin *Tripneustes gratilla*. *Plos One.* 5, e11372.
- Brewer, P. G., Peltzer, E. T., 2009. Limits to marine life. *Science.* 324, 347-348.
- Brune, A., Kühl, M., 1996. pH profiles of the extremely alkaline hindguts of soil-feeding termites (Isoptera: Termitidae) determined with microelectrodes. *J Insect Phys.* 42, 1121-1127.
- Burke, R. D., 1980. Podial sensory receptors and the induction of metamorphosis in echinoids. *J Exp Mar Biol Ecol.* 47, 223-234.
- Burke, R. D., 1981. Structure of the digestive tract of the pluteus larva of *Dendraster excentricus* (Echinodermata, Echinozoa). *Zoomorphology.* 98, 209-225.
- Burke, R. D., Tamboline, C. R., 1990. Ontogeny of an extracellular matrix component of sea urchins and its role in morphogenesis. *Dev Growth Diff.* 32, 461-471.
- Burnett, L., Terwilliger, N., Carroll, A., Jorgensen, D., Scholnick, D., 2002. Respiratory and acid-base physiology of the purple sea urchin, *Strongylocentrotus purpuratus*, during air exposure: presence and function of a facultative lung. *Biol. Bull.* 203, 42-50.
- Byrne, M., Ho, M., Selvakumaraswamy, P., Nguyen, H. D., Dworjanyn, S. A., Davis, A. R., 2009. Temperature, but not pH, compromises sea urchin fertilization and early development under near-future climate change scenarios. *P. Roy. Soc. B Bio.* 276, 1883-1888.
- Byrne, M., Ho, M., Wong, E., Soars, N. A., Selvakumaraswamy, P., Shepard-Brennand, H., Dworjanyn, S. A., Davis, A. R., 2011. Unshelled abalone and corrupted urchins: development of marine calcifiers in a changing ocean. *P Roy Soc B Bio.* 278, 2376-2383.
- Byrne, M., Prowse, T. A. A., Sewell, M. A., Dworjanyn, S., Williamson, J. E., Vaitilingon, D., 2008. Maternal provisioning for larvae and larval provisioning for

- juveniles in the toxopneustid sea urchin *Tripneustes gratilla*. *Mar Biol.* 155, 473-482.
- Byrne, M., Soars, N., Ho, M., Wong, E., McElroy, D., Selvakumaraswamy, P., Dworjanyn, S. A., Davis, A. R., 2010a. Fertilization in a suite of coastal marine invertebrates from south east Australia is robust to near-future ocean warming and acidification. *Mar Biol.* 175, 2061-2069.
- Byrne, M., Soars, N., Selvakumaraswamy, P., Dworjanyn, S. A., Davis, A. R., 2010b. Sea urchin fertilization in a warm, acidified and high $p\text{CO}_2$ ocean across a range of sperm densities. *Mar Environ Res.* 69, 234-239.
- Caldeira, K., Wickett, M. E., 2003. Anthropogenic carbon and ocean pH. *Nature.* 425, 365-365.
- Caldeira, K., Wickett, M. E., 2005. Ocean model predictions of chemistry changes from carbon dioxide emissions to the atmosphere and ocean. *J. Geophys. Res.* 110.
- Cameron, R. A., Hinegardner, R. T., 1974. Initiation of metamorphosis in laboratory cultured sea urchins. *Biol Bull.* 146, 335-342.
- Cao, L., Caldeira, K., 2008. Atmospheric CO_2 stabilization and ocean acidification. *Geophys Res Lett.* 35.
- Carefoot, T. H., 1967. Growth and nutrition of *Aplysia punctata* feeding on a variety of marine algae. *J Mar Biol Ass U.K.* 47, 565-589.
- Carr, R. S., Biedenbach, J. M., Nipper, M., 2006. Influence of potentially confounding factors on sea urchin porewater toxicity tests. *Arch Environ ContTox.* 51, 573-579.
- Checkley, D. M., Dickson, A. G., Takahashi, M., Radich, J. A., Eisenkolb, N., Asch, R., 2009. Elevated CO_2 enhances otolith growth in young fish. *Science.* 324, 1683.
- Cherr, G. N., Summers, R. G., Baldwin, J. D., Morrill, J. B., 1992. Preservation and visualization of the sea urchin embryo blastocoelic extracellular matrix. *Microsc Res Techniq.* 22, 11-22.
- Christiansen, J. S., Siikavuopio, S. I., 2007. The relationship between feed intake and gonad growth of single and stocked green sea urchin (*Strongylocentrotus droebachiensis*) in a raceway culture. *Aquaculture.* 262, 163-167.
- Claiborne, J. B., Edwards, S. L., Morrison-Shetlar, A. I., 2002. Acid-base regulation in fishes: Cellular and molecular mechanisms. *J Exp Zool.* 293, 302-319.
- Clark, D., Lamare, M., Barker, M., 2009. Response of sea urchin pluteus larvae (Echinodermata: Echinoidea) to reduced seawater pH: a comparison among tropical, temperate, and a polar species. *Mar. Biol.* 156, 1125-1137.
- Comeau, S., Gorsky, G., Alliouane, S., Gattuso, J. P., 2010a. Larvae of the pteropod *Cavolinia inflexa* exposed to aragonite undersaturation are viable but shell-less. *Mar. Biol.* 157, 2341-2345.
- Comeau, S., Gorsky, G., Jeffree, R., Teyssie, J. L., Gattuso, J. P., 2009. Impact of ocean acidification on a key Arctic pelagic mollusc (*Limacina helicina*). *Biogeosciences.* 6, 1877-1882.
- Comeau, S., Jeffree, R., Teyssie, J. L., Gattuso, J. P., 2010b. Response of the Arctic pteropod *Limacina helicina* to projected future environmental conditions. *Plos One.* 5, e11362.
- Conley, D. J., Carstensen, J., Aertebjerg, G., Christensen, P. B., Dalsgaard, T., Hansen, J. L. S., Josefson, A. B., 2007. Long-term changes and impacts of hypoxia in danish coastal waters. *Ecol Appl.* 17 Supplement, S165-S184.
- Conover, R. J., 1966. Assimilation of organic matter by zooplankton. *Limnol. Oceanogr.* 11, 338-345.

- Crawford, B. J., 1990. Changes in the arrangement of the extracellular matrix, larval shape, and mesenchyme cell migration during asteroid larval development. *J Morph.* 206, 147-161.
- Crise-Benson, N., Benson, S. C., 1979. Ultrastructure of collagen in sea urchin embryos. *Roux Arch Dev Biol.* 186, 65-70.
- Cummings, V., Hewitt, J., Van Rooyen, A., Currie, K., Beard, S., Thrush, S., Norkko, J., Barr, N., Heath, P., Halliday, N. J., Sedcole, R., Gomez, A., McGraw, C., Metcalf, V., 2011. Ocean acidification at high latitudes: potential effects on functioning of the Antarctic bivalve *Laternula elliptica*. *Plos One.* 6, e16069.
- Decker, G. L., Morrill, J. B., Lennarz, W. J., 1987. Characterization of sea urchin primary mesenchyme cells and spicules during biomineralization *in vitro*. *Development.* 101, 297-312.
- DeCoursey, T. E., 2008. Voltage-gated proton channels. *Cell Mol Life Sci.* 65, 2554-2573.
- Deigweiher, K., Hirse, T., Bock, C., Lucassen, M., Pörtner, H.-O., 2010. Hypercapnia induced shifts in gill energy budgets of Antarctic notothenioids. *J Comp Physiol B.* 180, 347-359.
- Deutzmann, R., Fowler, S., Zhang, X. M., Boone, K., Dexter, S., Boot-Handford, R. P., Rachel, R., Sarras, M. P., 2000. Molecular, biochemical and functional analysis of a novel and developmentally important fibrillar collagen (Hcol-I) in hydra. *Development.* 127, 4669-4680.
- Dickson, A. G., Millero, F. J., 1987. A comparison of the equilibrium constants for the dissociation of carbonic acid in seawater media. *Deep-Sea Res.* 34, 1733-1743. (Corrigenda. *Deep-Sea Res.* 36, 983).
- Dickson, A. G., Sabine, C. L., Christian, J. R., 2007. Guide to best practices for ocean CO₂ measurements. *PICES Special Publication.* 3, 191 pp.
- Doney, S. C., Fabry, V. J., Feely, R. A., Kleypas, J. A., 2009. Ocean acidification: the other CO₂ problem. *Annu Rev Marine Sci.* 1, 169-192.
- Dow, J. A. T., 1984. Extremely high pH in biological systems - a model for carbonate transport. *Am J Physiol.* 246, R633-R636.
- Dupont, S., Dorey, N., Thorndyke, M., 2010a. What meta-analysis can tell us about vulnerability of marine biodiversity to ocean acidification? *Estuar Coast Shelf S.* 89, 182-185.
- Dupont, S., Havenhand, J., Thorndyke, W., Peck, L., Thorndyke, M. C., 2008. CO₂-driven ocean acidification radically affect larval survival and development in the brittlestar *Ophiotrix fragilis*. *Mar Ecol Prog Ser.* 373, 285-294.
- Dupont, S., Lundve, B., Thorndyke, M., 2010b. Near future ocean acidification increases growth rate of the lecithotrophic larvae and juveniles of the sea star *Crossaster papposus*. *J Exp Zool. B.* 314B, 382-389.
- Dupont, S., Ortega-Martínez, O., Thorndyke, M. C., 2010c. Impact of near-future ocean acidification on echinoderms. *Ecotoxicology.* 19, 449-462.
- Ebert, T. A., 1967. Negative growth and longevity in the purple sea urchin *Strongylocentrotus purpuratus* (Stimpson). *Science.* 157, 557-558.
- Edwards, P. B., Ebert, T. A., 1991. Plastic responses to limited food availability and spine damage in the sea urchin *Strongylocentrotus purpuratus* (Stimpson). *J Exp Mar Biol Ecol.* 145, 205-220.
- Elkin, C., Marshall, D. J., 2007. Desperate larvae: influence of deferred costs and habitat requirements on habitat selection. *Mar. Ecol. Prog. Ser.* 335, 143-153.

- Elliott, J. M., Davison, W., 1975. Energy equivalents of oxygen-consumption in animal energetics. *Oecologia*. 19, 195-201.
- Ericson, J. A., Lamare, M. D., Morley, S. A., Barker, M. F., 2010. The response of two ecologically important Antarctic invertebrates (*Sterechinus neumayeri* and *Parborlasia corrugatus*) to reduced seawater pH: effects on fertilisation and embryonic development. *Mar. Biol.* 157, 2689-2702.
- Ettensohn, C. A., Malinda, K. M., 1993. Size regulation and morphogenesis: a cellular analysis of skeletogenesis in the sea urchin embryo. *Development*. 119, 155-167.
- Evans, D. H., Piermarini, P. M., Choe, K. P., 2005. The multifunctional fish gill: Dominant site of gas exchange, osmoregulation, acid-base regulation, and excretion of nitrogenous waste. *Physiol Rev.* 85, 97-177.
- Fabricius, K. E., Langdon, C., Uthicke, S., Humphrey, C., Noonan, S., De'ath, G., Okazaki, R., Muehllehner, N., Glas, M. S., Lough, J. M., 2011. Losers and winners in coral reefs acclimatized to elevated carbon dioxide concentrations. *Nature Climate Change*. 1, 165-169.
- Fabry, V. J., 2008. Marine calcifiers in a high-CO₂ ocean. *Science*. 320, 1020-1022.
- Feely, R. A., Sabine, C. L., Hernandez-Ayon, J. M., Ianson, D., Hales, B., 2008. Evidence for upwelling of corrosive "acidified" water onto the continental shelf. *Science*. 320, 1490-1492.
- Feely, R. A., Sabine, C. L., Lee, K., Berelson, W., Kleypas, J., Fabry, V. J., Millero, F. J., 2004. Impact of anthropogenic CO₂ on the CaCO₃ system in the oceans. *Science*. 305, 362-366.
- Fernandez, C., 1998. Seasonal changes in the biochemical composition of the edible sea urchin *Paracentrotus lividus* (Echinodermata: Echinoidea) in a lagoonal environment. *PSZN Mar Ecol.* 19, 1-11.
- Findlay, H. S., Wood, H. L., Kendall, M. A., Spicer, J. I., Twitchett, R. J., Widdicombe, S., 2009. Calcification, a physiological process to be considered in the context of the whole organism. *Biogeosciences Discuss.* 6, 2267-2284.
- Frost, B. W., 1972. Effects of size and concentration of food particles on the feeding behaviour of the marine planktonic copepod *Calanus pacificus*. *Limnol Oceanogr.* 17, 805-815.
- Furla, P., Benazet-Tambutte, S., Jaubert, J., Allemand, D., 1998. Diffusional permeability of dissolved inorganic carbon through the isolated oral epithelial layers of the sea anemone, *Anemonia viridis*. *J Exp Mar Biol Ecol.* 221, 71-88.
- Gazeau, F., Quiblier, C., Jansen, J. M., Gattuso, J.-P., Middleburg, J. J., Heip, C. H. R., 2007. Impact of elevated CO₂ on shellfish calcification. *Geophys Res Lett.* 34.
- George, S. B., 1999. Egg quality, larval growth and phenotypic plasticity in a forcipulate seastar. *J Exp Mar Biol Ecol.* 237, 203-224.
- Giese, A. C., Farmanfarmanian, A., Hilden, S., Doezema, P., 1966. Respiration during the reproductive cycle in the sea urchin, *Strongylocentrotus purpuratus*. *Biol Bull* 130, 192-201.
- Gnaiger, E., Calculation of energetic and biochemical equivalents of respiratory oxygen consumption. In: E. Gnaiger, H. Forstner, (Eds.), *Polarographic Oxygen Sensors: Aquatic and Physiological Applications*. Springer-Verlag, New York, 1983.
- González, M. L., López, D. A., Pérez, M. C., Castro, J. M., 2002. Effect of temperature on the scope for growth in juvenile scallops *Artopecten purpuratus* (Lamarck, 1819). *Aquacult Int.* 10, 339-349.

- Green, M. A., Jones, M. E., Boudreau, C. L., Moore, R. L., Westman, B. A., 2004. Dissolution mortality of juvenile bivalves in coastal marine deposits. *Limnol Oceanogr.* 49, 727-734.
- Greenwood, P. J., 1980. Growth, respiration and tentative energy budgets for two populations of the sea urchin *Parechinus angulosus* (Leske). *Estuar Coast Mar S.* 10, 347-367.
- Gruswitz, F., Chaudhary, S., Ho, J. D., Schlessinger, A., Pezeshki, B., Ho, C. M., Sali, A., Westhoff, C. M., Stroud, R. M., 2010. Function of human Rh based on structure of RhCG at 2.1 Å. *PNAS.* 107, 9638-9643.
- Guerinot, M. L., Patriquin, D. G., 1981. The association of N₂-fixing bacteria with sea urchins. *Mar Biol.* 62, 197-207.
- Guillard, R. R. L., Ryther, J. H., 1962. Studies of marine planktonic diatoms. I. *Cyclotella nana* Husted, and *Detonula confervacea* (Cleve). *Can J Microbiol.* 8, 229-239.
- Gutowska, M. A., Melzner, F., Langenbuch, M., Bock, C., Claireaux, G., Pörtner, H.-O., 2010a. Acid-base regulatory capacity in the cephalopod *Sepia officinalis* exposed to environmental hypercapnia. *J Comp Physiol B.* 180, 323-335.
- Gutowska, M. A., Melzner, F., Pörtner, H.-O., Meier, S., 2010b. Calcification in the cephalopod *Sepia officinalis* in response to elevated seawater pCO₂. *Mar Biol.* 157, 1653-1663.
- Gutowska, M. A., Pörtner, H.-O., Melzner, F., 2008. Growth and calcification in the cephalopod *Sepia officinalis* under elevated seawater pCO₂. *Mar Ecol Prog Ser.* 373, 303-309.
- Hall-Spencer, J. M., Rodolfo-Metalpa, R., Martin, S., Ransome, E., Fine, M., Turner, S. M., Rowley, S. J., Tedesco, D., Buia, M.-C., 2008. Volcanic carbon dioxide vents show ecosystem effects of ocean acidification. *Nature.* 454, 96-99.
- Hare, J. A., Cowen, R. K., 1997. Size, growth, development, and survival of the planktonic larvae of *Pomatomus saltatrix* (Pisces: Pomatomidae). *Ecology.* 78, 2415-2431.
- Haugen, H. A., Aagaard, P., Thyberg, B., Kjærstad, J., Langlet, D., Melaaen, M. C., Liljemark, S., Bergmo, P., Skagestad, R., Mathisen, A., Jarsve, E. M., Faleide, J. I., Bjørnsen, D., 2011. CCS in the Skagerrak/Kattegat area. *Energ Proc.* 4, 2324-2331.
- Hausman, R. E., Burnett, A. L., 1969. The mesoglea of hydra I. physical and histochemical properties. *J Exp Zool.* 171, 7-14.
- Havenhand, J., Buttler, F. R., Thorndyke, M. C., Williamson, J. E., 2008. Near-future levels of ocean acidification reduce fertilization success in a sea urchin. *Curr Biol.* 18, R651-R652.
- Heisler, N., 1989. Interaction between gas exchange, metabolism, and ion transport in animals: an overview. *Can J Zool.* 67, 2923-2935.
- HELCOM, 2009. Eutrophication in the Baltic Sea - An integrated thematic assessment of the effects of nutrient enrichment and eutrophication in the Baltic Sea region. *Bal Sea Environ Proc.* 115B.
- Hernandez, J. C., Russell, M. P., 2010. Substratum cavities affect growth-plasticity, allometry, movement and feeding rates in the sea urchin *Strongylocentrotus purpuratus*. *J Exp Biol.* 213, 520-525.
- Hibino, T., Ishii, Y., Levin, M., Nishino, A., 2006. Ion flow regulates left-right asymmetry in sea urchin development. *Dev. Genes Evol.* 216, 265-276.

- Highsmith, R. C., Emlet, R. B., 1986. Delayed metamorphosis: effect on growth and survival of juvenile sand dollars (Echinoidea: Clypeasteroidea). *Bull Mar Sci.* 39, 347-361.
- Hill, S. K., Lawrence, J. M., 2006. Interactive effects of temperature and nutritional condition on the energy budgets of the sea urchins *Arbacia punctulata* and *Lytechinus variegatus* (Echinodermata: Echinoidea). *J Mar Biol Ass U.K.* 86, 783-790.
- Hoegh-Guldberg, O., 1994. Uptake of dissolved organic matter by larval stage of the crown-of-thorns starfish *Acanthaster planci*. *Mar Biol.* 120, 55-63.
- Hoegh-Guldberg, O., Emlet, R. B., 1997. Energy use during the development of a lecithotrophic and a planktotrophic echinoid. *Biol Bull.* 192, 27-40.
- Hoegh-Guldberg, O., Mumby, P. J., Hooten, A. J., Steneck, R. S., Greenfield, P., Gomez, E., Harvell, C. D., Sale, P. F., Edwards, A. J., Caldeira, K., Knowlton, N., Eakin, C. M., Iglesias-Prieto, R., Muthiga, N., Bradbury, R. H., Dubi, A., Hatziolos, M. E., 2007. Coral reefs under rapid climate change and ocean acidification. *Science.* 318, 1737-1742.
- Hollertz, K., 2002. Feeding biology and carbon budget of the sediment-burrowing heart urchin *Bryopsis lyrifera* (Echinoidea: Spatangoida). *Mar Biol.* 140, 959-969.
- Holmes, R. M., Aminot, A., Kerouel, R., Hooker, B. A., Peterson, B. J., 1999. A simple and precise method for measuring ammonium in marine and freshwater ecosystems. *Can J Fish Aquat Sci.* 56, 1801-1808.
- Hu, M. Y.-A., Tseng, Y.-C., Stumpp, M., Gutowska, M. A., Kiko, R., Lucassen, M., Melzner, F., 2011. Elevated seawater $p\text{CO}_2$ differentially affects branchial acid-base transporters over the course of development in the cephalopod *Sepia officinalis*. *Am J Physiol - Reg I.* 300, R1100-R1114.
- Hughes, A. D., Kelly, M. S., Barnes, D. K. A., Catarino, A. I., Black, K. D., 2006. The dual functions of sea urchin gonads are reflected in the temporal variations of their biochemistry. *Mar Biol.* 148, 789-798.
- Hunt, B. P. V., Pakhomov, E. A., Hosie, G. W., Siegel, V., Ward, P., Bernard, K., 2008. Pteropods in Southern Ocean ecosystems. *Progr Oceanogr.* 78, 193-221.
- Hwang, S.-P. L., Lennarz, W. J., 1993. Studies on the cellular pathway involved in assembly of the embryonic sea urchin spicule. *Exp Cell Res.* 205, 383-387.
- Ikeda, T., 1977. The effect of laboratory conditions on the extrapolation of experimental measurements to the ecology of marine zooplankton. IV. Changes in respiration and excretion rates of Boreal zooplankton species maintained under fed and starved conditions. *Mar Biol.* 41, 241-252.
- IPCC, 2001. The third assessment report of the Intergovernmental Panel on Climate Change (IPCC). Cambridge University Press, Cambridge, UK and New York, USA.
- IPCC, 2007. The fourth assessment report of the Intergovernmental Panel on Climate Change (IPCC). Cambridge University Press, Cambridge, UK and New York, USA.
- Johansen, K., Vadas, R. L., 1967. Oxygen uptake and responses to respiratory stress in sea urchins. *Biol Bull.* 132, 16-22.
- Johnson, P. T., 1969. The coelomic elements of sea urchins (*Strongylocentrotus*) I. The normal coelomocytes; their morphology and dynamics in hanging drops. *J Invertebr Pathol.* 13, 25-41.
- Josephson, R. K., Schwab, W. E., 1979. Electrical properties of an excitable epithelium. *J Gen Physiol.* 74, 213-236.

- Katow, H., Solursh, M., 1979. Ultrastructure of blastocoel material in blastulae and gastrulae of the sea urchin *Lytechinus pictus*. *J Exp Zool.* 210, 561-567.
- Kawabe, T. T., Armstrong, P. B., Pollock, E. G., 1981. An extracellular fibrillar matrix in gastrulating sea urchin embryos. *Dev Biol.* 85, 509-515.
- Killian, C. E., Wilt, F. H., 2008. Molecular aspects of biomineralization of the echinoderm endoskeleton. *Chem Rev.* 106, 4463-4474.
- Klinger, T. S., 1984. Activities and kinetics of digestive alpha- and beta-glucosidase and beta-galactosidase of five species of echinoids. *Comp Biochem Physiol.* 78A, 597-600.
- Knoll, A. H., Barnbach, R. K., Payne, J. L., Pruss, S., Fischer, W. W., 2007. Paleophysiology and end-Permian mass extinction. *Earth Planet Sci Lett.* 256, 295-313.
- Kobayashi, N., 1980. Comparative Sensitivity of Various Developmental Stages of Sea-Urchins to Some Chemicals. *Mar Biol.* 58, 163-171.
- Körner, S., Das, S. K., Veenstra, S., Vermaat, J. E., 2001. The effect of pH variation at the ammonium/ammonia equilibrium in wastewater and its toxicity to *Lemna gibba*. *Aquat Bot.* 71, 71-78.
- Kroeker, K. J., Kordas, R. L., Crim, R. N., Singh, G. G., 2010. Meta-analysis reveals negative yet variable effects of ocean acidification on marine organisms. *Ecol Lett.* 13, 1419-1434.
- Kurihara, H., 2008. Effects of CO₂-driven ocean acidification on the early developmental stages of invertebrates. *Mar Ecol Prog Ser.* 373, 275-284.
- Kurihara, H., Shirayama, Y., 2004. Effects of increased atmospheric CO₂ on sea urchin early development. *Mar Ecol Prog Ser.* 274, 161-169.
- Langdon, C., Atkinson, M. J., 2005. Effect of elevated pCO₂ on photosynthesis and calcification of corals and interactions with seasonal change in temperature/irradiance and nutrient enrichment. *J Geophys Res.* 110.
- Langenbuch, M., Pörtner, H. O., 2002. Changes in metabolic rate and N excretion in the marine invertebrate *Sipunculus nudus* under conditions of environmental hypercapnia: identifying effective acid-base variables. *J Exp Biol.* 205, 1153-1160.
- Langenbuch, M., Pörtner, H. O., 2004. High sensitivity to chronically elevated CO₂ levels in a eurybathic marine sipunculid. *Aquat Toxicol.* 70, 55-61.
- Langer, G., Geisen, M., Baumann, K.-H., Kläs, J., Ribesell, U., Thoms, S., Young, J. R., 2006. Species-specific responses of calcifying algae to changing seawater carbonate chemistry. *Geochem Geophys Geosys.* 7.
- Lanning, G., Eilers, S., Pörtner, H. O., Sokolova, I. M., Bock, C., 2010. Impact of ocean acidification on energy metabolism of oyster *Crassostrea gigas* - changes in metabolic pathways and thermal response. *Mar Drugs.* 8, 2318-2339.
- Larsen, B. K., Pörtner, H. O., Jensen, F. B., 1997. Extra- and intracellular acid-base balance and ionic regulation in cod (*Gadus morhua*) during combined and isolated exposures to hypercapnia and copper. *Mar Biol.* 128, 337-346.
- Lau, D. C. C., Lau, S. C. K., Qian, P. Y., Qiu, J. W., 2009. Morphological plasticity and resource allocation in response to food limitation and hyposalinity in a sea urchin. *J Shellfish Res.* 28, 383-388.
- Lawrence, J. M., Edible sea urchins: use and life-history strategies. In: J. M. Lawrence, (Ed.), *Edible Sea Urchins Biology and Ecology*. Elsevier, Amsterdam, 2007, pp. 1-6.

- Lawrence, J. M., Plank, L. R., Lawrence, A. L., 2003. The effect of feeding frequency on consumption of food, absorption efficiency, and gonad production in the sea urchin *Lytechinus variegatus*. *Comp Biochem Physiol A*. 134, 69-75.
- Lebrato, M., Iglesias-Rodríguez, D., Feely, R. A., Greenley, D., Jones, D. O. B., Suarez-Bosche, N., Lampitt, R. S., Cartes, J. E., Green, D. R. H., Alker, B., 2010. Global contribution of echinoderms to the marine carbon cycle: CaCO₃ budget and benthic compartments. *Ecol Monogr*. 80, 441-467.
- Leong, P. K. K., Manahan, D. T., 1997. Metabolic importance of Na⁺/K⁺-ATPase activity during sea urchin development. *J Exp Biol*. 200, 2881-2892.
- Leong, P. K. K., Manahan, D. T., 1999. Na⁺/K⁺-ATPase activity during early development and growth of an antarctic sea urchin. *J Exp Biol*. 202, 2051-2058.
- Levitan, D. R., 1991. Skeletal changes in the test and jaws of the sea urchin *Diadema antillarum* in response to food limitation. *Mar Biol*. 111, 431-435.
- Lewis, E., Wallace, D. W. R., 1998. CO₂SYN-Program developed for the CO₂ system calculations. Carbon Dioxide Inf Anal Center Report ORNL/CDIAC-105.
- Lindinger, M. I., Lauren, D. J., McDonald, D. G., 1984. Acid-base-balance in the sea mussel, *Mytilus edulis*. 3. Effects of environmental hypercapnia on intracellular and extracellular acid-base-balance. *Mar Biol Lett*. 4, 371-381.
- Linser, P. J., Smith, K. E., Seron, T. J., Oviedo, M. N., 2009. Carbonic anhydrases and anion transport in mosquito midgut pH regulation. *J Exp Biol*. 212, 1662-1671.
- Lischka, S., Büdenbender, J., Boxhammer, T., Riebesell, U., 2011. Impact of ocean acidification and elevated temperatures on early juveniles of the polar shelled pteropod *Limacina helicina*: mortality, shell degradation, and shell growth. *Biogeosciences*. 8, 919-932.
- Livak, K. J., Schmittgen, T. D., 2001. Analysis of relative gene expression data using real-time quantitative PCR and the 2^{-ddCT} method. *Methods*. 25, 402-408.
- Livingston, B. T., Killian, C., Wilt, F., Cameron, A., Landrum, M. J., Ermolaeva, O., Sapojnikov, V., Maglott, D. R., Buchanan, A. M., Etensohn, C. A., 2006. A genome-wide analysis of biomineralization-related proteins in the sea urchin *Strongylocentrotus purpuratus*. *Dev Biol*. 300, 335-348.
- Love, A. C., Andrews, M. E., Raff, R. A., 2007. Gene expression patterns in a novel animal appendage: the sea urchin pluteus arm. *Evol Dev*. 9, 51-68.
- Lyons, D. A., Scheibling, R. E., 2007. Differences in somatic and gonadic growth of sea urchins (*Strongylocentrotus droebachiensis*) fed kelp (*Laminaria longicruris*) or the invasive alga *Codium fragile* ssp. *tomentosoides* are related to energy acquisition. *Mar Biol*. 152, 285-295.
- Maltby, L., Naylor, C., Calow, P., 1990. Effect of stress on a freshwater benthic detritivore: scope for growth in *Gammarus pulex*. *Ecotoxicol Environ Safety*. 19, 285-291.
- Mamelona, J., Pelletier, É., 2005. Green urchin as a significant source of fecal particulate organic matter within nearshore benthic ecosystems. *J Exp Mar Biol Ecol*. 314, 163-174.
- Manahan, D. T., 1990. Adaptations by invertebrate larvae for nutrient acquisition from seawater. *Am Zool*. 30, 147-160.
- Manahan, D. T., Crisp, D. J., 1982. The role of dissolved organic material in the nutrition of pelagic larvae - amino acid uptake by bivalve veligers. *Ame Zool*. 22, 635-646.
- Mann, K., Poustka, A. J., Mann, M., 2008. The sea urchin (*Strongylocentrotus purpuratus*) test and spine proteomes. *Proteome Science*. 6.

- Marsh, A. G., Leong, P. K. K., Manahan, D. T., 1999. Energy metabolism during embryonic development and larval growth of an antarctic sea urchin. *J Exp Biol.* 202, 2041-2050.
- Marsh, A. G., Manahan, D. T., 1999. A method for accurate measurements of the respiration rates of marine invertebrate embryos and larvae. *Mar Ecol Prog Ser.* 184, 1-10.
- Marshall, D. J., Pechenik, J. A., Keough, M. J., 2003. Larval activity levels and delayed metamorphosis affect post-larval performance in the colonial, ascidian *Diplosoma listerianum*. *Mar Ecol Prog Ser.* 246, 153-162.
- Marsham, S., Scott, G. W., Tobin, M. L., 2007. Comparison of nutritive chemistry of a range of temperate seaweeds. *Food Chem.* 100, 1331-1336.
- Martin, S., Richier, S., Pedrotti, M.-L., Dupont, S., Castejon, C., Gerakis, Y., Kerros, M.-E., Oberhänsli, F., Teyssié, J.-L., Gattuso, J. P., 2011. Early development and molecular plasticity in the Mediterranean sea urchin *Paracentrotus lividus* exposed to CO₂ driven ocean acidification. *J Exp Biol.* 214, 1357-1368.
- Matranga, V., Pinsino, A., Celi, M., Di Bella, G., Natoli, A., 2006. Impacts of UV-B radiation on short-term cultures of sea urchin coelomocytes. *Mar Biol.* 149, 25-34.
- Matyssek, R., Schnyder, H., Elstner, E. F., Munch, J. C., Pretzsch, H., Sandermann, H., 2002. Growth and parasite defence in plants; the balance between resource sequestration and retention: In lieu of a guest editorial. *Plant Biology.* 4, 133-136.
- Mehrbach, C., Culbertson, C. H., Hawley, J. E., Pytkowicz, R. M., 1973. Measurement of the apparent dissociation constants of carbonic acid in seawater at atmospheric pressure. *Limnol Oceanogr.* 18, 897-907.
- Meidel, S. K., Scheibling, R. E., 1999. Effects of food type and ration on reproductive maturation and growth of the sea urchin *Strongylocentrotus droebachiensis*. *Mar Biol.* 134, 155-166.
- Melzner, F., Gutowska, M. A., Langenbuch, M., Dupont, S., Lucassen, M., Thorndyke, M. C., Bleich, M., Pörtner, H.-O., 2009. Physiological basis for high CO₂ tolerance in marine ectothermic animals: pre-adaptation through lifestyle and otogeny? *Biogeosciences.* 6, 2313-2331.
- Meyer, E., Green, A. J., Moore, M., Manahan, D. T., 2007. Food availability and physiological state of sea urchin larvae (*Strongylocentrotus purpuratus*). *Mar Biol.* 152, 179-191.
- Michaelidis, B., Ouzounis, C., Palaras, A., Pörtner, H.-O., 2005. Effects of long-term moderate hypercapnia on acid-base balance and growth rate in marine mussels *Mytilus galloprovincialis*. *Mar Ecol Prog Ser.* 293, 109-118.
- Michaelidis, B., Spring, A., Pörtner, H. O., 2007. Effects of long-term acclimation to environmental hypercapnia on extracellular acid-base status and metabolic capacity in Mediterranean fish *Sparus aurata*. *Mar Biol.* 150, 1417-1429.
- Miles, H., Widdicombe, S., Spicer, J. I., Hall-Spencer, J., 2007. Effects of anthropogenic seawater acidification on acid-base balance in the sea urchin *Psammechinus miliaris*. *Mar Pollut Bull.* 54, 89-96.
- Miller, B. A., Emllet, R. B., 1999. Development of newly metamorphosed juvenile sea urchins (*Strongylocentrotus franciscanus* and *S. purpuratus*): morphology, the effects of temperature and larval food ration, and a method for determining age. *J Exp Mar Biol Ecol.* 235, 67-90.
- Miller, R. J., Mann, K. H., 1973. Ecological energetics of the seaweed zone in a marine bay on the Atlantic coast of Canada. III. Energy transformations by sea urchins. *Mar Biol.* 18, 99-114.

- Miner, B. G., 2005. Evolution of feeding structure plasticity in marine invertebrate larvae: a possible trade-off between arm length and stomach size. *J Exp Mar Biol Ecol.* 315, 117-125.
- Moore, H. B., McPherson, B. F., 1965. A contribution to the study of the productivity of the urchins *Tripneustes esculentus* and *Lytechinus variegatus*. *B Mar Sci.* 15, 855-871.
- Mubiana, V. K., Blust, R., 2007. Effects of temperature on scope for growth and accumulation of Cd, Co, Cu and Pb by the marine bivalve *Mytilus edulis*. *Mar Environ Res.* 63, 219-235.
- Mullin, M. M., Sloan, P. R., Eppley, R. W., 1966. Relationship between carbon content, cell volume, and area in phytoplankton. *Limnol Oceanogr.* 11, 307-311.
- Munday, P. L., Crawley, N. E., Nilsson, G. E., 2009. Interacting effects of elevated temperature and ocean acidification on the aerobic performance of coral reef fishes. *Mar Ecol Prog Ser.* 388, 235-242.
- Nakano, E., Okazaki, K., Iwamatsu, T., 1963. Accumulation of radioactive calcium in the larvae of the sea urchin *Pseudecentrotus depressus*. *Biol Bull.* 125, 125-136.
- Navarro, J. M., Urrutia, G. X., Carrasco, C., 2006. Scope for growth versus actual growth in the juvenile predatory gastropod *Chorus giganteus*. *J Mar Biol Ass U.K.* 86, 1423-1428.
- Nawata, C. M., Hirose, S., Nakada, T., Wood, C. M., Kato, A., 2010. Rh glycoprotein expression is modulated in pufferfish (*Takifugu rubripes*) during high environmental ammonia exposure. *J Exp Biol.* 213, 3150-3160.
- Nienhus, S., Palmer, A. R., Harley, D. G., 2010. Elevated CO₂ affects shell dissolution rate but not calcification rate in a marine snail. *Proc. R. Soc. B.* doi:10.1098/rspb.2010.0206.
- O'Donnell, M. J., Todgham, A. E., Sewell, M. A., Hammond, L. M., Ruggiero, K., Fanguie, N. A., Zippay, M. L., Hofmann, G. E., 2010. Ocean acidification alters skeletogenesis and gene expression in larval sea urchins. *Mar Ecol Prog Ser.* 398, 157-171.
- Okazaki, K., 1975. Spicule formation by isolated micromeres of the sea urchin embryo. *Am Zool.* 15, 567-581.
- Okazaki, K., Inoué, S., 1976. Crystal property of the larval sea urchin spicule. *Dev Growth Diff.* 18, 413-434.
- Onken, H., Moffett, D. F., 2009. Revisiting the cellular mechanisms of strong luminal alkalization in the anterior midgut of larval mosquitoes. *J Exp Biol.* 212, 373-377.
- Orr, J. C., Fabry, V. J., Aumont, O., Bopp, L., Doney, S. C., Feely, R. A., Gnanadesikan, A., Gruber, N., Ishida, A., Joos, F., Key, R. M., Lindsay, K., Maier-Reimer, E., Matear, R., Mofray, P., Mouchet, A., Najjar, R. G., Plattner, G.-K., Rodgers, K. B., Sabine, C. L., Sarmiento, J. L., Schlitzer, R., Slater, R. D., Totterdell, I. J., Weirig, M.-F., Yamanaka, Y., Yool, A., 2006. Anthropogenic ocean acidification over the twenty-first century and its impact on calcifying organisms. *Nature.* 437, 681-686.
- Otero-Villanueva, M. M., Kelly, M. S., Burnell, G., 2004. How diet influences energy partitioning in the regular echinoid *Psammechinus miliaris*; constructing an energy budget. *J Exp Mar Biol Ecol.* 304, 159-181.
- Pace, D. A., Manahan, D. T., 2006. Fixed metabolic costs for highly variable rates of protein synthesis in sea urchin embryos and larvae. *J Exp Biol.* 209, 391-392.

- Pane, E. F., Barry, J. P., 2007. Extracellular acid-base regulation during short-term hypercapnia is effective in a shallow-water crab, but ineffective in a deep-sea crab. *Mar Ecol Prog Ser.* 334, 1-9.
- Pearse, J. S., 2006. Ecological role of purple sea urchins. *Science.* 314, 940-941.
- Pechenik, J. A., 2006. Larval experience and latent effects - metamorphosis is not a new beginning. *Integr Comp Biol.* 46, 323-333.
- Pennington, J. T., Strathmann, R. R., 1990. Consequences of the calcite skeletons of planktonic echinoderm larvae for orientation, swimming, and shape. *Biol. Bull.* 179, 121-133.
- Petit, J. R., Jouzel, J., Raynaud, D., Barkov, N. I., Barnola, J. M., Basile, I., Bender, M., Chappellaz, J., Davis, M., Delaygue, G., Delmotte, M., Kotlyakov, V. M., Legrand, M., Lipenkov, V. Y., Lorius, C., Pepin, L., Ritz, C., Saltzman, E., Stievenard, M., 1999. Climate and atmospheric history of the past 420,000 years from the Vostok ice core, Antarctica *Nature.* 399, 429-436.
- Podolsky, R. D., McAlister, J. S., 2005. Developmental plasticity in *Macrophiothrix* brittlestars: are morphologically convergent larvae also convergently plastic? *Biol Bull.* 209, 127-138.
- Politi, Y., Arad, T., Klein, E., Weiner, S., Addadi, L., 2004. Sea urchin spine calcite forms via a transient amorphous calcium carbonate phase. *Science.* 306, 1161-1164.
- Politi, Y., Metzler, R. A., Abrecht, M., Gilbert, B., Wilt, F. H., Sagi, I., Addadi, L., Weiner, S., Gilbert, P. U. P. A., 2008. Transformation mechanisms of amorphous calcium carbonate into calcite in the sea urchin larval spicule. *PNAS.* 105, 17362-17366.
- Pond, D. W., Harris, R. P., Brownlee, C., 1995. A microinjection technique using a pH-sensitive dye to determine the gut pH of *Calanus helgolandicus*. *Mar Biol.* 123, 75-79.
- Pörtner, H.-O., 2008. Ecosystem effects of ocean acidification in times of ocean warming: a physiologist's view. *Mar Ecol Prog Ser.* 373, 203-217.
- Pörtner, H.-O., Dupont, S., Melzner, F., Storch, D., Thorndyke, M., Studies of metabolic rate and other characters across life stages. In: U. Riebesell, V. J. Fabry, L. Hansson, J.-P. Gattuso, (Eds.), *Guide to best practices for ocean acidification research and data reporting.* Publications Office of the European Union, Luxembourg, 2010, pp. 167-180.
- Pörtner, H.-O., Farrell, A. P., 2008. Physiology and climate change. *Science.* 322, 90-92.
- Pörtner, H. O., Langenbuch, M., Reipschläger, A., 2004. Biological impact of elevated ocean CO₂ concentrations: lessons from animal physiology and earth history. *J Oceanogr.* 60, 705-718.
- Powell, D. W., 1981. Barrier function of epithelia. *Am J Physiol.* 241, G275-G288.
- Propp, M. V., Ryabushko, V. I., Zhuchikhina, A. A., Propp, L. N., 1983. Seasonal changes in respiration, ammonia and phosphate excretion, and activity of carbohydrate-metabolism enzymes in four echinoderm species from the sea of Japan. *Comp Biochem Physiol B.* 75, 707-711.
- Ramakers, C., Ruijter, J. M., Deprez, R. H., Moorman, A. F., 2003. Assumption-free analysis of quantitative real-time polymerase chain reaction (PCR) data. *Neurosci Lett.* 13, 62-66.
- Raz, S., Hamilton, P. C., Wilt, F. H., Weiner, S., Addadi, L., 2003. The transient phase of amorphous calcium carbonate in sea urchin larval spicules: the involvement of

- proteins and magnesium ions in its formation and stabilization. *Adv. Funct. Mater.* 13, 480-486.
- Reardon, J., Foreman, J. A., Searcy, R., 1966. New reactants for the colourimetric determination of ammonia. *Clin Chim Acta.* 39, 403-405.
- Reipschläger, A., Pörtner, H.-O., 1996. Metabolic depression during environmental stress: the role of extracellular *versus* intracellular pH in *Sipunculus nudus*. *J Exp Biol.* 199, 1801-1807.
- Renaud, S. M., Thinh, L. V., Lambrinidis, G., Parry, D. L., 2002. Effect of temperature on growth, chemical composition and fatty acid composition of tropical Australian microalgae grown in batch cultures. *Aquaculture.* 211, 195-214.
- Riebesell, U., Schulz, K. G., Bellerby, R. G. J., Botros, M., Fritsche, P., Meyerhofer, M., Neill, C., Nondal, G., Oschlies, A., Wohlers, J., Zollner, E., 2007. Enhanced biological carbon consumption in a high CO₂ ocean. *Nature.* 450, 545-U10.
- Riebesell, U., Zondervan, I., Rost, B., Tortell, P. D., Zeebe, R. E., Morel, F. M. M., 2000. Reduced calcification of marine phytoplankton in response to increased atmospheric CO₂. *Nature.* 407, 364-467.
- Ries, J. B., Cohen, A. L., DMcCorkle, D. C., 2009. Marine calcifiers exhibit mixed responses to CO₂-induced ocean acidification. *Geology.* 37, 1131-1134.
- Rogers-Bennett, L., The ecology of *Strongylocentrotus franciscanus* and *Strongylocentrotus purpuratus*. In: J. M. Lawrence, (Ed.), *Edible Sea Urchins Biology and Ecology*. Elsevier, Amsterdam, 2007, pp. 393-426.
- Russell, M. P., 1998. Resource allocation plasticity in sea urchins: rapid, diet induced, phenotypic changes in the green sea urchin, *Strongylocentrotus droebachiensis* (Müller). *J Exp Mar Biol Ecol.* 220, 1-14.
- Sabine, C. L., Feely, R. A., Gruber, N., Key, R. M., Lee, K., Bullister, J. L., Wanninkhof, R., Wong, C. S., Wallace, D. W. R., Tilbrook, B., Millero, F. J., Peng, T. H., Kozyr, A., Ono, T., Rios, A. F., 2004. The oceanic sink for anthropogenic CO₂. *Science.* 305, 367-371.
- Sabourin, T. D., Stickle, W. B., 1981. Effects of salinity on respiration and nitrogen excretion in two species of echinoderms. *Mar Biol.* 65, 91-99.
- Sarazin, G., Michard, G., Prevot, F., 1999. A rapid and accurate spectroscopic method for alkalinity measurements in sea water samples. *Water Res.* 33, 290-294.
- Sarras, M. P., Madden, M. E., Zhang, X. M., Gunwar, S., Huff, J. K., Hudson, B. G., 1991. Extracellular matrix (mesoglea) of *Hydra vulgaris* .1. Isolation and characterization. *Dev Biol.* 148, 481-494.
- Sawabe, T., Oda, Y., Shiomi, Y., Ezura, Y., 1995. Alginate degradation by bacteria isolated from the gut of sea urchins and abalones. *Microb Ecol.* 30, 193-202.
- Scheibling, R. E., Hatcher, B. G., Ecology of *Strongylocentrotus droebachiensis*. In: J. M. Lawrence, (Ed.), *Edible Sea Urchins Biology and Ecology*. Elsevier, Amsterdam, 2007, pp. 353-382.
- Schiebel, R., 2002. Planktic foraminiferal sedimentation and the marine calcite budget. *Global Biogeochem cycl.* 16, 1065-1086.
- Schmid, V., Bally, A., Beck, K., Haller, M., Schlage, W. K., Weber, C., 1991. The extracellular matrix (mesoglea) of hydrozoan jellyfish and its ability to support cell adhesion and spreading. *Hydrobiologia.* 216, 3-10.
- Schneeberger, E. E., Lynch, R. D., 1984. Tight junctions - their structure, composition, and function. *Circ Res.* 55, 723-733.

- Selden, R., Johnson, A. S., Ellers, O., 2009. Waterborne cues from crabs induce thicker skeletons, smaller gonads and size-specific changes in growth rate in sea urchins. *Mar Biol.* 156, 1057-1071.
- Shapiro, S. S., Wilk, M. B., 1965. An analysis of variance test for normality. *Biometrika.* 52, 591-599.
- Shaposhnikova, T., Matveev, I., Napara, T., Podgornaya, O., 2005. Mesogleal cells of the jellyfish *Aurelia aurita* are involved in the formation of mesogleal fibres. *Cell Biology International.* 29, 952-958.
- Shilling, F. M., Bosch, I., 1994. 'Pre-feeding' embryos of antarctic and temperate echinoderms use dissolved organic material for growth and metabolic needs. *Mar Ecol Prog Ser.* 109, 173-181.
- Shilling, F. M., Manahan, D. T., 1990. Energetics of early development for the sea urchins *Strongylocentrotus purpuratus* and *Lytechinus pictus* and the Crustacean *Artemia* sp. *Mar Biol.* 106, 119-127.
- Shilling, F. M., Manahan, D. T., 1994. Energy metabolism and amino acid transport during early development of antarctic and temperate echinoderms. *Biol Bull.* 187, 398-407.
- Shimizu, H., Aufschnaiter, R., Li, L., Sarras, M. P., Borza, D. B., Abrahamson, D. R., Sado, Y., Zhang, X., 2008. The extracellular matrix of hydra is a porous sheet and contains type IV collagen. *Zoology.* 111, 410-418.
- Shirayama, Y., Thornton, H., 2005. Effect of increased atmospheric CO₂ on shallow water marine benthos. *J Geophys Res.* 110.
- Shirley, T. C., Stickle, W. B., 1982. Responses of *Leptasterias hexactis* (Echinodermata: Asteroidea) to low salinity II. Nitrogen metabolism, respiration and energy budget. *Mar Biol.* 69, 155-163.
- Siikavuopio, S. I., Dale, T., Mortensen, A., Foss, A., 2007a. Effects of hypoxia on feed intake and gonad growth in the green sea urchin, *Strongylocentrotus droebachiensis*. *Aquaculture.* 266, 112-116.
- Siikavuopio, S. I., Mortensen, A., Dale, T., Foss, A., 2007b. Effects of carbon dioxide exposure on feed intake and gonad growth in green sea urchin, *Strongylocentrotus droebachiensis*. *Aquaculture.* 266, 97-101.
- Sikes, C. S., Okazaki, K., Fink, R. D., 1981. Respiratory CO₂ and the supply of inorganic carbon for calcification of sea urchin embryos. *Comp Biochem Physiol A.* 70, 285-291.
- Silverman, J., Lazar, B., Cao, L., Caldeira, K., Erez, J., 2009. Coral reefs may start dissolving when atmospheric CO₂ doubles. *Geophys. Res. Lett.* 36, L05606, doi:10.1029/2008GL036282.
- Smith, M. M., Smith, L. C., Cameron, A., Urry, L. A., 2008. The larval stages of the sea urchin, *Strongylocentrotus purpuratus*. *J Morph.* 269, 713-733.
- Spicer, J. I., 1995. Oxygen and acid-base status of the sea urchin *Psammechinus miliaris* during environmental hypoxia. *Mar Biol.* 124, 71-76.
- Spicer, J. I., Taylor, A. C., Hill, A. D., 1988. Acid-base status in the sea urchins *Psammechinus miliaris* and *Echinus esculentus* (Echinodermata: Echinoidea) during emersion. *Mar Biol.* 99, 527-534.
- Spicer, J. I., Widdicombe, S., Needham, H. R., Berge, J. A., 2011. Impact of CO₂-acidified seawater on the extracellular acid-base balance of the northern sea urchin *Strongylocentrotus droebachiensis*. *J Exp Mar Biol Ecol.* 407, 19-25.

- Steneck, R. S., Graham, M. H., Bourque, B. J., Corbett, D., Erlandson, J. M., Estes, J. A., Tegner, M. J., 2002. Kelp forest ecosystems: biodiversity, stability, resilience and future. *Environ Conserv.* 29, 436-459.
- Strathmann, R. R., 1971. The feeding behavior of planktotrophic echinoderm larvae: mechanisms, regulation, and rates of suspensionfeeding. *J Exp Mar Biol Ecol.* 6, 109-160.
- Strathmann, R. R., 1989. Existence and functions of a gel filled primary body cavity in development of echinoderms and hemichordates. *Biol Bull.* 176, 25-31.
- Sumpter, J. P., 1992. Control of Growth of Rainbow-Trout (*Oncorhynchus-Mykiss*). *Aquaculture.* 100, 299-320.
- Sunday, J. M., Crim, R. N., Harley, C. D. G., Hart, M. W., 2011. Quantifying rates of evolutionary adaptation in response to ocean acidification. *Plos One.* 6, doi:10.1371/journal.pone.0022881.
- Thomsen, J., Gutowska, M. A., Saphörster, J., Heinemann, A., Fietzke, J., Hiebenthal, C., Eisenhauer, A., Körtzinger, A., Wahl, M., Melzner, F., 2010. Calcifying invertebrates succeed in a naturally CO₂ enriched coastal habitat but are threatened by high levels of future acidification. *Biogeosciences.* 7, 3879-3891.
- Thomsen, J., Melzner, F., 2010. Seawater acidification does not elicit metabolic depression in the blue mussel *Mytilus edulis*. *Mar Biol.* 157, 2667-2676.
- Thorsen, M. S., 1998. Microbial activity, oxygen status and fermentation in the gut of the irregular sea urchin *Echinocardium cordatum* (Spatangoida: Echinodermata). *Mar Biol.* 132, 423-433.
- Thorsen, M. S., 1999. Abundance and biomass of the gut-living microorganisms (bacteria, protozoa and fungi) in the irregular sea urchin *Echinocardium cordatum* (Spatangoida: Echinodermata). *Mar Biol.* 133, 353-360.
- Timpl, R., Glanville, R. W., Wick, G., Martin, G. R., 1979. Immunochemical study on basement membrane (type-IV) collagens. *Immunology.* 38, 109-116.
- Todgham, A. E., Hofmann, G. E., 2009. Transcriptomic response of sea urchin larvae *Strongylocentrotus purpuratus* to CO₂-driven seawater acidification. *J Exp Biol.* 212, 2579-2594.
- Vaitilingon, D., Morgan, R., Grosjean, P., Gosselin, P., Jangoux, M., 2001. Effects of delayed metamorphosis and food rations on the perimetamorphic events in the echinoid *Paracentrotus lividus* (Lamarck, 1816) (Echinodermata). *J Exp Mar Biol Ecol.* 262, 41-60.
- Van Weerd, J. H., Komen, J., 1998. The effects of chronic stress on growth in fish: a critical appraisal. *Comp Biochem Physiol A.* 120, 197-112.
- Vandenbroucke, I. I., Vandesompele, J., De Paepe, A., Messiaen, L., 2001. Quantification of splice variants using real-time PCR. *Nucleic Acids Res.* 29, e68.
- Verslycke, T., Janssen, C. R., 2002. Effects of a changing abiotic environment on the energy metabolism in the estuarine mysid shrimp *Neomysis integer* (Crustacea : Mysidacea). *J Exp Mar Biol Ecol.* 279, 61-72.
- Verslycke, T., Roast, S. D., Widdows, J., Jones, M. B., Janssen, C. R., 2004. Cellular energy allocation and scope for growth in the estuarine mysid *Neomysis integer* (Crustacea : Mysidacea) following chlorpyrifos exposure: a method comparison. *J Exp Mar Biol Ecol.* 306, 1-16.
- Voronezhskaya, E. E., Khabarova, M. Y., Nezlin, L. P., 2004. Apical sensory neurones mediate developmental retardation induced by conspecific environmental stimuli in freshwater pulmonate snails. *Development.* 131, 3671-3680.

- Walther, K., Anger, K., Pörtner, H. O., 2010. Effects of ocean acidification and warming on the larval development of the spider crab *Hyas araneus* from different latitudes (54° vs. 79° N). *Mar Ecol Prog Ser.* 417, 159-170.
- Weiss, R. F., 1974. Carbon dioxide in water and seawater: the solubility of a non-ideal gas. *Mar Chem.* 2, 203-215.
- Westbroeck, P., Brown, C. W., van Bleijswijk, J., Brownlee, C., Brummer, G. J., Conte, M., Egge, J., Fernández, E., Jordan, R., Knappertsbusch, M., Stefels, J., Veldhuis, M., van der Wal, P., Young, J., 1993. A model system approach to biological climate forcing. The example of *Emiliana huxleyi*. *Global Planet. Change.* 8, 27-46.
- Widdows, J., Johnson, D., 1988. Physiological energetics of *Mytilus edulis*: scope for growth. *Mar Ecol Prog Ser.* 46, 113-121.
- Wieser, W., Medgyesy, N., 1991. Metabolic rate and cost of growth in juvenile pike (*Esox lucius* L) and perch (*Perca fluviatilis* L) - the use of energy budgets as indicators of environmental change. *Oecologia.* 87, 500-505.
- Williams, J. C., 1994. Permeability of basement membranes to macromolecules. *Proceedings of the Society for Experimental Biology and Medicine.* 207, 13-19.
- Wilson, R. W., Millero, F. J., Taylor, J. R., Walsh, P. J., Christensen, V., Jennings, S., Grosell, M., 2008. Contribution of fish to the marine inorganic carbon cycle. *Science.* 323, 359-362.
- Wilt, F. H., 1999. Matrix and mineral in the sea urchin larval skeleton. *J Struct Biol.* 126, 216-226.
- Wilt, F. H., 2002. Biomineralization of the Spicules of sea urchin embryos. *Zool Sci.* 19, 253-261.
- Wilt, F. H., 2005. Developmental biology meets materials science: morphogenesis of biomaterialized structures. *Dev Biol.* 280, 15-25.
- Wilt, F. H., Killian, C. E., Hamilton, P., Croker, L., 2008. The dynamics of secretion during sea urchin embryonic skeleton formation. *Exp Cell Res.* 314, 1744-1752.
- Wilt, F. H., Killian, C. E., Livingston, B. T., 2003. Development of calcareous skeletal elements in invertebrates. *Differentiation.* 71, 237-250.
- Wolfson, J. L., Murdock, L. L., 1990. Diversity in digestive proteinase activity among insects. *J Chem Ecol.* 16, 1089-1102.
- Wood, H. L., Spicer, J. I., Kendall, M. A., Lowe, D. M., Widdicombe, S., 2011. Ocean warming and acidification; implications for the Arctic brittlestar *Ophiocten sericeum*. *Polar Biol.* 34, 1033-1044.
- Wood, H. L., Spicer, J. I., Lowe, D. M., Widdicombe, S., 2010. Interaction of ocean acidification and temperature; the high cost of survival in the brittlestar *Ophiura ophiura*. *Mar Biol.* 157, 2001-2013.
- Wood, H. L., Spicer, J. I., Widdicombe, S., 2008. Ocean acidification may increase calcification rates, but at a cost. *P Roy Soc B Bio.* 275, 1767-1773.
- Wu, S. C., Horng, J. L., Liu, S. T., Hwang, P. P., Wen, Z. H., Lin, C. S., Lin, L. Y., 2010. Ammonium-dependent sodium uptake in mitochondrion-rich cells of medaka (*Oryzias latipes*) larvae. *Am J Physiol Cell Physiol.* 298, C237-C250.
- Yajima, M., Kiyomoto, M., 2006. Study of larval and adult skeletogenic cells in developing sea urchin larvae. *Biol Bull.* 211, 183-192.
- Yajima, M., Wessel, G. M., 2011. Small micromeres contribute to the germline in the sea urchin. *Development.* 138, 237-243.
- Yu, P. C., Matson, P. G., Martz, T. R., Hofmann, G. E., 2011. The ocean acidification seascape and its relationship to the performance of calcifying marine

- invertebrates: Laboratory experiments on the development of urchin larvae framed by environmentally-relevant $p\text{CO}_2$ /pH. *J Exp Mar Biol Ecol.* 400, 288-295.
- Zeebe, R. E., Wolf-Gladrow, 2001. CO_2 in seawater: equilibrium, kinetics, isotopes. Elsevier Oceanography Series, Amsterdam.
- Zillén, L., Conley, D. J., Andrén, T., Andrén, E., Björck, S., 2008. Past occurrences of hypoxia in the Baltic Sea and the role of climate variability, environmental change and human impact. *Earth-Sci Rev.* 91, 77-92.

7 Eidesstattliche Erklärung

Meike Stumpp
Holtenauer Str 340
24106 Kiel

Erklärung gem. §9 der Promotionsordnung:

Ich erkläre hiermit,

- (i) dass die Abhandlung – abgesehen von der Beratung durch die Betreuerin oder den Betreuer – nach Inhalt und Form die eigene Arbeit ist,
 - (ii) dass diese Arbeit vor dem jetzigen Promotionsverfahren keinem anderen Promotionsverfahren unterzogen wurde
- und
- (iii) dass die Arbeit unter Einhaltung der Regeln guter wissenschaftlicher Praxis der Deutschen Forschungsgemeinschaft entstanden ist.

gez. Meike Stumpp

